STRUCTURE-FUNCTION ANALYSIS OF REOVIRUS BINDING TO JUNCTIONAL ADHESION MOLECULE-A

BY

Jacquelyn Andrea Campbell

Dissertation

Submitted to the Faculty of the

Graduate School of Vanderbilt University

in partial fulfillment of the requirements

for the degree of

DOCTOR OF PHILOSOPHY

in

Microbiology and Immunology

December, 2005

Nashville, Tennessee

Approved:

Earl Ruley

Phoebe Stewart

Luc Van Kaer

Richard Hoover

Jim Crowe

Terence S. Dermody

Dedicated to My Parents

Allan and Carol Campbell

ACKNOWLEDGEMENTS

I grew up hoping that I could someday find a good job. I am lucky to have found a path to a career I will always love. I could not have made it this far without the support of many people. I would like to especially thank the following for making it possible for me to have the opportunity to train at a wonderful place like Vanderbilt:

- My parents for their endless support, sacrifices, and love. Someday I hope to be as great a parent as you both are.
- The entire Hansberger family. One of the best parts of this experience was getting to know you.
- Mark Hansberger for being the best roommate, friend, and coworker I could have asked for.
- Terry Dermody for being an amazing mentor. I have felt lucky to have trained in your lab. You have shared a wealth of knowledge about life, wine, and science.
- All my friends, including Kary Kull and Paul King for their immense support. You have made Nashville a great place to live.
- My dissertation committee, Earl Ruley, Luc Van Kaer, Jim Crowe, Richard Hoover, and Phoebe Stewart for insightful advice on both science and career choices.
- Past and present members of the Dermody Lab. I've enjoyed your critical review of science, the warm atmosphere in which you all have contributed, and your friendship. I especially would like to thank Craig Forrest, both for outstanding technical and intellectual insight and for being a truly inspirational graduate student mentor.
- Bill and Lisa Rice for introducing me to science.

- Mr. Boldon for encouraging me early to try things I think might be nearly impossible.
- Dr. Richard Cowart for teaching me a little creativity and a Sigma catalog will take you places in science.
- Thank you to the Division of Pediatric Infectious Disease, the Department of Microbiology and Immunology, the Department of Pathology, and the Lamb Center for Pediatric Research for educational and financial support.

TABLE OF CONTENTS

LIST OF TABLES

LIST OF FIGURES

LIST OF ABBREVIATIONS

Ad	Adenovirus
AF-6	ALL-1 fusion partner from gene 6
CNS	Central nervous system
CAR	Coxsackievirus and adenovirus receptor
DNA	Deoxyribonucleic acid
dsRNA	Double-stranded ribonucleic acid
E. coli	*Escherichia coli*
FFU	Fluorescent focus unity
GFP	Green fluorescent protein
GST	Glutathione S-transferase
H	Hour
ICAM	Intercellular adhesion molecule
ISVP	Infectious subvirion particles
HIV	Human immunodeficiency virus
IG	Immunoglobulin
ISVP	Infectious subvirion particle
JAM	Junctional adhesion molecule
kD	Kilodalton
L	L929
mAb	Monoclonal antibody
Min	Minute
MDCK	Madin-Darby canine kidney

MEL	Murine erythroleukemia cells
MOI	Multiplicity of infection
mRNA	Message ribonucleic acid
MUPP-1	multiple PDZ domain containing protein-1
NGS	Normal goat serum
ORF	Open reading frame
PBS	Phosphate-buffered saline
PCR	Polymerase chain reaction
PFU	Plaque forming units
PKC	Protein kinase C
RNA	Ribonucleic acid
SA	Sialic acid
SDS	Sodium dodecyl sulphate
TER	Transepithelial resistance
T1	Type 1
T2	Type 2
T3	Type 3
V	Volts
Wt	Wild-type
ZO-1	Zonula occluden-1
ZO-2	Zonula occluden-2

CHAPTER I

BACKGROUND AND LITERATURE REVIEW

Overview of virus receptor utilization

Viral pathogenesis is a complex, multi-step process with many factors influencing disease development. In order for a virus to cause disease it must have the capacity to locate target organs. Virus attachment to cellular receptors is the first step in viral replication and thus plays a key role in viral tropism and disease. As such, virus-receptor engagement is a critical determinant of disease outcome and a potential target for antiviral therapy.

Viruses are capable of recognizing several types of cell-surface features including proteins and carbohydrates. Among the earliest reports of virus receptor identification was the suggestion in the late 1950s that influenza virus and coronavirus utilized carbohydrates such as sialic acid for receptors (75, 176). Carbohydrates serve as receptors for many families of viruses and, in some cases, these molecule play a key role in viral tropism and pathogenesis (11, 16, 198). Since the advent of molecular cloning, many proteinacetous viral receptors have been identified.

Three important themes have emerged from the identification and study of virus receptors (52). First, viruses have adapted to utilize receptors that facilitate a variety of normal cellular functions. Virus receptors may be highly specialized proteins with limited tissue distribution or more ubiquitous components of cellular membranes. One commonality amongst many virus receptors is that they are cell-junction associated proteins that function in maintaining cell-cell contacts, including integrins, coxsackievirus and adenovirus receptor (CAR) (23), junctional adhesion molecule-A (JAM-A) (10), Nectin, and intercellular adhesion molecule-1 (ICAM-1) (76, 150).

Second, many viruses use more than a single receptor to effect multi-step attachment to cells or mediate independent binding and internalization events. Receptors were long thought of as an adsorptive docking point for virus attachment. It is now established that interactions between viruses and receptors are much more complex than the original simplistic "lock and key" model in which a single viral protein interacted with a single cellular receptor to gain access to the cell. For example, HIV entry into cells requires multiple interactions with receptors (45). Initial binding of the HIV attachment protein, gp120, to CD4 is required but not sufficient for virus infection (40). Following engagement of CD4, gp120 undergoes conformational changes allowing interactions with a coreceptor, which depending on the strain, may be either CXCR4 or CCR5 (54, 194). Upon gp120 interaction with both CD4 and a coreceptor, the viral fusion protein is exposed, resulting in membrane fusion and viral entry (108).

Third, in addition to serving as an attachment point for the virus, virus-receptor engagement also can activate receptor-linked signaling pathways, including those that initiate innate immune responses or induce apoptosis. Upon binding to the cell surface, viruses frequently commandeer the signaling cascades elicited by many receptors such as integrins, cytokine receptors, and growth factor receptors (104, 111, 181).

Although receptors have been identified for several virus families, little is known about the functions of individual receptors in viral tropism and disease. This key gap in knowledge represents a long-standing barrier to efforts to define how viruses select specific cellular targets. Moreover, given the critical importance of the attachment step in viral pathogenesis, new insights into the structure and function of viral attachment proteins and their cell-surface receptors will be required to understand disease mechanisms and illuminate new targets for therapeutic intervention.

Reovirus introduction

Reoviruses were first isolated in 1950s. This family of viruses was coined reoviruses because they were isolated from the respiratory and enteric tracts and not associated with a specific disease (*re*spirator *e*nteric *o*rphan virus) (138). Reoviruses are nonenveloped viruses that contain a segmented, double-stranded RNA (dsRNA) genome (166). The genome consists of ten gene segments that encode eleven proteins, eight of which are structural proteins whereas three are not associated with the virion and termed "nonstructural proteins". The virion consists of two concentric protein shells (Figure 1). The outer capsid contains proteins λ2, μ1, σ3, and σ1. The inner protein shell is termed the core and consists of proteins λ1, λ2, λ3, μ2 and σ2 (166).

After attachment to the cell surface, the virus is internalized by receptor-mediated endocytosis. Within endosomes, virions undergoes acid-dependent, proteolytic disassembly to form infectious subvirion particles (ISVPs). ISVPs penetrate the endosomal membrane and release the transcriptionally active core into the cytoplasm. Following synthesis of viral proteins and replication of viral genomic dsRNA, progeny virions are assembled and released fro the cell (Figure 2) (166).

Mammalian orthoreoviruses have served as one of the most richly exploited models of viral pathogenesis. There are three major reovirus serotypes each represented by a prototype strain: type 1 Lang (T1L), type 2 Jones (T2J), and type 3 Dearing (T3D). All three serotypes are capable of infecting most mammals, including humans, but disease progression is restricted to the very young (168).

Following oral inoculation of newborn mice, both type 1 reovirus and type 3 reovirus undergo primary replication in the intestinal epithelium and Peyer's patches (190). However,

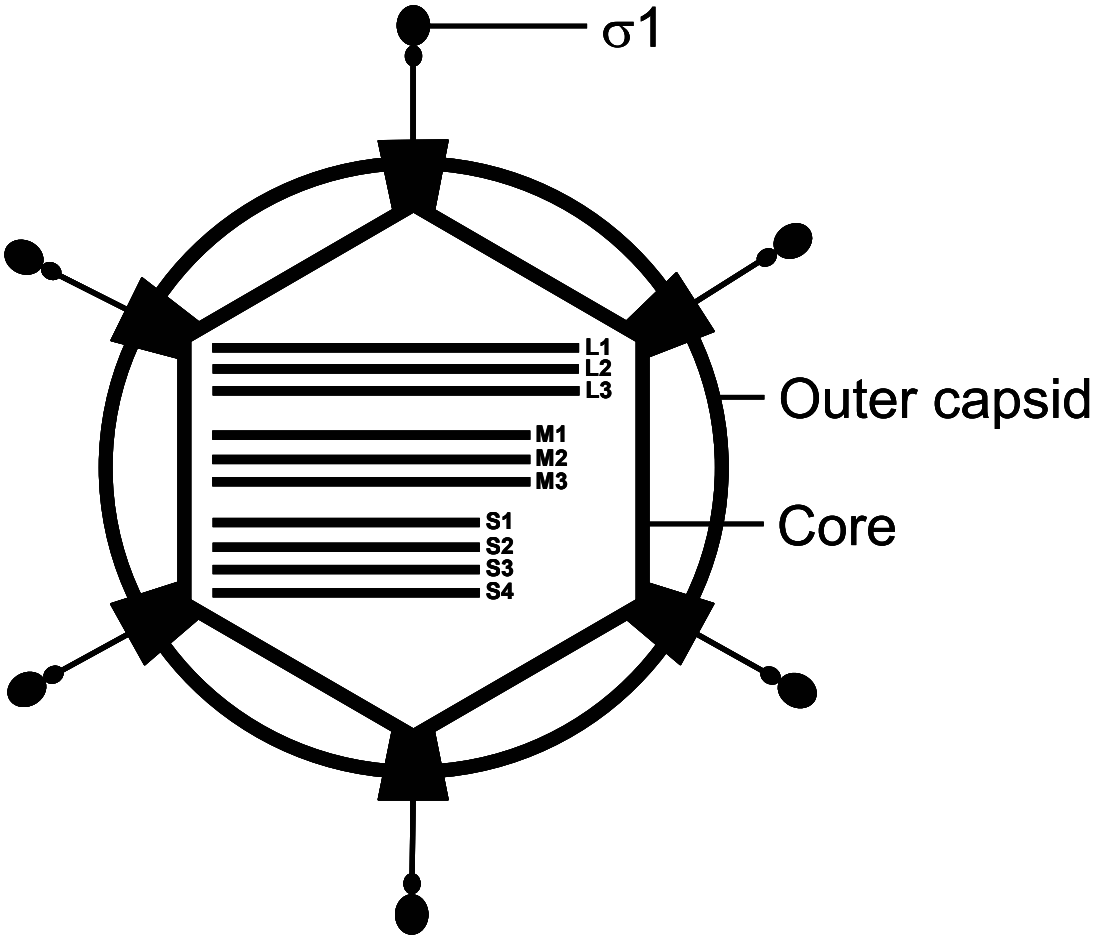

Figure 1. The reovirus virion. The reovirus virion contains two concentric protein shells termed outer capsid and core. The core contains 10 dsRNA gene segments that are classified by size as large (L), medium (M), or small (S). The viral attachment protein, σ1, is depicted as a ball and stick model protruding from the outer capsid.

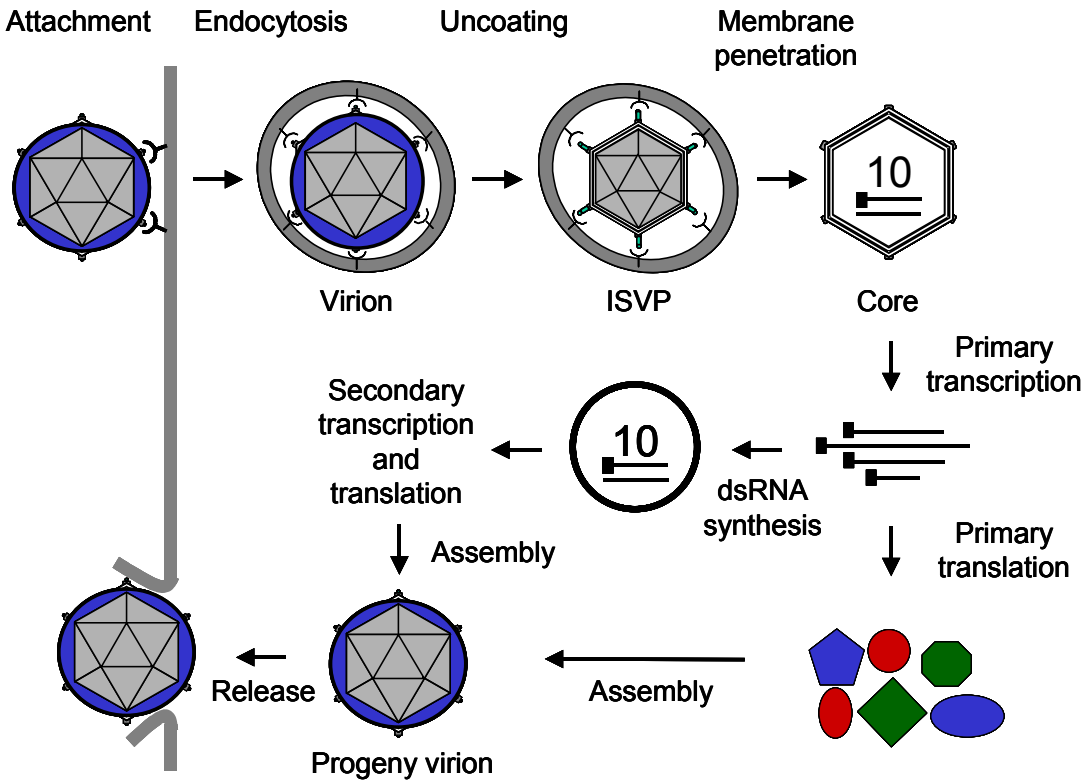

Figure 2. The reovirus replication cycle. Reovirus attaches to the cell surface and enters by receptor-mediated endocytosis. Disassembly occurs in the endosome, resulting in the formation of ISVPs. ISVPs penetrate the membrane and the core is released into the cytoplasm to begin transcription. Following synthesis of viral proteins and replication of viral genomic dsRNA, progeny virions are assembled and released from the cell.

after primary replication there is a marked dichotomy in both the route of spread and tropism between the two serotypes. Type 1 reovirus spreads hematogenously to ependymal cells where it causes sub-acute hydrocephalus (167, 183, 184). Type 3 reovirus spreads by neural routes to the CNS where it infects neurons and causes acute, lethal encephalitis (114, 167, 183, 184). This difference in spread and tissue tropism has been mapped using type 1 and type 3 reovirus reassortant viruses to the S1 gene, which encodes the viral attachment protein, σ1 (167, 183, 184). The link between σ1 and the route of dissemination in the host and cell tropism within the CNS has made its structure and function the focus of considerable interest.

General properties of σ1

The first experimental insights into σ1 structure came from composite transmission electron micrographs of σ1 molecules purified from virions (64) (Figure 3). These images confirmed earlier predictions of a fiber-like structure of σ1 (13) and clearly revealed two distinct morphological domains: a long N-terminal fibrous tail that inserts into the viral capsid and a C-terminal globular head that projects away from the virion surface. The σ1 protein exhibits substantial flexibility at several discrete regions within the fibrous tail.

Additional clues about key structural features of σ1 were revealed by increasingly sophisticated analyses of its amino acid sequence over many years. Following an N-terminal hydrophobic region that comprises 30 residues and likely serves as the primary anchor of the protein into the capsid, the σ1 sequence contains an extended region characterized by heptad repeats with non-polar residues at the first and fourth positions of the repeating unit (50).

Such repeats are characteristic of α-helical coiled coils (182) in which amphipathic helices are wrapped around each other to form dimers, trimers, or tetramers. Accordingly, the N-terminal portion of σ1 was predicted to form an oligomeric α-helical coiled coil

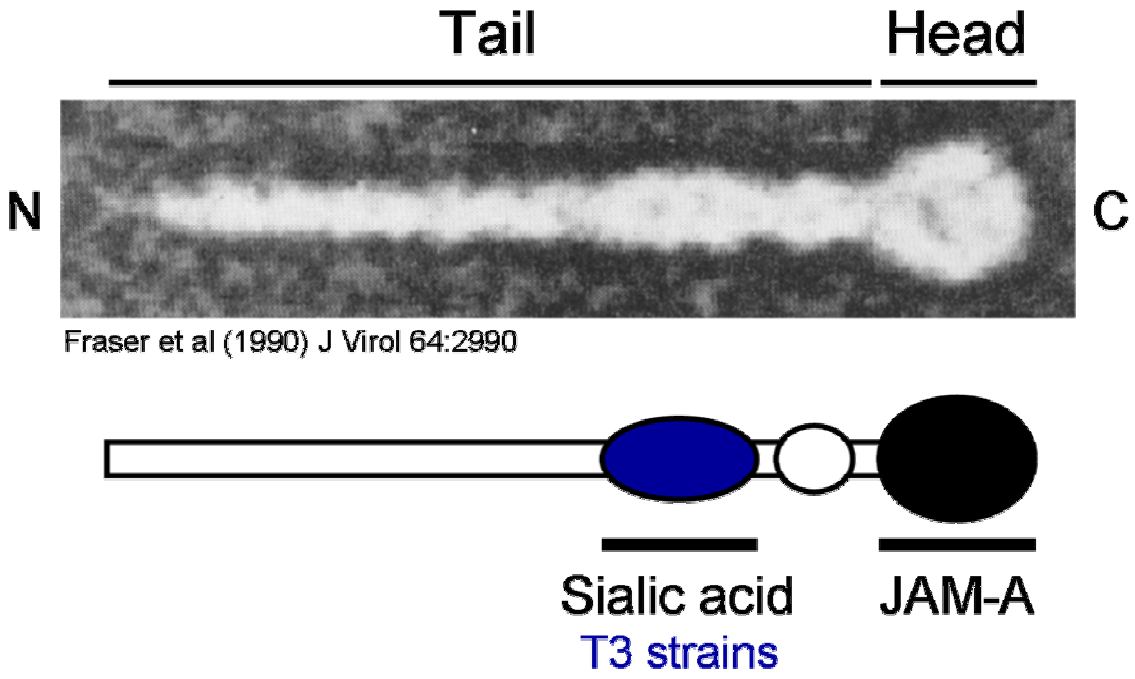

Figure 3. Electron micrograph and model of σ1. The top panel is a composite transmission electron micrographs of σ1 molecules purified from virions. The lower panel is a model of σ1 receptor binding domains for serotype 3 reovirus strains.

structure (13). The actual oligomeric state of σ1 was the subject of some controversy, as dimeric (99, 196), trimeric (100, 152), and tetrameric (14, 64) structures were proposed. More complex sequence analyses and correlation of sequence data with the observed morphology eventually led to a plausible model for the domain architecture of σ1. This model postulated three major structurally distinct regions of σ1, each accounting for about one third of its sequence. The N-terminal third was predicted to form an α-helical coiled coil structure, the second third a fiber-like region composed primarily of β-sheet structure, and the final third a globular head domain (117), While this model served to explain several properties of σ1, a high-resolution structure was required to accurately describe its features and correlate them with functional data.

Structural analyses of σ1 were complicated by the flexible, fiber-like nature of the protein, its poor solubility, and difficulties in producing significant quantities of well-folded and functional protein. Several groups have expressed full-length σ1 protein in bacteria, eukaryotic cells, and *in vitro* using cell lysates (25, 57, 84, 107, 127), and others relied on the use of protein purified from whole virions (115, 196). The small amounts of protein recovered using these approaches were sufficient for biochemical experiments but inadequate for extensive structural studies of σ1. However, a breakthrough came with the development of an internally truncated σ1 construct that lacked a portion of the predicted N-terminal coiled coil while retaining the hydrophobic sequence at the N-terminus and the C-terminal two thirds of the protein (35). This truncated form of σ1 was expressed in insect cells using a baculovirus vector, and substantial amounts of folded and stable truncated σ1 protein were purified. Cleavage of this construct with trypsin resulted in a stable and soluble fragment (residues 246-455) that formed functional oligomers (35).

Structural analysis of the C-terminal σ1 fragment firmly established the oligomeric state of the molecule as a trimer (37). The structure has provided a wealth of information about the architecture of σ1 and potential roles of its structural features in viral attachment (Figure 4). The structure also suggests that σ1 is a dynamic molecule poised to undergo conformational rearrangements, perhaps in response to viral attachment or disassembly. The crystallized protein forms a homotrimer that features a slender tail domain (residues 246-309) and a compact head (residues 310-455). The tail consists of three triple β-spiral repeats, a rare trimerization motif that has so far only been seen in one other protein, the adenovirus fiber (113). The β-spiral is characterized by short, vertically-oriented β-strands that wind around each other and bury a substantial number of hydrophobic residues at the center. The head domain is formed from two Greek keys which assemble into a compact ß-barrel (37).

Reovirus receptors

Early studies examining the capacity of reovirus strains to agglutinate erythrocytes isolated from different species of animals documented a serotype-specific difference in hemagglutination that was genetically mapped using reassortant viruses to the σ1-encoding S1 gene (124, 185). Hemagglutination produced by type 3 reovirus is inhibited by pretreatment of erythrocytes with various proteases or neuraminidase (2), suggesting that sialic acid is the erythrocyte structure bound by type 3 reovirus. Type 3 reovirus binding to some types of cells is also reduced by neuraminidase treatment, indicating that cell-surface sialic acid-containing glycoconjugates contribute to productive type 3 reovirus attachment (68, 136). Both T1L and T3D reoviruses can infect L929 cells, a murine fibroblast cell line commonly used to propagate reovirus. However, only sialic acid-binding type 3 strains can infect murine erythroleukemia (MEL) cells (36, 135). Serial passage of non-sialic-acid-

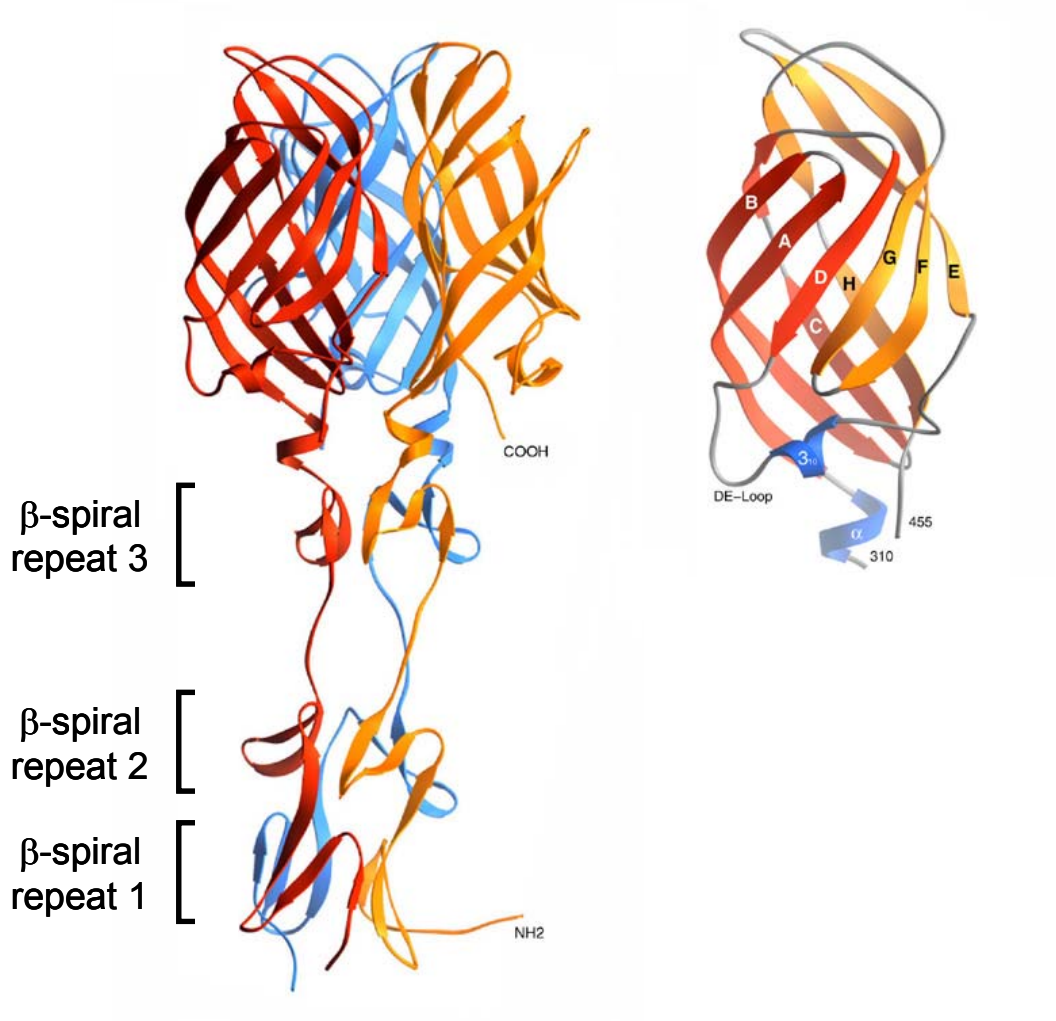

Figure 4. The structure of σ1. (**A**) Ribbon drawing of the σ1 trimer. The three σ1 monomers are shown in red, orange and blue. Each monomer consists of a head domain formed by a compact ß-barrel and a fibrous tail with three ß-spiral repeats. (**B**) Enlarged view of the σ1 head domain. The two Greek key motifs, shown in red and orange, form a compact, cylindrical ß-sheet that contains eight ß-strands (A–H). With the exception of the DE loop, the connections between the ß-strands are very tight.

binding type 3 strains in MEL cells results in selection of viral variants that have acquired the capacity to bind sialic acid (36). The variants have substitutions at only three positions (Asn198, Arg202, and Pro204). In each case, the substituted residues are present in all sialic acid-binding type 3 strains sequenced to date.

Junctional adhesion molecule-A

Many proteins have been proposed to function as reovirus receptors, including the beta-adrenergic receptor (42), epidermal growth factor receptor (155), and a p65/p95 complex (131). However, to date only junctional adhesion molecule-A (JAM-A) has been shown to directly interact with reovirus attachment protein σ1 and confer reovirus infection to nonpermissive cells (10). JAM-A was identified as a reovirus receptor using an expression cloning approach in which a non-sialic acid-binding reovirus strain was employed as an affinity ligand. COS-7 cells were transfected with cDNAs from an NT2 teratoma cell library and screened for the capacity to support reovirus binding. Using this approach, four plasmids were identified, each of which encoded JAM-A. Three lines of evidence support the contention that JAM-A is a receptor for reovirus. First, JAM-A-specific monoclonal antibodies (mAbs) block reovirus binding and infection. Second, transfection of nonpermissive cells with JAM-A-encoding cDNA confers efficient reovirus growth. Third, and most importantly, the σ1 head domain of strain T3D interacts directly with the JAM-A ectodomain, as assessed by surface plasmon resonance (10).

JAM-A was first identified by screening a panel of mAbs raised against endothelial cells in an attempt to characterize proteins localized to endothelial tight junctions (105). The human (h) homolog of JAM-A is a 299 amino acid, type I transmembrane protein that is a member of the immunoglobulin (Ig) superfamily (123) (Figure 5). JAM-A is expressed in

many tissues, with the highest levels being found in the kidney, liver, and lung (188). The JAM-A cytoplasmic tail has a classical type II PDZ binding motif and is phosphorylated by Protein kinase C (PKC) upon platelet activation (59, 122). Several adaptor proteins have been identified as possible binding partners of the JAM-A cytoplasmic tail, including Zonula occluden-1 (ZO-1), ALL-1 fusion partner from gene 6 (AF-6), multiple PDZ domain containing protein-1 (MUPP-1), and CASK (59, 77, 105). JAM-A is proposed to form homodimers located at tight junctions of polarized cells and may play a role in leukocyte migration and tight junction formation through homotypic interactions (18, 106).

JAM-A belongs to a group of related proteins termed the junctional adhesion molecule family. Two JAM-A homologs, JAM-B and JAM-C, share approximately 36% amino acid identity with JAM-A and have overlapping but also distinct tissue distribution in comparison to JAM-A. While all JAM family members are expressed by endothelial cells, JAM-B is predominantly expressed in the heart, and JAM-C is mainly expressed in the brain and kidney (4, 44). Unlike JAM-B, which mediates homotypic interactions, JAM-C forms heterodimers with JAM-B (3). Each of the JAM family members has been proposed to be involved in leukocyte transmigration, but only JAM-A serves as a reovirus receptor (29, 129).

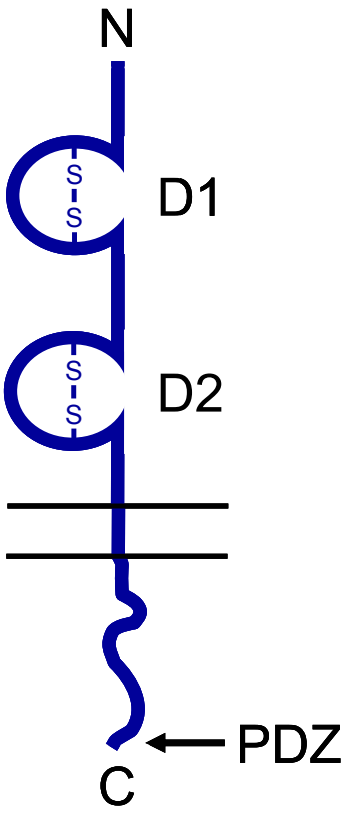

Figure 5. A structural model for JAM-A. JAM-A contains two immunoglobulin domains. The D1 domain is membrane distal and is responsible for homodimerization of the protein, the D2 domain is membrane proximal. The extracellular portion of the protein is followed by a putative membrane spanning domain and a cytoplasmic tail which is 38 aa long. The cytoplasmic tail contains a classical type II PDZ domain-binding motif.

Significance of the research

At the onset of this research, key unanswered questions included: Is JAM-A a serotype-independent reovirus receptor? What sequences in σ1 and JAM-A are required for σ1-JAM-A biophysical interactions? What are the physiological consequences of reovirus infection of polarized cells where JAM-A is expressed in tight junctions? Answers to these questions will contribute to an understanding of the molecular basis of reovirus-cell attachment and pathogenesis.

The mammalian reoviruses provide an attractive experimental system to study the role of virus-receptor interactions in the pathogenesis of viral infections, especially those involving the nervous system. The reovirus attachment protein, σ1, is the primary determinant of viral growth in the intestine, spread from the intestine to the central nervous system (CNS), and tropism for distinct types of neural tissues. Because σ1 mediates multiple steps in reovirus-host interaction, it is ideally suited for studies of mechanisms by which viral attachment determines the outcome of CNS infections. Studies of molecular determinants of reovirus receptor engagement will generate new knowledge about fundamental mechanisms used by viral attachment proteins to interact with cellular receptors to mediate viral tropism and organ-specific disease.

CHAPTER II

JUNCTIONAL ADHESION MOLECULE-A SERVES AS A RECEPTOR FOR PROTOTYPE AND FIELD-ISOLATE STRAINS OF MAMMALIAN REOVIRUS

Introduction

There are at least three serotypes of reovirus, which can be differentiated by the capacity of anti-reovirus antisera to neutralize viral infectivity and inhibit hemagglutination (134, 137). Each of the reovirus serotypes is represented by a prototype strain: type 1 Lang/53 (T1L/53), type 2 Jones/55 (T2J/55), and type 3 Dearing/55 which differ mainly in σ1 sequence (T3D/55) (56, 117).

Reoviruses appear to infect most mammalian species, but disease is restricted to the very young (reviewed in (163)). Reovirus infections of newborn mice have been used as the preferred experimental system for studies of reovirus pathogenesis. Sequence polymorphisms in reovirus attachment protein σ1 play an important role in determining sites for reovirus infection in the infected host (11, 92, 183, 184).

There are two distinct receptor-binding regions in σ1. A region in the fibrous tail domain of type 3 σ1 binds to α-linked sialic acid (9, 35, 36). A distinct region in the type 1 σ1 tail domain also binds to cell-surface carbohydrate (35), and recent evidence suggests that sialic acid may be involved in the binding of T1L/53 to intestinal cells (80). A second receptor-binding site is located in the head domain of both type 1 and type 3 σ1 proteins (10, 116).

An expression-cloning approach was used to identify junctional adhesion molecule-A (JAM-A) as a receptor for prototype strains T1L/53 and T3D/55 (10). JAM-A is a 35 kDa, type I transmembrane protein that is a member of the immunoglobulin superfamily (102,

106). JAM-A contains two immunoglobulin-like domains, a single transmembrane region, and a short cytoplasmic tail. JAM-A is expressed in a variety of tissues including epithelial and endothelial barriers (102, 106, 123), where it is thought to regulate tight-junction permeability and mediate leukocyte trafficking (48, 102, 106, 123).

The prototype reovirus strains type 1 Lang/53 (T1L/53) and type 3 Dearing/55 (T3D/55) JAM-A as a receptor (10). The C-terminal half of the T3D/55 σ1 protein interacts directly with JAM-A, but the determinants of receptor-binding specificity have not been identified (10). The goal of this study was to determine whether JAM-A also mediates the attachment of the prototype reovirus strain type 2 Jones/55 (T2J/55) and a panel of field-isolate strains representing each of the three serotypes. The results indicate that JAM-A, but not the related JAM family members JAM-B or JAM-C, is a receptor for prototype and field-isolate strains of the three reovirus serotypes. Analysis of conserved and variable sequences in the σ1 head, together with existing structural information for σ1 and JAM-A, suggests an especially high tolerance for surface variation while maintaining specificity for receptor utilization. These findings enhance an understanding of the molecular basis of reovirus binding to JAM-A and provide clues about mechanisms of reovirus attachment.

Results

JAM-A serves as a receptor for prototype strains of the three reovirus serotypes

Our previous work indicates that JAM-A serves as a receptor for prototype reovirus strains T1L/53 and T3D/55 (10). To confirm these observations, and to test whether JAM-A is used as a receptor by T2J/55, HeLa cells were treated with PBS, hCAR-specific antiserum as a control, or hJAM-A-specific mAb J10.4 prior to viral adsorption. Infected cells were

quantified by indirect immunofluorescence using an anti-reovirus serum (Figure 6). Treatment of cells with CAR-specific antiserum had no effect on the capacity of these prototype strains to infect HeLa cells. In sharp contrast, treatment with mAb J10.4 resulted in a concentration-dependent inhibition of infection for all three strains. The minimum concentration of mAb J10.4 required to reduce infectivity of these strains by 50% was between 0.1 and 1.0 μg per ml (Figure 6). Infectivity of all three strains was reduced by approximately 90% following treatment of cells with 100 μg per ml mAb J10.4.

JAM-B and JAM-C do not serve as receptors for prototype strains of reovirus

JAM-A is the only JAM family member tested to date that functions as a receptor for T1L/53 (129). To determine whether JAM family members in addition to JAM-A serve as reovirus receptors for other reovirus prototype strains, CHO cells, which are poorly permissive for reovirus infection (63), were transfected with cDNAs encoding hJAM-A, hJAM-B, or hJAM-C. Cells also were transfected with hCAR as a negative control. Following confirmation of cell-surface expression of the receptor constructs (Figure 7), transfected cells were tested for the capacity to support reovirus infection. Infected cells were quantified by indirect immunofluorescence using an anti-reovirus serum (Figure 7). Only CHO cells transfected with hJAM-A were capable of supporting efficient infection of each of the three prototype reovirus strains, whereas cells transfected with hJAM-B and hJAM-C did not support infection of any of these strains in excess of those transfected with hCAR (Figure 7). Therefore, JAM family member JAM-A, but not JAM-B or JAM-C, functions as a receptor for prototype strains of reovirus.

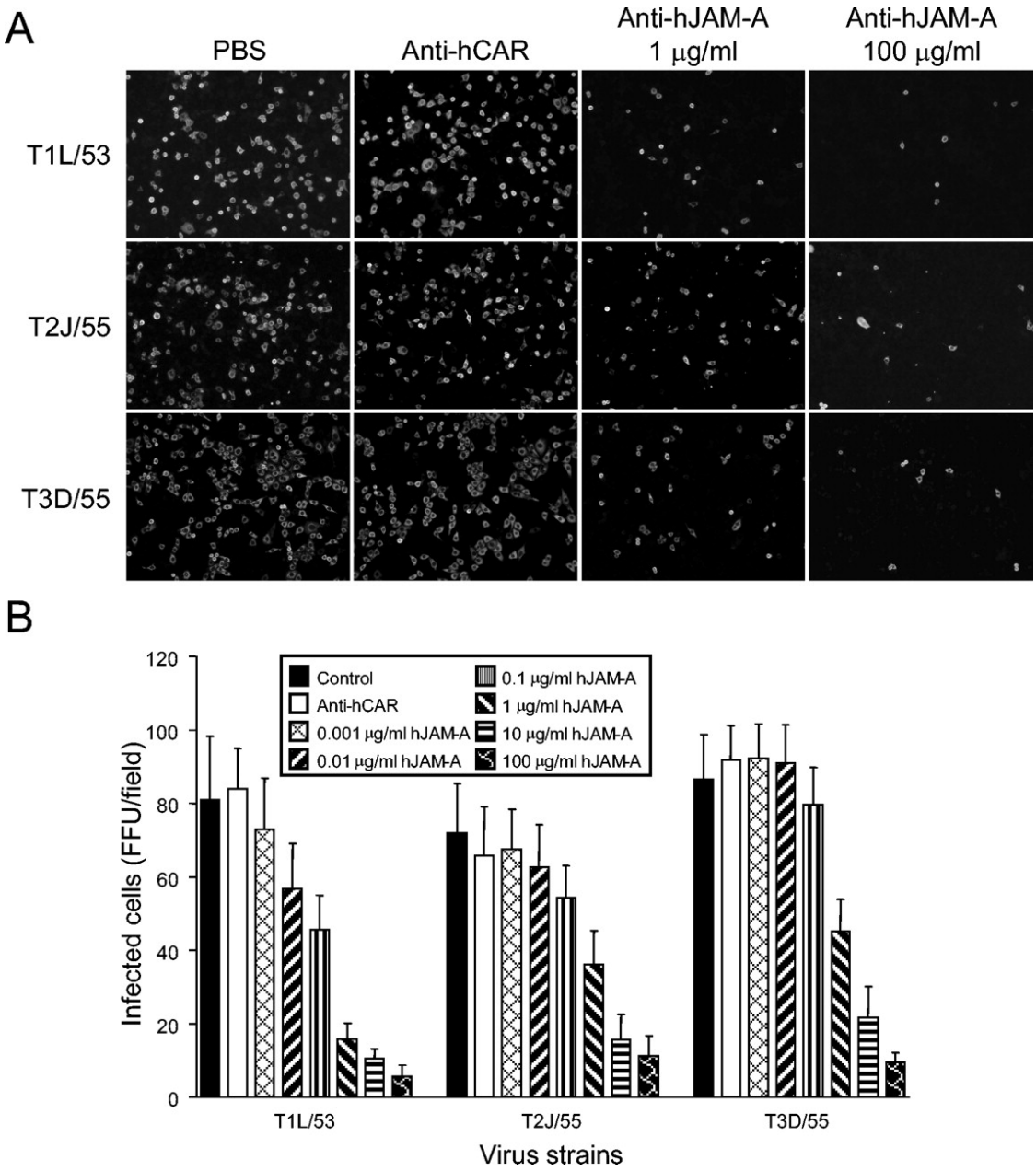

Figure 6. JAM-A blockade reduces infection of prototype reovirus strains. HeLa cells at equivalent degrees of confluence as a control, JAM-A-specific mAb J10.4 prior to adsorption with T1L/53, T2J/55, or T3D/55 at an MOI of 0.1 FFU per cell. After incubation for 20 h, the cells were fixed and newly synthesized viral proteins were detected by indirect immunofluorescence. (A) Representative fields of view. (B) Reovirus-infected cells were quantified by counting fluorescent cells in a minimum of three random fields of view per well for three wells at a magnification of x20. The results are presented as the mean FFU per field. Error bars indicate standard deviations.

JAM-A serves as a receptor for field-isolate strains of reovirus

Strains of each of the three reovirus serotypes have been isolated from many mammalian hosts over a period in excess of 50 years (73, 85). A type 3 reovirus strain isolated from the cerebrospinal fluid of a child with meningitis is capable of using JAM-A as a receptor (164). However, the receptor-binding properties of other field-isolate strains have not been reported. To determine whether JAM-A is used as a receptor by other field-isolate strains of reovirus, CHO cells were transfected with hJAM-A, hJAM-B, or hJAM-C and tested for the capacity to support reovirus infection. Ten strains, encompassing four type 1, two type 2, and four type 3 viruses (Table 1), were used in these experiments. In parallel with findings made using prototype reovirus strains, each of the field-isolate strains tested was capable of utilizing hJAM-A but not hJAM-B or hJAM-C as a receptor (Figure 8).

Analysis of deduced σ1 amino acid sequences of JAM-A-binding reovirus strains

To gain insight into σ1 residues that mediate interactions between reovirus and JAM-A, we analyzed the amino acid sequences of the σ1 proteins of the three prototype and ten field-isolate strains chosen for study. For these experiments, we determined the σ1-encoding S1 gene sequences of T1C23/59, T1C50/60, T1Neth/84, T1Neth/85, T2Neth/73, and T2Neth/84, and compared these sequences to those reported previously (Table 1). RT-PCR primers complementary to the nontranslated regions of the type 1 and type 2 S1 genes were designed to facilitate amplification of entire S1 genes from infected L-cell lysates.

To define evolutionary relationships of the S1 gene sequences determined in this study with those of the other reovirus strains sequenced to date, we constructed phylogenetic trees by using variation in the σ1-encoding S1 gene nucleotide sequences and the maximum parsimony method as applied in the program PAUP (Figure 9). The

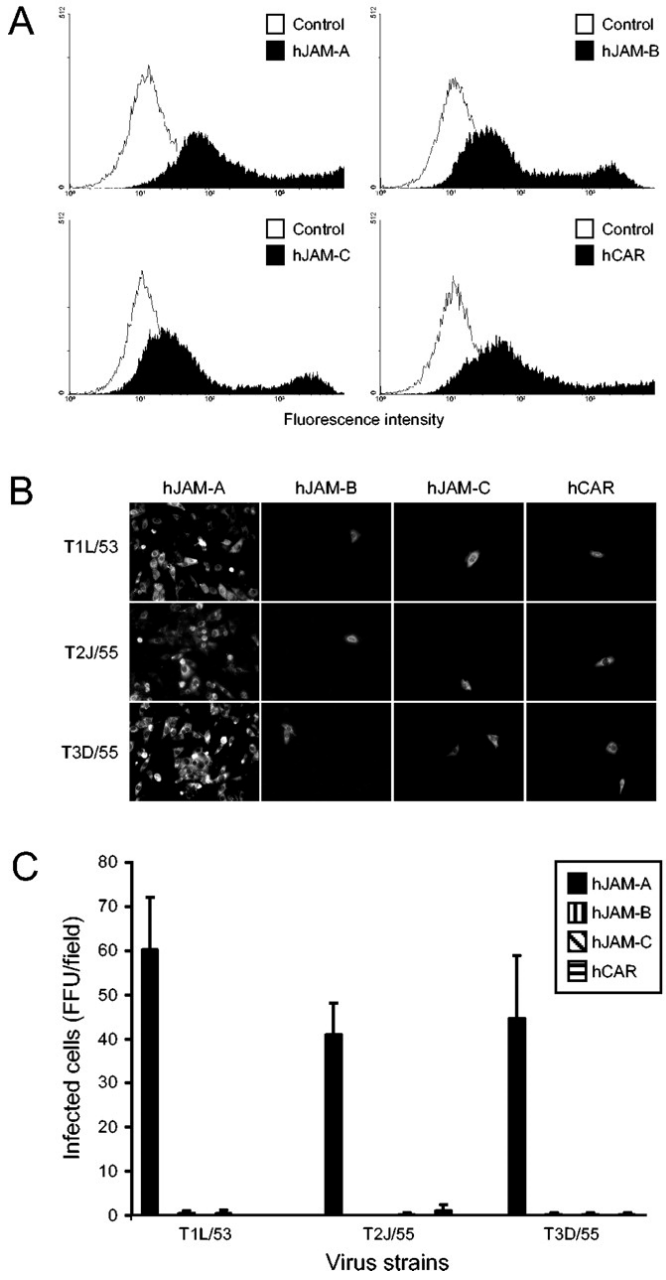

Figure 7. CHO cells transfected with hJAM-A support growth of prototype reovirus strains. (A) CHO cells were transiently transfected with a plasmid encoding hCAR, hJAM-A, hJAM-B, or hJAM-C. Following incubation for 24 h to permit receptor expression, cells were incubated with receptor-specific MAbs, and the cell surface expression of receptor constructs was assessed by flow cytometry. (B) Transfected CHO cells were adsorbed with T1L/53, T2J/55, or T3D/55 at an MOI of 0.1 FFU per cell. Reovirus proteins were detected by indirect immunofluorescence at 20 h postinfection. Representative fields of view are shown. Magnification, x20. (C) Reovirus-infected cells were quantified by counting fluorescent cells in five random fields of view per well for three wells. The results are presented as the mean FFU per field. Error bars indicate standard deviations.

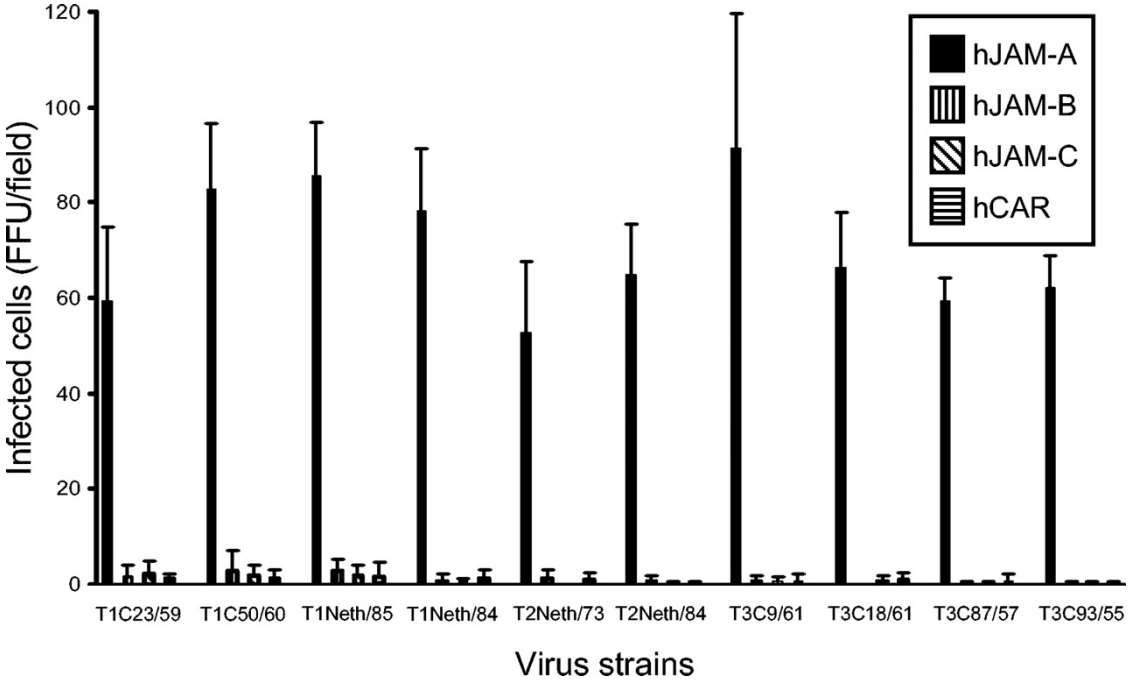

Figure 8. Expression of JAM-A confers infectivity on field-isolate reovirus strains. CHO cells were transiently transfected with a plasmid encoding hCAR, hJAM-A, hJAM-B, or hJAM-C. Following incubation for 24 h to permit receptor expression, the cells were adsorbed with the indicated field-isolate strains at an MOI of 1 FFU per cell. Reovirus proteins were detected by indirect immunofluorescence at 20 h postinfection and quantified by counting of the fluorescent cells in three random fields of view per well for three wells. The results are presented as the mean FFU per field. Error bars indicate standard deviations.

most noteworthy feature of the S1 phylogenetic tree is that the strains cluster into distinct lineages based on serotype. A phylogenetic tree generated by using the same data set and the neighbor joining algorithm of the phylogenetic analysis program, MacVector (MacVector 2001, version 7.1.1), has a topology identical to the tree generated by PAUP (data not shown). Therefore, phylogenetic analysis indicates that the S1 genes of reovirus strains cluster tightly into three lineages defined by serotype. Concordantly, changes in the deduced amino acid sequences of σ1 protein within a given serotype are confined to a small number of residues. As each of the strains investigated here is capable of using JAM-A as a receptor, the location of these changes provides clues about areas that can vary in surface structure without impeding the capacity to engage this molecule. Thus, these changes define areas that are unlikely to interact with JAM-A.

Sequence variability within type 3 σ1 protein

Structural information is available for the T3D/55 σ1 protein (37). We therefore carried out a structure-based comparison of the deduced amino acid sequences of σ1 proteins of type 3 field-isolate strains with that of prototype T3D/55 to define regions of conserved and variable sequence within a serotype (Figure 10). Substantial variability is seen between residues 240 and 250, a region that lies just N-terminal to the first β-spiral repeat in the crystallized fragment and is disordered in the crystal structure. The σ1 fragment was obtained by trypsin cleavage of a longer construct after residue Arg245 (37). The fact that trypsin cleaves σ1 at only this position suggests that Arg245 lies in an exposed loop that likely possesses some flexibility. Exposed areas in the second and third β-spiral repeats of the crystallized fragment also contain a number of substitutions. Because these areas are

TABLE 1. Strains used for studies of JAM-A utilization by reoviruses

Virus strain[a]	Abbreviation	GenBank accession no.	Reference
T1/Human/Ohio/Lang/1953	T1L/53	M35963	45, 50
T1/Bovine/Maryland/clone23/1959	T1C23/59	AY862134	31
T1/Bovine/Maryland/clone50/1960	T1C50/60	AY862133	31
T1/Human/Netherlands/1/1984	T1Neth/84	AY862136	29
T1/Human/Netherlands/1/1985	T1Neth/85	AY862135	29
T2/Human/Ohio/Jones/1955	T2J/55	M35964	46, 50
T2/Human/Netherlands/1/1973	T2Neth/73	AY862137	29
T2/Human/Netherlands/1/1984	T2Neth/84	AY862138	29
T3/Human/Ohio/Dearing/1955	T3D/55	NC_004277	46, 50
T3/Human/Wash.D.C./clone93/1955	T3C93/55	L37675	31
T3/Human/Wash.D.C./clone87/1957[b]	T3C87/57	L37677	48
T3/Bovine/Maryland/clone18/1961	T3C18/61	L37684	31
T3/Murine/France/clone9/1961	T3C9/61	L37676	31

[a] Strain nomenclature is as follows: serotype/species of origin/place of origin/strain designation/year of isolation.

[b] This strain has also been designated T3/Human/Wash.D.C./Abney/1957.

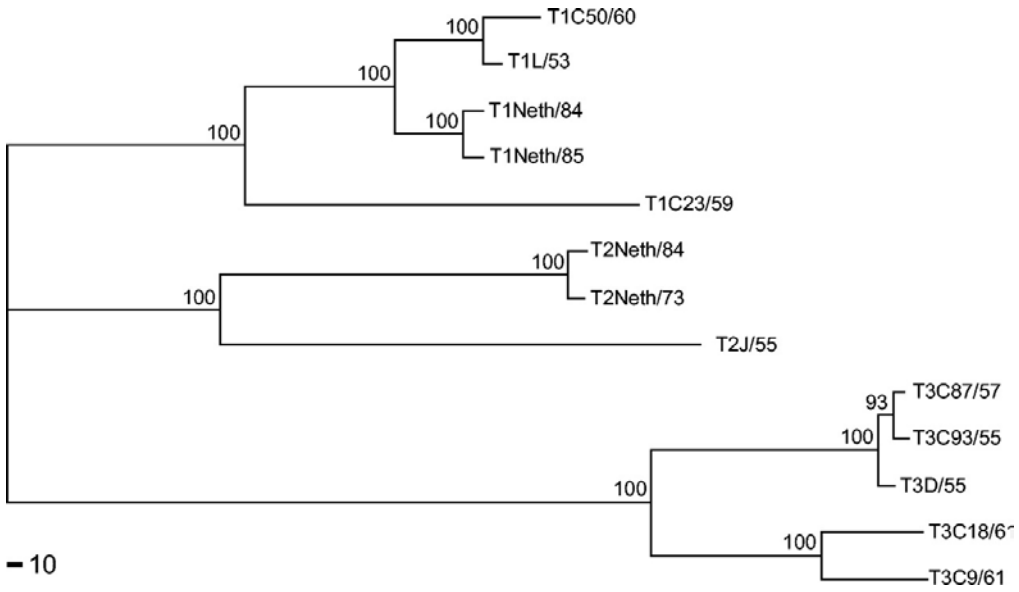

Figure 9. Phylogenetic relationships among S1 gene nucleotide sequences of 13 reovirus strains. A phylogenetic tree for the σ1-encoding S1 gene sequences of the strains shown in Table 1 was constructed by using the maximum parsimony method as applied in the program PAUP. The tree is rooted at its midpoint. Bootstrap values of >50% (indicated as a percentage of 1,000 repetitions) for major branches are shown at the nodes. Bar, distance resulting from 10 nucleotide changes.

variable, they are unlikely to significantly contribute to JAM-A binding.

Most of the remaining substitutions are located at the top of the σ1 trimer, forming a highly variable "plateau" that is also unlikely to bind to JAM-A. Some of the observed variations on the plateau are anticipated to alter the structure of the molecule. For example, the replacement of Ser435 with Met in T3D9/61 and T3D18/61 is likely to cause significant structural changes as Ser435 is partially buried in the T3D/55 structure (37). Because they are exposed at the protein surface, the polymorphisms seen on the plateau may allow viral escape from antibody recognition. In contrast, the lower portion of the head domain is highly invariant, suggesting that the base of the σ1 head is primarily responsible for interactions with JAM-A.

Sequence variability within σ1 protein of the three reovirus serotypes

Alignment of the deduced σ1 amino acid sequences of all of the strains chosen for study shows that only 36 of the 210 residues in the crystallized fragment of T3D/55 σ1 (37) are conserved (Figure 11). The variability among the serotypes is substantially greater than the variability within each serotype. Mapping of the conserved residues onto the crystal structure of T3D/55 σ1 shows that many of these residues are buried, especially those located at the base of the σ1 head trimer interface (Figure 12). A large fraction of the remaining conserved residues cluster in a single, solvent-exposed region at the lower edge of the β-barrel. Again, the regions that are most variable within type 3 σ1 (the β-spiral region and the "top" of the extended, contiguous area of conserved residues is located at the base of the head domain, and additional, smaller areas of conservation are found along the side of this domain. Because these regions are conserved in the JAM-A-binding strains investigated here, they

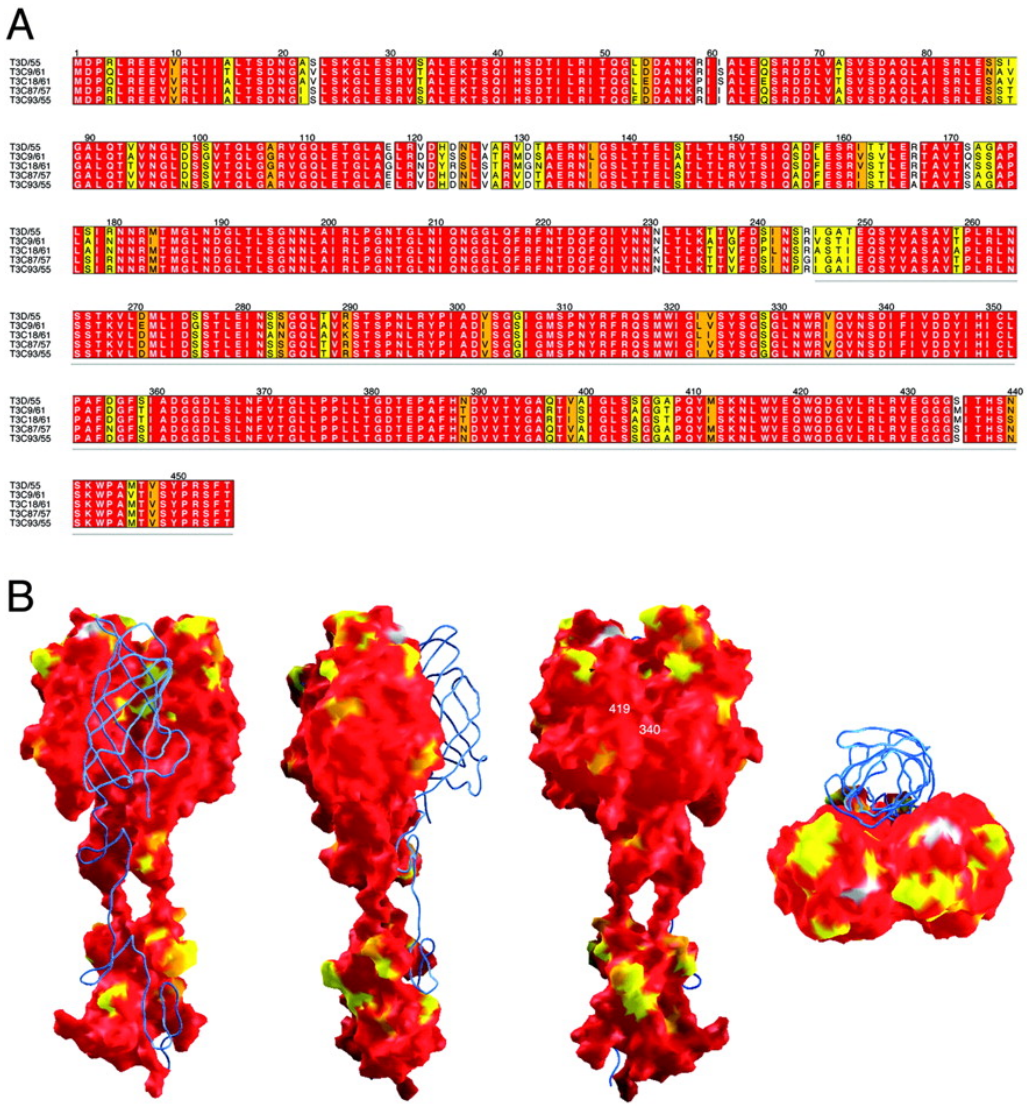

Figure 10. Sequence conservation and structural variability within the type 3 σ1 protein. (A) Alignment of deduced amino acid sequences of the σ1 proteins of prototype strain T3D/55 and four type 3 field-isolate strains. The alignment was generated by using the program ALSCRIPT, with default conservation parameters applied according to the following color scheme: red, identical residues; orange, conserved residues at 80% conservation; yellow, conserved residues at 60% conservation; white, nonconserved residues. The 80% conservation threshold identifies closely related amino acids (e.g., Ile and Leu), whereas the 60% threshold identifies more distantly related amino acids (e.g., Ser and Ala, both of which have small side chains). The amino acid positions in the alignment are numbered above the sequences. The gray line indicates residues present in the crystallized fragment of T3D/55 σ1. (B) Structure of the σ1 trimer, with residues colored according to the same color code as that used for panel A. Four different views are shown. For each of the views, two σ1 monomers are shown in surface representation, and the other is depicted as a blue ribbon tracing corresponding to the α-carbon backbone. The first three views each differ by 90° along a vertical axis; the fourth view shows the molecule in the third view after rotation by 90° along a horizontal axis. The positions of residues 340 and 419 are marked in the third panel from the left.

mark potential contact points for this receptor.

The large conserved area at the base of the head domain is formed primarily by a stretch of residues (Asn369 to Glu384 in T3D/55 σ1) within a 3_{10} helix and long loop between β-strands D and E (37) (Figure 12). This region also includes Trp421 at the end of β-strand F. The conserved region is fairly hydrophobic, with the side chains of Val371, Leu379, and Trp421 accounting for a large portion of the surface area predicted to be involved in JAM-A binding. A second, smaller cluster of conserved residues (Leu331, Trp333, Ile360, and His438 in T3D/55 σ1) lies above this putative JAM-A-binding surface, near the top of the trimer (Figure 12). While most of the side chains of these residues are buried, structural features of this cluster may contribute to receptor binding. The remaining surface area of the σ1 trimer, especially near the top of the head and the head-to-head contacts, is almost entirely devoid of conserved residues.

A neutralization-resistant variant of reovirus T3D/55 uses JAM-A as a receptor

Variants of T3D/55 selected for resistance to neutralization by mAb 9BG5 ((149)) have mutations at Asp340 or Glu419 in the σ1 head (15) (Figure 12). These variants have alterations in central nervous system (CNS) tropism following infection of newborn mice (148). The single mutation in variant K σ1, Glu419 to Lys (15), segregates genetically with the altered growth and tropism of this virus in the murine CNS (92). To determine whether a with increasing concentrations of JAM-A-specific mAb J10.4 resulted in a dose-dependent inhibition of viral infection, while CAR-specific antiserum had no effect on viral infectivity. At the maximal concentration of mAb J10.4 used (100 μg per ml), infectivity was nearly abolished, demonstrating that variant K is capable of using JAM-A as a receptor (Figure 13).

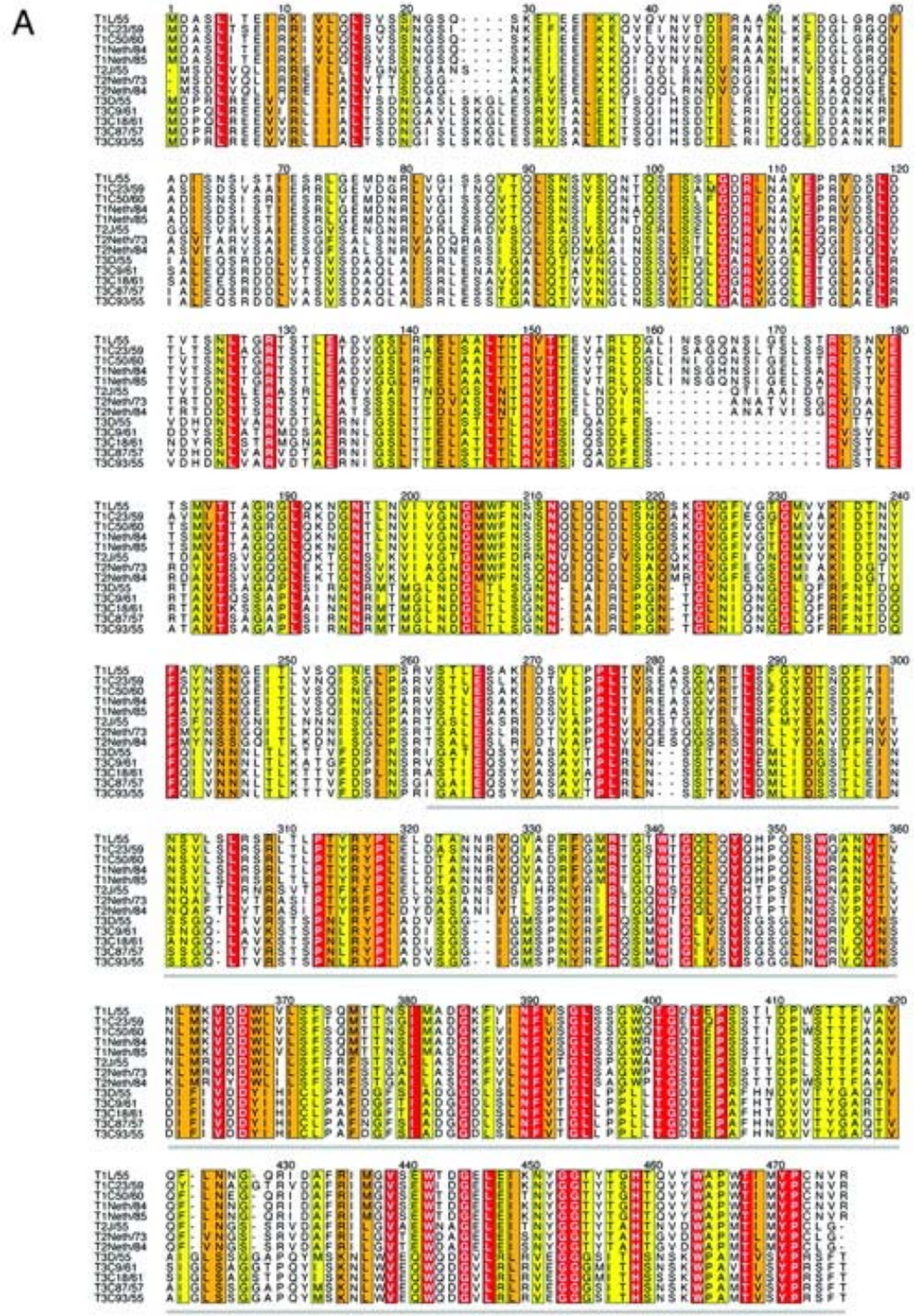

Figure 11. Sequence conservation within the σ1 proteins of the three reovirus serotypes. Alignment of deduced amino acid sequences of the σ1 proteins of 3 prototype and 10 field-isolate reovirus strains. The alignment was generated by using ALSCRIPT and the scheme described in the legend to Figure 10. Gaps in the aligned sequences are indicated by dots.

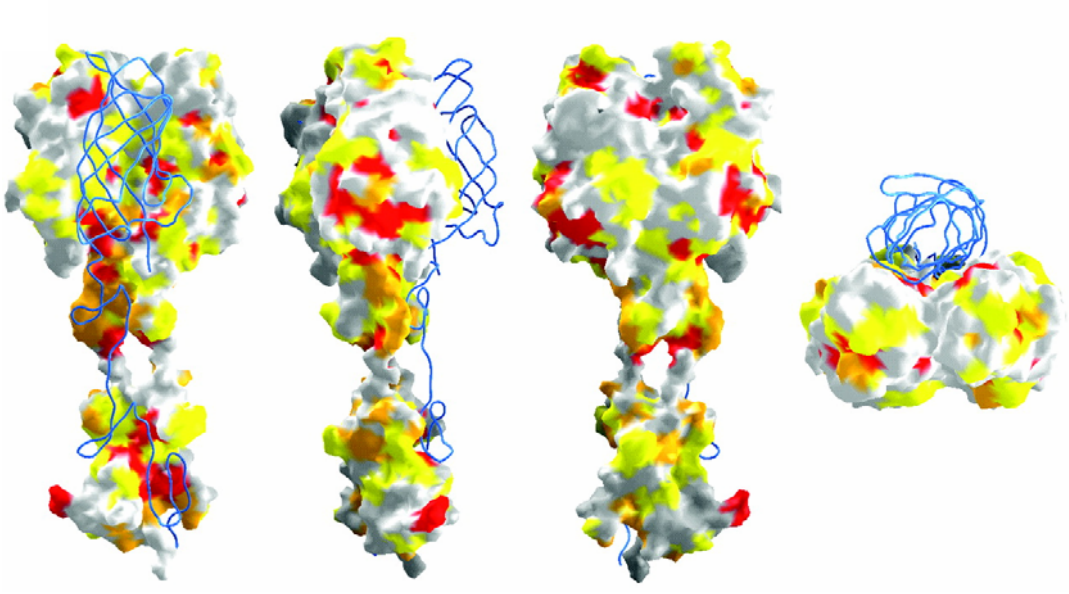

Figure 12. Structural variability within the σ1 proteins of the three reovirus serotypes. Mapping of residues onto the σ1 structure, using the same color code as that depicted in Figure 10. The four views correspond to those in Figure 10.

Thus, the mechanism of altered pathogenicity of variant K appears to be independent of JAM-A utilization.

Discussion

Examination of receptor usage by diverse virus families, including arenavirus (30, 147), adenovirus (23, 67, 140, 192), and measles virus (55, 103, 158), has led to the discovery that receptor usage by some viruses varies based on viral clade, serotype, or adaptation to passage in cell culture. We undertook this study to determine whether JAM-A is used as a receptor for both prototype and field-isolate strains of reovirus. The results demonstrate that each of the prototype and field-isolate reovirus strains tested, regardless of serotype, species, or geographical region of isolation, is capable of utilizing JAM-A as receptor.

Prior to this work, sequence information for the S1 gene segment of type 1 and type 2 reovirus strains was limited to prototype strains T1L/53 and T2J/55. In this study, we determined the S1 sequences of four type 1 and two type 2 field-isolate strains. Phylogenetic analysis of the deduced σ1-encoding S1 gene sequences revealed that these reovirus field-isolate strains associate into discrete lineages defined by serotype. Given that all reovirus strains tested to date are capable of using JAM-A as a receptor, it seems plausible that σ1 interacts with JAM-A through residues that are conserved among the serotypes, including the newly characterized type 1 and type 2 field-isolate strains. The observation that JAM-A is used as a receptor by all reovirus strains tested was unexpected since the σ1 protein is highly divergent among the three serotypes. For example, sequence analysis of the prototype strains reveals that the σ1 head domain of T1L/53 and T2J/55 share 50% identical residues, while that of T1L/53 and T3D/55 share only 27%.

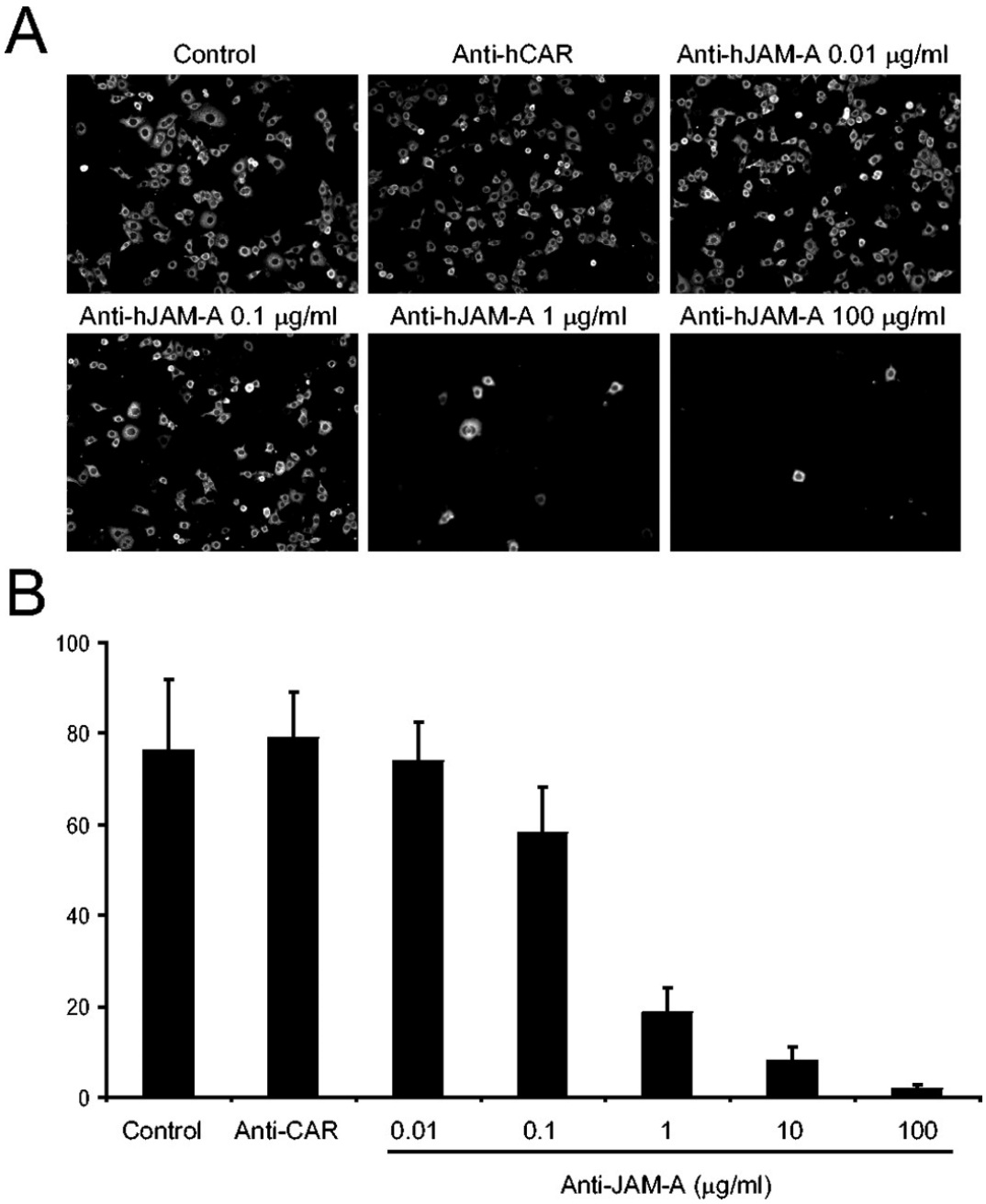

Figure 13. JAM-A is used as a receptor for a neutralization-resistant variant of reovirus T3D/55. HeLa cells were pretreated with PBS, an hCAR-specific antiserum, or the hJAM-A-specific mAb J10.4 prior to adsorption with variant K at an MOI of 1 FFU per cell. Reovirus proteins were detected by indirect immunofluorescence at 20 h postinfection. (A) Representative fields of view. (B) Reovirus-infected cells were quantified by counting fluorescent cells in three random fields of view per well for three wells. The results are presented as the mean FFU per field. Error bars indicate standard deviations.

Substantial evidence has accumulated to suggest that the σ1 head domain binds to cellular receptors. Truncated forms of σ1 containing only the head domain are capable of specific cell interactions (57, 58). Concordantly, proteolysis of T3D/55 virions leads to release of a C-terminal receptor-binding fragment of σ1 (residues 246 to 455) (34) and a resultant loss in infectivity (116). This fragment of σ1 is capable of binding to JAM-A on a biosensor surface with nanomolar affinity (10). Preliminary findings from our laboratory indicate that an even smaller fragment of T3D/55 σ1, corresponding to the head domain and a single β-spiral repeat, is capable of binding to JAM-A (Guglielmi, K. M., Schelling, P., Stehle, T., and Dermody T. S., unpublished observations). Thus, the σ1 head promotes interactions with JAM-A that are distinct from interactions with sialic acid mediated by the σ1 tail.

While most of the residues conserved in the σ1 proteins of the strains tested are scattered throughout the molecule, examination of the σ1 surface reveals a single, extended patch of conserved residues at the lower edge of the σ1 head. We think that this region may form part of a JAM-A-binding surface. This conserved region is formed mostly by residues in the vicinity of a long loop connecting β-strands D and E of the eight-stranded β-barrel that forms the σ1 head. Although it is easily accessible to ligand, this site is somewhat recessed into the protein surface and surrounded by protruding, non-conserved residues on all three edges of the trimer. Only residues from a single monomer contribute to the putative JAM-A-binding region and its borders, and the regions are not involved in σ1 intersubunit contacts. Thus, the location of conserved residues within the trimer suggests that each σ1 monomer can independently bind to a JAM-A molecule.

Although it may serve as the primary contact point for the receptor, the putative JAM-A binding site in σ1 is relatively small, measuring about 15Å in length and 10Å in width. Most other interactions between viral ligands and proteinaceous receptors cover somewhat larger areas. It is therefore likely that additional regions of σ1 contribute to interactions with JAM-A. We note that the putative JAM-A binding site lies at the lower edge of a large, concave surface formed by β-strands B, A, D and G of σ1. Residues on this surface, which almost entirely covers one side of the β-barrel, would easily be accessible to a receptor and do not participate in inter-subunit contacts. The top of the σ1 head is formed by three prominent protrusions, one from each β-barrel. These protrusions are entirely devoid of conserved residues among the serotypes and also exhibit significant sequence drift within type 3 σ1. It is therefore highly unlikely that the top of the σ1 head participates in receptor binding, again implicating regions on the side of each β-barrel as the most likely areas of contact with JAM-A.

Neutralization-resistant variants of reovirus T3D/55 selected using σ1-specific mAb 9BG5 contain mutations in the σ1 head that segregate genetically with alterations in neural tropism (15, 92, 148, 149). Since reovirus tropism in the murine CNS is determined at least in part by σ1-receptor interactions (53, 157), it is possible that the antibody-selected mutations in the σ1 head alter receptor binding. However, we found that variant K, which has a Glu to Lys mutation at amino acid 419, uses JAM-A as a receptor. This observation suggests that the mutation in variant K σ1 alters interactions of this strain with cell-surface receptors other than JAM-A or influences a post-attachment step in reovirus replication. It is noteworthy that amino acid 419 is adjacent to the σ1 head trimer interface in the vicinity of amino acid 340 (37) (Figure 10), which also is targeted for mutation in neutralization-

resistant variants of T3D/55 (15). It is possible that mutations at these sites alter σ1 subunit interactions required for viral assembly or disassembly.

Reovirus serotypes exhibit striking differences in tropism and pathogenesis in the murine CNS. Type 1 reovirus spreads to the CNS hematogenously and infects ependymal cells (167, 184), resulting in subacute hydrocephalus (183). In contrast, type 3 reovirus spreads to the CNS by neural routes and infects neurons (114, 167, 184), causing lethal encephalitis (156, 183). Analysis of reassortant viruses containing gene segments derived from T1L/53 and T3D/55 demonstrated that the pathway of viral spread in the host (167) and tropism for neural tissues (53, 184) segregate with the σ1-encoding S1 gene.

These findings suggest that σ1 determines the CNS cell types that serve as targets for reovirus infection, presumably by its capacity to bind to receptors expressed by specific CNS cells. Since all strains of reovirus tested are capable of utilizing JAM-A as a receptor, engagement of JAM-A alone does not explain the differences in tropism and virulence displayed by the different reovirus serotypes in the murine CNS. It is possible that JAM-A serves as a serotype-independent reovirus receptor at some sites within the host and that other receptors, perhaps carbohydrate in nature, confer serotype-dependent tropism. In support of a role for cell-surface carbohydrate in reovirus disease, the capacity to bind sialic acid enhances the spread of type 3 reovirus within the host and targets the virus to bile duct epithelial cells, leading to obstructive jaundice (9). It is also possible that serotype-dependent differences in pathogenesis are influence by one or more post-binding events.

The role of JAM-A utilization in reovirus infection in vivo is not known. JAM-A is expressed on many cell types, including intestinal epithelium, bile duct epithelium, lung epithelium, leukocytes, and CNS endothelial cells (106), which serve as sites for reovirus infection in mice (175). It will be interesting to determine whether JAM-A functions as a

reovirus receptor at these sites in infected animals. Mice with targeted disruption of the JAM-A gene are viable and fertile (32). These mice exhibit accelerated migration of dendritic cells to lymph nodes, which is associated with enhanced contact hypersensitivity (32). No other developmental or immune abnormalities have been noted. Studies of reovirus infections using JAM-A-deficient animals should clarify the function of JAM-A in reovirus pathogenesis and disease.

CHAPTER III

CRYSTAL STRUCTURE OF HUMAN JUNCTIONAL ADHESION MOLECULE-A: IMPLICATIONS FOR REOVIRUS BINDING

Introduction

Immunoglobulin (Ig) and Ig-like proteins are extensively studied because of their importance in the immune system, intercellular interactions, and interactions with microbial pathogens (145). Proteins within the immunoglobulin superfamily are highly modular and consist of Ig-like domains. Ig-like domains can be classified as being one of the following sets; variable-like domains, the V set, the constant-like domains, the C1 and C2 sets, and the intermediate set, the I set (78). JAM-A is a member of the Ig superfamily with two extracellular Ig-like domains, a single transmembrane region, and a short cytosolic tail.

The crystal structure of the extracellular region of murine JAM-A (mJAM-A) revealed a dimer stabilized by interactions involving the membrane-distal Ig-like domain (95). The contacts that facilitate JAM-A dimerization are interesting in that they occur via the GFCC' face of the membrane distal (D1) Ig-like domain (36, 126). The only other molecules demonstrated to form homodimers using similar interdimer contacts are the human coxsackievirus and adenovirus receptor (hCAR) and CD2 (24, 121). The structure of hCAR in complex with the adenovirus fiber knob revealed that fiber engages the D1 domain of hCAR using residues involved in hCAR homodimer formation and that knob mimics the hCAR-hCAR interaction (24, 64). Biophysical evidence suggests that fiber-hCAR interactions are thermodynamically favored over hCAR-hCAR interactions,

providing support for a model in which residues in the hCAR dimer interface preferentially bind fiber over hCAR (28). The structural similarities between the reovirus and adenovirus attachment proteins and between their cognate receptors, paired with the absolute conservation of residues in mJAM-A and hJAM-A that mediate homodimer formation, suggest that reovirus engages the D1 domain of hJAM-A and that residues involved in hJAM-A dimerization are important for reovirus attachment (36).

The crystal structure of a JAM-A-binding fragment of a σ1 revealed numerous structural and functional similarities to the adenovirus attachment protein, fiber, suggesting an evolutionary link in the receptor-binding strategies of reoviruses and adenoviruses (37). Most adenovirus serotypes initiate infection by binding to the coxsackievirus and adenovirus receptor (CAR) (23). The crystal structure of the adenovirus fiber knob in complex with CAR is known (24). Although no structural information is currently available for a reovirus-receptor complex, analysis of the crystallized σ1 fragment revealed a region that is likely involved in the interaction with JAM-A (37). This putative JAM-A-binding site forms a recessed groove at the lower edge of the σ1head that contains many of the residues conserved in prototype strains of the three reovirus serotypes. The location of this site suggests that each σ1monomer can independently interact with a JAM-A molecule.

To enhance an understanding of how reovirus mediates cell tropism and initiates organ-specific disease, we used a genetic approach combined with structural analyses to define reovirus JAM-A interactions. Through utilization of chimeric JAM-A-CARreceptor constructs, we identified the D1 domain of JAM-A to be necessary and sufficient for reovirus binding. In order to understand the structure-function relationships

within JAM-A that mediate reovirus binding, we determined the crystal structure of the hJAM-A ectodomain. Analysis of this structure allows us to identify regions of the D1 domain that are most likely involved in the binding of σ1. Moreover, comparison of the structures of hJAM-A and mJAM-A reveals differences in the dimeric arrangements of the molecules despite absolute conservation of residues at the interface, suggesting that the JAM-A dimer is dynamic and can undergo rearrangement and perhaps dissociation. Finally, we show that the structure of the JAM-A dimer closely resembles that of the CAR dimer, mirroring the close resemblance of the reovirus and adenovirus attachment proteins and suggesting that the similarities extend beyond conservation of structure toward conserved strategies of attachment and entry.

Results

Identification of hJAM-A domains required for reovirus attachment

We previously have shown that JAM-A is a serotype-independent reovirus receptor (10). However, specific sequences in JAM-A required for reovirus attachment were not known prior to the initiation of this work. To identify domains in JAM-A required for reovirus binding and infection, we generated receptor chimeras using hJAM-A and Ig superfamily relative hCAR (Figure 14). hCAR is incapable of supporting reovirus binding and infection (10) and was selected as the chimera partner for these studies because of its structural similarities to JAM-A (129). A PCR-based approach was used to reciprocally exchange sequences encoding either the D1 or D2 Ig-like domains of wild-type receptor cDNAs. We also generated single-domain deletion mutants of hJAM-

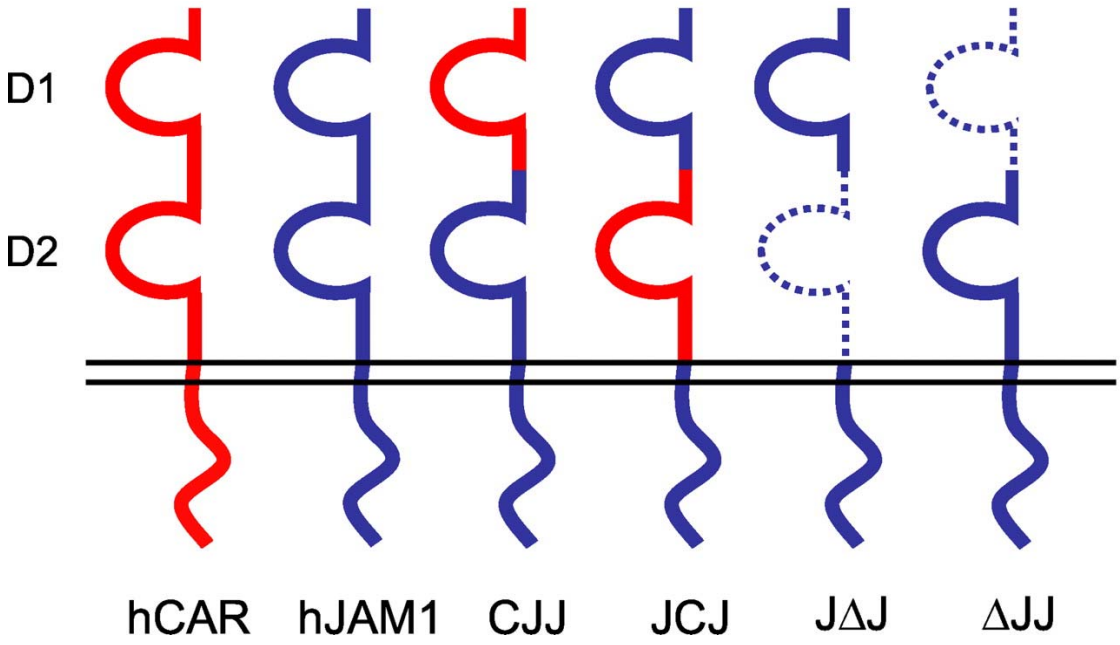

Figure 14. Chimeric and deletion mutant receptor constructs for studies of reovirus binding and growth. Ig superfamily proteins hCAR (*red*) and hJAM-A (*blue*) were used to generate chimeric receptor constructs in which Ig-like domains were reciprocally exchanged. Single Ig-like domains of hJAM-A also were deleted. Nomenclature indicates origin or deletion of domains D1, D2, and cytoplasmic tail (*left* to *right*) relative to wild-type hCAR or hJAM-A.

A to complement data obtained using the chimeric receptor molecules. CHO cells, which lack expression of both JAM-A and CAR (23, 106), were transiently transfected with plasmids encoding wild-type hJAM-A and hCAR, chimeric receptor molecules CJJ and JCJ, and hJAM-A deletion mutants JΔJ and ΔJJ. Cell-surface expression of each construct and the capacity of reovirus to bind transfected cells were assessed by flow cytometry (Figure 15). All constructs were detected at the cell surface. Chimera-transfected cells stained with both hJAM-A- and hCAR-specific antisera, indicating that the molecules are indeed chimeric (Figure 15). Prototype reovirus strain T1L bound cells expressing wild-type hJAM-A, chimera JCJ, and deletion mutant JΔJ but failed to bind cells expressing hCAR, chimera CJJ, or deletion mutant ΔJJ (Figure 15). T3 reovirus strain T3SA- also bound cells expressing constructs that contained the D1 domain of hJAM-A (data not shown). These data demonstrate that both T1 and T3 reoviruses engage the membrane-distal D1 domain of hJAM-A.

Reovirus infection and growth in CHO cells expressing chimeric and deletion mutant receptors

To determine the role of specific JAM-A domains in reovirus infection, CHO cells were transiently transfected with plasmids encoding the hCAR-hJAM-A chimeras or hJAM-A domain-deletion mutants. Transfected cells were adsorbed with T1L, and the capacity of reovirus to infect these cells was assessed by indirect immunofluorescence.

Consistent with the binding experiments, reovirus protein expression was detected after infection of cells expressing wild-type hJAM-A, chimera JCJ, and deletion mutant JΔJ (Figure 16). As a control, adenovirus infection also was tested by adsorbing transfected cells with Ad 5-GFP. This Ad5-GFP was constructed from a plasmid which

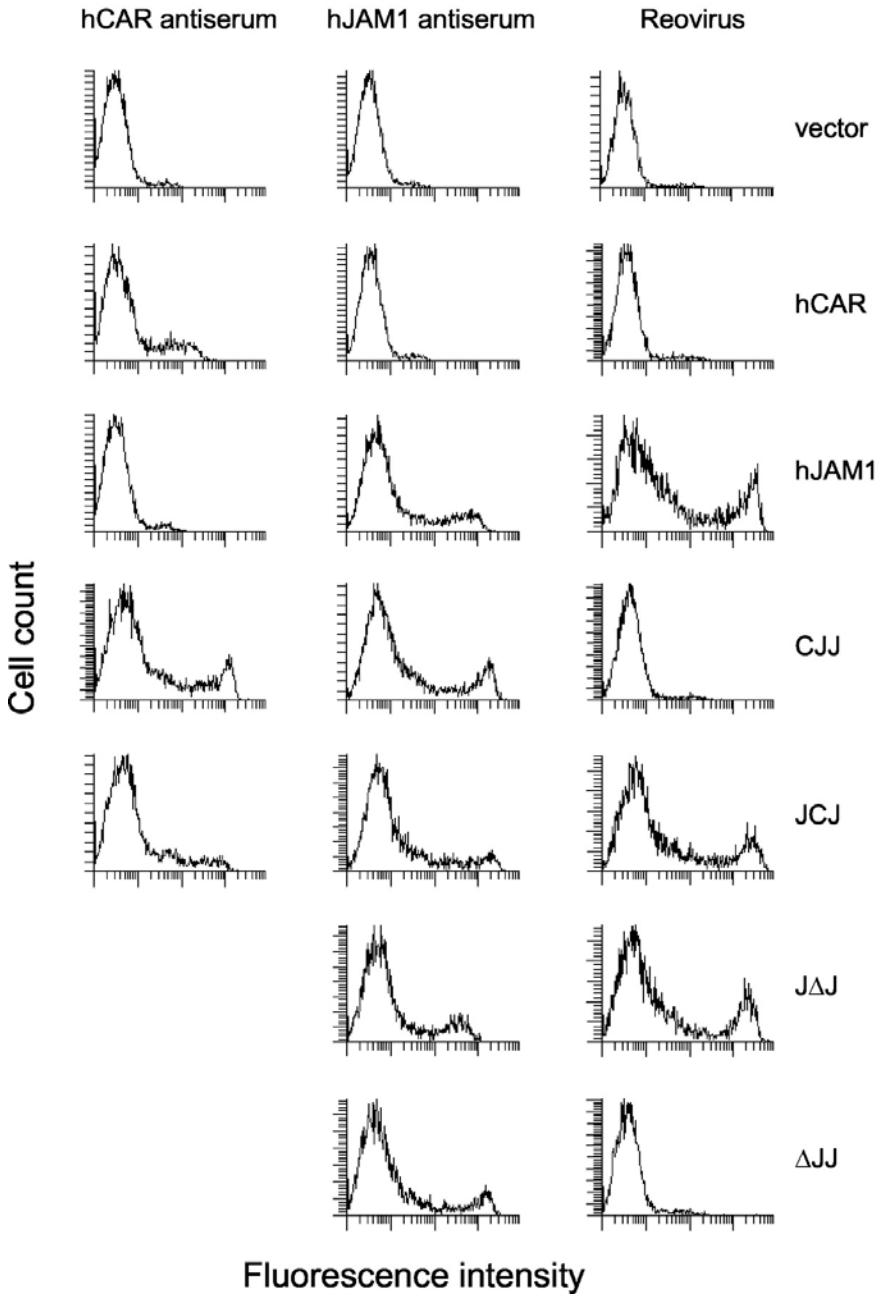

Figure 15. Reovirus engages the D1 domain of hJAM-A. CHO cells were transiently transfected with plasmids encoding the indicated receptor constructs. Following incubation for 24 h to permit receptor expression, cells (1 x 10^6) were stained with hCAR or hJAM-A-specific antisera or adsorbed with reovirus T1L (1 x 10^{11} particles). Cell surface expression of receptor constructs and virus binding were assessed by flow cytometry.

contained a 2.3-kb, cytomegalovirus (CMV) promoter-driven enhanced green fluorescent protein (EGFP) gene (derived from pEGFP-1 [Clontech, Palo Alto, Calif.]) inserted into the E3 region of Ad5 (141). Cells expressing hCAR and CJJ supported infection by adenovirus (data not shown), demonstrating that these molecules also can serve as functional virus receptors. To provide further support for the role of hJAM-A D1 in reovirus infection, viral replication was assessed 24 h after adsorption by plaque assay. T1L produced substantially higher yields in cells expressing hJAM-A, JCJ, and JΔJ in comparison to yields in cells expressing receptors that lack the hJAM-A D1 domain (Figure 16). Together, these data indicate that the D1 domain of hJAM-A is required for reovirus attachment, infection, and growth.

Overall structure of hJAM-A

To better understand structure-function relationships of JAM-A which mediate binding to reovirus, a GST–hJAM-A fusion protein was constructed. The extracellular portion of hJAM-A was cloned into a vector encoding glutathione S-transferase (GST) followed by a thrombin cleavage site to produce a GST-hJAM-A fusion protein. The protein was expressed in bacteria and purified using a glutathione column followed by cleavage with thrombin. The protein was further purified by ion-exchange chromatography and size-exclusion. Crystals were obtained by using 8 mg/ml protein and 16% PEG 6K, 18% isopropanol, 0.1 M sodium citrate as precipitant.

The polypeptide chain of the extracellular region of hJAM-A folds into two concatenated Ig-like domains, termed D1 and D2 (Figure 17). The N-terminal D1 domain contains two antiparallel β-sheets (strands ABED and GFCC'C"), which classifies it as an Ig-like domain of the variable type (V-set). Although the fold of D2 is very

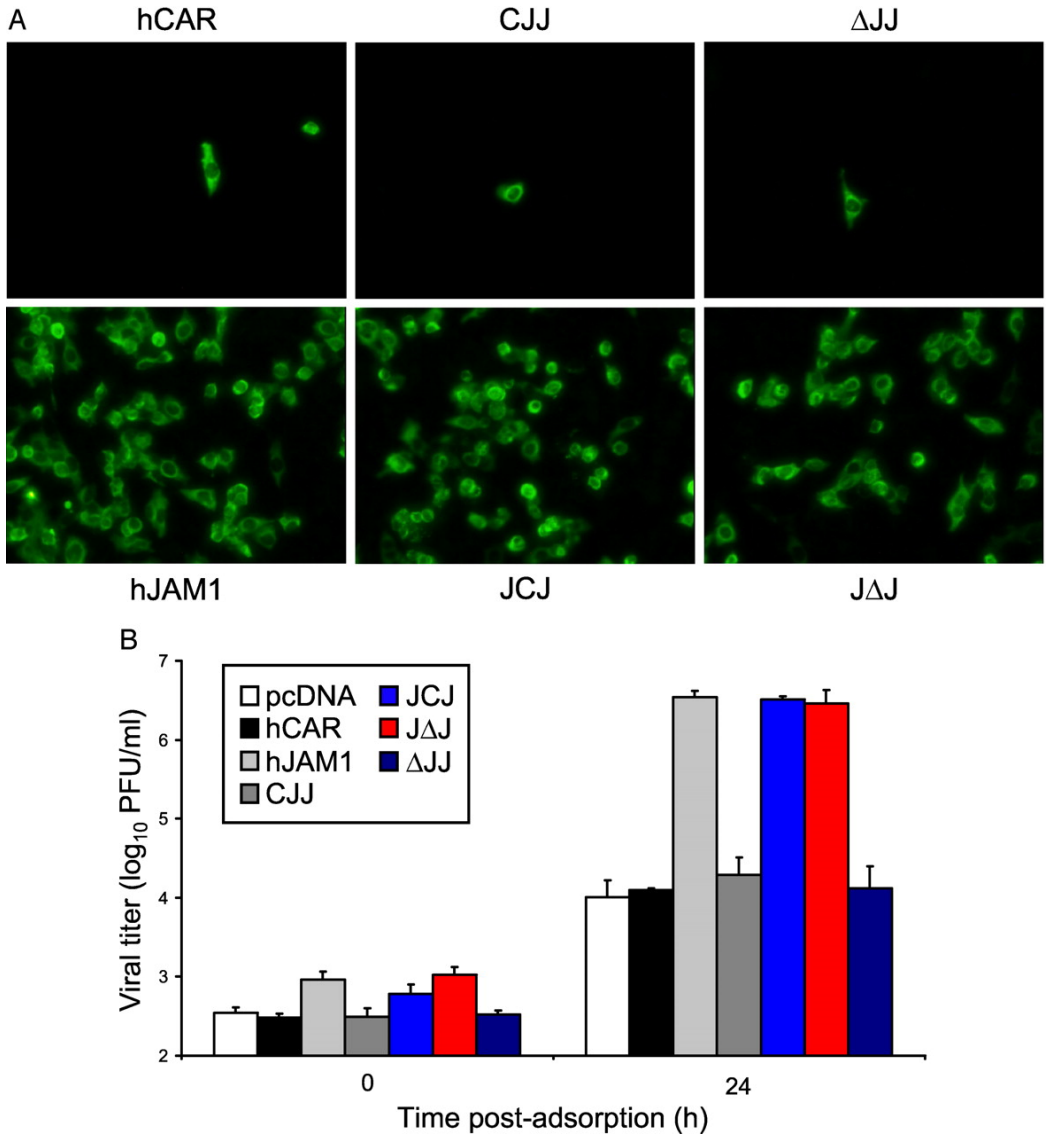

Figure 16. The D1 domain of hJAM-A is required for reovirus infection and replication. CHO cells were transiently transfected with plasmids encoding the indicated receptor constructs and incubated for 24 h to permit receptor expression. (*A*) Transfected cells (4 x 10^5) were infected with reovirus T1L at an MOI of 1 FFU per cell and incubated at 37 °C for 20 h. Cells were fixed and stained for reovirus protein, and infected cells were identified by indirect immunofluorescence. Representative images are shown. (*B*) transfected cells (2 x 10^5) were adsorbed with reovirus T1L at an MOI of 1 PFU per cell. Reovirus growth was assessed by plaque assay at 0 and 24 h postadsorption. Shown are mean viral titers for three independent experiments. The error bars indicate standard deviations.

similar to that of D1, this domain has a much shorter C' strand, and it lacks the C" strand. These differences indicate that D2 is an intermediate type (I-set) Ig-like domain (78) and not a V-set Ig-like domain, as reported for mJAM-A D2 (95). Analysis with DALI (82) shows that the prototypical I-set domain, telokin (78), is among the closest structural homologs of hJAM-A D2. Both D1 and D2 of hJAM-A have the classical disulfide bond between β-strands B and F. The hJAM-A structure exhibits a pronounced elbow angle of ~125° between the two domains. As expected, the overall structure of each hJAM-A D1D2 monomer resembles that of mJAM-A D1D2 (95), although there are conformational differences between the two proteins in surface loops and at the interdomain interface. Our structure also allows us to trace a long loop between β-strands C' and D (C'D loop) in D2 that was disordered in the model for mJAM-A D1D2.

The asymmetric unit of the hJAM-A crystals contains two independent but virtually identical chains (termed A and B). Each chain assembles into a U-shaped homodimer with crystallographic 2-fold symmetry. The dimer interface features an extensive contact between the D1 domains and is reminiscent of an arm-wrestling grip, with the GFCC' faces of the two N-terminal domains interlocking at an angle of ~90° (Figure 17). Two crystallographically independent dimers are observed. One is formed by chain A and its symmetry mate A, and the other is formed by chains B and B. Two observations suggest that the hJAM-A dimer is physiologically relevant: (*i*) the purified protein elutes at the expected molecular mass for a dimer (48 kDa) by size-exclusion chromatography and (*ii*) a similar dimeric structure was seen in the crystals of mJAM-A (95). With the exception of the dimeric interaction, the arrangements of the molecules in the hJAM-A and mJAM-A crystals are not related.

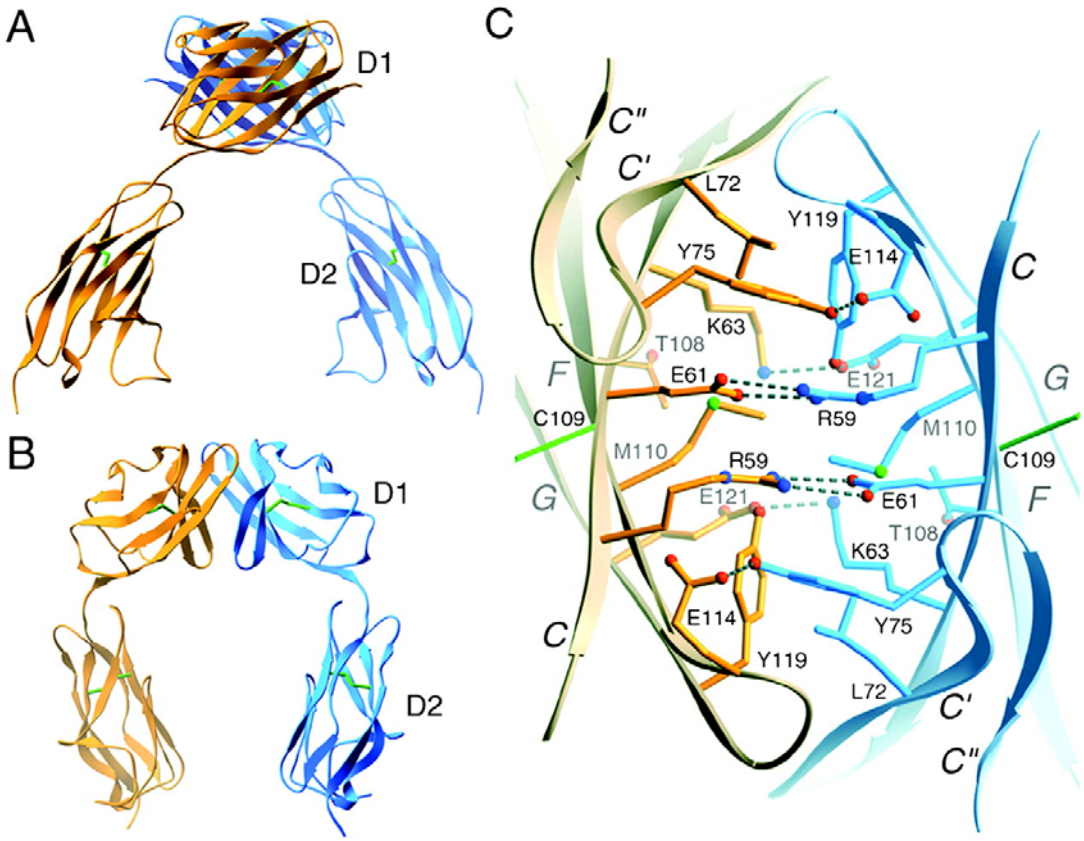

Figure 17. Structure of hJAM-A. (*A* and *B*) Ribbon drawings of the hJAM-A dimer, with one monomer shown in orange and the other in blue. Two orthogonal views are displayed. Disulfide bonds are shown in green. (*C*) View of the interface between two hJAM-A monomers. The interface is formed by residues on the GFCC' faces of two D1 domains. The view is along a crystallographic dyad. Hydrogen bonds and salt bridges are represented by broken cylinders. Amino acids are labeled in single-letter code.

Interaction of hJAM-A with reovirus attachment protein σ1

The crystal structure of the reovirus attachment protein σ1 revealed a putative binding site for JAM-A at the lower edge of the σ1 head domain (37). To investigate whether other JAM family members serve as reovirus receptors, we transiently transfected CHO cells with hJAM-A, hJAM-B, or hJAM-C and assayed transfected cells for the capacity to support reovirus infection. Expression of JAM proteins at the cell surface was confirmed by flow cytometry (Figure 20). In contrast to cells transfected with hJAM-A, cells transfected with hJAM-B or hJAM-C were not infected by reovirus (Figure 20). Our findings clearly demonstrate that reovirus recognizes structural features that are present in hJAM-A but not in hJAM-B or hJAM-C.

To define structural features unique to JAM-A and potentially involved in contacting σ1, we identified conserved sequences in hJAM-A and mJAM-A that are not conserved in the other two JAM family members (Figure 20). Both hJAM-A and mJAM-A serve as reovirus receptors, whereas hJAM-B and hJAM-C do not. Because the D1 domain of hJAM-A is necessary and sufficient for interaction with σ1 (Figures 15 and 16), our analysis was restricted to that domain. Residues unique to hJAM-A D1 and mJAM-A D1, and therefore likely to participate in σ1 binding, cluster in three main areas (Figure 20): a region at the dimer interface (shown in orange) and two surface-exposed regions at the "back" of the molecule, opposite the dimer interface (shown in green and magenta, respectively). All three areas are candidates for interaction with σ1.

Interestingly, the "top" of the hJAM-A dimer does not contain conserved residues, and therefore we hypothesize that σ1 either engages the side of the hJAM-A dimer (via the magenta or green surfaces) or the JAM-A dimer interface (via the orange surface). The green surface near the top of D1 comprises the BC loop and the beginning of strand C. This surface

is most complementary in shape and size to the proposed JAM-A-binding region of σ1 (37) and, thus, it is a good candidate for σ1–JAM-A interactions. The equivalent regions in JAM-B and JAM-C likely have a different structure because of two-residue insertions (Figure 20), perhaps explaining the inability of these proteins to serve as reovirus receptors. The magenta-colored regions at the "back" of the protein contain three solvent-exposed side chains, Lys-47, Thr-88, and Thr-95, which also could participate in the interaction with σ1.

The interdimer interface of JAM-A (the orange surface in Figure 20) is not accessible to σ1 in the context of a JAM-A–JAM-A dimer. However, σ1 might engage this surface in monomeric forms of JAM-A. Such a mechanism of binding is identical to the strategy used by the adenovirus fiber knob to bind the monomeric form of CAR (24). Indeed, comparison of the sequences of JAM-A and CAR shows that JAM-A residues highlighted in orange cluster in the same region as the CAR residues known to bind fiber (Figure 20). Although we have no evidence to suggest that σ1 binds to JAM-A in a similar manner, the similarities exhibited by σ1 and fiber, and between JAM-A and CAR, indicate that such an interaction might occur. The affinity of the σ1 head domain for hJAM-A is in the nanomolar range (6×10^{-8} M) (10). Although the affinity of JAM-A for itself is not known, studies using recombinant mJAM-A demonstrated that a significant portion of this protein is monomeric under physiologic conditions (18). This finding suggests that JAM-A–JAM-A interactions are weak. Therefore, it seems plausible that σ1 binds to monomeric JAM-A, perhaps by engaging residues that form the JAM-A–JAM-A interface.

Structure of the dimer

Residues involved in hJAM-A homodimer formation are exclusively located on the concave GFCC' face of D1. The dimer interface includes four buried salt bridges (Arg-59–

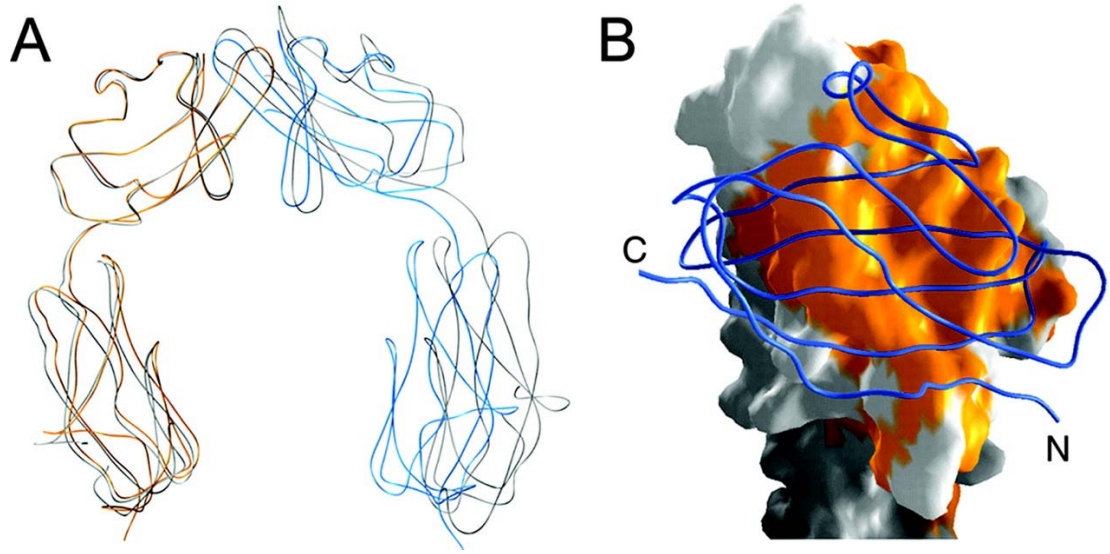

Figure 18. Comparison of dimeric arrangements in hJAM-A and mJAM-A. (*A*) Superposition of dimeric structures of hJAM-A (colored as in Fig. 14) and mJAM-A (gray). The superposition is based on D1 residues of one monomer only (the orange monomer of hJAM-A). (*B*) Conservation of residues at the mJAM-A and hJAM-A D1 domain dimer interfaces. One hJAM-A monomer is shown in surface representation, and the other is shown as a blue ribbon. Residues that are strictly conserved in mJAM-A are shown in orange and cover the entire dimer interface.

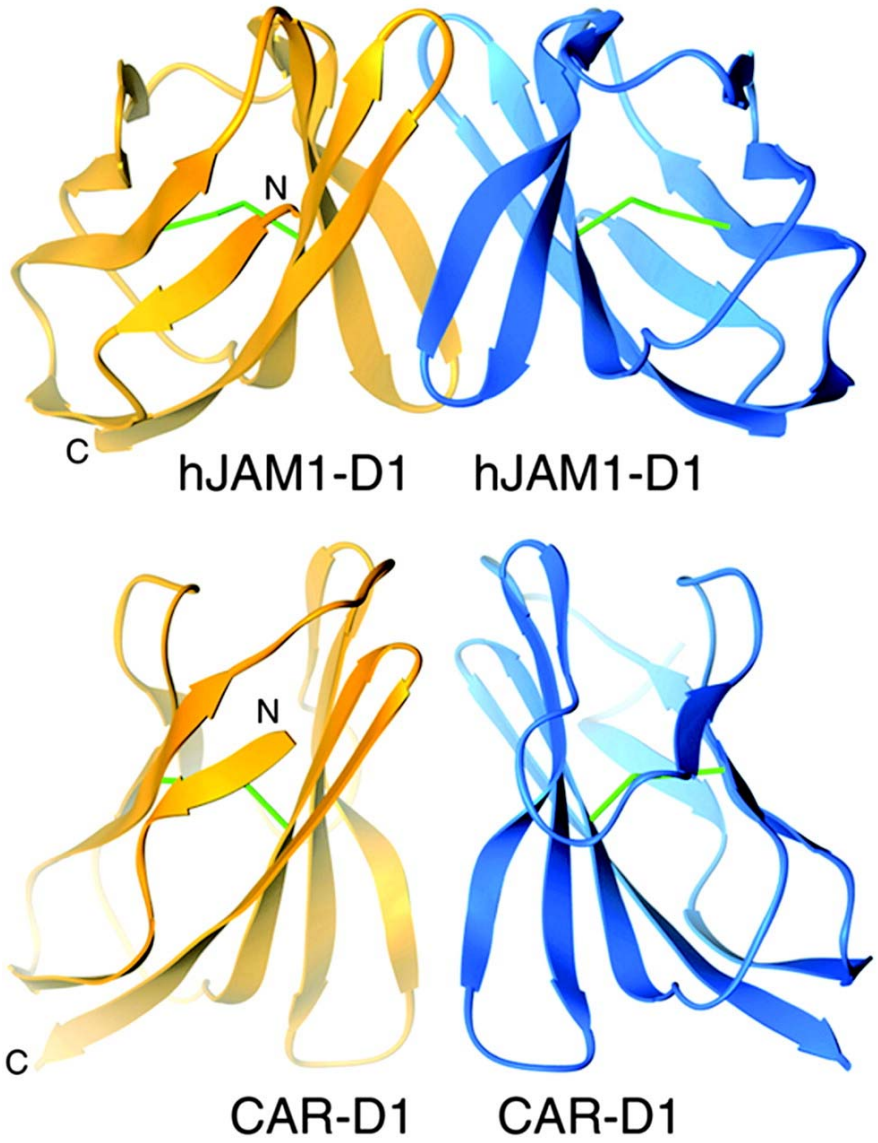

Figure 19. Dimeric structures of virus receptors hJAM-A and CAR. The D1 domains of hJAM-A (*Upper*) and CAR (*Lower*) engage in a conserved mode of dimerization based on interactions between the concave GFCC' β-sheets. Disulfide bonds are in green.

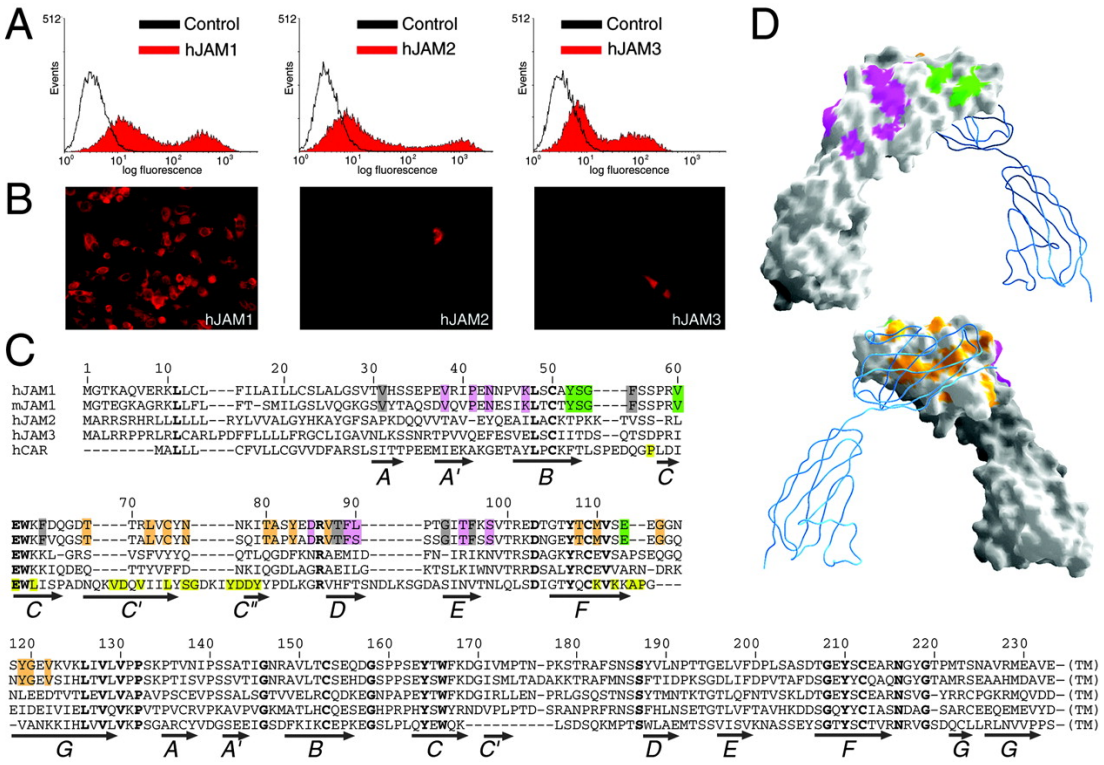

Figure 20. Interaction of reovirus with hJAM-A. (*A*) Transiently transfected CHO cells display surface expression of JAM family members. CHO cells were transiently transfected with hJAM-A, hJAM-B, or hJAM-C and screened for surface expression of JAM proteins by flow cytometry. (*B*) Transfection of CHO cells with hJAM-A, but not hJAM-B or hJAM-C, rescues infection by reovirus strain T1L. Shown are infected cells as detected by indirect immunofluorescence using rabbit antireovirus sera. (*C*) Sequence alignment, with residues conserved in hJAM-A and mJAM-A, but not in hJAM-B or hJAM-C, highlighted in orange, magenta, and green. Arrows indicate β-strands. CAR residues contacting the adenovirus fiber knob in the complex are highlighted in yellow. Residues conserved in all sequences are shown in bold. (*D*) The hJAM-A D1D2 dimer viewed from opposite angles, with one monomer shown in surface representation and the other shown as a blue ribbon. The side chains of conserved residues from *C* were mapped onto the hJAM-A D1D2 surface by using the same color code. Residues colored in orange, green, or magenta cluster in three different surface areas. Residues shaded gray in *C* are buried and not visible in this representation.

Glu-61, Glu-61–Arg-59, Lys-63–Glu-121, and Glu-121–Lys-63) as well as several hydrophobic contacts (Leu-72–Tyr-119, Met-110–Met-110, and Tyr-119–Leu-72) (Figure 18). Hydrogen bonds exist between the Tyr-75 and Glu-114 side chains.

Although the GFCC' face of D1 also mediates homodimer formation in the mJAM-A D1D2 structure (95), the relative arrangements of the D1 domains in the two dimers are noticeably different (Figure 18). The mJAM-A interdomain interface contains only two salt bridges and fewer additional contacts (95). The Lys-63–Glu-121 and Met-110–Met-110 interactions at the center of the hJAM-A interface are absent in mJAM-A, as are the hydrogen bonds involving Tyr-75, Glu-114, and their symmetry-related counterparts. These differences result in a smaller interface in mJAM-A (Figure 18). Using the program SURFACE and a standard probe radius of 1.4 Å, we calculate buried surface areas of 1,380 and 1,200 $Å^2$ for the hJAM-A and mJAM-A dimers, respectively.

The observed differences in the hJAM-A and mJAM-A dimers are noteworthy given the near absolute conservation of residues at the dimer interfaces (Figure 18). The GFCC' faces of hJAM-A and mJAM-A (residues 58–75 and 105–122 of hJAM-A) can be superimposed onto each other with an root means squared deviation of 0.4 Å for the 36 Cα atoms. There are only six substitutions among these 36 aa, and none of the substituted residues engage in dimer contacts (distances >4 Å). Thus, differences in the arrangement of the hJAM-A and mJAM-A dimer interfaces cannot be explained by altered contacts mediated by substituted residues. Instead, these differences are likely caused by crystal packing forces involving other regions of the molecules, and they indicate that small movements of one monomer with respect to the other can occur.

The dynamic nature of the JAM-A dimer interface may result in part from its dependence on ionic interactions, which is unusual for protein–protein interfaces. Low

pH and moderately high ionic strength lead to dissociation of the mJAM-A dimer (18), indicating that ionic interactions represent the principal means of association. We note that both structures were obtained by using conditions of low ionic strength and at pH values at which acidic side chains are expected to be deprotonated. Thus, salt bridges are expected to exist in both cases. However, the free energy contribution of salt bridges in an aqueous environment is small (139). The JAM-A dimer interface, which is stabilized primarily by salt bridges and contains several solvent molecules, is therefore especially likely to undergo rearrangement or dissociation.

Discussion

Experiments reported here were performed to define the molecular basis of reovirus attachment to hJAM-A. The capacity of reovirus to bind, infect, and replicate to high titers in cells expressing chimeric hCAR-hJAM-A receptor constructs and single domain deletion mutants demonstrates that the membrane-distal D1 domain of hJAM-A is an essential component of the reovirus receptor function of hJAM-A (Figures 18 and 19). Several viruses have been demonstrated to engage cellular receptors via the most distal domain of an Ig superfamily receptor, including adenovirus (hCAR) (24, 65), coxsackievirus (hCAR) (79), human immunodeficiency virus (CD4) (97), measles virus (SLAM) (119), poliovirus (PVR) (21), and rhinovirus (ICAM-1) (94). Thus, utilization of the membrane-distal D1 domain of hJAM-A by reovirus provides additional evidence for a common theme in viral attachment.

The attachment proteins of adenovirus and reovirus share structural and functional properties, which has led to speculation that they have a common ancestor (37). Remarkably, the receptors for both viruses, CAR and JAM-A, respectively, also share key structural properties. CAR forms a homodimer (171) that is structurally similar to the

hJAM-A homodimer and also is formed by interactions between the GFCC' β-sheets of the N-terminal D1 domains (Figure 19). Although the contacts between CAR monomers are somewhat more hydrophobic and do not directly involve salt bridges (171), several charged residues are present at the CAR–CAR interface (Glu-56, Asp-68, Lys-121). It is possible that these side chains interact via water molecules. Moreover, the relative arrangement of the two CAR monomers is highly similar to that observed for the two hJAM-A monomers (Figure 19). Both contacts involve concave GFCC' β-sheets that face each other at an angle of ~90° and bury an almost identical amount of solvent (1,300 $Å^2$ for the CAR–CAR dimer (171) and 1,380 $Å^2$ for hJAM-A–hJAM-A).

Homodimeric structures have been observed in a number of other Ig superfamily proteins (31, 89, 91, 120, 193), but only one of these proteins, CD2, forms dimers via the GFCC' β-sheet of D1 (26, 89). However, it is noteworthy that several Ig superfamily receptors engage viral ligands via the GFCC' β-sheet. The HIV glycoprotein gp120 binds to residues on the GFCC' face of its receptor CD4 (97), and the same region of CD4 also interacts with its natural ligand MHC class II (180). Complexes of rhinoviruses and coxsackievirus A21 with their receptor intercellular adhesion molecule-1 (ICAM-1) also show that the interactions involve residues at the top of ICAM-1 D1, a region that includes part of the GFCC' face (20, 195). Moreover, the adenovirus fiber knob engages the same area of the GFCC' face that mediates formation of the CAR–CAR dimer (24, 171). The structure of the complex between fiber knob and CAR shows a trimeric knob decorated with three copies of monomeric CAR (24, 171).

Analysis of the crystal-packing arrangement of the mJAM-A molecules has led to a model of JAM-A interactions at tight junctions (95). In this model, a JAM-A dimer located

at the surface of one cell engages a dimer on the opposing cell via contacts in D1, producing an extensive network of contacts between dimers. Although our crystals contain two crystallographically nonequivalent copies of hJAM-A, we do not observe a similar contact involving either of these molecules, and thus our structural analysis does not provide supporting evidence for the model presented by Kostrewa *et al.* (95). In the hJAM-A crystals, two alternative contacts between hJAM-A dimers that could form the basis for interactions in tight junctions exist. However, neither of these contacts is observed in the mJAM-A crystal lattice.

One interpretation of the available crystallographic data is that contacts between JAM-A dimers in tight junctions involve low-affinity interactions that depend on the presence of additional proteins, and these interactions cannot be easily reproduced by using conditions that promote crystallization. Another interpretation is that the JAM-A dimer itself, which is observed in the crystals of hJAM-A and mJAM-A, represents a physiologic contact present in tight junctions. In this interpretation, JAM-A monomers would engage JAM-A monomers on apposing cells to help mediate homophilic cell–cell interactions. The dimensions for such a model suggest that it deserves consideration, because it would lead to a separation of cells of ~85 Å, similar to the observed distances between cells at tight junctions of ~100 Å. CAR is also thought to mediate homophilic interactions between cells (43, 83, 179), and the homodimeric structure of CAR has been interpreted to depict an interaction between CAR monomers from apposing cells (171).

Of the virus receptors whose structures have been solved, only adenovirus receptor hCAR and reovirus receptor JAM-A have been demonstrated to form homodimers by contacts between the GFCC' β-strands of apposing D1 domains (95, 129, 171). Moreover, there are numerous similarities in the attachment proteins of adenovirus and reovirus: 1) both

form trimers; 2) both insert into pentamers of capsid proteins at the virion 5-fold symmetry axes; 3) both have fibrous domains formed by unique triple β-spiral structural motifs; and 4) both have globular, virion-distal domains formed by β-barrel structures with unique and identical β-strand connectivity. These similarities suggest functionally convergent evolution of two large, nonenveloped viruses (151). Additionally, the observation that hJAM-A and hCAR share numerous structural and functional similarities leads to the hypothesis that adenovirus and reovirus engage their receptors using similar mechanisms.

The crystal structure of the hJAM-A ectodomain provides insights into how JAM-A functions in tight junction formation and viral attachment. A key feature of JAM-A is its capacity to form dimers via an extensive interface in its N-terminal domain. This interface is distinguished from traditional protein–protein interfaces by its highly polar character and its capacity to accommodate substantial rearrangements. The latter is evidenced by the different dimeric structures of hJAM-A and mJAM-A despite absolute conservation of residues at the interface. We think it possible that the dynamic nature of the interface plays a role in mediating and perhaps facilitating transitions between monomeric and dimeric forms of JAM-A. Moreover, the dynamic nature of the interface likely distinguishes JAM-A from the other JAM family members, JAM-B and JAM-C, both of which contain substitutions that are predicted to alter the stability of the interface. Previous work from our laboratory has shown that the adenovirus and reovirus attachment proteins share many structural and functional features (37). Here we show that the similarities also extend to their receptors. The crystal structure of hJAM-A features a dimeric arrangement that closely resembles that seen in the adenovirus receptor, CAR. Parallels in the structures of these molecules are especially intriguing in light of the recent observation that CAR, like JAM-A, is a component of cell–cell junctions (43, 83, 179). Thus, both viral and cellular determinants of adenovirus and

reovirus binding exhibit striking structural similarities, which suggest conserved strategies of attachment among these viruses.

CHAPTER IV

A CHIMERIC ADENOVIRUS VECTOR ENCODING REOVIRUS ATTACHMENT PROTEIN σ1 TARGETS CELLS EXPRESSING JUNCTIONAL ADHESION MOLECULE-A

Introduction

Adenovirus (Ad) vectors are potent gene-delivery vehicles capable of eliciting both mucosal and systemic immune responses (142). Ad vectors are advantageous because the can tolerate large fragments of DNA and have a low frequency of nonhomologous chromosomal integration (81). Human Ad serotypes 2 and 5 (Ad2 and Ad5) bind and enter cells by using the combined interactions of the fiber and penton base proteins with cellular receptors. The fiber protein is an elongated trimer with an N-terminal fibrous tail domain (shaft) and a C-terminal globular head domain (knob). Ad2 and Ad5 engage the coxsackievirus and Ad receptor (CAR) (23, 161) via a binding site located in the knob [Roelvink, 1998 #3093]. CAR is a member of the Ig superfamily (23, 161) expressed at regions of cell-cell contact (43). After fiber-mediated attachment, the penton base binds to cell surface α_v integrins, which mediate internalization (187).

Although Ad5 vectors transduce many types of cells, the efficiency of these vectors is limited if cells lack one or more Adenovirus receptors (86). For example, dendritic cells (DCs) do not express CAR and are poorly transduced by Ad5 (160). This relatively poor transduction of DCs can be enhanced by engineering the vector to target alternative receptors (22, 125). Ad serotypes that bind to other receptors (e.g., CD46 (67) mediate increased transduction of immunologically relevant cells (177), but these vectors are more promiscuous than Ad5 and deliver genes into cells that may not contribute to vaccination and thus may

increase toxicity. Therefore, although potent, current Ad vectors lack sufficient specificity to function in some applications.

The reovirus attachment protein, σ1, plays a key role in targeting the virus to distinct cell types, including those at mucosal surfaces (1, 27, 189, 190). Similar to the Ad fiber, reovirus σ1 is an elongated trimer with head-and-tail morphology [Furlong, 1988 #370;Banerjea, 1988 #77;;Fraser, 1990 #3682]. A domain in the fibrous tail of T3D σ1 binds to α-linked sialic acid (9, 35, 36, 49), whereas the head binds to JAM-A (10).

The structures of the Ad fiber (172) and reovirus σ1 (37) proteins are strikingly similar (Figure 19). The two proteins are the only structures known to date to form trimers by using triple β-spiral motifs. The fiber shaft most likely is composed entirely of β-spiral repeats (172), whereas the σ1 tail is predicted to also contain an α-helical coiled-coil N-terminal to the β-spiral region (37). The head domains of both proteins are formed by eight antiparallel β-strands with identical interstrand connectivity. Therefore, although Ad and reovirus belong to different virus families and have few overall properties in common, the observed similarities between the attachment proteins and receptors of these viruses suggest a conserved mechanism of binding.

Based on the structural similarities between Ad fiber and reovirus σ1, we engineered chimeric fiber-σ1 attachment proteins to exploit the JAM-A and sialic acid-binding properties of σ1. Of those tested, only a near-full-length version of σ1 grafted onto the virion-insertion domain of Ad fiber (Fibtail-T3D σ1) formed trimers and assembled onto Ad particles. We show here that when the fiber gene in the Ad5 genome is replaced with Fibtail-T3D σ1, the resulting virus, Ad5-T3Dσ1, is capable of infecting intestinal epithelial cells expressing JAM-A and sialic acid and primary human DCs expressing JAM-A. These data provide

proof of principle for the development of chimeric Ad vectors encoding reovirus σ1 for gene delivery to mucosal surfaces. This work also establishes a foundation for the use of Ad-σ1 chimeric viruses as a template to enable facile reverse genetic manipulation of the reovirus attachment protein for studies of virus–cell and virus–host interactions. Results presented in this chapter were gathered in collaboration with Skip Mercier and Michael Barry at Baylor College of Medicine.

Results

Design and Characterization of a Functional Fiber-σ1 Chimera

Based on the structural similarities between Ad5 fiber and reovirus σ1 (Figure 21), we engineered three Ad fiber-reovirus σ1 chimeras with increasingly larger portions of σ1 protein replacing structurally homologous regions of fiber (Figure 22A). Fibshaft-T3Dσ1 contains the N-terminal 21 β-spiral repeats of fiber fused to the head domain of T3Dσ1. Fib8-T3Dσ1 contains the N-terminal eight β-spiral repeats of fiber fused to the T3D σ1 β-spiral and head domains. Fibtail-T3Dσ1 contains the N-terminal 44 aa virion-anchoring domain (41) fused to T3Dσ1 lacking only the N-terminal 17 amino acids. After transfection of CHO cells, each of the chimeric attachment proteins was expressed, but only Fibtail-T3Dσ1 formed trimers (Figure 22B and data not shown), suggesting that only this chimera maintains native folding.

Production and characterization of an Ad vector expressing a chimeric fiber-σ1 attachment protein

The Fibtail-T3Dσ1 gene was recombined into an Ad5 genome lacking E1 and E3 to

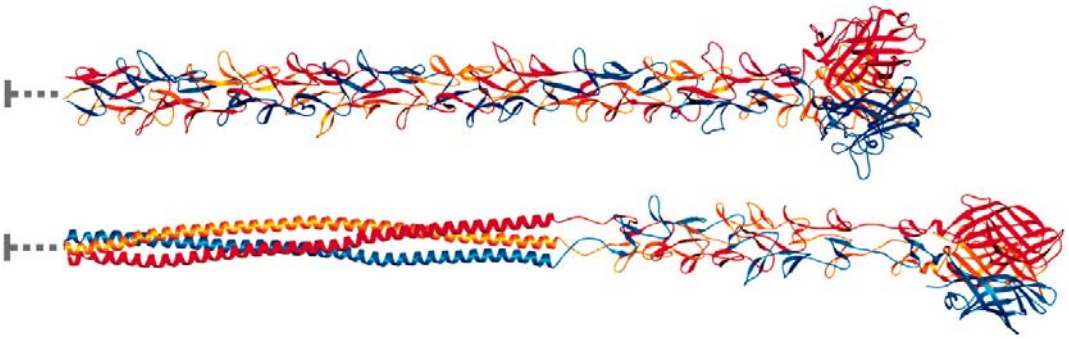

Figure 21. Full-length models of Ad5 fiber (*Upper*) and reovirus σ1 (*Lower*). The three monomers within each trimer are shown in red, orange, and blue. Both proteins have head-and-tail morphology, with an eight-stranded β-barrel domain forming the head. The Ad5 fiber model was generated by adding 17 β-spiral repeats to the four present in the crystal structure of an Ad2 fragment, which also has 21 β-spiral repeats. Sequence predictions suggest that 1 contains an N-terminal 135-residue α-helical coiled coil followed by eight β-spiral repeats and the globular head domain. The σ1 model was generated by first adding five β-spiral repeats to the N terminus of the crystallized fragment. This model then was joined with a 135-residue trimeric coiled coil formed by elongating an existing coiled-coil structure. The N-terminal 45 and 39 residues of fiber and σ1, respectively, are not included in the model, because they form a virion-anchoring structure (indicated by gray lines).

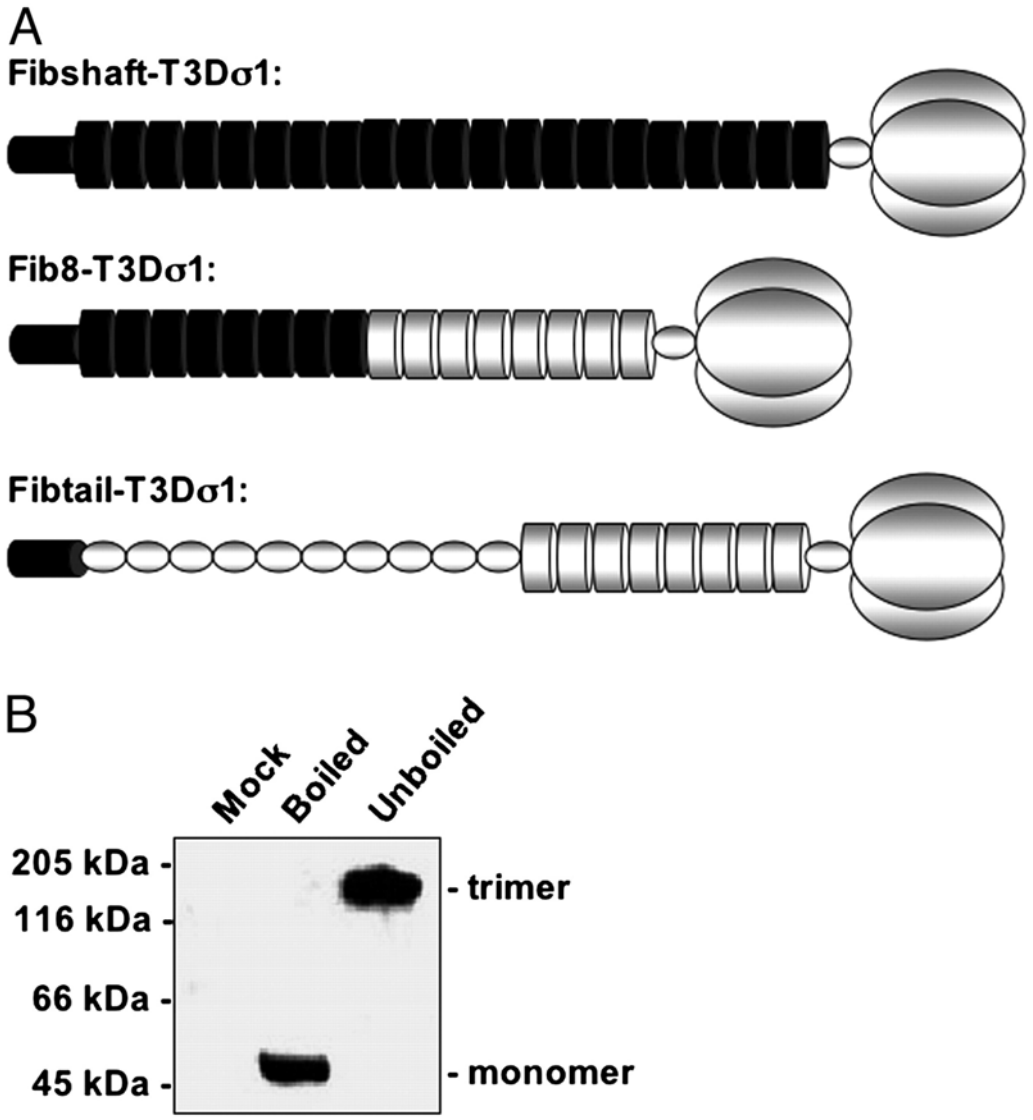

Figure 22. Design and expression of chimeric fiber-σ1 attachment proteins. (*A*) Schematic diagram of the chimeric fiber-σ1 attachment proteins described in the text. Regions corresponding to fiber and σ1 in the diagrams are shaded black and gray, respectively (not drawn to scale). Fiber tail, which mediates virion anchoring, is represented as a small cylinder, the α-helical coiled coils as small ovals, the β-spiral repeats as large cylinders, and the head domain as three large ovals. (*B*) Immunoblots of denatured (boiled) and native (unboiled) lysates of CHO cells transfected with plasmid expressing Fibtail-T3Dσ1 probed with a serum (1561) that recognizes the N-terminal region of Ad5 fiber.

replace the fiber gene by using λphage red recombinase (128). During the cloning process, two c-Myc tags (C2) and one hexahistidine tag (H6) were added to the C terminus of Fibtail-T3Dσ1 (Fibtail-T3Dσ1C2H6) to facilitate protein detection. The resulting virus, Ad5-T3Dσ1, was rescued by transfection and production in 633 fiber-expressing cells (178). After amplification in 633 cells, the virus was passaged in 293A cells to eliminate fiber from the virions and allow only Fibtail-T3Dσ1C2H6 to be encapsidated.

To determine whether Fibtail-T3Dσ1C2H6 was encapsidated onto Ad5 virions, CsCl-purified Ad5, Ad5-BAP-TR, which contains biotinylated fibers (125), and Ad5T3Dσ1 were analyzed by immunoblotting using antibodies specific for either the fiber N terminus or the c-Myc epitope tag (Figure 23A). Comparison of the immunoblots demonstrated that Fibtail-T3Dσ1C2H6 was encapsidated onto Ad5 virions at levels similar to those of fiber on Ad5 and Ad5-BAP-TR. As anticipated, the anti-c-Myc antibody recognized both Ad5-BAP-TR and Ad5-T3Dσ1, which contain c-Myc tags but not wild-type fiber. Coomassie blue staining demonstrated that relative amounts of the capsid proteins of wild-type Ad5 and Ad5-T3Dσ1were comparable (Figure 23B). Thus, Fibtail-T3Dσ1C2H6 is encapsidated onto Ad virions and enables normal virion maturation.

Transient transfection of CHO cells with JAM-A rescues infection by Ad5-T3Dσ1

To determine whether the chimeric Fibtail-T3Dσ1 attachment protein could bind to JAM-A, CHO cells were transfected with plasmids expressing hCAR, hJAM-A, and mJAM-A and tested for infection by luciferase-expressing Ad5-T3Dσ1. CHO cells were chosen for these studies, because they lack both CAR and JAM-A and are poorly infected by both Ad and reovirus (63). Transduction of CHO cells by Ad5-T3Dσ1 was increased substantially by expression of either hJAM-A or mJAM-A but not by expression of hCAR (Figure 24A), the

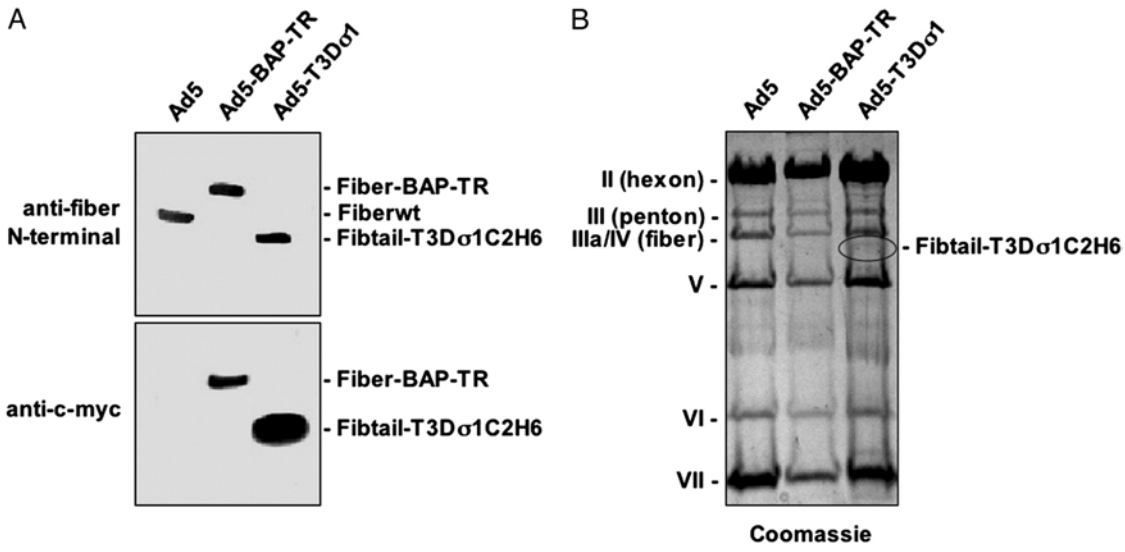

Figure 23. Characterization of Ad5-T3Dσ1. Ad5 virions expressing wild-type fiber (Fiberwt), CAR-ablated biotinylated fiber (Fiber-BAP-TR), and Fibtail-T3D 1C2H6 were precipitated with trichloroacetic acid. (*A*) Precipitated particles (4 x 10^{10} per lane) were resolved by SDS/PAGE and immunoblotted with anti-c-Myc mAb 9E10 or antiserum 1561, which recognizes the N-terminal region of Ad5 fiber. (*B*) Precipitated particles (1.5 x 10^{11} per lane) were resolved by SDS/PAGE and stained with Coomassie blue.

receptor for Ad5 (23, 161). These data indicate that the JAM-A-binding domain of Ad5-T3Dσ1 is functional and can target JAM-A-expressing cells in a species-independent fashion.

Inhibition of binding to JAM-A and sialic acid blocks Ad5-T3Dσ1 infection of Caco-2 cells

We next tested the capacity of hJAM-A-specific mAb J10.4 and *C. perfringens* neuraminidase to inhibit transduction by Ad5-T3Dσ1. Caco-2 intestinal epithelial cells, a model for enteric mucosal surfaces (93, 170), were used for these experiments, because these cells express CAR, JAM-A, and sialic acid (10, 39). Transduction by Ad5-T3Dσ1 was inhibited 50% by JAM-A-specific mAb J10.4 and 80% by neuraminidase (Figure 24B). Combined treatment with both mAb J10.4 and neuraminidase reduced transduction nearly 95%. In contrast, isotype-matched hCAR-specific mAb RmcB, used as a negative control, did not diminish luciferase transduction (Figure 24B).

To ensure that JAM-A-dependent transduction by Ad5-T3Dσ1 depends on σ1 and not another Ad protein, we tested the capacity of the T3D σ1-specific mAb 9BG5 [Burstin, 1982 #362] to block infection of Caco-2 cells. In contrast to T1L σ1-specific mAb 5C6 (174), mAb 9BG5 inhibited transduction in a dose-dependent fashion (data not shown). We noted a similar decrease in transduction efficiency after incubation of Ad5-T3Dσ1 with sialoglycophorin, which is known to interact with reovirus T3Dσ1 (49), before infection (data not shown). These results demonstrate that transduction by Ad5-T3Dσ1 requires σ1 and its receptors, JAM-A and sialic acid.

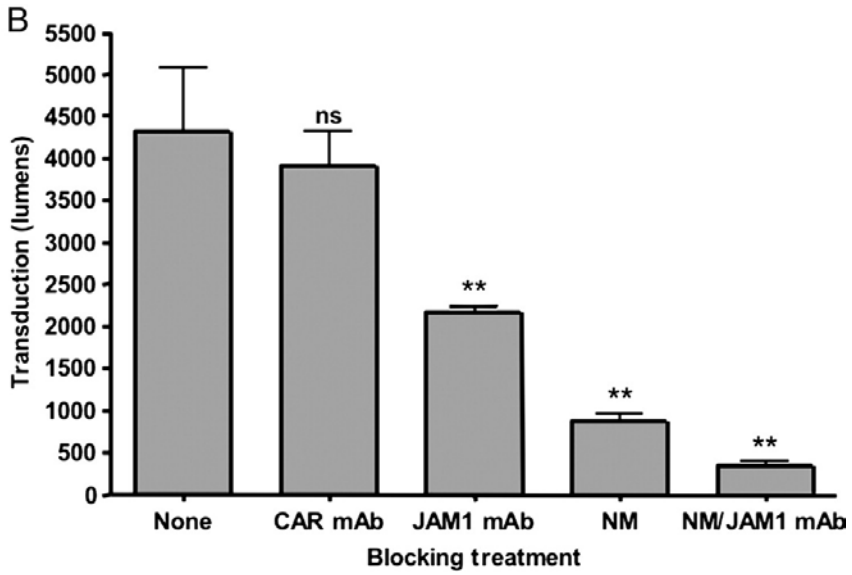

Figure 24. Ad5-T3Dσ1 transduction is mediated by JAM-A and sialic acid. (*A*) CHO cells were transiently transfected with plasmids encoding hCAR, hJAM-A, or mJAM-A. After 48 h of incubation to permit receptor expression, cells were adsorbed with 5,000 particles per cell of Ad5-T3Dσ1 and harvested 24 h later for luciferase assay. Transduction was measured in lumens. (*B*) Caco-2 cells were either untreated or treated with 10 μg/ml hCAR-specific mAb RmcB (CAR mAb), 10 μg/ml hJAM-A-specific mAb J10.4 (JAM-A mAb), 333 milliunits/ml *C. perfringens* neuraminidase (NM), or both JAM-A mAb and neuraminidase. Cells were adsorbed with 5,000 particles per cell of Ad5-T3Dσ1 and harvested 24 h later for luciferase assay. Transduction was measured in lumens. The results are presented as the means for three independent experiments. Error bars indicate SD. A paired Student's *t* test was performed to compare transduction of transfected or treated cells versus mock or untreated cells (*, $P < 0.01$; **, $P < 0.05$; ns, not significant).

Ad5-T3Dσ1 Transduces Primary Human DCs

DCs play important roles in the induction of adaptive immune responses (8). To determine whether Ad5-T3Dσ1 is capable of transducing DCs, we infected primary cultures of human DCs with Ad5 and Ad5-T3Dσ1. DCs express JAM-A but not CAR (Figure 25A), which is consistent with previous observations (132). Transduction of DCs by Ad5-T3Dσ1 was substantially more efficient than by Ad5 (Figure 25B). Moreover, transduction was eliminated almost completely by treatment with hJAM-A-specific mAb J10.4 (Figure 25B). These findings suggest that Ad5-T3Dσ1 may have utility for transducing CAR-negative DCs at mucosal and other sites.

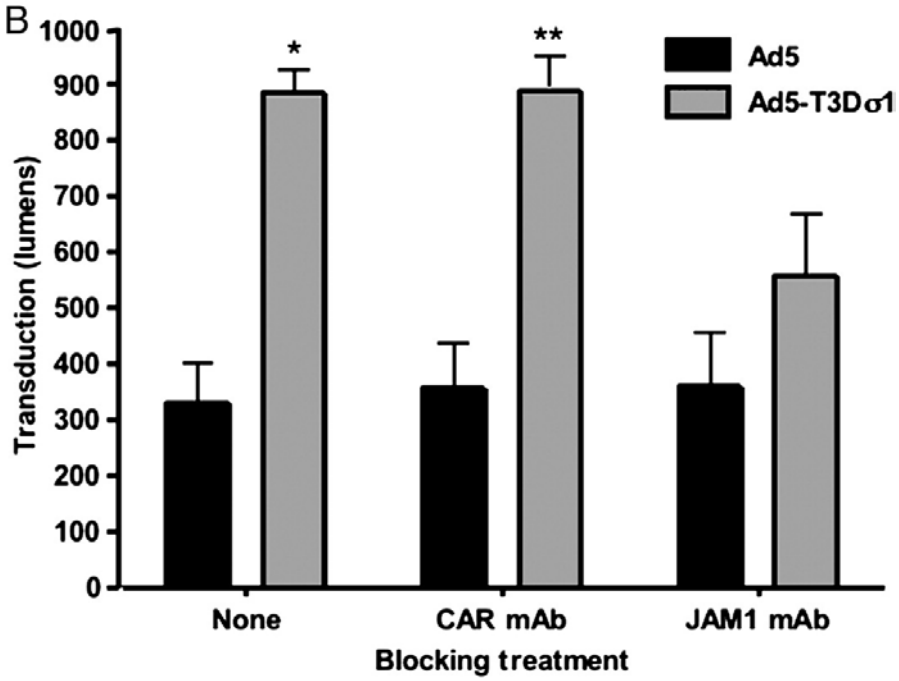

Figure 25. Ad5 and Ad5-T3Dσ1 transduction of primary human DCs. (*A*) DCs were assessed for surface expression of CAR and JAM-A by flow cytometry by using hCAR-specific mAb RmcB and hJAM-A-specific mAb J10.4, respectively. (*B*) DCs were either untreated or treated with 10 μg/ml hCAR-specific mAb RmcB (CAR mAb) or hJAM-A-specific mAb J10.4 (JAM-A mAb) before adsorption with 5,000 particles per cell of either Ad5 or Ad5-T3Dσ1. Cells were harvested 24 h later for luciferase assay. Transduction was measured in lumens. The results are presented as the means for three independent experiments. Error bars indicate SD. A paired Student's *t* test was performed to compare transduction by Ad5 versus Ad5-T3D 1 (*, $P < 0.01$; **, $P < 0.05$).

Discussion

In this study, we fused two structurally homologous viral attachment proteins, Ad fiber and reovirus σ1, to produce a functional chimeric virus, Ad5-T3Dσ1. Of the three fiber-σ1 chimeras tested, only Fibtail-T3Dσ1 bearing the Ad5 fiber virion-insertion domain fused to an almost-full-length version of T3D σ1 protein formed trimers and assembled onto Ad virions. The lack of trimerization of Fib8-T3Dσ1 and Fibshaft-T3Dσ1 was surprising, because both the head and tail regions of σ1 contain trimerization domains (69), whereas the fiber knob domain initiates and maintains trimerization (84). Because only Fibtail-T3Dσ1 formed trimers, it is likely that the C-terminal trimerization domain of σ1 is insufficient for trimerization of the fiber shaft. Alternatively, it is possible that the chimeric Fib8-T3Dσ1 and Fibshaft-T3Dσ1 proteins do not form trimers, because the fused β-spiral junctions are imperfectly matched.

In Ad5-T3Dσ1 virions, Fibtail-T3Dσ1 was encapsidated at levels comparable with wild-type fiber. Furthermore, the capsid protein profile of Ad5-T3Dσ1 is similar to that of wild-type Ad5. Most importantly, experiments using receptor-transfected cells, antibodies, and reagents that block σ1-sialic acid interactions provide compelling evidence that Ad5-T3Dσ1 displaying Fibtail-T3Dσ1 retains both the JAM-A and sialic acid-binding functions of the T3Dσ1 protein.

We envision at least four applications for chimeric Ad vectors in which the CAR-binding functions of fiber have been replaced with the JAM-A and sialic acid-binding functions of σ1. First, Ad vectors based on fiber-σ1 chimeras may serve to efficiently target mucosal sites for enhanced induction of immune responses at mucosal surfaces.

Second, because JAM-A and sialic acid are expressed on a variety of cells, Ad5-T3Dσ1 and its derivatives may have utility for transducing cells deficient in CAR (e.g., DCs and certain types of cancer cells). Third, because σ1 incorporates its own trimerization motifs, fiber-σ1 fusions may provide a trimeric scaffold for the display of other cell-targeting ligands in a manner analogous to fiber-fibritin chimeras (96). In support of this approach, we recently appended single-chain antibodies onto truncated forms of Fibtail-T3Dσ1 for delivery of Ad vectors to cells expressing antibody targets (unpublished data). Fourth, Ad vectors based on Ad5-T3Dσ1 can be used as a simple genetic platform for directed mutagenesis of σ1 for studies of reovirus tropism and receptor-linked signaling.

Recently, an additional report has been published that characterizes an Ad5 vector that produces a mosaic virus expressing both the Ad5 and reovirus attachment proteins (162). This study confirms that Ad5 tropism can be modified by the exchange or addition of the Ad5 fiber with σ1 binding properties. Interestingly, the modified Ad5-σ1 vector enhanced infectivity of cancer cell lines that lack CAR expression (162).

The opportunity to use Ad vectors encoding fiber-σ1 chimeras for mucosal targeting is especially appealing. Increased delivery of antigens to intestinal epithelial cells and Peyer's patch lymphocytes by such vectors might result in more potent and less toxic gene-based vaccines. Reovirus binds to murine microfold cells (1, 189, 190), and the σ1 protein plays an important role in conferring this tropism (1, 80). Interactions of Ad5-σ1 vectors with microfold cells may facilitate efficient delivery to underlying Peyer's patches for induction of immune responses in the gut. Alternatively, σ1-bearing Ad vectors may directly infect DCs at the luminal surface, which are known to shuttle bacteria across epithelial monolayers by opening tight junctions and sampling the intestinal lumen (132).

DCs express tight junction proteins, including JAM-A (132), which are hypothesized to facilitate epithelial barrier penetration. Our finding that Ad5-T3Dσ1 transduces primary DCs more efficiently than wild-type Ad5 suggests that Ad5-σ1 vectors may be useful for antigen gene delivery to DCs in the intestine and other sites.

Findings described in this report indicate that Ad vectors can be efficiently targeted to cells expressing JAM-A and sialic acid by the reovirus attachment protein σ1. By virtue of the capacity to infect both intestinal epithelial cells and DCs, Ad5-σ1 vectors may have utility in the induction of immune responses at mucosal surfaces and thus prevention of infection at the site of pathogen entry. These vectors also will allow a precise determination of the contribution of the JAM-A- and sialic acid-binding properties of σ1 to interactions of σ1 with cells *in vivo*. This approach should lead to improved Ad vectors for gene delivery and enhance an understanding of σ1 biology.

CHAPTER V

REOVIRUS ENTRY INTO POLARIZED EPITHELIAL CELLS DISRUPTS TIGHT JUNCTION INTEGRITY

Introduction

JAM-A is essential for reovirus infection of numerous cell types (10, 109, 129). However, the biochemical consequences of reovirus interactions with JAM-A in tight junctions have not been elucidated. JAM-A is an important component of tight junctions that form between endothelial and epithelial cells (102, 106, 123). Tight junctions serve as a semipermeable barrier between cells, establish distinct apical and basolateral regions in polarized epithelia, and function as critical sites for endocytosis and signaling (7, 197).

Tight junctions are composed of transmembrane proteins clustered at the apical portion of the lateral membrane (112). These transmembrane proteins are adhesion molecules that mediate cell-cell contacts (7, 197). Scaffolding proteins are tethered to the cytoplasmic tails of the transmembrane proteins. These proteins are involved in the recruitment and maintenance of the junctional complex (112).

The cytoplasmic tail of JAM-A interacts with several tight junction-associated proteins, including AF-6 (59), PAR-3 (60, 88), and ZO-1 (19, 59) in a PDZ-domain-dependent manner. ZO-1 belongs to the zonula occludens family, which also includes ZO-2 and ZO-3. The zonula occludens family of proteins is hypothesized to function in mediating protein-protein interactions through modular PDZ domains and participate as components of signal transduction pathways (72). ZO-1 functions as a transcriptional regulator through its interactions with ZO-1–associated nucleic acid binding protein (ZONAB) (6).

It is not known how reovirus accesses JAM-A on polarized cells, nor whether reovirus binding to JAM-A leads to intracellular signaling events that influence viral

replication or alter tight junction integrity. In the infected host, reovirus might engage JAM-A on the apical surface of intestinal epithelial cells. Since JAM-A is a tight junction protein, apical infection by reovirus would require disruption of tight junctions to liberate the receptor. Reovirus also may infect the basolateral surfaces of intestinal cells following transcytosis through microfold (M) cells (191). Current data do not favor one model over the other.

To determine the route by which reovirus infects polarized cells most efficiently and to elucidate whether reovirus alters the tight junction protein complex during viral attachment and internalization, we utilized MDCK and Caco-2 cell culture systems, which are well-established models for studies of tight junctions in polarized epithelium (144). We found that reovirus preferentially infects the apical surface of polarized cells and that infection is dependent on JAM-A. Reovirus binding to polarized cells alters the distribution of JAM-A and tight junction-associated protein ZO-1 and induces disruptions in transepithelial resistance (TER) of infected epithelial monolayers. These results suggest that reovirus disrupts tight junction integrity during viral entry.

Results

Reovirus entry into cells disrupts JAM-A distribution

To test whether reovirus alters the distribution of JAM-A during entry, we examined the intracellular localization of this receptor during a timecourse of reovirus entry into JAM-A-expressing CHO cells. Cells were grown on glass coverslips and adsorbed with T1L at 4^{o}C for 45 min. The inoculum was replaced with fresh medium, and cells were incubated at 37^{o}C. Cells were fixed in methanol and stained for JAM-A at 10 min intervals for 60 min. Subcellular distribution of these proteins was determined by using immunofluorescence

microscopy (Figure 26). In the untreated and 0 min timepoints, JAM-A localization was tightly confined to regions of cell-cell contact. At early timepoints following reovirus infection, JAM-A was apparent in the cytoplasm. After 30 minutes of infection the JAM-A signal was localized to punctate bodies within the cytoplasm with minimal staining at the cell surface. These results demonstrate that reovirus entry into JAM-A-expressing cells induces receptor internalization.

Apical infection of polarized cells by reovirus is JAM-A-dependent

To investigate whether reovirus preferentially infects apical or basolateral surfaces of polarized cells, Caco-2 cells were grown on transwell supports and allowed to form polarized monolayers. The extent of polarization of the transwells was determined by measuring the TER prior to the onset of experimentation. Cells were adsorbed either apically or basolaterally with T1L and incubated at 37^{o}C for 24 h. Following incubation, infected cells were quantified using an immunofluorescence assay (Figure 27). We found that apical infection of Caco-2 cells by T1L was substantially more efficient than basolateral infection.

To test the requirement for JAM-A as a receptor in polarized cells, Caco-2 cells were grown to confluency on glass coverslips and treated with JAM-A-specific mAb J10.4 prior to apical infection with T1L. Pretreatment of cells with JAM-A-specific mAb J10.4 efficiently reduced T1L infection (Figure 28). These findings suggest that apical infection of Caco-2 cells by T1L is dependent on utilization of JAM-A as a receptor.

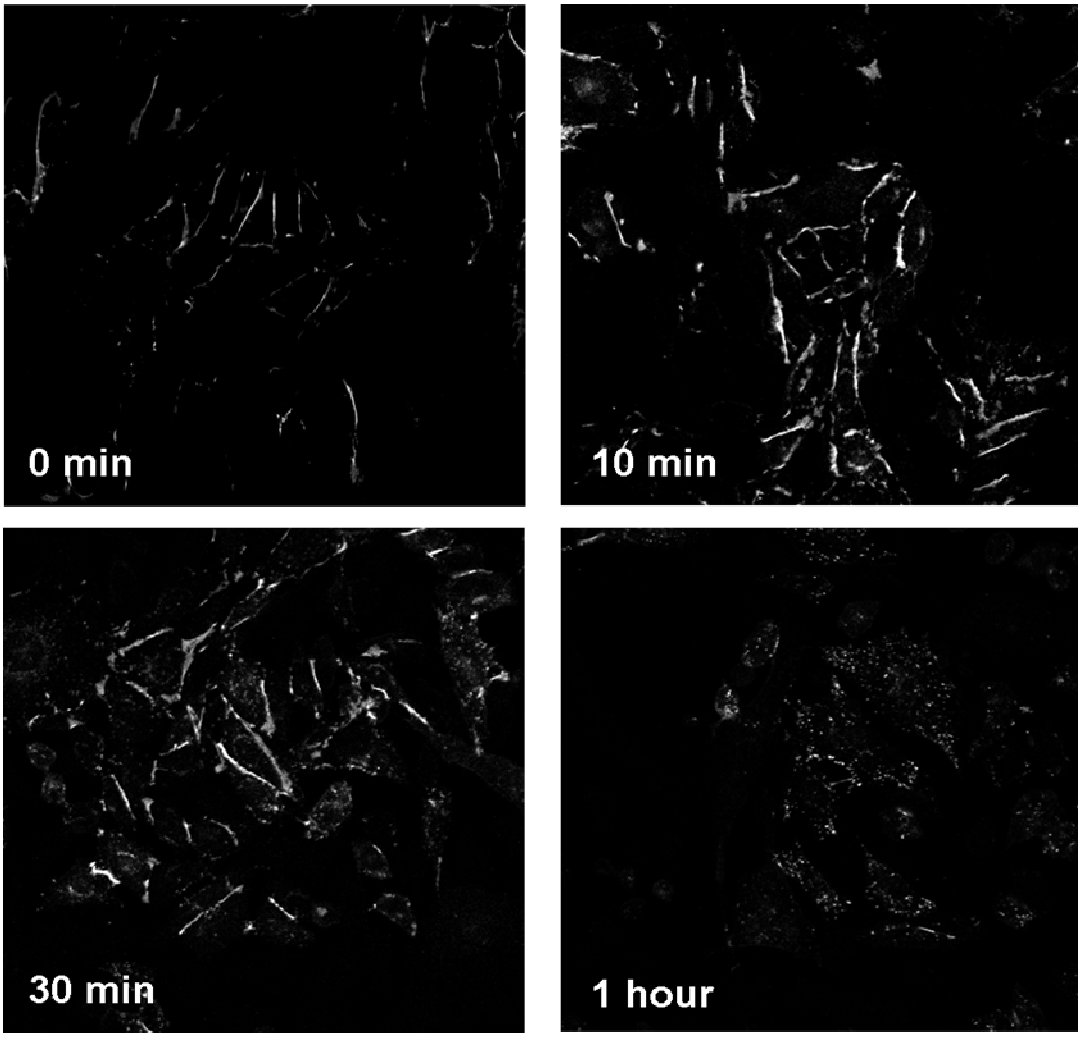

Figure 26. Reovirus infection of JAM-A-expressing cells alters JAM-A localization. JAM-A expressing CHO cells were grown to confluency on glass coverslips. Monolayers were adsorbed T1L at an MOI of $5X10^3$ particles per cell at 4°C for 45 min. Cells were warmed to 37°C for the times shown, stained with JAM-A-specific mAb J10.4, and visualized using immunofluorescence microscopy.

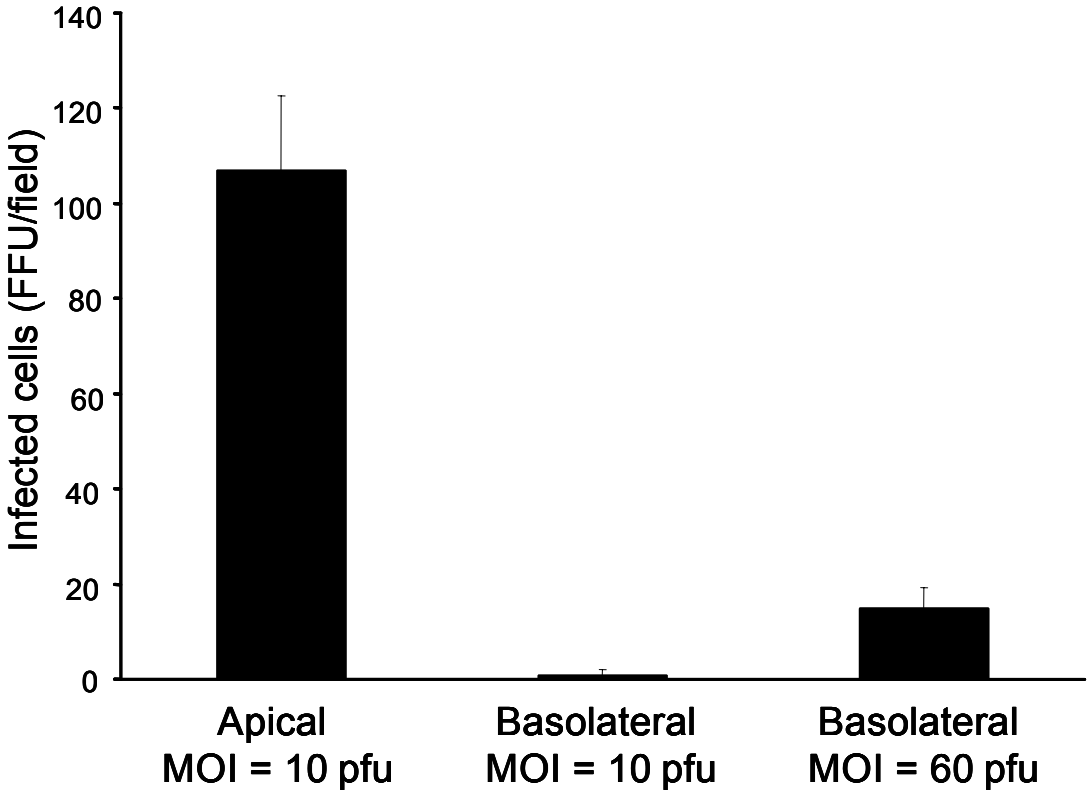

Figure 27. Reovirus infection is most efficient following adsorption to the apical surface of polarized cells. Caco-2 cells were plated to confluency on 0.33-cm^2 permeable supports and cultured for 14 days. Monolayers were adsorbed either apically or basolaterally with T1L at an MOI of 10 or 60 PFU per cell. Infected cells were detected by indirect immunofluorescence and quantified by counting fluorescent cells in three random fields of view per well in three wells. Error bars indicate standard deviations.

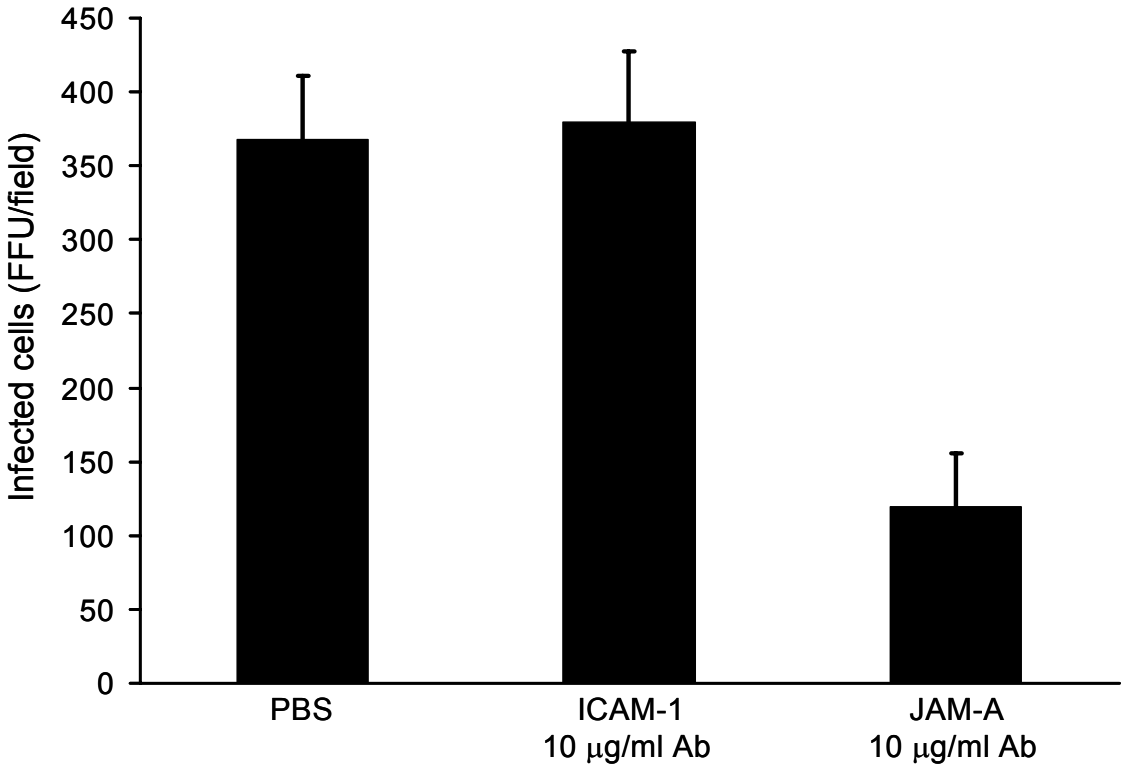

Figure 28. Apical infection of polarized cells is JAM-A dependent. Caco-2 cells were grown to confluency on glass coverslips. Monolayers were adsorbed apically with T1L at an MOI of 10 PFU per cell in the presence or absence of PBS, anti-ICAM-1 mAb, or anti-hJAM-A mAb J10.4. Infected cells were detected by indirect immunofluorescence and quantified by counting fluorescent cells in three random fields of view per well in three wells. For both experiments, results are presented as the mean FFU per field. Error bars indicate standard deviations.

Reovirus entry of polarized cells alters ZO-1 localization

To test whether reovirus alters the distribution of tight junction proteins, we examined the intracellular location of ZO-1, which interacts with the JAM-A cytoplasmic tail (19, 59), during a timecourse of reovirus entry into epithelial cells. Confluent MDCK cells were adsorbed with reovirus T1L, and ZO-1 location was monitored by immunofluorescence microscopy (Figure 29). ZO-1 was redistributed from regions of intercellular contacts to the cytoplasm and nucleus during the 40 min observation interval, coincident with reovirus entry and disassembly (5, 153). Thus, reovirus entry into MDCK cells alters the intracellular distribution of JAM-A-associated protein ZO-1, suggesting that reovirus perturbs the function of epithelial tight junctions.

Reovirus entry of polarized epithelial cells alters TER

To test whether reovirus binding to JAM-A disrupts the barrier activity of tight junctions in polarized cells, polarized MDCK cells were grown on transwell supports and adsorbed with T1L at 37^{o}C. The monolayers were monitored at 15-min intervals for a total of 120 min for changes in TER using an epithelial volt-Ohm meter (Figure 30). As negative controls, cells were treated in the absence of viral adsorption with PBS or pretreatment with

JAM-A-specific mAb J10.4, which does not disrupt intact tight junctions (102). Reovirus induced a time-dependent increase in paracellular permeability with kinetics that paralleled the redistribution of ZO-1. Importantly, reovirus-induced alterations in TER were diminished by incubation of cells with J10.4 mAb prior to viral adsorption. These findings suggest that reovirus alters tight junction integrity, which may be important for viral growth in certain types of cells and dissemination in the host.

Reovirus entry of non-polarized cells alters ZO-1 localization

Experiments described thus far demonstrate that reovirus binding to JAM-A alters the subcellular distribution of ZO-1 during a timecourse of reovirus entry into polarized cells. ZO-1 is also expressed in non-polarized cell types that are permissive for reovirus infection (87, 101). To confirm that ZO-1 redistributes during reovirus entry, HeLa cells were adsorbed with reovirus T3D and incubated at 37^{o}C for 0 or 30 minutes. Nuclear and cytoplasmic extracts were prepared after lysis in a hypotonic buffer containing 10 mM HEPES (pH 7.9), 10 mM KCl, and 1.5 mM $MgCl_2$. Nuclear and cytoplasmic proteins were resolved by SDS-PAGE and immunoblotted using a ZO-1-specific polyclonal antiserum (Figure 31). Following entry of T3D, the relative abundance of ZO-1 in the cytoplasm was diminished in comparison to mock infection. Additionally, a cleavage fragment of ZO-1 appears in the nucleus 30 minutes following infection with T3D. These biochemical data compliment the observation of ZO-1 nuclear accumulation following reovirus entry using immunofluorescence microscopy and suggest that reovirus internalization leads to a redistribution of ZO-1 from the cell surface to the nucleus.

Discussion

Although many examples exist of viruses utilizing cell adhesion molecules as receptors, little is known about how viral attachment proteins encounter these subcellularly restricted proteins and the cellular response of these interactions. We have previously demonstrated that JAM-A is a serotype-independent reovirus receptor and that efficient entry of reovirus into numerous cell types including HeLa, CHO, and dendritic cells is dependent on JAM-A utilization (10, 109, 129). Prior to studies in this chapter, it was unknown what role JAM-A plays in reovirus infection of polarized cells.

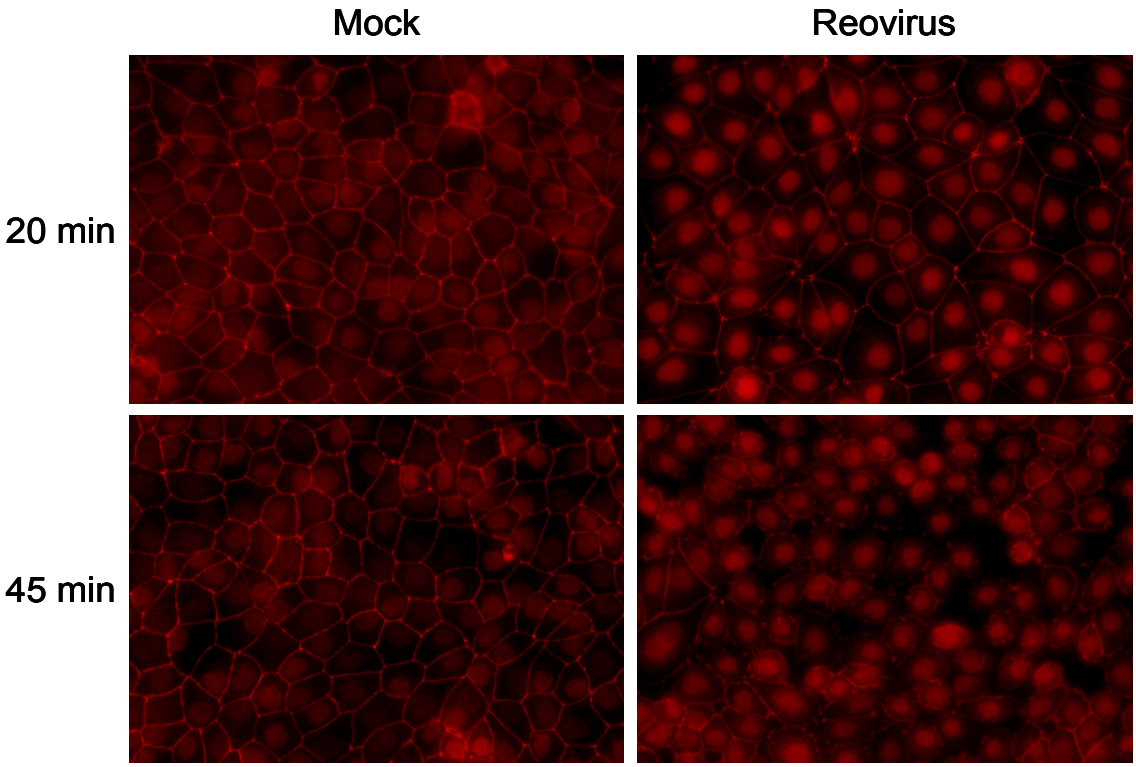

Figure 29. Intracellular distribution of ZO-1 following reovirus infection of MDCK cells. MDCK cells were plated to confluency and cultured for five days. Cells were either infected with T1L at an MOI of 10^2 PFU per cell or treated with PBS (mock). Cells were incubated at 37°C for the times shown, stained with a polyclonal ZO-1 antiserum, and visualized using immunofluorescence microscopy.

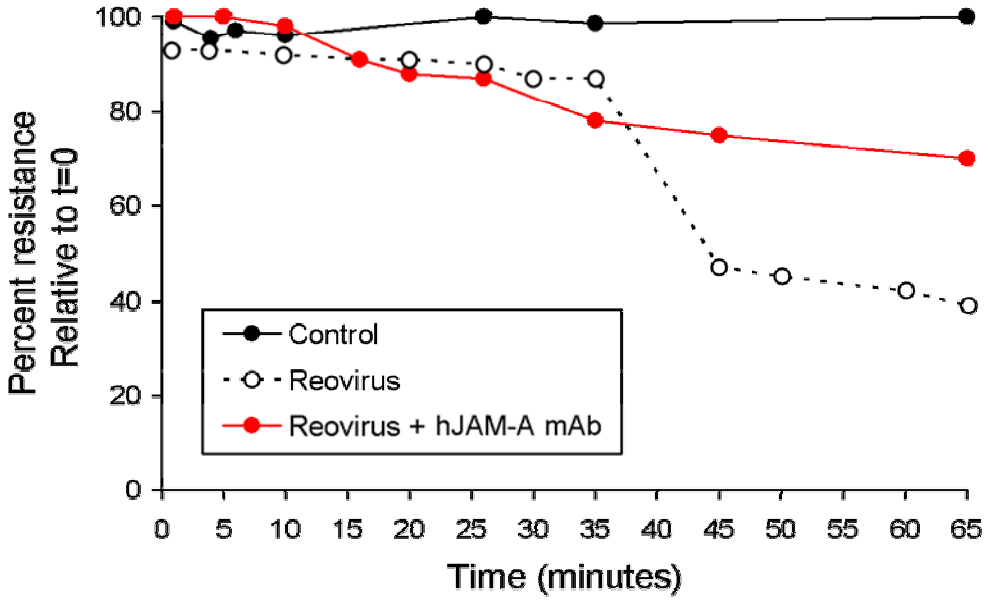

Figure 30. Changes in TER following reovirus infection of MDCK cells. MDCK cells were plated to confluency on 0.33-cm^2 permeable supports and cultured for 12 days. Monolayers were adsorbed apically with PBS (control) or T1L at an MOI of 10^2 PFU per cell in the presence or absence of anti-hJAM-A mAb J10.4 (hJAM-A mAb). Monolayers were monitored for changes in TER for the times shown using an epithelial volt-Ohm meter. The results are presented as percent resistance relative to the zero time point (baseline resistance = 350 Ω).

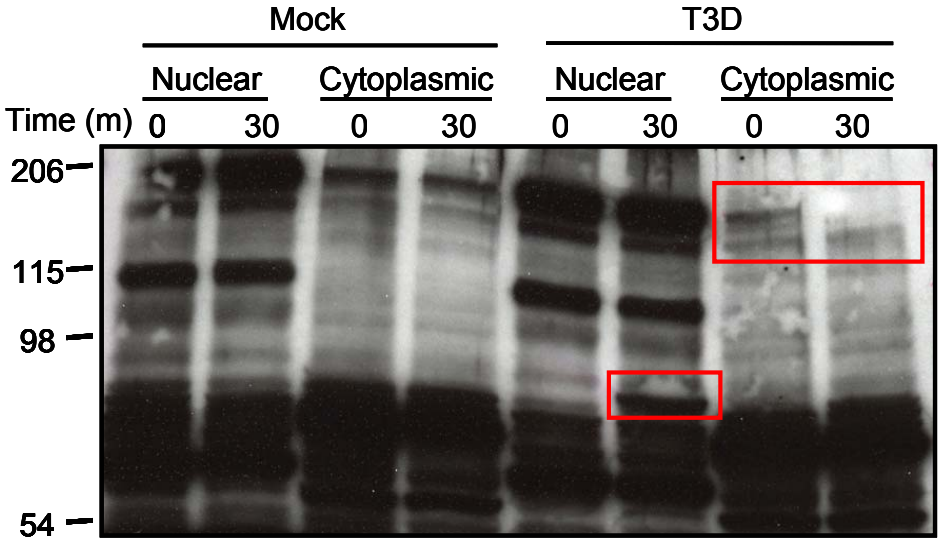

Figure 31. Reovirus entry into HeLa cells alters ZO-1 distribution. HeLa cells were plated to confluency and adsorbed with T3D at an MOI of 100 PFU per cell for 0 or 30 minutes. At the indicated timepoints, nuclear and cytoplasmic extracts were prepared, resolved by SDS-PAGE, and immunoblotted using a polyclonal ZO-1-specific antiserum. Positions of MW standards (in kD) are shown.

Results presented here demonstrate that reovirus infection of polarized epithelial cells is most efficient following apical adsorption and is dependent on JAM-A utilization. At early time points in reovirus infection, JAM-A redistributes from regions of cell-cell contact to punctuate bodies within the cytoplasm. Concurrently, ZO-1 localization changes from regions of intercellular contacts to the cytoplasm and nucleus. Paracellular permeability as assessed by TER is increased with kinetics that parallel the redistribution of ZO-1. Reovirus-induced TER alterations are diminished with pretreatment with JAM-A-specific mAb J10.4, demonstrating that these effects are JAM-A dependent.

The capacity of reovirus to use JAM-A as a receptor has implications for reovirus infection and pathogenesis. Regulation of tight junction formation is important for development and maintenance of epithelial and endothelial barriers (17). JAM-A-specific mAbs prevent the reorganization of disrupted tight junctions in cultured intestinal epithelial cells (102) and promote tight junction breakdown of the endothelium lining CNS blood vessels, resulting in enhanced disease in response to viral or bacterial infections (98). If reovirus-JAM-A interactions lead to a similar destabilization of tight junctions in CNS endothelium, this effect might promote disruption of the blood-brain barrier, permitting cerebral edema and neural inflammation, conditions associated with reovirus-induced encephalitis (10, 71, 165) .

Reovirus-induced tight junction dysregulation within the intestinal epithelium might promote infection of enteric epithelial cells and underlying Peyer's patches, thereby providing an opportunity for systemic dissemination. A similar mechanism has been proposed for adenovirus interactions of epithelial surfaces. During adenovirus infection, the viral fiber protein is shed from infected cells and binds to its receptor, CAR, which like JAM-A, is also expressed at tight junctions (43). Fiber-CAR interactions are hypothesized to disrupt tight junctions and allow virus escape (179). This model fits with data presented in

Chapter II demonstrating that σ1 binds to residues involved in JAM-A homodimer formation, which provides support for the idea that σ1-JAM-A interactions may disrupt tight junctions.

Until recently, ZO-1 was presumed to function primarily as a tight junction regulator through its action as an organizational scaffold that tethers transmembrane proteins to signaling molecules and the cytoskeleton (61, 62, 110). The discovery that ZO-1 acts in concert with ZONAB as a transcriptional regulator suggests that tight junction proteins serve as platforms for cell signaling at both the cell membrane and the nucleus. To date, the only stimuli identified to result in nuclear accumulation of ZO-1 are the remodeling of cell-cell contacts of maturing monolayers and wound healing (74). Our finding that reovirus-JAM-A interactions result in a nuclear translocation of ZO-1 suggests that ZO-1 is involved in cellular responses elicited by microbes.

Utilization or disruption of tight junctions is a common theme for many microorganisms including viruses, bacteria, and fungi (38, 143, 179). This theme of disrupting or commandeering tight junction proteins by diverse pathogens may highlight common signaling strategies, one of which may be to modulate the transcriptional machinery to render the cell more permissive for pathogen replication. For example, disruption of tight junctions and accumulation of ZO-1 in the nucleus could induce cytoskeletal rearrangements, induce signal transduction events, and alter the transcriptional program of the cell. Any of these events could result in a more favorable environment for pathogen growth and dissemination. Alternatively, microbial-induced disruption of tight junctions may result in induction of innate host defense mechanisms. Rapid relocalization of ZO-1 or other junctional proteins to the nucleus may serve a cellular sensor function in which tight junction disruption is an early indicator of cellular invasion.

The discovery that reovirus-JAM-A interactions leads to a redistribution of ZO-1,

expands our knowledge of the physiologic effects of virus-receptor interactions and highlights a potential role for the tight junction in regulating the cellular response to viral infection. This work expands our understanding of viral receptors and highlights that they are not simply attachment moieties. Virus-receptor interactions are capable of disrupting cell-cell interactions and induce signal transduction pathways. It will be fascinating to explore the biological consequences of these biochemical events elicited by reovirus receptor engagement.

CHAPTER VI

SUMMARY AND FUTURE DIRECTIONS

The first step in viral replication is mediated by a specific and structurally regulated relationship between the viral attachment protein and its cognate receptor. Defining the precise interactions that mediate virus-receptor engagement is crucial for understanding the mechanisms underlying viral pathogenesis. Although many viral receptors have been identified, little is known about the biophysical events that mediate cellular entry, the involvement of viral replication in signal transduction, and the function of these molecules in viral tropism and pathogenesis. A thorough understanding of mechanisms of viral attachment is essential for uncovering the role of receptors in pathogenesis at an organismal level and the rational design of antiviral therapeutics targeting the virus attachment step. The work described in this dissertation was performed to enhance an understanding of structure-function relationships between σ1 and JAM-A and to seek insight into the physiological consequences of reovirus-receptor engagement.

The data presented in this thesis support the following conclusions: 1) reovirus attachment is achieved through binding of the D-E loop of σ1 to the JAM-A dimer interface (Chapter II and III); 2) in polarized epithelial cells, the binding of σ1 to the JAM-A dimer interface disrupts tight junction integrity (Chapter V); 3) and disruption of tight junction integrity by reovirus leads to the internalization of JAM-A and subsequent nuclear re-distribution of ZO-1 (Chapter V). This chapter summarizes the data presented in this dissertation and highlights future directions for this research.

Molecular mechanisms of reovirus attachment

Results from Chapter II demonstrate that JAM-A is a serotype-independent reovirus receptor and the only JAM family member capable of mediating reovirus entry. This work led to the identification of a highly conserved cluster of residues found at the base of the σ1 head termed the D-E loop. The D-E loop is a logical candidate for a receptor-binding domain because it is highly conserved among JAM-A-binding strains, it is surface exposed, and it is accessible to a ligand.

Future studies should be directed toward definition of the specific interactions that govern σ1 engagement of JAM-A. To test the hypothesis that the D-E loop mediates JAM-A binding, mutations can be engineered into a bacterially expressed GST-T3D σ1 head construct using PCR-based methods. The affinities of purified mutant σ1 proteins for JAM-A can be determined by surface plasmon resonance. After identification of mutant σ1 proteins that exhibit a decreased affinity for JAM-A, the biological relevance of these mutations should be tested by using the reovirus-Ad5 chimera system (Chapter IV). Should results from experiments using chimeric adenoviruses be difficult to interpret, full-length wt and mutant σ1 proteins, along with outer-capsid proteins σ3 and μ1, can be expressed in insect cells using recombinant baculoviruses and recoated onto reovirus core particles (33). Recoated core particles can be tested for the capacity to bind and infect cells.

The experiments described in Chapter III identified the D1 domain of JAM-A to be both necessary and sufficient for reovirus binding and infection. The D1 domain is the membrane distal immunoglobulin-like domain that mediates JAM-A homodimerization. Subsequent to this work, mutagenesis studies demonstrated that residues intimately associated with the JAM-A dimer interface are critical for reovirus interactions with JAM-A (63). This finding suggests that σ1 engages JAM-A using sequences involved in

dimer formation. To test this theory and establish the structural basis of JAM-A interactions with σ1, the structures of σ1 in complex with JAM-A should be solved using X-ray crystallography. This work is currently being performed in collaboration with the laboratory of Thilo Stehle.

The role of JAM-A in reovirus-induced disruptions of tight junction integrity

The experiments described in Chapter V we determined that apical route entry of reovirus is most permissive for reovirus infection of polarized epithelial cells. This infection is dependent on binding to JAM-A and results in disruption of JAM-A localization during a timecourse of reovirus entry. Additionally, infection of polarized epithelial cells results in alteration of ZO-1 localization and an increase of paracellular permeability, suggesting that reovirus entry disrupts tight junction integrity.

Immediate future steps should focus on defining the minimal viral components necessary for disruption of tight junction integrity and the physiological consequences of this alteration. To determine whether changes in the distribution of tight junction-associated proteins are attributable to σ1 interactions with JAM-A, virus should be treated prior to adsorption T1 σ1-specific mAb which blocks reovirus binding to JAM-A. I predict that antibody treatment will inhibit the capacity of reovirus to alter the intracellular distribution of JAM-A and JAM-A-associated proteins. Additionally, a bacterially expressed T3D σ1 head construct should be used in experiments to study the capacity of σ1, in the absence of other viral components, to disrupt tight junction integrity.

To test whether alterations in tight junction protein distribution require steps in reovirus replication subsequent to attachment, cells should be treated with either ammonium chloride, which arrests acid-dependent disassembly of virions in cellular endosomes (51,

153) or ribavirin, which blocks viral transcription (130). Given the tempo of the observed changes, less than 1h, I anticipate that neither treatment will interfere with the capacity of reovirus to alter the distribution of JAM-A and JAM-A-associated proteins following attachment.

To define the dynamics of tight junction disruption and ZO-1 distribution during reovirus entry into living cells, we will use a ZO-1-green fluorescent protein (GFP) fusion construct can be used (133). ZO-1-GFP exhibits subcellular colocalization with endogenous ZO-1 and has no demonstrable effects on cell growth or TER of transfected cells (133). MDCK cells should be transfected with ZO-1-GFP, infected with reovirus, and imaged for ZO-1 localization using confocal video microscopy for real-time analysis.

To investigate the role of ZO-1 in reovirus entry and infection, epithelial cells lacking ZO-1 expression should be infected and monitored for alterations in tight junction integrity, reovirus entry, and infection (169). ZO-1 has been demonstrated to alter transcriptional regulation following migration to the nucleus (6). It would be interesting to investigate whether reovirus-induced nuclear localization of ZO-1 results in alteration of the transcriptional program. To test this hypothesis, ZO-1 deficient cells can be utilized to define gene expression patterns through microarray analysis following reovirus infection in the presence and absence of ZO-1 expression.

The role of JAM-A in reovirus pathogenesis

JAM-A is a receptor for prototype and field-isolate strains of reovirus. However, the function of JAM-A in reovirus-induced disease is unknown. The dramatic differences exhibited by T1 and T3 reovirus strains in viral tropism and disease in mice segregate with the σ1-encoding S1 gene [Weiner, 1980 #210;[Weiner, 1977 #189;Weiner, 1980

#210;Tardieu, 1982 #212;Dichter, 1984 #147]]. These findings suggest that different reovirus serotypes engage unique receptors and that receptor distribution is an important determinant of reovirus pathogenesis. However, all reovirus strains tested to date are capable of using JAM-A as a receptor (10, 29). I think it possible that JAM-A serves as a serotype-independent reovirus receptor at some sites in the host, and other as yet unidentified receptors may confer serotype-dependent tropism in the CNS. In support of this possibility, a p65/p95 complex has been suggested to serve as a T3 reovirus receptor in the murine nervous system (131). Alternatively, utilization of coreceptors, perhaps carbohydrate in nature, may permit reovirus infection of specific cells or tissues. In support of this idea, reovirus strains that vary in sialic acid binding also vary in cell tropism and disease pathogenesis in the hepatobiliary system (11). To distinguish between these possibilities, JAM-A-null mice should be infected with reovirus strains that bind to JAM-A but not sialic acid and monitor infected mice for viral growth and disease. If JAM-A is a tissue-specific reovirus receptor, reovirus should infect some sites in JAM-A-null mice but not others. If coreceptor utilization is required for tropism in the context of JAM-A expression, JAM-A-null mice should be resistant to reovirus infection.

Conclusions

With this research, we seek to establish a precise understanding of virus-receptor interactions in reovirus target-cell selection and pathogenesis. The studies performed in this thesis are a blend of molecular genetics, cell imaging, and structural analyses designed to provide a comprehensive assessment of the structure and function of reovirus attachment protein σ1 and its cell-surface receptors. The long-term goal of this work is to identify key intermolecular interactions between virus and the cell that define obligate, sequential steps

leading to tissue- and organ-specific infection and disease. Knowledge gained fron this research also might enable the targeting of vaccine or gene therapy vectors, such as σ1-expressing chimeric adenoviruses, to specific sites in the host. Identification of signaling pathways activated by reovirus binding would represent a particularly intriguing area of future research. Experiments to extend such observations will be designed to explore how receptor-linked signaling pathways influence viral growth and cell death. Because this work affords the opportunity to couple atomic resolution studies of reovirus-receptor interactions with studies of reovirus target cell selection in the infected host, it may serve as a general model for ligand-receptor binding and aid in the rational design of anti-infective therapies based on inhibition of pathogen-receptor interactions.

CHAPTER VII

DETAILED METHODS OF PROCEDURE

Cells, viruses, and antibodies

Spinner-adapted murine L929 (L) cells were grown in either suspension or monolayer cultures in Joklik's modified Eagle's minimal essential medium (Irvine Scientific, Santa Ana, Calif.) supplemented to contain 5% fetal bovine serum (Gibco-BRL, Gaithersburg, Md.), 2 mM L-glutamine, 100 U of penicillin per ml, 100 mg of streptomycin per ml, and 0.25 mg of amphotericin per ml (Gibco-BRL). HeLa, MDCK, and Caco-2 cells were maintained in monolayer cultures in Dulbecco's minimal essential medium (Gibco-BRL) supplemented to contain 10% fetal bovine serum, L-glutamine, and antibiotics as described for L cells. Chinese hamster ovary (CHO) cells were maintained in Ham's F12 medium supplemented with fetal bovine serum, L-glutamine, and antibiotics as described for HeLa cells.

The prototype reovirus strains T1L/53, T2J/55, and T3D/55 are laboratory stocks. The field-isolate reovirus strains used in this study are shown in Table 1. Variant K, a neutralization-resistant variant of T3D/55, was selected and characterized as previously described (15, 148, 149). Green fluorescent protein-encoding serotype 5 adenovirus (Ad 5-GFP) was provided by Dr. Jeffrey Bergelson (University of Pennsylvania). Viral stocks were prepared by plaque purification and passage in L cells (173). Purified virions were prepared by using second- and third-passage L-cell lysate stocks as previously described (66, 135). Viral particle concentrations were determined by measurements of the optical density at 260 nm, using a conversion factor of 2.1×10^{12} viral particles per optical

density unit (146). The particle-to-PFU ratio of stocks used for viral infectivity assays was approximately 250 to 1.

Rabbit hCAR-specific antiserum was provided by Jeffrey Bergelson (University of Pennsylvania). Rabbit polyclonal hJAM-B- and hJAM-C-specific antisera were generated as previously described (70). The murine hJAM-A-specific monoclonal antibody (MAb) J10.4 was purified from mouse ascites by using protein A-Sepharose (102). The immunoglobulin G (IgG) fractions of polyclonal rabbit antisera raised against T1L/53 and T3D/55 (186) were purified by using protein A-Sepharose (9). A mixture of these sera was capable of recognizing all strains of reovirus used in this study.

Fluorescent-focus assays of viral infectivity

Monolayers of HeLa cells in 96-well plates (Costar, Cambridge, Mass.) (3×10^4 cells per well) were pretreated for 1 h with phosphate-buffered saline (PBS), hCAR-specific antiserum, or the hJAM-A-specific MAb J10.4 at various concentrations prior to the adsorption of virus at room temperature for 1 h. Following removal of the inoculum, the cells were washed with PBS and incubated at 37°C for 20 h to permit the completion of a single round of viral replication. Monolayers were fixed with 1 ml of methanol at –20°C for a minimum of 30 min, washed twice with PBS, blocked with 2.5% immunoglobulin-free bovine serum albumin (Sigma-Aldrich, St. Louis, Mo.) in PBS, and incubated at room temperature for 1 h with protein-A-affinity-purified polyclonal rabbit anti-reovirus serum at a 1:800 dilution in PBS-0.5% Triton X-100. The monolayers were washed twice with PBS-0.5% Triton X-100 and incubated with a 1:1,000 dilution of goat anti-rabbit immunoglobulin conjugated with the Alexa Fluor 546 fluorophore (Molecular Probes, Eugene, Oreg.). The monolayers were washed twice with PBS, and infected cells were visualized by indirect

immunofluorescence using an Axiovert 200 inverted microscope modified for fluorescence microscopy (Carl Zeiss, New York, N.Y.). Infected cells were identified by the presence of intense cytoplasmic fluorescence that was excluded from the nucleus. No background staining of uninfected control monolayers was noted. Reovirus antigen-positive cells were quantified by counting the fluorescent cells in at least three random fields of view per well in triplicate at a magnification of x20.

Transient transfection and infection of CHO cells

CHO cells were transiently transfected with an empty vector or with plasmids encoding receptor constructs by the use of Lipofectamine PLUS reagent (Invitrogen, San Diego, Calif.) as previously described (10). After 24 h of incubation to allow receptor expression, transfected cells were allowed to adsorb to the virus at a multiplicity of infection (MOI) of 1 fluorescent focus unit (FFU) per cell, incubated for an additional 20 h, fixed with methanol, and stained for reovirus proteins by use of an antireovirus serum at a 1:800 dilution. Images were captured at a magnification of x20 with a Zeiss Axiovert 200 inverted microscope.

Sequence analysis of the S1 gene

Viral genomes were extracted from infected L-cell lysates by the use of Trizol (Life Technologies, Rockville, Md.) according to the protocol supplied by the manufacturer. S1 gene segments were amplified by reverse transcription-PCR (RT-PCR) using 10 U of avian myeloblastosis virus reverse transcriptase (Promega Biosciences, San Luis Obispo, Calif.), 2.5 U *Taq* DNA polymerase (Promega Biosciences), and primers complementary to the 5' and 3' nontranslated regions of the S1 genes of the reovirus prototype strains. The type 1 S1 forward primer was 5' GGATCCGCTATTCGCGCCTATGGATG, and the reverse primer

was 5' GGGTTCGCGCTAGATTCA. The type 2 S1 forward primer was 5' GCTATTCGCACTCATGTCGGATCTAGTGCAGC, and the reverse primer was 5' GATGAGTCGCCACTGTGCCGAGTGGA. The type 1 5' forward primer contained nucleotides that resulted in a primer-derived sequence for the first two amino acids (M and D), and the type 2 5' forward primer contained nucleotides that resulted in a primer-derived sequence for the first six amino acids (M, S, D, L, V, and Q). The amplification products were cloned into the pCR 2.1 vector (Invitrogen). Sequences of at least two independent RT-PCR clones for each S1 gene segment were determined by automated sequencing.

Phylogenetic analysis of S1 gene nucleotide sequences

Sequences were aligned by using the program ClustalX (159). Phylogenetic trees were constructed from variations in the σ1-encoding S1 gene nucleotide sequences by the maximum parsimony method using the heuristic search algorithm within the program PAUP v4.0b10 (154). Trees were rooted at the midpoint. The branching orders of the phylograms were verified statistically by resampling the data 1,000 times in a bootstrap analysis using the branch and bound algorithm as applied in PAUP.

Sequence alignment and structural modeling methods

Sequences were aligned by using the program ClustalW (http://www.ebi.ac.uk/clustalw/). Alignments were rendered in ALSCRIPT (12), using different colors to highlight different degrees of sequence similarity. Sequence changes were mapped onto the crystal structure of T3D/55 σ1 (37) by using the program GRASP (118).

Generation of chimeric and mutant receptor constructs

Nomenclature of chimeric and deletion mutant constructs indicates exchanged or deleted domains relative to wild-type hCAR or hJAM-A from amino to carboxyl termini. Chimeric receptor CJJ (hCAR residues 1-141; hJAM-A residues 133-299) and deletion mutants JΔJ (hJAM-A residues 133-234 deleted) and ΔJJ (hJAM-A residues 29-132 deleted) were generated using PCR to insert a HindIII endonuclease restriction site at the 3' or 5' end of respective amino-terminal or carboxyl-terminal receptor fragments. Chimera JCJ (hJAM-A residues 1-128, hCAR residues 138-227, hJAM-A residues 235-299) and full-length D1 point mutant receptors were generated by overlap extension PCR. All chimeric and mutant receptor PCR products were digested with restriction endonucleases and ligated into plasmid pcDNA3.1+ (Invitrogen). The fidelity of cloning was confirmed by automated sequencing.

Flow cytometric analysis of receptor expression and virus binding

CHO cells were transiently transfected and incubated for 24 h to allow receptor expression. Cells were detached from plates by incubation with 20 mM EDTA in PBS. Cells (1×10^6) were incubated with hCAR- or hJAM-A-specific antiserum at dilutions of 1:750 or 1:1000, respectively, or incubated with reovirus T1L or T3SA- (1×10^5 particles/cell) on ice for ~60 min. Virus-adsorbed cells were washed with PBS and incubated with clarified, combined T1L/T3D antiserum at 1:1000 dilution on ice for ~60 min. All samples were washed with PBS and incubated with phycoerythrin-conjugated goat anti-rabbit IgG secondary antiserum (Molecular Probes, Inc.) at a 1:1000 dilution on ice for ~30 min. Cells were washed twice with PBS and fixed with 2% paraformaldehyde in PBS. Cells were analyzed using a FACScan flow cytometer (Becton-Dickinson).

Transient transfection and infection of CHO cells expressing chimeric receptor constructs

CHO cells were transiently transfected with empty vector or plasmids encoding wild-type, chimeric, or deletion mutant receptors using LipofectAMINE and PLUS reagent (Invitrogen) as previously described (129). Cells were incubated for 24 h to allow receptor expression and then infected with reovirus T1L at multiplicities of infection of 1 fluorescent focus unit/cell and 1 plaque-forming unit/cell for fluorescent focus and plaque assays, respectively. For fluorescent focus assays, infected cells were processed for indirect immunofluorescence as previously above and previously (9). For plaque assays, viral titers in cell lysates were determined at 0 and 24 h after adsorption as previously described (173). In brief, monolayers of L cells were infected in duplicate with serial 10-fold dilutions of sample. After viral attachment (37ºC, 1 h), cells were overlayed with a 50%-50% (vol/vol) mixture of completed 2X medium 199 and 2% Bacto-Agar dissolved in deionized distilled water. Monolayers were overlayed a second time at 3 days post inoculation. A final overlay with 2X medium 199 containing 1% agar and .04% neutral red was performed 6 days after inoculation. Plaques were counted 12-24 h after the neutral overlay. The viral titer is reported as plaque forming units per ml of original sample.

Protein expression, purification, and crystallization of hJAM-A

A cDNA corresponding to the extracellular region of hJAM-A (residues 27–233) was cloned into the pGEX-4T-3 expression vector (Amersham Pharmacia), which encodes N-terminal GST followed by a thrombin cleavage site. GST–hJAM-A fusion protein was expressed in *Escherichia coli* and purified by affinity chromatography using glutathione beads. hJAM-A was released from the beads by thrombin cleavage and further purified by anion-exchange chromatography. The cleaved protein contains three additional non-native

amino acids (Gly-24, Ser-25, and Met-26) at the N terminus. A final gel filtration step resulted in a homogenous peak that corresponded to a dimer of 48 kDa. Higher-order oligomers were not observed. Crystals were obtained by using 8 mg/ml protein and 16% PEG 6K, 18% isopropanol, 0.1 M sodium citrate as precipitant. The final pH of the mixture was 6.0.

Structure determination of hJAM-A

The crystals belong to space group C2 (a = 116.8 Å, b = 61.8 Å, c = 82.9 Å, β = 120.01°) and contain two molecules in their asymmetric unit. Before data collection, crystals were cryoprotected with 15% glycerol and then flash-frozen in liquid nitrogen. Diffraction data were collected at NSLS beamline X25 and processed with HKL (121). The structure was determined by molecular replacement using the structure of mJAM-A (95). Rotation and translation searches were performed separately with the N- and C-terminal domains of mJAM-A in AMORE , which yielded two clear solutions for each domain. The free R factor (28) for the combined solutions was 45.1% (8–3.5 Å) after rigid body refinement. Alternating rounds of model building in O (90) and refinement in X-PLOR (28) produced a model with good refinement statistics. Bulk solvent correction and noncrystallographic symmetry constraints were used throughout the refinement. The final model contains residues 25–233 of both chains and 124 water molecules. PROCHECK analysis shows no residues in disallowed regions in the Ramachandran plot.

Generation of chimeric fiber-σ1 attachment proteins

Fiber-σ1 fusion constructs were generated by using λphage red recombinase (128) expressed in *Escherichia coli* strain BW25113/pKD46 (46) obtained from the *E. coli* Genetic Stock Center (http://cgsc.biology.yale.edu) as follows: Fibshaft-T3Dσ1, consisting of the N-terminal 396 aa of Ad5 fiber fused to amino acid 292 of T3D σ1; Fib8-T3Dσ1, consisting of the N-terminal 170 aa of Ad5 fiber fused to amino acid 167 of T3D σ1; and Fibtail-T3Dσ1, consisting of the N-terminal 44 aa of Ad5 fiber fused to amino acid 18 of T3Dσ1. Sequences encoding the reovirus T3Dσ1 protein flanked by a bovine growth hormone polyadenylation signal and a zeocin-resistance gene were amplified by using *Pfu* polymerase (Stratagene) and primers containing 39-nt overhangs homologous to the pCMVfiber plasmid. The pCMVfiber plasmid, containing the Ad5 fiber gene expressed from a CMV immediate-early promoter, was cotransformed with the PCR product into the λphage red strain BW25113/pKD46. Recombinants were selected by using zeocin-containing agar plates.

Fibtail-T3Dσ1 was subcloned into a plasmid containing sequences homologous to E4 and then recombined into the Ad5 genome to replace the fiber gene using red recombinase. To aid in detection of the chimeric protein, two c-Myc tags (C2), and one hexahistidine tag (H6) were added to the C terminus of the chimera (Fibtail-T3DσC2H6) before recombination. The recombinants were screened for loss of the fiber gene by restriction endonuclease mapping and sequencing.

Ad vectors used are based on the AdEasy system (Q-BIOgene) and carry the full E1- and E3-deleted Ad5 genome with the firefly luciferase gene, an internal ribosome entry site, and the humanized *Renilla* GFP expressed from a cytomegalovirus (CMV) immediate-early promoter in the E1 region. CHO cells were transfected with plasmids encoding fiber-σ1

chimeras by using Lipofectamine-PLUS (Invitrogen), and cell extracts were harvested for SDS/PAGE. Immunoblots were performed as described (125).

Generation of a chimeric Ad vector

Linearized Ad genome encoding the Fibtail-T3Dσ1C2H6 chimera was transfected into 633 cells and maintained in the presence of 0.3 μM dexamethasone and 4 μg/ml polybrene. Virus was propagated, purified by CsCl gradient centrifugation, and quantitated as described (47). The resultant recombinant virus, Ad5-T3Dσ1, was amplified for a final round by using 293A cells to remove any residual fiber from newly assembled virions.

CsCl-banded Ad5, CAR-ablated biotinylated Ad [Ad5-BAP-TR [Parrott, 2003 #5103]], and Ad5-T3Dσ1 were precipitated with trichloroacetic acid. Pellets were resuspended in loading buffer, and 4 x 10^{10} particles per lane were resolved by SDS/PAGE and immunoblotting. For total protein analysis, precipitated virus (1.5 x 10^{11} particles per lane) was resolved by SDS/PAGE, and gels were stained with Coomassie blue.

Transduction of CHO cells transfected with receptor constructs

CHO cells were transfected with plasmids expressing hCAR, hJAM-A, or murine (m)JAM-A (24, 63). After 48 h, the cells were washed once with Hanks' balanced salt solution (GIBCO) with 1% BSA (HBSS-BSA) and adsorbed with 5,000 particles per cell of Ad5-T3Dσ1 at 4°C for 30 min. Cells were washed twice with HBSS-BSA, and fresh medium was added. After incubation at 37°C for 24 h, cells were lysed, and luciferase activity (in lumens) was measured as described (125).

Transduction of Caco-2 cells and primary DCs after receptor blockade

Cells were harvested, washed with HBSS-BSA, and incubated in suspension with 10 μg/ml of either hCAR-specific mAb RmcB or hJAM1-specific mAb J10.4 at 4°C for 30 min. Alternatively, cells were treated with 333 milliunits/ml of *Clostridium perfringens* neuraminidase type X (Sigma) at 37°C for 30 min to remove cell-surface sialic acid, followed by two washes with HBSS-BSA. Cells then were adsorbed with 5,000 particles per cell of Ad5-T3D-1 at 4°C for an additional 30 min, washed twice, and seeded onto 24-well plates in fresh medium. After incubation at 37°C for 24 h, cells were harvested for determination of luciferase activity.

Reovirus infection assays of polarized epithelial cells

MDCK cells were plated to confluency on 0.33-cm^2 permeable supports and cultured for 12 days. Monolayers were adsorbed apically with PBS (control) or T1L at an MOI of 10^2 PFU per cell in the presence or absence of anti-hJAM-A mAb J10.4. Monolayers were monitored for changes in TER for the times shown using an epithelial volt-Ohm meter. The results are presented as percent resistance relative to the zero time point (baseline resistance = 350 Ω).

Localization of TJ-associated proteins in polarized epithelial cells as determined by microscopy

Intracellular distribution of ZO-1 following reovirus infection of MDCK cells. MDCK cells were plated to confluency and cultured for five days. Cells were either infected with T1L at an MOI of 10^2 PFU per cell or treated with PBS (mock). Cells were incubated at

37°C for the times shown, stained with a polyclonal ZO-1 antiserum (Zymed), and visualized using immunofluorescence microscopy.

Biochemical examination of TJ-associated proteins in HeLa cells

HeLa cells were adsorbed with reovirus T3D at an MOI of 100 PFU per cell and incubated at 37°C for 0 or 30 minutes. Nuclear and cytoplasmic extracts were prepared after lysis in a hypotonic buffer containing 10 mM HEPES (pH 7.9), 10 mM KCl, and 1.5 mM $MgCl_2$. Nuclear and cytoplasmic proteins were resolved by SDS-PAGE and immunoblotted using a ZO-1-specific polyclonal antiserum (Zymed).

APPENDIX A

JUNCTIONAL ADHESION MOLECULE-A SERVES AS A RECEPTOR FOR PROTOTYPE AND FIELD-ISOLATE STRAINS OF REOVIRUS

Jacquelyn A. Campbell, Pierre Schelling, J. Denise Wetzel, Elizabeth M. Johnson, J. Craig Forrest, Greame A. R. Wilson, Michel Aurrand-Lions, Beat A. Imhof, [6]Thilo Stehle, and Terence S. Dermody

Journal of Virology. 79(13):7967-7978, 2005

JOURNAL OF VIROLOGY, July 2005, p. 7967–7978 Vol. 79, No. 13
0022-538X/05/$08.00+0 doi:10.1128/JVI.79.13.7967–7978.2005

Junctional Adhesion Molecule A Serves as a Receptor for Prototype and Field-Isolate Strains of Mammalian Reovirus

Jacquelyn A. Campbell,[1,2] Pierre Schelling,[3] J. Denise Wetzel,[2,4] Elizabeth M. Johnson,[1,2] J. Craig Forrest,[1,2] Greame A. R. Wilson,[5] Michel Aurrand-Lions,[6] Beat A. Imhof,[6] Thilo Stehle,[3] and Terence S. Dermody[1,2,4]*

Departments of Microbiology and Immunology[1] and Pediatrics[4] and Elizabeth B. Lamb Center for Pediatric Research,[2] Vanderbilt University School of Medicine, Nashville, Tennessee 37232; Amgen Inc., Thousand Oaks, California 91320[5]; Department of Pathology, Centre Medical Universitaire, Geneva, Switzerland[6]; and Laboratory of Developmental Immunology, Massachusetts General Hospital and Harvard Medical School, Boston, Massachusetts 02114[3]

Received 6 January 2005/Accepted 17 March 2005

Reovirus infections are initiated by the binding of viral attachment protein σ1 to receptors on the surface of host cells. The σ1 protein is an elongated fiber comprised of an N-terminal tail that inserts into the virion and a C-terminal head that extends from the virion surface. The prototype reovirus strains type 1 Lang/53 (T1L/53) and type 3 Dearing/55 (T3D/55) use junctional adhesion molecule A (JAM-A) as a receptor. The C-terminal half of the T3D/55 σ1 protein interacts directly with JAM-A, but the determinants of receptor-binding specificity have not been identified. In this study, we investigated whether JAM-A also mediates the attachment of the prototype reovirus strain type 2 Jones/55 (T2J/55) and a panel of field-isolate strains representing each of the three serotypes. Antibodies specific for JAM-A were capable of inhibiting infections of HeLa cells by T1L/53, T2J/55, and T3D/55, demonstrating that strains of all three serotypes use JAM-A as a receptor. To corroborate these findings, we introduced JAM-A or the structurally related JAM family members JAM-B and JAM-C into Chinese hamster ovary cells, which are poorly permissive for reovirus infection. Both prototype and field-isolate reovirus strains were capable of infecting cells transfected with JAM-A but not those transfected with JAM-B or JAM-C. A sequence analysis of the σ1-encoding S1 gene segment of the strains chosen for study revealed little conservation in the deduced σ1 amino acid sequences among the three serotypes. This contrasts markedly with the observed sequence variability within each serotype, which is confined to a small number of amino acids. Mapping of these residues onto the crystal structure of σ1 identified regions of conservation and variability, suggesting a likely mode of JAM-A binding via a conserved surface at the base of the σ1 head domain.

Mammalian orthoreoviruses (referred to as reoviruses in this article) are nonenveloped viruses with genomes of 10 discrete segments of double-stranded RNA (reviewed in reference 41). There are at least three serotypes of reoviruses, which can be differentiated by the capacity of antireovirus antisera to neutralize viral infectivity and inhibit hemagglutination (47, 50). Each of the reovirus serotypes is represented by a prototype strain, namely, type 1 Lang/53 (T1L/53), type 2 Jones/55 (T2J/55), and type 3 Dearing/55 (T3D/55). Reoviruses appear to infect most mammalian species, but disease is restricted to the very young (reviewed in reference 63). Reovirus infections of newborn mice have been used as the preferred experimental system for studies of reovirus pathogenesis. Sequence polymorphisms in reovirus attachment protein σ1 play an important role in determining sites of reovirus infection in the infected host (4, 32, 69, 70).

The σ1 protein is an elongated trimer with a head-and-tail morphology. The N-terminal σ1 tail partially inserts into the virion via "turrets" formed by the pentameric λ2 protein, while the C-terminal σ1 head projects away from the virion surface (1, 25, 26). A crystal structure of the C-terminal half of T3D/55 σ1 revealed that the head contains three β-barrel domains (one from each trimer), each of which is constructed from eight antiparallel β-strands (16). Sequence analysis and structural modeling have suggested that the N-terminal half of the tail is formed from an α-helical coiled coil (6, 21, 40) and the C-terminal half is formed from a triple β-spiral (16, 56). The overall structural topology of the β-spiral and head domains of σ1 is strikingly similar to that of the adenovirus attachment protein, fiber (16, 37, 56).

There are two distinct receptor-binding regions in σ1. A region in the fibrous tail domain of type 3 σ1 binds to α-linked sialic acid (2, 14, 15, 18). A distinct region in the type 1 σ1 tail domain also binds to cell surface carbohydrates (14), and recent evidence suggests that sialic acid may be involved in the binding of T1L/53 to intestinal cells (30). A second receptor-binding site is located in the head domains of both the type 1 and type 3 σ1 proteins (3, 39).

An expression-cloning approach was used to identify junctional adhesion molecule A (JAM-A) as a receptor for the prototype strains T1L/53 and T3D/55 (3). JAM-A is a 35-kDa type I transmembrane protein that is a member of the immunoglobulin superfamily (34, 36). JAM-A contains two immunoglobulin-like domains, a single transmembrane region, and a short cytoplasmic tail. JAM-A is expressed in a variety of

* Corresponding author. Mailing address: Lamb Center for Pediatric Research, D7235 MCN, Vanderbilt University School of Medicine, Nashville, TN 37232. Phone: (615) 343-9943. Fax: (615) 343-9723. E-mail: terry.dermody@vanderbilt.edu.

tissues, including epithelial and endothelial barriers (34, 36, 43), where it is thought to regulate tight-junction permeability and mediate leukocyte trafficking (17, 34, 36, 43).

The crystal structures of the murine (m) and human (h) homologs of JAM-A, both of which are functional reovirus receptors (3), indicate that JAM-A forms homodimers via extensive hydrophobic and ionic contacts between apposing membrane-distal (D1) immunoglobulin-like domains (33, 44). Residues that facilitate interdimer interactions are strictly conserved between mJAM-A and hJAM-A (33, 44). JAM-A dimers are thought to be physiologically relevant, perhaps functioning in tight-junction barrier integrity or the diapedesis of inflammatory cells (8, 33, 44). Recent biochemical studies of reovirus–JAM-A interactions suggested that σ1 binds to a monomeric version of JAM-A and contacts residues in the vicinity of the JAM-A dimer interface (24). This strategy of cell attachment is strikingly similar to that used by adenovirus fiber to bind to the coxsackievirus and adenovirus receptor (CAR) (10, 66), an immunoglobulin superfamily member that shares considerable structural homology with JAM-A (57).

For this study, we determined whether JAM-A serves as a receptor for the prototype type 2 strain T2J/55 and a panel of four type 1, two type 2, and four type 3 field-isolate strains. The results indicate that JAM-A, but not the related JAM family members JAM-B and JAM-C, is a receptor for prototype and field-isolate strains of the three reovirus serotypes. An analysis of conserved and variable sequences in the σ1 head, together with existing structural information for σ1 and JAM-A, suggested an especially high tolerance for surface variation in the protein while maintaining the specificity for receptor utilization. These findings enhance our understanding of the molecular basis of reovirus binding to JAM-A and provide clues about the mechanisms of reovirus attachment.

MATERIALS AND METHODS

Cells, viruses, and antibodies. Spinner-adapted murine L929 (L) cells were grown in either suspension or monolayer cultures in Joklik's modified Eagle's minimal essential medium (Irvine Scientific, Santa Ana, Calif.) supplemented to contain 5% fetal bovine serum (Gibco-BRL, Gaithersburg, Md.), 2 mM L-glutamine, 100 U of penicillin per ml, 100 mg of streptomycin per ml, and 0.25 mg of amphotericin per ml (Gibco-BRL). HeLa cells were maintained in monolayer cultures in Dulbecco's minimal essential medium (Gibco-BRL) supplemented to contain 10% fetal bovine serum, L-glutamine, and antibiotics as described for L cells. Chinese hamster ovary (CHO) cells were maintained in Ham's F12 medium supplemented with fetal bovine serum, L-glutamine, and antibiotics as described for HeLa cells.

The prototype reovirus strains T1L/53, T2J/55, and T3D/55 are laboratory stocks. The field-isolate reovirus strains used in this study are shown in Table 1. Variant K, a neutralization-resistant variant of T3D/55, was selected and characterized as previously described (7, 54, 55). Viral stocks were prepared by plaque purification and passage in L cells (67). Purified virions were prepared by using second- and third-passage L-cell lysate stocks as previously described (26, 49). Viral particle concentrations were determined by measurements of the optical density at 260 nm, using a conversion factor of 2.1×10^{12} viral particles per optical density unit (52). The particle-to-PFU ratio of stocks used for viral infectivity assays was approximately 250 to 1.

Rabbit hCAR-specific antiserum was provided by Jeffrey Bergelson (University of Pennsylvania). Rabbit polyclonal hJAM-B- and hJAM-C-specific antisera were generated as previously described (28). The murine hJAM-A-specific monoclonal antibody (MAb) J10.4 was purified from mouse ascites by using protein A-Sepharose (34). The immunoglobulin G (IgG) fractions of polyclonal rabbit antisera raised against T1L/53 and T3D/55 (71) were purified by using protein A-Sepharose (2). A mixture of these sera was capable of recognizing all strains of reovirus used in this study.

TABLE 1. Strains used for studies of JAM-A utilization by reoviruses

Virus strain[a]	Abbreviation	GenBank accession no.	Reference
T1/Human/Ohio/Lang/1953	T1L/53	M35963	45, 50
T1/Bovine/Maryland/clone23/1959	T1C23/59	AY862134	31
T1/Bovine/Maryland/clone50/1960	T1C50/60	AY862133	31
T1/Human/Netherlands/1/1984	T1Neth/84	AY862136	29
T1/Human/Netherlands/1/1985	T1Neth/85	AY862135	29
T2/Human/Ohio/Jones/1955	T2J/55	M35964	46, 50
T2/Human/Netherlands/1/1973	T2Neth/73	AY862137	29
T2/Human/Netherlands/1/1984	T2Neth/84	AY862138	29
T3/Human/Ohio/Dearing/1955	T3D/55	NC_004277	46, 50
T3/Human/Wash.D.C./clone93/1955	T3C93/55	L37675	31
T3/Human/Wash.D.C./clone87/1957[b]	T3C87/57	L37677	48
T3/Bovine/Maryland/clone18/1961	T3C18/61	L37684	31
T3/Murine/France/clone9/1961	T3C9/61	L37676	31

[a] Strain nomenclature is as follows: serotype/species of origin/place of origin/strain designation/year of isolation.
[b] This strain has also been designated T3/Human/Wash.D.C./Abney/1957.

Fluorescent-focus assays of viral infectivity. Monolayers of HeLa cells in 96-well plates (Costar, Cambridge, Mass.) (3×10^4 cells per well) were pretreated for 1 h with phosphate-buffered saline (PBS), hCAR-specific antiserum, or the hJAM-A-specific MAb J10.4 at various concentrations prior to the adsorption of virus at room temperature for 1 h. Following removal of the inoculum, the cells were washed with PBS and incubated at 37°C for 20 h to permit the completion of a single round of viral replication. Monolayers were fixed with 1 ml of methanol at −20°C for a minimum of 30 min, washed twice with PBS, blocked with 2.5% immunoglobulin-free bovine serum albumin (Sigma-Aldrich, St. Louis, Mo.) in PBS, and incubated at room temperature for 1 h with protein-A–affinity-purified polyclonal rabbit antireovirus serum at a 1:800 dilution in PBS–0.5% Triton X-100. The monolayers were washed twice with PBS–0.5% Triton X-100 and incubated with a 1:1,000 dilution of goat anti-rabbit immunoglobulin conjugated with the Alexa Fluor 546 fluorophore (Molecular Probes, Eugene, Oreg.). The monolayers were washed twice with PBS, and infected cells were visualized by indirect immunofluorescence using an Axiovert 200 inverted microscope modified for fluorescence microscopy (Carl Zeiss, New York, N.Y.). Infected cells were identified by the presence of intense cytoplasmic fluorescence that was excluded from the nucleus. No background staining of uninfected control monolayers was noted. Reovirus antigen-positive cells were quantified by counting the fluorescent cells in at least three random fields of view per well in triplicate at a magnification of ×20.

Transient transfection and infection of CHO cells. CHO cells were transiently transfected with an empty vector or with plasmids encoding receptor constructs by the use of Lipofectamine PLUS reagent (Invitrogen, San Diego, Calif.) as previously described (3). After 24 h of incubation to allow receptor expression, transfected cells were allowed to adsorb to the virus at a multiplicity of infection (MOI) of 1 fluorescent focus unit (FFU) per cell, incubated for an additional 20 h, fixed with methanol, and stained for reovirus proteins by use of an anti-reovirus serum at a 1:800 dilution. Images were captured at a magnification of ×20 with a Zeiss Axiovert 200 inverted microscope.

Flow cytometric analysis of receptor expression. CHO cells were transiently transfected with receptor constructs, incubated for 24 h, and detached from the plates by incubation with 20 mM EDTA in PBS. Cells (10^6) were incubated with the hCAR-specific antiserum, the hJAM-A-specific MAb J10.4, or an antibody specific for hJAM-B or hJAM-C (28), washed with PBS, and incubated with a phycoerythrin-conjugated goat anti-rabbit or anti-rat IgG secondary antibody (Molecular Probes) at a 1:1,000 dilution on ice for 30 min. The cells were washed twice with PBS and analyzed with a FACScan flow cytometer (Becton-Dickinson, Palo Alto, Calif.).

Sequence analysis of the S1 gene. Viral genomes were extracted from infected L-cell lysates by the use of Trizol (Life Technologies, Rockville, Md.) according to the protocol supplied by the manufacturer. S1 gene segments were amplified by reverse transcription-PCR (RT-PCR) using 10 U of avian myeloblastosis virus reverse transcriptase (Promega Biosciences, San Luis Obispo, Calif.), 2.5 U *Taq* DNA polymerase (Promega Biosciences), and primers complementary to the 5′ and 3′ nontranslated regions of the S1 genes of the reovirus prototype strains. The type 1 S1 forward primer was 5′ GGATCCGCTATTCGCGCCTATGG

ATG, and the reverse primer was 5′ GGGTTCGCGCTAGATTCA. The type 2 S1 forward primer was 5′ GCTATTCGCACTCATGTCGGATCTAGTGC AGC, and the reverse primer was 5′ GATGAGTCGCCACTGTGCCGAGT GGA. The type 1 5′ forward primer contained nucleotides that resulted in a primer-derived sequence for the first two amino acids (M and D), and the type 2 5′ forward primer contained nucleotides that resulted in a primer-derived sequence for the first six amino acids (M, S, D, L, V, and Q). The amplification products were cloned into the pCR 2.1 vector (Invitrogen). Sequences of at least two independent RT-PCR clones for each S1 gene segment were determined by automated sequencing.

Phylogenetic analysis of S1 gene nucleotide sequences. Sequences were aligned by using the program ClustalX (62). Phylogenetic trees were constructed from variations in the σ1-encoding S1 gene nucleotide sequences by the maximum parsimony method using the heuristic search algorithm within the program PAUP v4.0b10 (58). Trees were rooted at the midpoint. The branching orders of the phylograms were verified statistically by resampling the data 1,000 times in a bootstrap analysis using the branch and bound algorithm as applied in PAUP.

Sequence alignment and structural modeling methods. Sequences were aligned by using the program ClustalW (http://www.ebi.ac.uk/clustalw/). Alignments were rendered in ALSCRIPT (5), using different colors to highlight different degrees of sequence similarity. Sequence changes were mapped onto the crystal structure of T3D/55 σ1 (16) by using the program GRASP (42).

RESULTS

JAM-A serves as a receptor for prototype strains of the three reovirus serotypes. Our previous work indicated that JAM-A serves as a receptor for the prototype reovirus strains T1L/53 and T3D/55 (3). To confirm these observations and to test whether JAM-A is used as a receptor by T2J/55, we treated HeLa cells with PBS, an hCAR-specific antiserum as a control, or the hJAM-A-specific MAb J10.4 prior to viral adsorption. Infected cells were quantified by indirect immunofluorescence using an antireovirus serum (Fig. 1A). The treatment of cells with the CAR-specific antiserum had no effect on the capacity of the prototype strains to infect HeLa cells. In sharp contrast, the treatment with MAb J10.4 resulted in a concentration-dependent inhibition of infection for all three strains. The minimum concentrations of MAb J10.4 required to reduce the infectivities of these strains by 50% were between 0.1 and 1.0 μg per ml (Fig. 1B). The infectivities of all three strains were reduced approximately 90% following the treatment of cells with 100 μg per ml MAb J10.4.

JAM-B and JAM-C do not serve as receptors for prototype strains of reovirus. JAM-A is the only JAM family member tested to date that functions as a receptor for T1L/53 (44). To determine whether other JAM family members in addition to JAM-A serve as reovirus receptors for other reovirus prototype strains, we transfected CHO cells, which are poorly permissive for reovirus infection (24), with a cDNA encoding hJAM-A, hJAM-B, or hJAM-C. Cells also were transfected with hCAR as a negative control. After confirmation of the cell surface expression of the receptor constructs (Fig. 2A), the transfected cells were tested for the capacity to support reovirus infection. Infected cells were quantified by indirect immunofluorescence using an antireovirus serum (Fig. 2B). Only CHO cells transfected with hJAM-A were capable of supporting an efficient infection of each of the three prototype reovirus strains, whereas cells transfected with hJAM-B and hJAM-C did not support the infection of any of these strains in excess of that supported by cells transfected with hCAR (Fig. 2C). Therefore, the JAM family member JAM-A, but not JAM-B or JAM-C, functions as a receptor for prototype strains of reovirus.

JAM-A serves as a receptor for field-isolate strains of reovirus. Strains of each of the three reovirus serotypes have been isolated from many mammalian hosts over a period in excess of 50 years (29, 31). A type 3 reovirus strain isolated from the cerebrospinal fluid of a child with meningitis is capable of using JAM-A as a receptor (64). However, the receptor-binding properties of other field-isolate strains have not been reported. To determine whether JAM-A is used as a receptor by other field-isolate strains of reovirus, we transfected CHO cells with hJAM-A, hJAM-B, or hJAM-C and tested them for the capacity to support reovirus infection. Ten strains, encompassing four type 1, two type 2, and four type 3 viruses (Table 1), were used in these experiments. In parallel with the findings for prototype reovirus strains, each of the field-isolate strains tested was capable of utilizing hJAM-A, but not hJAM-B or hJAM-C, as a receptor (Fig. 3).

Analysis of deduced σ1 amino acid sequences for JAM-A-binding reovirus strains. To gain insight into the σ1 residues that mediate interactions between reoviruses and JAM-A, we analyzed the amino acid sequences of the σ1 proteins of the 3 prototype and 10 field-isolate strains chosen for study. For these experiments, we determined the σ1-encoding S1 gene sequences of the strains T1C23/59, T1C50/60, T1Neth/84, T1Neth/85, T2Neth/73, and T2Neth/84 and compared these sequences to those reported previously (Table 1). RT-PCR primers complementary to the nontranslated regions of the type 1 and type 2 S1 genes were designed to facilitate the amplification of entire S1 genes from infected L-cell lysates.

To define the evolutionary relationships of the S1 gene sequences determined for this study with those of the other reovirus strains sequenced to date, we constructed phylogenetic trees by using variation in the σ1-encoding S1 gene nucleotide sequences and the maximum parsimony method as applied in the program PAUP (Fig. 4). The most noteworthy feature of the S1 phylogenetic tree is that the strains clustered into distinct lineages based on their serotypes. A phylogenetic tree generated by using the same data set and the neighbor-joining algorithm of the phylogenetic analysis program MacVector (MacVector 2001, version 7.1.1) had a topology identical to that of the tree generated by PAUP (data not shown). Therefore, our phylogenetic analysis indicates that the S1 genes of reovirus strains cluster tightly into three lineages defined by serotype. Concordantly, changes in the deduced amino acid sequences of the σ1 protein within a given serotype are confined to a small number of residues. Since each of the strains investigated for this study was capable of using JAM-A as a receptor, the locations of these changes provide clues about areas that can vary in surface structure without impeding the capacity to engage this molecule. Thus, these changes define areas that are unlikely to interact with JAM-A.

Sequence variability within type 3 σ1 protein. Structural information is available for the T3D/55 σ1 protein (16). We therefore carried out a structure-based comparison of the deduced amino acid sequences of the σ1 proteins of type 3 field-isolate strains with that of the prototype T3D/55 to define regions of conserved and variable sequences within a serotype (Fig. 5). Substantial variability is seen between residues 240 and 250, a region that lies just N-terminal to the first β-spiral repeat in the crystallized fragment and is disordered in the crystal structure. The σ1 fragment was obtained by trypsin

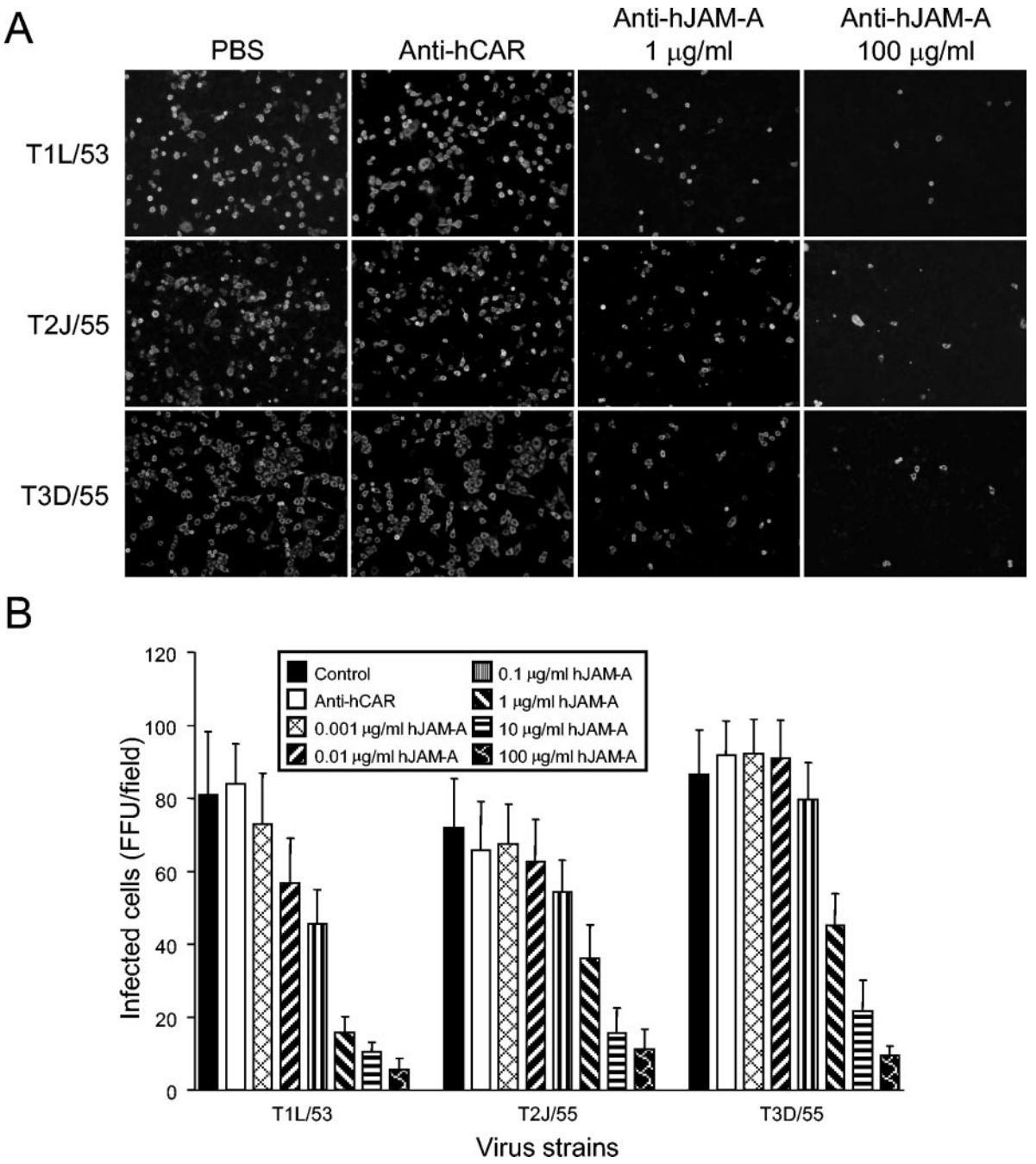

FIG. 1. JAM-A blockade reduces infection of prototype reovirus strains. HeLa cells at equivalent degrees of confluence were pretreated with PBS, an hCAR-specific antiserum as a control, or the hJAM-A-specific MAb J10.4 prior to adsorption with T1L/53, T2J/55, or T3D/55 at an MOI of 0.1 FFU per cell. After incubation for 20 h, the cells were fixed and permeabilized with methanol. Newly synthesized viral proteins were detected by the incubation of cells with a polyclonal rabbit antireovirus serum followed by incubation with an anti-rabbit immunoglobulin–Alexa-546 serum for the visualization of infected cells by indirect immunofluorescence. (A) Representative fields of view. (B) Reovirus-infected cells were quantified by counting fluorescent cells in a minimum of three random fields of view per well for three wells at a magnification of ×20. The results are presented as the mean FFU per field. Error bars indicate standard deviations.

cleavage of a longer construct after residue Arg245 (16). The fact that trypsin cleaves σ1 at only this position suggests that Arg245 lies in an exposed loop that likely possesses some flexibility. Exposed areas in the second and third β-spiral repeats of the crystallized fragment also contain several substitutions. Because these areas are variable, they are unlikely to contribute significantly to JAM-A binding.

Most of the remaining substitutions are located at the top of the σ1 trimer, forming a highly variable "plateau" that is also unlikely to bind to JAM-A. Some of the observed variations on

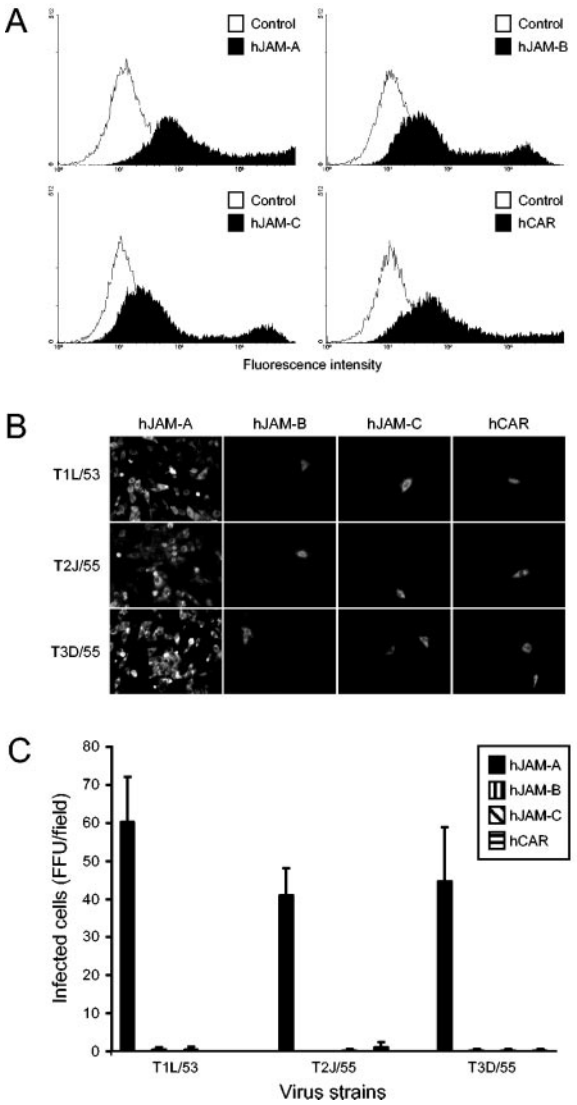

FIG. 2. CHO cells transfected with hJAM-A support growth of prototype reovirus strains. (A) CHO cells were transiently transfected with a plasmid encoding hCAR, hJAM-A, hJAM-B, or hJAM-C. Following incubation for 24 h to permit receptor expression, cells were incubated with receptor-specific MAbs, and the cell surface expression of receptor constructs was assessed by flow cytometry. (B) Transfected CHO cells at equivalent degrees of confluence were adsorbed with T1L/53, T2J/55, or T3D/55 at an MOI of 0.1 FFU per cell. Reovirus proteins were detected by indirect immunofluorescence at 20 h postinfection. Representative fields of view are shown. Magnification, ×20. (C) Reovirus-infected cells were quantified by counting fluorescent cells in five random fields of view per well for three wells. The results are presented as the mean FFU per field. Error bars indicate standard deviations.

the plateau are anticipated to alter the structure of the molecule. For example, the replacement of Ser435 with Met in T3D9/61 and T3D18/61 is likely to cause significant structural changes, as Ser435 is partially buried in the T3D/55 structure (16). Because they are exposed at the protein surface, the polymorphisms seen on the plateau may allow viral escape from antibody recognition. In contrast, the lower portion of the head domain is highly invariant, suggesting that the base of the σ1 head is primarily responsible for interactions with JAM-A.

Sequence variability within σ1 proteins of the three reovirus serotypes. An alignment of the deduced σ1 amino acid sequences for all of the strains chosen for study showed that only 36 of the 210 residues in the crystallized fragment of T3D/55 σ1 (16) are conserved (Fig. 6). There is substantially more variability among the serotypes than that within each serotype. Mapping of the conserved residues onto the crystal structure of T3D/55 σ1 showed that many of these residues are buried, especially those located at the base of the σ1 head-trimer interface (Fig. 6). A large fraction of the remaining conserved residues cluster in a single, solvent-exposed region at the lower edge of the β-barrel. Again, the regions that are most variable within type 3 σ1 (the β-spiral region and the "top" of the trimer) are also most variable among the different serotypes. In contrast, an extended, contiguous area of conserved residues is located at the base of the head domain, and additional, smaller areas of conservation are found along the side of this domain. Because these regions are conserved in the JAM-A-binding strains investigated here, they mark potential contact points for this receptor.

The large conserved area at the base of the head domain is formed primarily by a stretch of residues (Asn369 to Glu384 in T3D/55 σ1) within a 3_{10} helix and a long loop between β-strands D and E (16) (Fig. 6). This region also includes Trp421 at the end of β-strand F. The conserved region is fairly hydrophobic, with the side chains of Val371, Leu379, and Trp421 accounting for a large portion of the surface area predicted to be involved in JAM-A binding. A second, smaller cluster of conserved residues (Leu331, Trp333, Ile360, and His438 in T3D/55 σ1) lies above this putative JAM-A-binding surface, near the top of the trimer (Fig. 6). While most of the side chains of these residues are buried, the structural features of this cluster may contribute to receptor engagement. The remaining surface area of the σ1 trimer, especially near the top of the head and the head-to-head contacts, is almost entirely devoid of conserved residues.

A neutralization-resistant variant of reovirus T3D/55 uses JAM-A as a receptor. Variants of T3D/55 selected for their resistance to neutralization by the use of MAb 9BG5 (55) have a mutation at Asp340 or Glu419 in the σ1 head (7) (Fig. 5B). These variants have alterations in central nervous system (CNS) tropism following infections of newborn mice (54). The single mutation in variant K of σ1, Glu419 to Lys (7), segregates genetically with the altered growth and tropism of this virus in the murine CNS (32). To determine whether a neutralization-resistant variant of T3D/55 retained the capacity to use JAM-A as a receptor, we treated HeLa cells with PBS, an hCAR-specific antiserum as a negative control, or the hJAM-A-specific MAb J10.4 prior to infection with variant K. Infected cells were quantified by indirect immunofluorescence using an antireovirus serum (Fig. 7). The treatment of cells with increasing concentrations of the JAM-A-specific MAb J10.4 resulted in a dose-dependent inhibition of viral infection, while the CAR-specific antiserum had no effect on viral infectivity. At the maximal concentration of MAb J10.4 used (100 μg per ml), infectivity was nearly abolished, demonstrating that variant K is capable of using JAM-A as a receptor (Fig. 7).

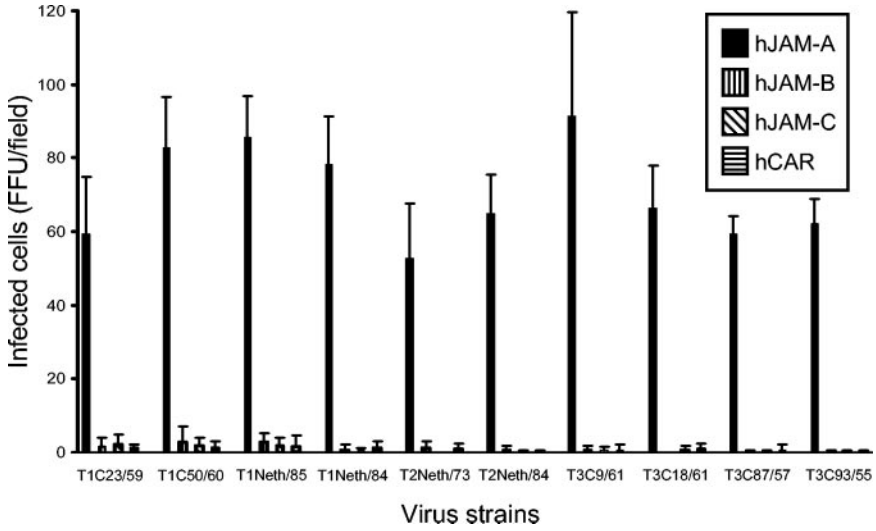

FIG. 3. Expression of JAM-A confers infectivity on field-isolate reovirus strains. CHO cells were transiently transfected with a plasmid encoding hCAR, hJAM-A, hJAM-B, or hJAM-C. Following incubation for 24 h to permit receptor expression, the cells were adsorbed with the indicated field-isolate strains at an MOI of 1 FFU per cell. Reovirus proteins were detected by indirect immunofluorescence at 20 h postinfection and quantified by counting of the fluorescent cells in three random fields of view per well for three wells. The results are presented as the mean FFU per field. Error bars indicate standard deviations.

Thus, the mechanism of the altered pathogenicity of variant K appears to be independent of JAM-A utilization.

DISCUSSION

An examination of receptor usage by diverse virus families, including arenaviruses (11, 53), adenoviruses (9, 27, 51, 72), and measles virus (20, 35, 61), has led to the discovery that receptor usage by some viruses varies based on the viral clade, serotype, or adaptation to passaging in cell culture. We undertook this study to determine whether JAM-A is used as a receptor by both prototype and field-isolate strains of reoviruses. The results demonstrate that each of the prototype and field-isolate reovirus strains tested, regardless of their serotype, species, or geographical region of isolation, is capable of utilizing JAM-A as a receptor.

Prior to this work, sequence information for the S1 gene segments of type 1 and type 2 reovirus strains was limited to the prototype strains T1L/53 and T2J/55. In this study, we determined the S1 sequences of four type 1 and two type 2 field-isolate strains. A phylogenetic analysis of the deduced σ1-encoding S1 gene sequences revealed that these reovirus field-isolate strains are associated with discrete lineages defined by serotype. Given that all reovirus strains tested to date

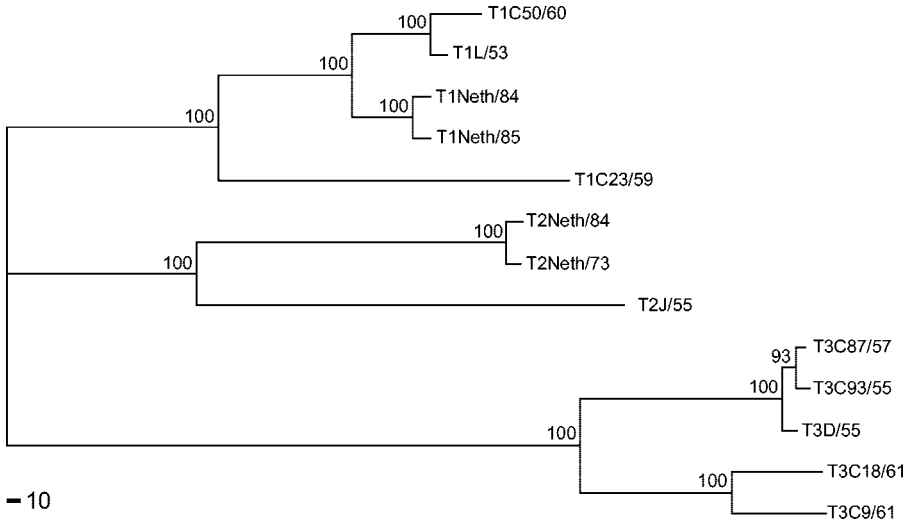

FIG. 4. Phylogenetic relationships among S1 gene nucleotide sequences of 13 reovirus strains. A phylogenetic tree for the σ1-encoding S1 gene sequences of the strains shown in Table 1 was constructed by using the maximum parsimony method as applied in the program PAUP. The tree is rooted at its midpoint. Bootstrap values of >50% (indicated as a percentage of 1,000 repetitions) for major branches are shown at the nodes. Bar, distance resulting from 10 nucleotide changes.

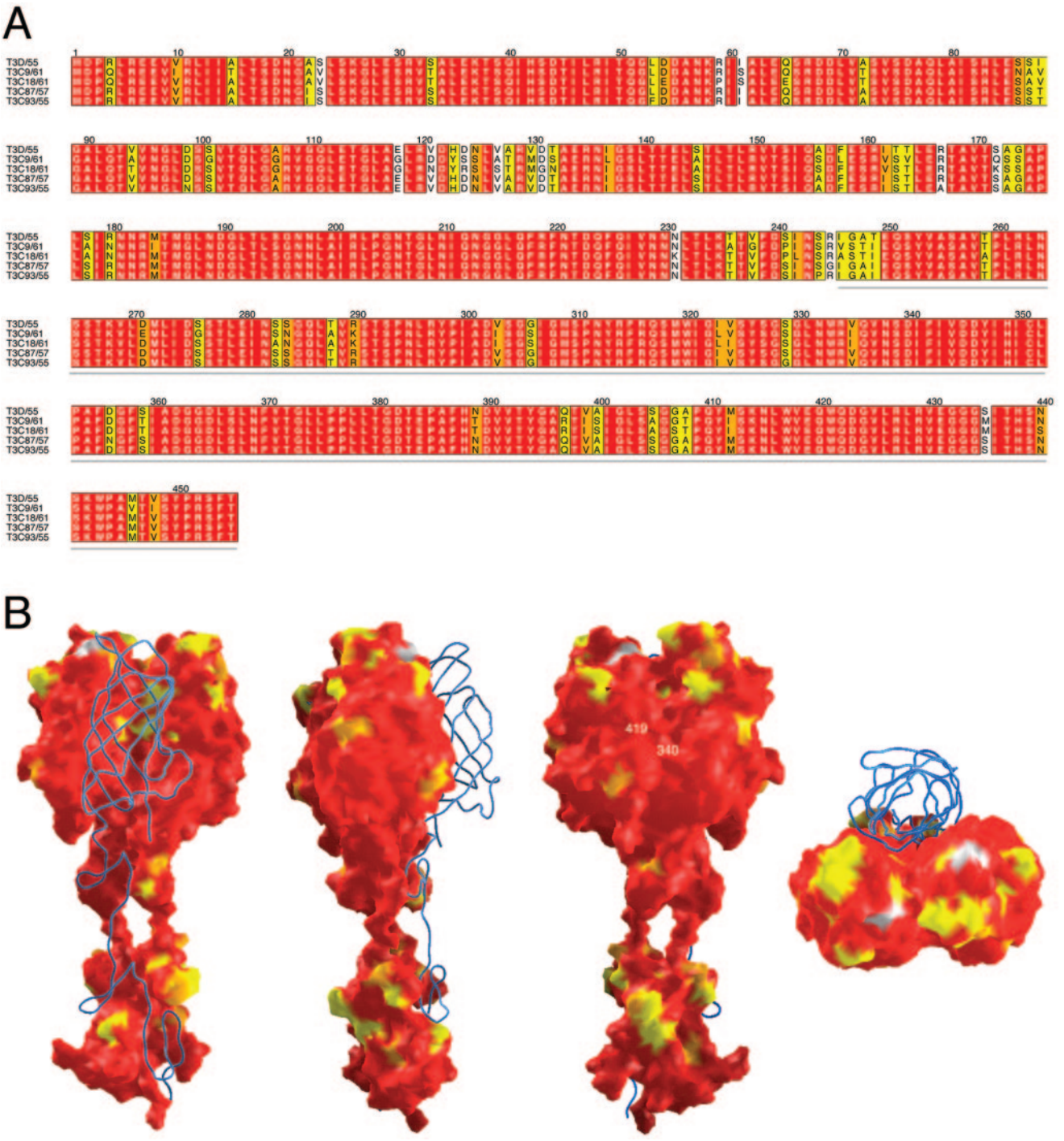

FIG. 5. Sequence conservation and structural variability within the type 3 σ1 protein. (A) Alignment of deduced amino acid sequences of the σ1 proteins of prototype strain T3D/55 and four type 3 field-isolate strains. The alignment was generated by using the program ALSCRIPT (5), with default conservation parameters applied according to the following color scheme: red, identical residues; orange, conserved residues at 80% conservation; yellow, conserved residues at 60% conservation; white, nonconserved residues. The 80% conservation threshold identifies closely related amino acids (e.g., Ile and Leu), whereas the 60% threshold identifies more distantly related amino acids (e.g., Ser and Ala, both of which have small side chains). The amino acid positions in the alignment are numbered above the sequences. The gray line indicates residues present in the crystallized fragment of T3D/55 σ1 (16). (B) Structure of the σ1 trimer, with residues colored according to the same color code as that used for panel A. Four different views are shown. For each of the views, two σ1 monomers are shown in surface representation, and the other is depicted as a blue ribbon tracing corresponding to the α-carbon backbone. The first three views each differ by 90° along a vertical axis; the fourth view shows the molecule in the third view after rotation by 90° along a horizontal axis. The positions of residues 340 and 419 are marked in the third panel from the left.

A

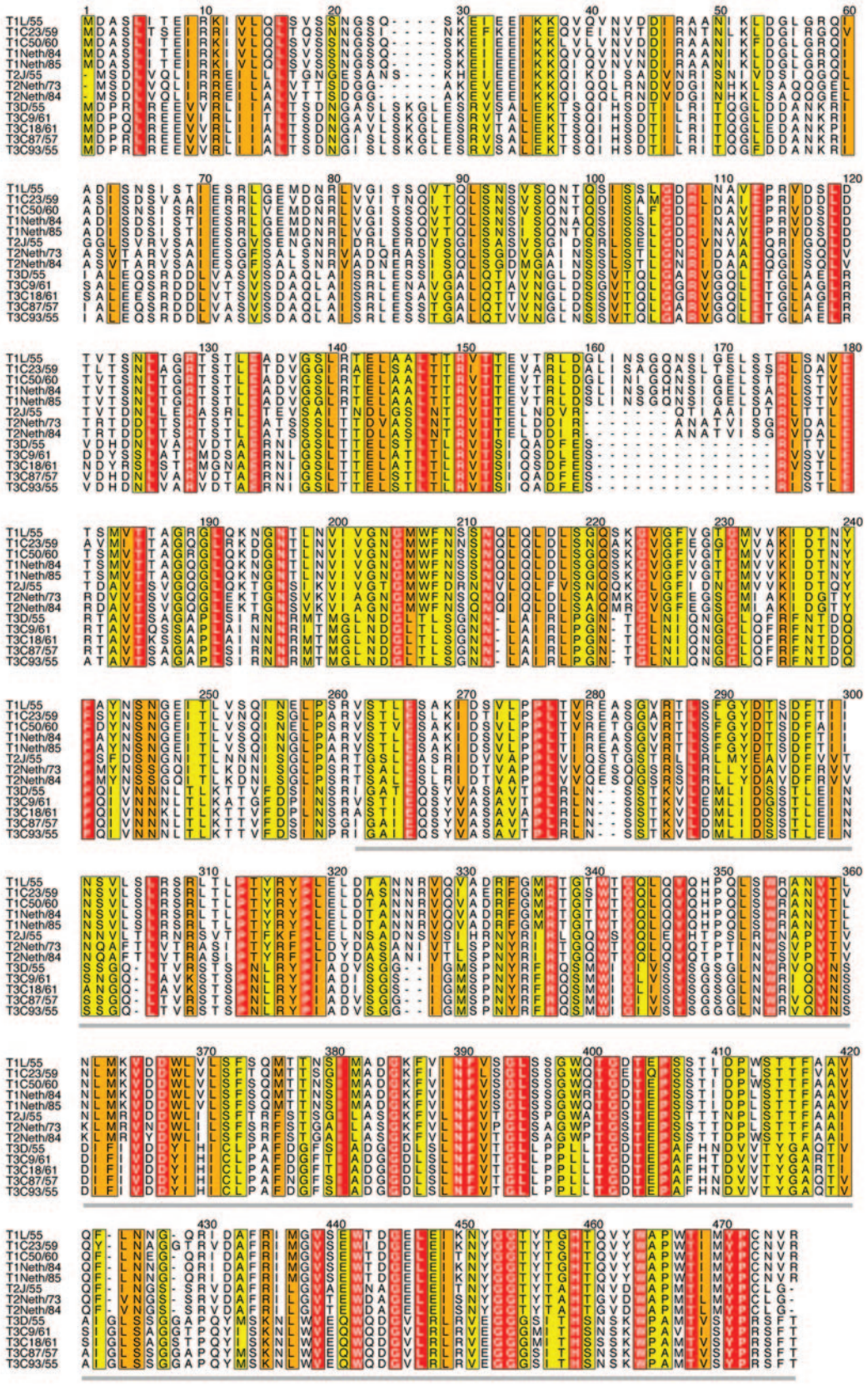
T1L/55
T1C23/59
T1C50/60
T1Neth/84
T1Neth/85
T2J/55
T2Neth/73
T2Neth/84
T3D/55
T3C9/61
T3C18/61
T3C87/57
T3C93/55

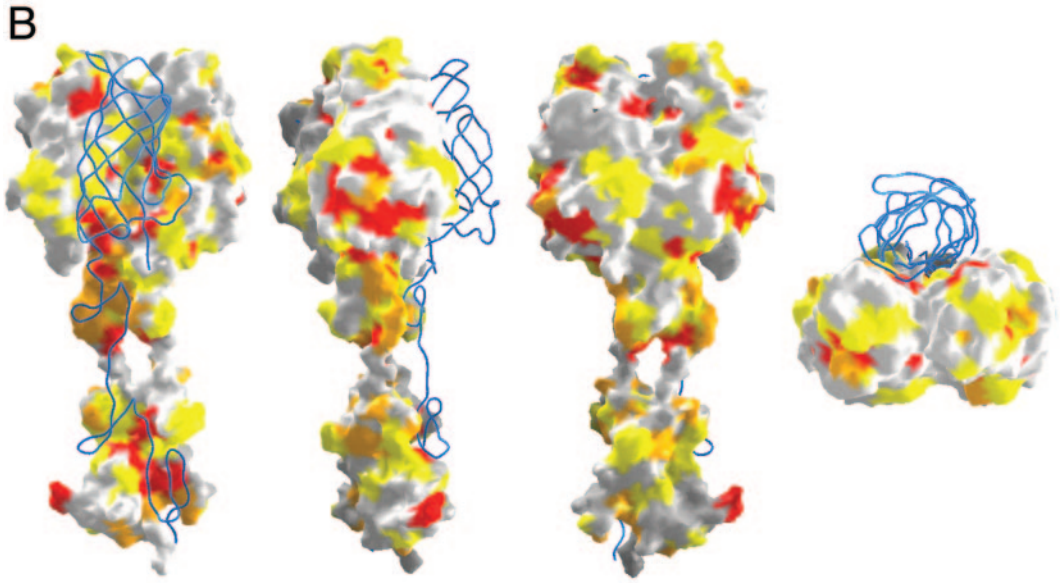

FIG. 6. Sequence conservation and structural variability within the σ1 proteins of the three reovirus serotypes. (A) Alignment of deduced amino acid sequences of the σ1 proteins of 3 prototype and 10 field-isolate reovirus strains. The alignment was generated by using ALSCRIPT and the scheme described in the legend to Fig. 5. Gaps in the aligned sequences are indicated by dots. (B) Mapping of residues onto the σ1 structure, using the same color code as that depicted in Fig. 5. The four views correspond to those in Fig. 5B.

are capable of using JAM-A as a receptor, it seems plausible that σ1 interacts with JAM-A through residues that are conserved among the serotypes, including the newly characterized type 1 and type 2 field-isolate strains. The observation that JAM-A is used as a receptor by all reovirus strains tested was unexpected since the σ1 protein is highly divergent among the three serotypes. For example, a sequence analysis of the prototype strains revealed that the σ1 head domains of T1L/53 and T2J/55 share 50% identical residues, while those of T1L/53 and T3D/55 share only 27% of their residues.

Substantial evidence has accumulated to suggest that the σ1 head domain binds to cellular receptors. Truncated forms of σ1 containing only the head domain are capable of specific cell interactions (22, 23). Concordantly, proteolysis of T3D/55 virions leads to the release of a C-terminal receptor-binding fragment of σ1 (residues 246 to 455) (13) and a resultant loss in infectivity (39). This fragment of σ1 is capable of binding to JAM-A on a biosensor surface with an affinity in the nanomolar range (3). Preliminary findings from our laboratory indicate that an even smaller fragment of T3D/55 σ1, corresponding to the head domain and a single β-spiral repeat, is capable of binding to JAM-A (K. M. Guglielmi, P. Schelling, T. Stehle, and T. S. Dermody, unpublished observations). Thus, the σ1 head promotes interactions with JAM-A that are distinct from the interactions with sialic acid mediated by the σ1 tail.

While most of the residues conserved among the σ1 proteins of the strains tested are scattered throughout the molecule, an examination of the σ1 surface revealed a single extended patch of conserved residues at the lower edge of the σ1 head. We think that this region may form part of a JAM-A-binding surface. This conserved region is formed mostly by residues in the vicinity of a long loop connecting β-strands D and E of the eight-stranded β-barrel that forms the σ1 head. Although it is easily accessible to ligands, this site is somewhat recessed into

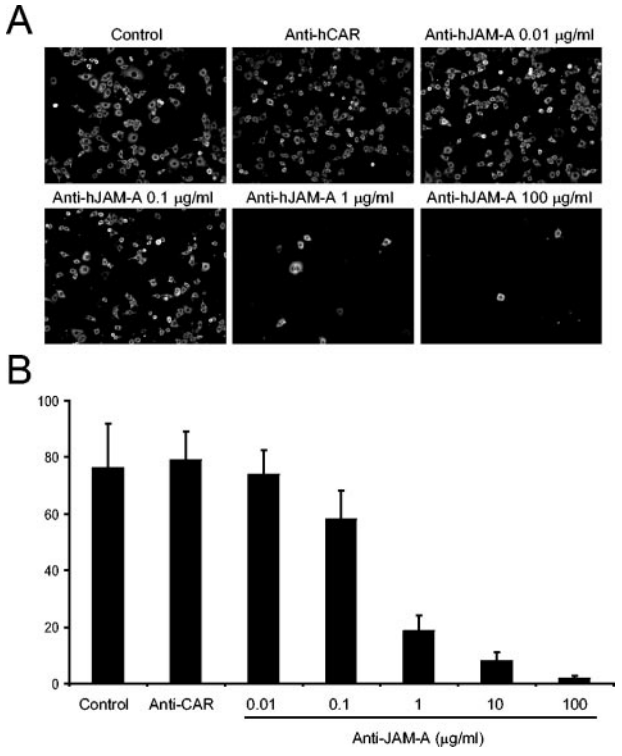

FIG. 7. JAM-A is used as a receptor for a neutralization-resistant variant of reovirus T3D/55. HeLa cells at equivalent degrees of confluence were pretreated with PBS, an hCAR-specific antiserum, or the hJAM-A-specific MAb J10.4 prior to adsorption with variant K at an MOI of 1 FFU per cell. Reovirus proteins were detected by indirect immunofluorescence at 20 h postinfection. (A) Representative fields of view. (B) Reovirus-infected cells were quantified by counting fluorescent cells in three random fields of view per well for three wells. The results are presented as the mean FFU per field. Error bars indicate standard deviations.

the protein surface and is surrounded by protruding, nonconserved residues on all three edges of the trimer. Only residues from a single monomer contribute to the putative JAM-A-binding region and its borders, and the regions are not involved in σ1 intersubunit contacts. Thus, the location of conserved residues within the trimer suggests that each σ1 monomer can independently bind to a JAM-A molecule.

Although it may serve as the primary contact point for the receptor, the putative JAM-A-binding site in σ1 is relatively small, measuring about 15 Å long and 10 Å wide. Most other interactions between viral ligands and proteinaceous receptors cover somewhat larger areas. It is therefore likely that additional regions of σ1 contribute to interactions with JAM-A. We noted that the putative JAM-A-binding site lies at the lower edge of a large, concave surface formed by β-strands B, A, D, and G of σ1. Residues on this surface, which almost entirely covers one side of the β-barrel, would easily be accessible to a receptor and do not participate in intersubunit contacts. The top of the σ1 head is formed by three prominent protrusions, with one coming from each β-barrel. These protrusions are entirely devoid of conserved residues among the serotypes and also exhibit significant sequence drift within type 3 σ1 proteins. It is therefore highly unlikely that the top of the σ1 head participates in receptor binding, again implicating regions on the side of each β-barrel as the most likely areas of contact with JAM-A.

Neutralization-resistant variants of the reovirus T3D/55 selected by using the σ1-specific MAb 9BG5 contain mutations in the σ1 head that segregate genetically with alterations in neural tropism (7, 32, 54, 55). Since reovirus tropism in the murine CNS is determined at least in part by σ1-receptor interactions (19, 60), it is possible that the antibody-selected mutations in the σ1 head alter receptor binding. However, we found that variant K, which has a Glu-to-Lys mutation at amino acid 419, uses JAM-A as a receptor. This observation suggests that the mutation in σ1 of variant K alters the interactions of this strain with cell surface receptors other than JAM-A or influences a postattachment step in reovirus replication. It is noteworthy that amino acid 419 is adjacent to the σ1 head trimer interface in the vicinity of amino acid 340 (16) (Fig. 5), which is also targeted for mutation in neutralization-resistant variants of T3D/55 (7). It is possible that mutations at these sites alter σ1 subunit interactions required for viral assembly or disassembly.

Reovirus serotypes exhibit striking differences in tropism and pathogenesis in the murine CNS. Type 1 reoviruses spread to the CNS hematogenously and infect ependymal cells (65, 70), resulting in subacute hydrocephalus (69). In contrast, type 3 reoviruses spread to the CNS by neural routes and infect neurons (38, 65, 70), causing lethal encephalitis (59, 69). An analysis of reassortant viruses containing gene segments derived from T1L/53 and T3D/55 demonstrated that the pathway of viral spread in the host (65) and tropism for neural tissues (19, 70) segregate with the σ1-encoding S1 gene. These findings suggest that σ1 determines the CNS cell types that serve as targets for reovirus infection, presumably by its capacity to bind to receptors expressed by specific CNS cells. Since all strains of reovirus tested are capable of utilizing JAM-A as a receptor, the engagement of JAM-A alone does not explain the differences in tropism and virulence displayed by the different reovirus serotypes in the murine CNS. It is possible that JAM-A serves as a serotype-independent reovirus receptor at some sites within the host and that other receptors, perhaps carbohydrate in nature, confer serotype-dependent tropism. In support of a role for cell surface carbohydrates in reovirus disease, the capacity to bind sialic acid enhances the spread of type 3 reoviruses within the host and targets the virus to bile duct epithelial cells, leading to obstructive jaundice (4). It is also possible that serotype-dependent differences in pathogenesis are influenced by one or more postbinding events.

The role of JAM-A utilization in reovirus infections in vivo is not known. JAM-A is expressed on many cell types, including intestinal epithelium, bile duct epithelium, lung epithelium, leukocytes, and CNS endothelial cells (36), which serve as sites of reovirus infection in mice (68). It will be interesting to determine whether JAM-A functions as a reovirus receptor at these sites in infected animals. Mice with a targeted disruption of the JAM-A gene are viable and fertile (12). These mice exhibit an accelerated migration of dendritic cells to lymph nodes, which is associated with enhanced contact hypersensitivity (12). No other developmental or immune abnormalities have been noted. Studies of reovirus infections using JAM-A-deficient animals should clarify the function of JAM-A in reovirus pathogenesis and disease.

ACKNOWLEDGMENTS

We thank members of our laboratory for many useful discussions and Annie Antar, Jim Chappell, and Kristen Guglielmi for reviews of the manuscript. We are grateful to Jeff Bergelson for providing the hCAR-specific serum, Chuck Parkos for providing the hJAM-A-specific MAb J10.4, and the Nashville Veterans Affairs Hospital Flow Cytometry Facility for assistance and data analysis. We are grateful to Kevin Coombs, Max Nibert, and Ken Tyler for kindly contributing stocks of reovirus field-isolate strains.

This research was supported by Public Health Service awards T32 CA09385 (J.A.C. and J.C.F.), R01 AI38296 (T.S.D.), and R01 GM67853 (T.S. and T.S.D.) and by the Elizabeth B. Lamb Center for Pediatric Research. Additional support was provided by Public Health Service awards CA68485 to the Vanderbilt Cancer Center and DK20593 to the Vanderbilt Diabetes Research and Training Center.

REFERENCES

1. **Banerjea, A. C., K. A. Brechling, C. A. Ray, H. Erikson, D. J. Pickup, and W. K. Joklik.** 1988. High-level synthesis of biologically active reovirus protein sigma 1 in a mammalian expression vector system. Virology **167:**601–612.
2. **Barton, E. S., J. L. Connolly, J. C. Forrest, J. D. Chappell, and T. S. Dermody.** 2001. Utilization of sialic acid as a coreceptor enhances reovirus attachment by multistep adhesion strengthening. J. Biol. Chem. **276:**2200–2211.
3. **Barton, E. S., J. C. Forrest, J. L. Connolly, J. D. Chappell, Y. Liu, F. Schnell, A. Nusrat, C. A. Parkos, and T. S. Dermody.** 2001. Junction adhesion molecule is a receptor for reovirus. Cell **104:**441–451.
4. **Barton, E. S., B. E. Youree, D. H. Ebert, J. C. Forrest, J. L. Connolly, T. Valyi-Nagy, K. Washington, J. D. Wetzel, and T. S. Dermody.** 2003. Utilization of sialic acid as a coreceptor is required for reovirus-induced biliary disease. J. Clin. Investig. **111:**1823–1833.
5. **Barton, G. J.** 1993. ALSCRIPT: a tool to format multiple sequence alignments. Protein Eng. **6:**37–40.
6. **Bassel-Duby, R., A. Jayasuriya, D. Chatterjee, N. Sonenberg, J. V. Maizel, Jr., and B. N. Fields.** 1985. Sequence of reovirus haemagglutinin predicts a coiled-coil structure. Nature **315:**421–423.
7. **Bassel-Duby, R., D. R. Spriggs, K. L. Tyler, and B. N. Fields.** 1986. Identification of attenuating mutations on the reovirus type 3 S1 double-stranded RNA segment with a rapid sequencing technique. J. Virol. **60:**64–67.
8. **Bazzoni, G., O. M. Martinez-Estrada, F. Mueller, P. Nelboeck, G. Schmid, T. Bartfai, E. Dejana, and M. Brockhaus.** 2000. Homophilic interaction of junctional adhesion molecule. J. Biol. Chem. **275:**30970–30976.
9. **Bergelson, J. M., J. A. Cunningham, G. Droguett, E. A. Kurt-Jones, A. Krithivas, J. S. Hong, M. S. Horwitz, R. L. Crowell, and R. W. Finberg.** 1997.

Isolation of a common receptor for coxsackie B viruses and adenoviruses 2 and 5. Science **275:**1320–1323.
10. **Bewley, M. C., K. Springer, Y. B. Zhang, P. Freimuth, and J. M. Flanagan.** 1999. Structural analysis of the mechanism of adenovirus binding to its human cellular receptor, CAR. Science **286:**1579–1583.
11. **Cao, W., M. D. Henry, P. Borrow, H. Yamada, J. H. Elder, E. V. Ravkov, S. T. Nichol, R. W. Compans, K. P. Campbell, and M. B. Oldstone.** 1998. Identification of alpha-dystroglycan as a receptor for lymphocytic choriomeningitis virus and Lassa fever virus. Science **282:**2079–2081.
12. **Cera, M. R., A. Del Prete, A. Vecchi, M. Corada, I. Martin-Padura, T. Motoike, P. Tonetti, G. Bazzoni, W. Vermi, F. Gentili, S. Bernasconi, T. N. Sato, A. Mantovani, and E. Dejana.** 2004. Increased DC trafficking to lymph nodes and contact hypersensitivity in junctional adhesion molecule-A-deficient mice. J. Clin. Investig. **114:**729–738.
13. **Chappell, J. D., E. S. Barton, T. H. Smith, G. S. Baer, D. T. Duong, M. L. Nibert, and T. S. Dermody.** 1998. Cleavage susceptibility of reovirus attachment protein σ1 during proteolytic disassembly of virions is determined by a sequence polymorphism in the σ1 neck. J. Virol. **72:**8205–8213.
14. **Chappell, J. D., J. L. Duong, B. W. Wright, and T. S. Dermody.** 2000. Identification of carbohydrate-binding domains in the attachment proteins of type 1 and type 3 reoviruses. J. Virol. **74:**8472–8479.
15. **Chappell, J. D., V. L. Gunn, J. D. Wetzel, G. S. Baer, and T. S. Dermody.** 1997. Mutations in type 3 reovirus that determine binding to sialic acid are contained in the fibrous tail domain of viral attachment protein σ1. J. Virol. **71:**1834–1841.
16. **Chappell, J. D., A. Prota, T. S. Dermody, and T. Stehle.** 2002. Crystal structure of reovirus attachment protein σ1 reveals evolutionary relationship to adenovirus fiber. EMBO J. **21:**1–11.
17. **Del Maschio, A., A. De Luigi, I. Martin-Padura, M. Brockhaus, T. Bartfai, P. Fruscella, L. Adorini, G. Martino, R. Furlan, M. G. De Simoni, and E. Dejana.** 1999. Leukocyte recruitment in the cerebrospinal fluid of mice with experimental meningitis is inhibited by an antibody to junctional adhesion molecule (JAM). J. Exp. Med. **190:**1351–1356.
18. **Dermody, T. S., M. L. Nibert, R. Bassel-Duby, and B. N. Fields.** 1990. A σ1 region important for hemagglutination by serotype 3 reovirus strains. J. Virol. **64:**5173–5176.
19. **Dichter, M. A., and H. L. Weiner.** 1984. Infection of neuronal cell cultures with reovirus mimics in vitro patterns of neurotropism. Ann. Neurol. **16:**603–610.
20. **Dörig, R. E., A. Marcil, A. Chopra, and C. D. Richardson.** 1993. The human CD46 molecule is a receptor for measles virus (Edmonston strain). Cell **75:**295–305.
21. **Duncan, R., D. Horne, L. W. Cashdollar, W. K. Joklik, and P. W. K. Lee.** 1990. Identification of conserved domains in the cell attachment proteins of the three serotypes of reovirus. Virology **174:**399–409.
22. **Duncan, R., D. Horne, J. E. Strong, G. Leone, R. T. Pon, M. C. Yeung, and P. W. K. Lee.** 1991. Conformational and functional analysis of the C-terminal globular head of the reovirus cell attachment protein. Virology **182:**810–819.
23. **Duncan, R., and P. W. K. Lee.** 1994. Localization of two protease-sensitive regions separating distinct domains in the reovirus cell-attachment protein sigma 1. Virology **203:**149–152.
24. **Forrest, J. C., J. A. Campbell, P. Schelling, T. Stehle, and T. S. Dermody.** 2003. Structure-function analysis of reovirus binding to junctional adhesion molecule 1. Implications for the mechanism of reovirus attachment. J. Biol. Chem. **278:**48434–48444.
25. **Fraser, R. D. B., D. B. Furlong, B. L. Trus, M. L. Nibert, B. N. Fields, and A. C. Steven.** 1990. Molecular structure of the cell-attachment protein of reovirus: correlation of computer-processed electron micrographs with sequence-based predictions. J. Virol. **64:**2990–3000.
26. **Furlong, D. B., M. L. Nibert, and B. N. Fields.** 1988. Sigma 1 protein of mammalian reoviruses extends from the surfaces of viral particles. J. Virol. **62:**246–256.
27. **Gaggar, A., D. M. Shayakhmetov, and A. Lieber.** 2003. CD46 is a cellular receptor for group B adenoviruses. Nat. Med. **9:**1408–1412.
28. **Gliki, G., K. Ebnet, M. Aurrand-Lions, B. A. Imhof, and R. H. Adams.** 2004. Spermatid differentiation requires the assembly of a cell polarity complex downstream of junctional adhesion molecule-C. Nature **431:**320–324.
29. **Goral, M. I., M. Mochow-Grundy, and T. S. Dermody.** 1996. Sequence diversity within the reovirus S3 gene: reoviruses evolve independently of host species, geographic locale, and date of isolation. Virology **216:**265–271.
30. **Helander, A., K. J. Silvey, N. J. Mantis, A. B. Hutchings, K. Chandran, W. T. Lucas, M. L. Nibert, and M. R. Neutra.** 2003. The viral sigma1 protein and glycoconjugates containing alpha2-3-linked sialic acid are involved in type 1 reovirus adherence to M cell apical surfaces. J. Virol. **77:**7964–7977.
31. **Hrdy, D. B., L. Rosen, and B. N. Fields.** 1979. Polymorphism of the migration of double-stranded RNA segments of reovirus isolates from humans, cattle, and mice. J. Virol. **31:**104–111.
32. **Kaye, K. M., D. R. Spriggs, R. Bassel-Duby, B. N. Fields, and K. L. Tyler.** 1986. Genetic basis for altered pathogenesis of an immune-selected antigenic variant of reovirus type 3 Dearing. J. Virol. **59:**90–97.
33. **Kostrewa, D., M. Brockhaus, A. D'Arcy, G. E. Dale, P. Nelboeck, G. Schmid, F. Mueller, G. Bazzoni, E. Dejana, T. Bartfai, F. K. Winkler, and M. Hennig.** 2001. X-ray structure of junctional adhesion molecule: structural basis for homophilic adhesion via a novel dimerization motif. EMBO J. **20:**4391–4398.
34. **Liu, Y., A. Nusrat, F. J. Schnell, T. A. Reaves, S. Walsh, M. Ponchet, and C. A. Parkos.** 2000. Human junction adhesion molecule regulates tight junction resealing in epithelia. J. Cell Sci. **113:**2363–2374.
35. **Manchester, M., D. S. Eto, A. Valsamakis, P. B. Liton, R. Fernandez-Munoz, P. A. Rota, W. J. Bellini, D. N. Forthal, and M. B. A. Oldstone.** 2000. Clinical isolates of measles virus use CD46 as a cellular receptor. J. Virol. **74:**3967–3974.
36. **Martin-Padura, I., S. Lostaglio, M. Schneemann, L. Williams, M. Romano, P. Fruscella, C. Panzeri, A. Stoppacciaro, L. Ruco, A. Villa, D. Simmons, and E. Dejana.** 1998. Junctional adhesion molecule, a novel member of the immunoglobulin superfamily that distributes at intercellular junctions and modulates monocyte transmigration. J. Cell Biol. **142:**117–127.
37. **Mercier, G. T., J. A. Campbell, J. D. Chappell, T. Stehle, T. S. Dermody, and M. A. Barry.** 2004. A chimeric adenovirus vector encoding reovirus attachment protein σ1 targets cells expressing junctional adhesion molecule 1. Proc. Natl. Acad. Sci. USA **101:**6188–6193.
38. **Morrison, L. A., R. L. Sidman, and B. N. Fields.** 1991. Direct spread of reovirus from the intestinal lumen to the central nervous system through vagal autonomic nerve fibers. Proc. Natl. Acad. Sci. USA **88:**3852–3856.
39. **Nibert, M. L., J. D. Chappell, and T. S. Dermody.** 1995. Infectious subvirion particles of reovirus type 3 Dearing exhibit a loss in infectivity and contain a cleaved σ1 protein. J. Virol. **69:**5057–5067.
40. **Nibert, M. L., T. S. Dermody, and B. N. Fields.** 1990. Structure of the reovirus cell-attachment protein: a model for the domain organization of σ1. J. Virol. **64:**2976–2989.
41. **Nibert, M. L., and L. A. Schiff.** 2001. Reoviruses and their replication, p. 1679–1728. *In* D. M. Knipe, P. M. Howley, D. E. Griffin, R. A. Lamb, M. A. Martin, B. Roizman, and S. E. Straus (ed.), Fields virology, 4th ed. Lippincott-Raven, Philadelphia, Pa.
42. **Nicholls, A., K. A. Sharp, and B. Honig.** 1991. Protein folding and association: insights from the interfacial and thermodynamic properties of hydrocarbons. Proteins **11:**281–296.
43. **Ozaki, H., K. Ishii, H. Horiuchi, H. Arai, T. Kawamoto, K. Okawa, A. Iwamatsu, and T. Kita.** 1999. Cutting edge: combined treatment of TNF-alpha and IFN-gamma causes redistribution of junctional adhesion molecule in human endothelial cells. J. Immunol. **163:**553–557.
44. **Prota, A. E., J. A. Campbell, P. Schelling, J. C. Forrest, T. R. Peters, M. J. Watson, M. Aurrand-Lions, B. Imhof, T. S. Dermody, and T. Stehle.** 2003. Crystal structure of human junctional adhesion molecule 1: implications for reovirus binding. Proc. Natl. Acad. Sci. USA **100:**5366–5371.
45. **Ramos-Alvarez, M., and A. B. Sabin.** 1954. Characteristics of poliomyelitis and other enteric viruses recovered in tissue culture from healthy American children. Proc. Soc. Exp. Biol. **87:**655–661.
46. **Ramos-Alvarez, M., and A. B. Sabin.** 1958. Enteropathogenic viruses and bacteria. Role in summer diarrheal diseases of infancy and early childhood. JAMA **167:**147–158.
47. **Rosen, L.** 1960. Serologic grouping of reovirus by hemagglutination-inhibition. Am. J. Hyg. **71:**242–249.
48. **Rosen, L., J. F. Hovis, F. M. Mastrota, J. A. Bell, and R. J. Huebner.** 1960. Observations on a newly recognized virus (Abney) of the reovirus family. Am. J. Hyg. **71:**258–265.
49. **Rubin, D. H., D. B. Weiner, C. Dworkin, M. I. Greene, G. G. Maul, and W. V. Williams.** 1992. Receptor utilization by reovirus type 3: distinct binding sites on thymoma and fibroblast cell lines result in differential compartmentalization of virions. Microb. Pathog. **12:**351–365.
50. **Sabin, A. B.** 1959. Reoviruses: a new group of respiratory and enteric viruses formerly classified as ECHO type 10 is described. Science **130:**1387–1389.
51. **Segerman, A., J. P. Atkinson, M. Marttila, V. Dennerquist, G. Wadell, and N. Arnberg.** 2003. Adenovirus type 11 uses CD46 as a cellular receptor. J. Virol. **77:**9183–9191.
52. **Smith, R. E., H. J. Zweerink, and W. K. Joklik.** 1969. Polypeptide components of virions, top component and cores of reovirus type 3. Virology **39:**791–810.
53. **Spiropoulou, C. F., S. Kunz, P. E. Rollin, K. P. Campbell, and M. B. Oldstone.** 2002. New World arenavirus clade C, but not clade A and B viruses, utilizes alpha-dystroglycan as its major receptor. J. Virol. **76:**5140–5146.
54. **Spriggs, D. R., R. T. Bronson, and B. N. Fields.** 1983. Hemagglutinin variants of reovirus type 3 have altered central nervous system tropism. Science **220:**505–507.
55. **Spriggs, D. R., and B. N. Fields.** 1982. Attenuated reovirus type 3 strains generated by selection of haemagglutinin antigenic variants. Nature **297:**68–70.
56. **Stehle, T., and T. S. Dermody.** 2003. Structural evidence for common functions and ancestry of the reovirus and adenovirus attachment proteins. Rev. Med. Virol. **13:**123–132.
57. **Stehle, T., and T. S. Dermody.** 2004. Structural similarities in the cellular receptors used by adenovirus and reovirus. Viral Immunol. **17:**129–143.
58. **Swofford, D. L.** 2002. PAUP—phylogenetic analysis using parsimony (and other methods), version 4.0b10. Sinauer Associates, Sunderland, Mass.

59. **Tardieu, M., M. L. Powers, and H. L. Weiner.** 1983. Age-dependent susceptibility to reovirus type 3 encephalitis: role of viral and host factors. Ann. Neurol. **13:**602–607.
60. **Tardieu, M., and H. L. Weiner.** 1982. Viral receptors on isolated murine and human ependymal cells. Science **215:**419–421.
61. **Tatsuo, H., N. Ono, K. Tanaka, and Y. Yanagi.** 2000. SLAM (CDw150) is a cellular receptor for measles virus. Nature **406:**893–897.
62. **Thompson, J. D., T. J. Gibson, F. Plewniak, F. Jeanmougin, and D. G. Higgins.** 1997. The CLUSTAL_X windows interface: flexible strategies for multiple sequence alignment aided by quality analysis tools. Nucleic Acids Res. **25:**4876–4882.
63. **Tyler, K. L.** 2001. Mammalian reoviruses, p. 1729–1745. *In* D. M. Knipe, P. M. Howley, D. E. Griffin, R. A. Lamb, M. A. Martin, B. Roizman, and S. E. Straus (ed.), Fields virology, 4th ed. Lippincott-Raven, Philadelphia, Pa.
64. **Tyler, K. L., E. S. Barton, M. L. Ibach, C. Robinson, T. Valyi-Nagy, J. A. Campbell, P. Clarke, S. M. O'Donnell, J. D. Wetzel, and T. S. Dermody.** 2004. Isolation and molecular characterization of a novel type 3 reovirus from a child with meningitis. J. Infect. Dis. **189:**1664–1675.
65. **Tyler, K. L., D. A. McPhee, and B. N. Fields.** 1986. Distinct pathways of viral spread in the host determined by reovirus S1 gene segment. Science **233:** 770–774.
66. **van Raaij, M. J., E. Chouin, H. van der Zandt, J. M. Bergelson, and S. Cusack.** 2000. Dimeric structure of the coxsackievirus and adenovirus receptor D1 domain at 1.7 A resolution. Structure Fold Des. **8:**1147–1155.
67. **Virgin, H. W., IV, R. Bassel-Duby, B. N. Fields, and K. L. Tyler.** 1988. Antibody protects against lethal infection with the neurally spreading reovirus type 3 (Dearing). J. Virol. **62:**4594–4604.
68. **Virgin, H. W., K. L. Tyler, and T. S. Dermody.** 1997. Reovirus, p. 669–699. *In* N. Nathanson (ed.), Viral pathogenesis. Lippincott-Raven, New York, N.Y.
69. **Weiner, H. L., D. Drayna, D. R. Averill, Jr., and B. N. Fields.** 1977. Molecular basis of reovirus virulence: role of the S1 gene. Proc. Natl. Acad. Sci. USA **74:**5744–5748.
70. **Weiner, H. L., M. L. Powers, and B. N. Fields.** 1980. Absolute linkage of virulence and central nervous system tropism of reoviruses to viral hemagglutinin. J. Infect. Dis. **141:**609–616.
71. **Wetzel, J. D., J. D. Chappell, A. B. Fogo, and T. S. Dermody.** 1997. Efficiency of viral entry determines the capacity of murine erythroleukemia cells to support persistent infections by mammalian reoviruses. J. Virol. **71:**299–306.
72. **Wu, E., S. A. Trauger, L. Pache, T. M. Mullen, D. J. von Seggern, G. Siuzdak, and G. R. Nemerow.** 2004. Membrane cofactor protein is a receptor for adenoviruses associated with epidemic keratoconjunctivitis. J. Virol. **78:**3897–3905.

APPENDIX B

ISOLATION AND CHARACTERIZATION OF A NOVEL TYPE 3 REOVIRUS FROM A CHILD WITH MENINGITIS

Tyler KL, Barton ES, Ibach ML, Robinson C, Campbell JA, O'Donnell SM, Valyi-Nagy T, Clarke P, Wetzel JD, Dermody TS.

Journal of Infectious Diseases. 189(9):1664-75; 2004

MAJOR ARTICLE

Isolation and Molecular Characterization of a Novel Type 3 Reovirus from a Child with Meningitis

Kenneth L. Tyler,[1,2,3,4] Erik S. Barton,[6,9,a] Maria L. Ibach,[5] Christine Robinson,[1,4] Jacquelyn A. Campbell,[6,9] Sean M. O'Donnell,[8,9] Tibor Valyi-Nagy,[7,9,a] Penny Clarke,[1,4] J. Denise Wetzel,[8,9] and Terence S. Dermody,[6,8,9]

Departments of [1]Neurology, [2]Medicine, and [3]Microbiology and Immunology, University of Colorado Health Science Center, [4]Denver Veterans Affairs Medical Center, and [5]Department of Pathology, Children's Hospital, Denver, Colorado; Departments of [6]Microbiology and Immunology, [7]Pathology, and [8]Pediatrics, and [9]Elizabeth B. Lamb Center for Pediatric Research, Vanderbilt University School of Medicine, Nashville, Tennessee

Mammalian reoviruses are nonenveloped viruses that contain a segmented, double-stranded RNA genome. Reoviruses infect most mammalian species, although infection with these viruses in humans is usually asymptomatic. We report the isolation of a novel reovirus strain from a 6.5-week-old child with meningitis. Hemagglutination and neutralization assays indicated that the isolate is a serotype 3 strain, leading to the designation T3/Human/Colorado/1996 (T3C/96). Sequence analysis of the T3C/96 S1 gene segment, which encodes the viral attachment protein, σ1, confirmed the serotype assignment for this strain and indicated that T3C/96 is a novel reovirus isolate. T3C/96 is capable of systemic spread in newborn mice after peroral inoculation and produces lethal encephalitis. These results suggest that serotype 3 reoviruses can cause meningitis in humans.

Mammalian reoviruses are nonenveloped viruses that contain a genome of 10 discrete segments of double-stranded RNA (dsRNA) [1]. There are 3 major reovirus serotypes, which are differentiated by the capacity of antisera to neutralize viral infectivity and inhibit hemagglutination [2, 3]. Reoviruses have a wide geographic distribution and can infect virtually all mammals, including humans [4].

Reoviruses were originally called respiratory enteric orphans on the basis of their repeated isolation from respiratory and enteric tracts of children with asymptomatic illness [2]. Only mild respiratory or gastrointestinal symptoms are observed when infection is symptomatic [4–7]. There are few studies of human reovirus-associated neurological disease [8]. These studies generally relied on serological analysis or isolation of reovirus from stool samples for diagnosis, which is diagnostically inconclusive, because of the frequency of asymptomatic reovirus infections. Three studies have described the isolation of reovirus directly from cerebrospinal fluid (CSF) or neural tissue samples obtained from individuals with meningitis or encephalitis, as described elsewhere [9–11]. In these studies, there was no molecular or virological analysis of the isolated strain performed. Therefore, little is known about the biologic characteristics of reovirus strains that cause human CNS disease.

In contrast to human reovirus infection, infection of newborn mice is highly pathogenic. After oral inoculation in mice, reovirus is taken up by intestinal M cells [12] and undergoes primary replication in lymphoid tissue of Peyer's patches. T1 reovirus spreads to the CNS hematogenously and infects ependymal cells [13, 14], which results in hydrocephalus [15]. In contrast, T3 reovirus spreads to the CNS neurally, infects neurons [13, 14, 16], and causes lethal encephalitis [15, 17]. The pathways of viral spread in the host [13] and pattern

Received 28 August 2003; accepted 17 October 2003; electronically published 15 April 2004.

Financial support: National Science Foundation (support to E.S.B.); Public Health Service (grants T32 CA09385 to J.A.C., T32 AI07474 to S.M.O. and T.V.-N., R01 AI38296 to T.S.D., CA68485 to Vanderbilt-Ingram Cancer Center, and DK20593 to Vanderbilt Diabetes Research and Training Center); Department of Veterans Affairs (REAP and MERIT awards to K.L.T.); US Army Medical Research and Material Command (grant DAMD17-98-1-8614 to K.L.T.); Vanderbilt University Research Council (support to E.S.B.); Elizabeth B. Lamb Center for Pediatric Research; Revler-Lewin Family Professorship of Neurology (support to K.L.T.).

[a] Present affiliations: Department of Pathology, Washington University School of Medicine, St. Louis, Missouri (E.S.B.); Department of Pathology, University of Illinois, Chicago (T.V.-N.).

Reprints or correspondence: Dr. Terence Dermody, Elizabeth B. Lamb Center for Pediatric Research, D7235 MCN, Vanderbilt University School of Medicine, Nashville, TN 37232 (terry.dermody@vanderbilt.edu); Dr. Kenneth Tyler, Neurology B-182, University of Colorado Health Sciences Center, 4200 E. 9th Ave., Denver, CO 80262 (ken.tyler@uchsc.edu)

The Journal of Infectious Diseases 2004;189:1664–75

0022-1899/2004/18909-0015$15.00

Table 1. Reovirus strains used for T3C/96 S1 gene sequence analysis.

Virus strain[a]	Abbreviation	GenBank accession no.	Reference(s)
T1/Human/Ohio/Lang/1953	T1L/53	M35963	[2, 66]
T2/Human/Ohio/Jones/1955	T2J/55	M35964	[2, 67]
T3/Human/Ohio/Dearing/1955	T3D/55	NC_004277	[2, 67]
T3/Human/Washington, DC/clone 93/1955	T3C93/55	L37675	[68]
T3/Human/Washington, DC/Abney/1957	T3A/57	L37677	[69]
T3/Human/Washington, DC/clone 84/1957	T3C84/57	L37678	[44]
T3/Bovine/Maryland/clone 31/1959	T3C31/59	L37683	[68]
T3/Bovine/Maryland/clone 43/1960	T3C43/60	L37682	[68]
T3/Bovine/Maryland/clone 44/1960	T3C44/60	L37681	[44]
T3/Bovine/Maryland/clone 45/1960	T3C45/60	L37680	[44]
T3/Human/Tahiti/clone 8/1960	T3C8/60	L37679	[68]
T3/Bovine/Maryland/clone 18/1961	T3C18/61	L37684	[68]
T3/Murine/France/clone 9/1961	T3C9/61	L37676	[68]
T3/Human/Colorado/1996	T3C/96	AY 302467	Present study

[a] Strains are named according to the following scheme: serotype/species of origin/place of origin/strain designation/year of isolation [70].

of neurotropism [14, 18] segregate with the viral S1 gene, which encodes the viral attachment protein [19, 20]. The σ1 protein which determines the CNS cell types that serve as targets for reovirus infection, presumably by its capacity to bind receptors expressed on specific CNS cells.

The σ1 protein is a fibrous trimer with an elongated tail domain that inserts into the virion and a globular head domain that projects away from the virion surface [21–23]. T1 and T3 σ1 contain receptor-binding domains in both the tail and head regions. A domain in the T3 σ1 tail binds α-linked sialic acid [24, 25], and another domain in the head of both T1 and T3 σ1 binds junctional adhesion molecule 1 (JAM1) [26]. The T1 σ1 tail also binds cell-surface carbohydrate [25]. As a consequence of a sequence polymorphism in the tail of T3D/55 σ1, the sialic acid– and JAM1-binding domains are dissociable by treatment of virions with intestinal proteases, such as trypsin or chymotrypsin [27, 28], which may determine the attenuated virulence of T3D/55 after oral inoculation [29].

Engagement of reovirus receptors also induces postbinding signaling events that influence disease pathogenesis. Reovirus induces apoptosis in cultured cells [30–33], including neurons [34], and in vivo [35, 36]. Neurovirulent strains induces apoptosis to a greater extent than nonneurovirulent strains [30, 31, 34, 37]. Analysis of T1L/53 $\times$ T3D/55 reassortant viruses indicates that differences in apoptosis efficiency are determined primarily by the σ1-encoding S1 gene [30, 31, 37], which suggests that receptor engagement influences the magnitude of the apoptotic response. In concordance with this idea, the most apoptogenic reovirus strains bind to both sialic acid [37] and JAM1 [26].

In the present study, we report the isolation of a T3 reovirus designated T3/Human/Colorado/1996 (T3C/96) from the CSF of a 6.5-week-old child with meningitis. The T3C/96 S1 gene sequence was determined and compared to all previously reported T3 reovirus S1 gene sequences. The capacity of T3C/96 to bind sialic acid and JAM1 and to cause encephalitis in mice was assessed. The results indicate that T3C/96 is a novel T3 reovirus capable of systemic spread to the CNS after peroral inoculation of newborn mice and provide direct evidence that T3 reovirus can be neurovirulent in humans.

MATERIALS AND METHODS

Cells, viruses, and antibodies. Spinner-adapted murine L929 (L) cells grown in suspension or on monolayer cultures and HeLa cell monolayers were maintained as described elsewhere [30, 32]. Prototype reovirus strains T1L/53 and T3D/55 and reovirus field isolate strains (table 1) are laboratory stocks. Virus titers were determined by use of plaque assay [38], and purified virus and particle concentrations were determined, as described elsewhere [21, 39]. Antibodies used included murine σ1-specific monoclonal antibody (MAb) 5C6 (T1 σ1) [40], MAb 9BG5 (T3 σ1) [41], and JAM1-specific MAb J10.4 [42].

Electron microscopy. Supernatant of infected rhesus monkey kidney (RMK) cells was clarified by centrifugation at 1000 *g* for 10 min at 22°C. Clarified supernatant was placed in an Airfuge EM-90 rotor (Beckman Coulter) containing a Formvar-coated grid (Electron Microscopy Sciences) and was centrifuged at 100,000 *g* for 30 min at 22°C. The grid was stained with 2% phosphotungstic acid (1 min) and was examined by use of a Zeiss EM10 electron microscope.

Hemagglutination (HA) assays. Purified reovirus virions (10^{11} particles) were serially diluted in 50 μL of PBS in 96-well round-bottom microtiter plates (Corning-Costar). Calf eryth-

rocytes (Colorado Serum) were washed twice with PBS and were resuspended at a concentration of 1% (vol/vol) in PBS. Erythrocytes (50 μL) were added to wells containing virus and incubated for 2 h at 4°C.

Neutralization assays. T1 and T3 σ1-specific MAbs were serially diluted 2-fold in gelatin saline and were incubated with 10^3 pfu/mL of T3C/96 virions for 1 h at 37°C. Samples were titrated in duplicate on L-cell monolayers by use of plaque assay [38]. Data are presented as the percentage of control plaque-forming units (virions untreated by antibody).

Sequence analysis of the S1 gene. The S1 gene segment of T3C/96 was amplified by use of reverse-transcriptase polymerase chain reaction (RT-PCR), using primers complementary to the 5′ and 3′ nontranslated regions (NTRs) [43], and then was cloned into the pCR 2.1 vector (Invitrogen) and sequenced by use of T4 DNA polymerase (Sequenase 2.0; United States Biochemical). Sequences of the NTRs were determined by use of direct dsRNA sequencing, using purified viral genomic RNA [44]. The S1 gene nucleotide sequences of independent isolates of T3C/96 were determined in independent laboratories and were found to be identical.

Phylogenetic analysis of S1 gene nucleotide sequences. Phylogenetic trees were constructed from variation in the σ1-encoding S1 gene nucleotide sequences by use of the neighbor-joining algorithm (phylogenetic analysis program; MacVector 2001, version 7.1.1; Accelrys). Branching orders of the phylograms were verified statistically by resampling the data 1000 times in a bootstrap analysis, using the branch and bound algorithm (MacVector).

Fluorescent-focus assays of viral infectivity. HeLa cell monolayers (2×10^5 cells/well) were pretreated with PBS, coxsackie and adenovirus receptor (CAR)–specific MAb RmcB (20 μg/mL) [45, 46], *Arthrobacter ureafaciens* neuraminidase (40 mU/mL; ICN Biomedicals), or JAM1-specific MAb J10.4 (20 μg/mL) [42] before adsorption of virus for 1 h at room temperature. Inoculum was removed, and cells were washed with PBS and were incubated for 20 h at 37°C, to permit completion of a single round of viral replication. Cells were fixed with 1 mL of methanol for 30 min at −20°C. Fixed monolayers were washed twice with PBS, blocked with 5% immunoglobulin-free bovine serum albumin (Sigma-Aldrich) in PBS, and incubated for 30 min at 37°C with protein-A–affinity–purified polyclonal rabbit antireovirus serum [47] at a 1:800 dilution in PBS/0.5% Triton X-100. Monolayers were washed twice with PBS/0.5% Triton X-100 and were incubated with a 1:1000 dilution of goat anti–rabbit immunoglobulin serum conjugated with Alexa Fluor 546 fluorophore (Molecular Probes). Monolayers were washed twice with PBS/0.5% Triton X-100, and infected cells were visualized by indirect immunofluorescence by use of a Zeiss Photomicroscope III microscope modified for fluorescence microscopy. Infected cells were identified by the presence of intense cytoplasmic fluorescence that was excluded from the nucleus. No background staining of uninfected control monolayers was detected. Reovirus antigen-positive cells were quantitated by counting fluorescent cells in 3 random fields of view/well in triplicate at a 20× magnification.

Mice and inoculations. ND4 Swiss Webster mice aged 2–3 days with an average weight of 2 g (Harlan) were inoculated either intracranially or perorally with purified virus. Before inoculation, all mice from simultaneously delivered litters were pooled and randomly subdivided into litters of 8–11 mice/dam. For intracranial inoculations, 5 μL of purified virus diluted in gelatin saline was delivered into the right cerebral hemisphere by use of a Hamilton syringe and a 30-gauge needle [48]. For peroral inoculations, 50 μL of purified virus diluted in gelatin saline was delivered into the stomach by passage of a polyethylene catheter 0.61 mm in diameter (BD Biosciences) through the esophagus [49]. At various times after inoculation, mice were killed, and brains were harvested into 2 mL of gelatin saline. Brains were homogenized by freezing (−70°C) and thawing (37°C), which was then followed by sonication. Virus titer in brain homogenates was determined by plaque assay [38].

The LD_{50} of reovirus was determined by use of ND4 Swiss Webster mice aged 2–3 days. Litters of mice were inoculated either intracranially or perorally with a single dose of reovirus and were checked daily for survival. Moribund mice were killed. The LD_{50} of reovirus was calculated by use of the method of Reed and Muench [50]. All animal experiments were performed under institutionally approved protocols in Association for Assessment and Accreditation of Laboratory Animal Care–approved facilities.

Histological and immunohistochemical staining for reovirus antigen. At various times after intracranial inoculation of neonatal mice, mice were killed. Brains were fixed in 10% buffered formaldehyde for 24–48 h at 4°C, paraffin embedded, and thin sectioned. Deparaffinized tissue samples were stained with hematoxylin-eosin.

For immunohistochemical staining, deparaffinized tissue samples were rehydrated by incubation in PBS for 20 min at room temperature. Endogenous peroxidase was quenched by incubation in 0.3% peroxide in methanol for 30 min. Tissue samples were blocked by incubation in PBS containing 1.5% normal goat serum for 20 min. After the blocking solution was removed, tissue samples were incubated for 30 min in rabbit antireovirus serum (1:800 in blocking solution) that was first purified by protein-A affinity chromatography and was preadsorbed against methanol-fixed L-cell monolayers. Antigen-positive cells were visualized by use of avidin-biotin–conjugated horseradish peroxidase (Vectastain ABC) and 3,3′-diaminobenzadine (DAB) substrate, according to the manufacturer's instructions (Vector Laboratories). After DAB staining, tissue samples were rinsed in deionized water and were counterstained

for 45 s with hematoxylin, dehydrated in 95% ethanol, air dried, and mounted under coverslips by use of Accu-Mount 60 reagent (Baxter Healthcare).

RESULTS

Case report. A 6.5-week-old female infant who was delivered vaginally at 35 weeks gestation had a 3-day history of irritability, decreased appetite, vomiting, and high-pitched cry. After vital signs were notable for temperature of 38.8°C (pr), heart rate of 166 beats/min, respiratory rate of 36 breaths/min, and blood pressure of 72/30 mmHg. The child was in mild respiratory distress, with grunting while breathing room air. Her neck was supple, chest and cardiac examinations were normal, and her abdomen was soft and nontender. Neurological examination was remarkable for lethargy, normal cranial nerves, muscle tone, and reflexes. An episode consistent with a generalized seizure was noted in the emergency department.

Her hematocrit was 27.7%, white blood cell (WBC) count was 9500 cells/mm^3, and platelet count was 412,000 platelets/mm^3. CSF contained a WBC count of 22 cells/mm^3 (77% neutrophils, 9% bands, and 14% lymphocytes), a protein level of 67 mg/dL, and a glucose level of 44 mg/dL. The serum glutamate oxaloacetate transaminase level was 64 IU/L (normal, <60 IU/L), and the conjugated bilirubin level was 0.5 mg/dL (normal, <0.3 mg/dL). Alkaline phosphatase, serum glutamate pyruvate transaminase, and gamma glutamyltransferase levels were normal. Bacterial cultures of blood and CSF were sterile. CSF PCR assay was negative for enteroviruses and herpes simplex virus. During her 5 days of hospitalization, the patient developed transient abdominal distension and watery diarrhea. No erythrocytes or leukocytes were observed after microscopy of stool samples, and stool cultures were negative for enteric pathogens, as were tests for rotavirus antigen and electron microscopy for rotavirus particles. She gradually recovered and was discharged from the hospital without obvious neurological sequelae.

Isolation and virological characterization of a novel T3 reovirus strain. CSF was inoculated onto primary human diploid fibroblast (MRC-5), human epithelial carcinoma (Hep-2), and primary RMK cell monolayers. The RMK cell cultures developed a granular, nonsloughing pattern of cytopathic effect (CPE). Supernatant of these cells was used to infect MRC-5 cells, which developed similar CPE. Electron microscopy of infected cells demonstrated icosahedral nonenveloped viral particles characteristic of mammalian reovirus (figure 1*A*).

The original RMK cell lysate was used to inoculate flasks of murine L cells, which developed a characteristic reovirus CPE. Plaque assay of lysates demonstrated round 1–2 mm plaques. Electrophoretic analysis of infected L-cell lysates demonstrated the presence of 10 viral gene segments (figure 1*B*). The largest

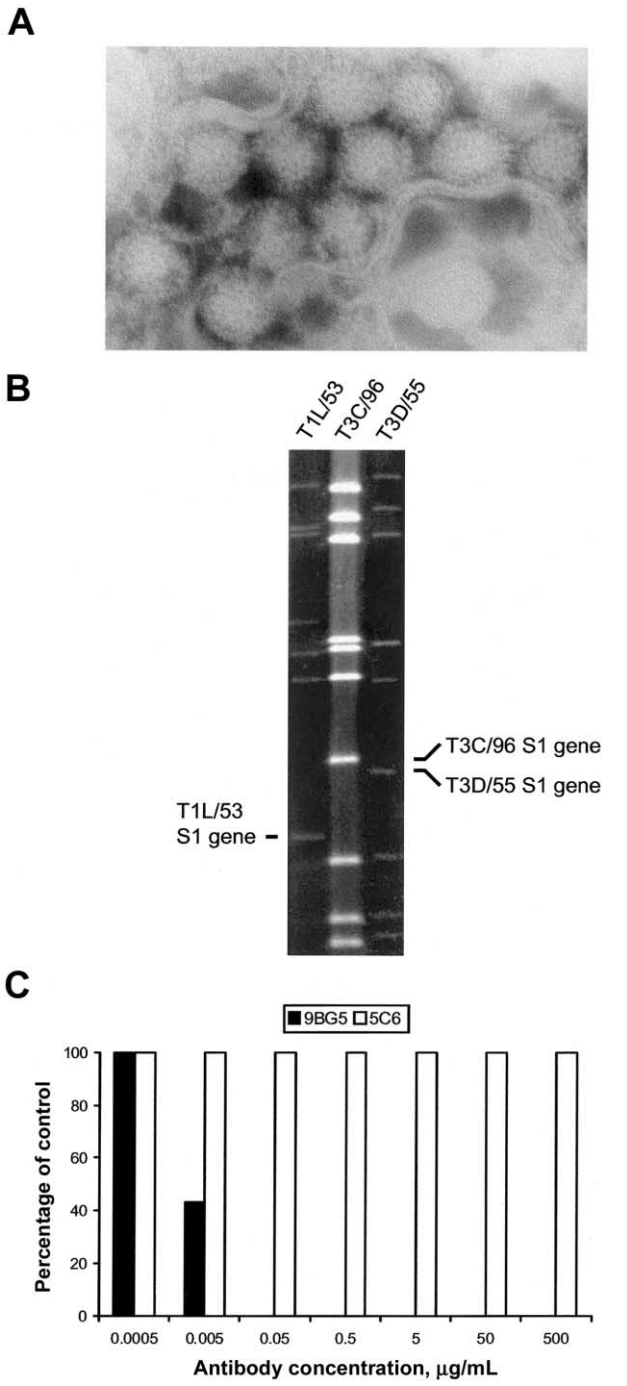

Figure 1. Strain characterization of T3C/96. *A,* Electron micrograph of T3C/96 after growth in primary rhesus monkey kidney cells. *B,* Electrophoretic analysis of reovirus strains T1L/53, T3C/96, and T3D/55. Approximately equal numbers of reovirus particles were resolved by acrylamide gel electrophoresis. Viral double-strand RNA (dsRNA) gene segments were visualized after staining of the gel with ethidium bromide. Position of the serotype-determining S1 gene segment is indicated for each strain. *C,* Neutralization of T3C/96 with σ1-specific monoclonal antibodies (MAbs). T3C/96 virions were incubated for 1 h at 37°C with either the T1σ1-specific MAb 5C6 or the T3 σ1-specific MAb 9BG5 at the concentrations shown. Viral titer was determined by plaque assay, using L cells. Data are the mean of 2 experiments.

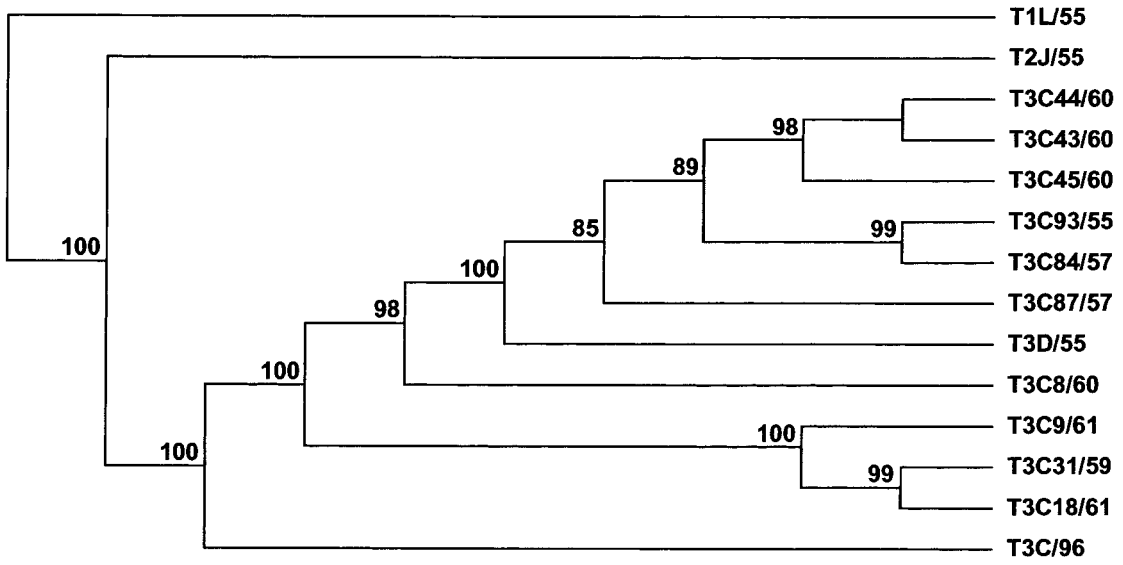

Figure 2. Phylogenetic tree based on S1 gene nucleotide sequences of 14 reovirus strains. Phylogenetic tree for 1416 nt of the S1 gene (nt 12–1370) of the strains shown in table 1 was constructed by use of the neighbor-joining algorithm of MacVector (version 7.1.1; Accelrys). Bootstrap values >50% (indicated as a percentage of 1000 repetitions) for major branches are shown at the nodes. The tree is unrooted.

of the S-class gene segments (S1) migrated slowly in the acrylamide gel, a characteristic of T3 reovirus strains (figure 1*B*). Virus produced after infection of L cells agglutinated bovine erythrocytes (HA observed at virus concentrations $\geq 6.25 \times 10^4$ pfu/well), which is characteristic of HA produced by T3 reovirus (data not shown) [51, 52]. The CSF isolate was efficiently neutralized by T3 σ1-specific MAb 9BG5 (>50% plaque reduction at 5 ng/mL), but not by T1 σ1-specific MAb 5C6 (no plaque reduction at ≤ 500 μg/mL) (figure 1*C*). The new reovirus isolate was designated T3C/96.

Sequence analysis of the T3C/96 S1 gene. The reovirus S1 gene, encoding viral attachment protein σ1 [19, 20], is the major genetic determinant of neurovirulence in infected mice [14, 15]. Therefore, we determined the sequence of the T3C/96 S1 gene (GenBank accession no. AY302467). The 5′ and 3′ NTRs of all T3 reovirus S1 genes sequenced to date are highly conserved [44]. RT-PCR primers complementary to the NTRs were designed to permit amplification of the entire T3C/96 S1 gene from infected L-cell lysates. A PCR product of the expected size (~1.4 kb) was obtained. The S1 gene cDNA was cloned and sequenced. NTRs of the T3C/96 S1 gene were directly sequenced by use of dsRNA as template. Nucleotide sequences of the prototype T3D/55 and the novel T3C/96 S1 genes shared 69% positional identity, which provided sequence confirmation of the assignment of this new isolate as a T3 strain.

To define the evolutionary relationship of the T3C/96 S1 gene with the S1 genes of other reovirus strains sequenced to date, we constructed phylogenetic trees by use of variation in the S1 gene nucleotide sequences and the neighbor-joining algorithm (figure 2). The most noteworthy feature of the S1 phylogenetic tree is that the S1 gene sequence of T3C/96 is substantially divergent from all other T3 strains analyzed. However, the T3C/96 S1 gene is more closely related to the S1 genes of the other T3 strains than to those of either T1 or T2 strains. A phylogenetic tree generated by use of the maximum likelihood method (Phylogeny Inference Package) [53] had a topology identical to the tree generated by using the neighbor-joining algorithm (data not shown). Therefore, T3C/96 is the first member of a highly divergent clade of T3 reovirus.

Comparison of the deduced amino acid sequences of the T3D/55 and T3C/96 σ1 proteins confirms their evolutionary relationship, with the sequences sharing 74.3% positional identity (figure 3*A*). Secondary structure predictions for the 2 proteins are strikingly similar (data not shown). Notably, both T3D/55 and T3C/96 σ1 possess amino-terminal regions with high α-helical predictions and contain regions of sequence between amino-terminal residues 200–300 with high β-sheet predictions.

The deduced aa sequence of T3C/96 σ1 protein was compared with that of T3D/55 across known functional domains (figure 3*B*). The region between aa residues 198 and 204 has been linked genetically [24, 52, 54] and biochemically [25] to the capacity of T3D/55 to bind sialic acid. The sequence of T3C/96 σ1 was identical to that of T3D/55 across this region, which is consistent with the capacity of T3C/96 to produce HA and suggests that T3C/96 uses α-linked sialic acid as a coreceptor. Sequence polymorphism at aa 249 influenced the susceptibility of T3 σ1 protein to cleavage by intestinal proteases [28]. T3C/96 encoded a hydrophobic isoleucine at aa 249, which is a characteristic of all T3 strains that possess protease-resistant

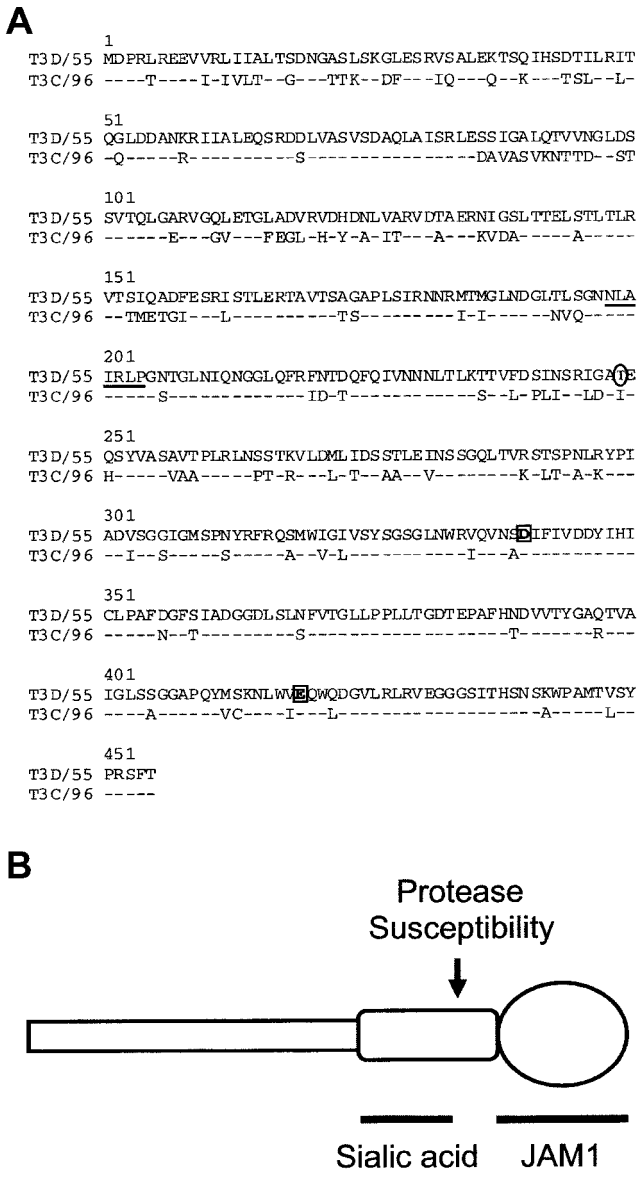

Figure 3. Sequence analysis of the T3C/96 σ1 protein. *A,* Alignment of deduced amino acid sequences of the σ1 proteins of T3D/55 and T3C/96. T3D/55 σ1 protein aa residues 1–455 are shown by use of the single-letter aa code. aa Residues in T3C/96 σ1 that are identical to the T3D/55 sequence are indicated by dashes. aa Positions are numbered above the sequences. aa Residues in the predicted sialic acid–binding domain [24, 25, 52, 54] are underlined. A sequence that confers sensitivity to cleavage by intestinal proteases [28] is circled. aa Residues identified to be important for neuronal tropism [55, 56] are boxed. *B,* Functional domains of σ1 protein. JAM1, junctional adhesion molecule 1.

σ1 proteins [28]. Two aa residues in the σ1 head domain (aa 340 and 419) have been genetically implicated in reovirus neurotropism [55, 56]. These aa residues are identical in the T3D/55 and T3C/96 σ1 proteins, and aa residues in the immediate vicinity of these 2 sites are highly conserved. Thus, the divergent strain T3C/96 conserves several domains of σ1 known to be important for reovirus neurovirulence.

T3C/96 receptor utilization. To determine whether T3C/96 is capable of using sialic acid and JAM1 as functional receptors, HeLa cells were treated with neuraminidase, JAM1-specific MAb J10.4, or both neuraminidase and MAb J10.4 before adsorption with T3C/96. Infected cells were quantitated by use of indirect immunofluorescence, using an antireovirus serum (figure 4). Compared to either untreated cells or cells treated with CAR-specific MAb RmcB as a control, treatment of cells with neuraminidase to remove cell-surface sialic acid resulted in a 61% reduction in the number of infected cells. Treatment of cells with JAM1-specific MAb J10.4 resulted in a 47% reduction in the number of infected cells. However, when cells were treated with both neuraminidase and MAb J10.4, infection by T3C/96 was virtually abolished. Therefore, T3C/96 is capable of using both sialic acid and JAM1 as receptors, which confirms predictions made by analysis of its σ1 protein sequence.

Pathogenesis of T3C/96 in mice. To test the capacity of T3C/96 to infect CNS tissue, newborn mice were inoculated intracranially with either T3C/96 or T3D/55 and were killed at various times after inoculation. Infectious virus present in homogenized brain tissue samples was quantitated by use of plaque assay (figure 5). Similar to T3D/55, T3C/96 replicated efficiently in CNS tissues, producing yields 10,000-fold greater than input 4 days after inoculation and sustaining high titers in the brain up to 12 days after infection. These data indicate that T3C/96 can infect and grow to high titer in the murine CNS.

To assess the neurovirulence of T3C/96, litters of newborn mice were inoculated intracranially with increasing doses (10^1–10^4 pfu/mouse) of either T3D/55 or T3C/96, and mortality was monitored daily for 21 days after inoculation (figure 6*A*). T3D/55 is neurovirulent after intracranial infection, displaying an LD_{50} of ~100 pfu, which is consistent with previously studies, as described elsewhere [38, 57, 58]. Infection with T3C/96 also resulted in lethality, although with somewhat reduced virulence, compared with T3D/55 (LD_{50}, ~ 3000 pfu). These results indicate that T3C/96 is virulent after direct inoculation of the virus into the brain.

To determine whether T3C/96 is virulent after a natural route of infection, newborn mice were inoculated perorally with 10^5, 10^6, or 10^7 pfu/mouse of either T3D/55 or T3C/96 and were monitored daily for mortality (figure 6*B*). In contrast to results obtained after intracranial inoculation, we found that only T3C/96 was virulent after peroral inoculation. At the highest dose of virus used, no mice survived infection with T3C/96, whereas 90% of T3D-infected mice survived. Thus, T3C/96 can disseminate from the murine intestine to the CNS and produce a lethal infection.

To assess pathologic changes associated with T3C/96 infection in the CNS, brain section samples derived from mice killed 2, 4, and 6 days after intracranial inoculation with either 10^4

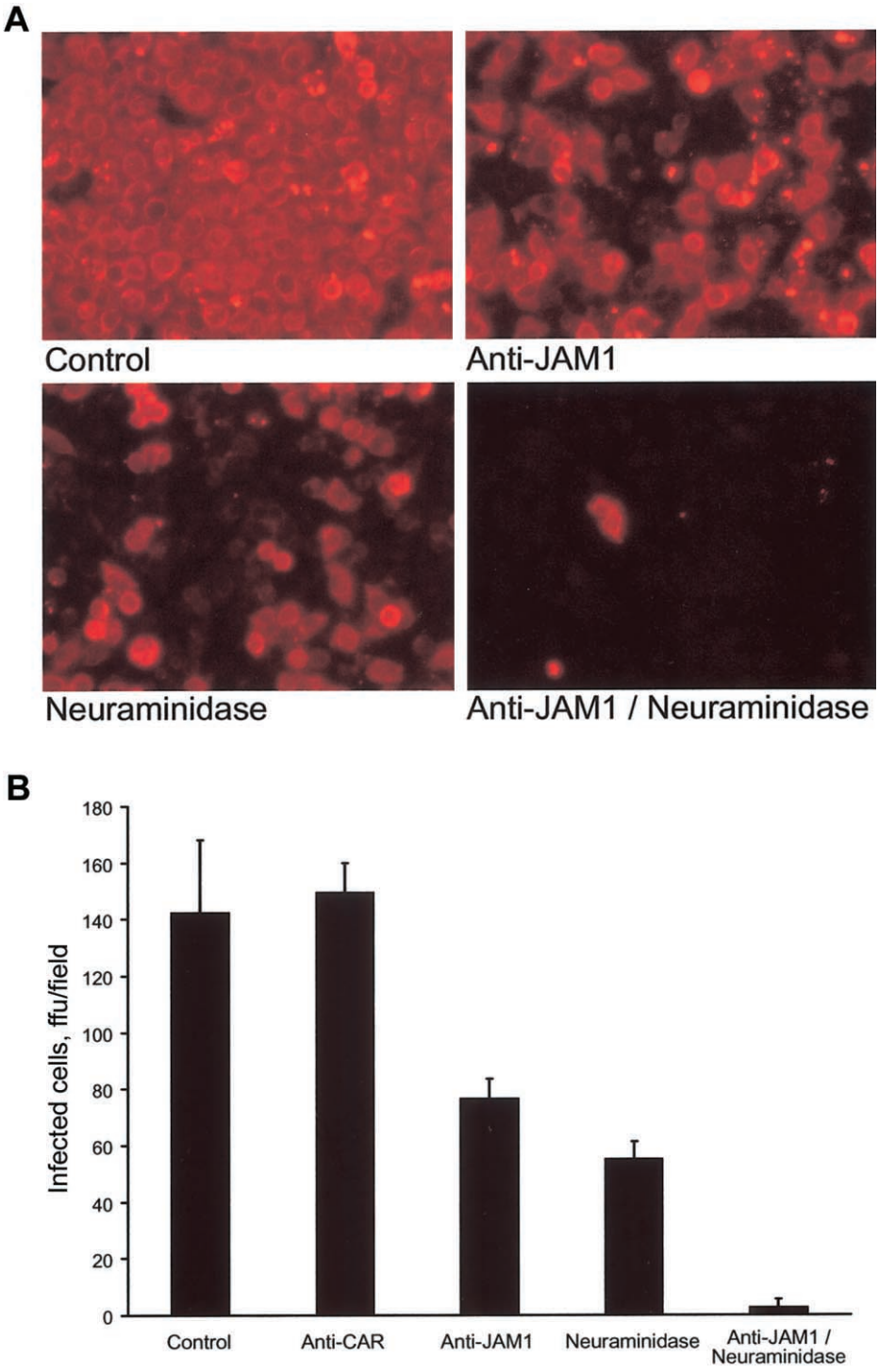

Figure 4. Effect of neuraminidase and junctional adhesion molecule 1 (JAM1)–specific monoclonal antibody (MAb) on growth of T3C/96. HeLa cells (2×10^5 cells) were pretreated with PBS, coxsackie and adenovirus receptor (CAR)–specific MAb RmcB (20 μg/mL) [45, 46], neuraminidase (40 mU/mL), JAM1-specific MAb J10.4 (20 μg/mL) [42], or neuraminidase and MAb J10.4 before adsorption with T3C/96 at an MOI of 1 fluorescent focus unit (ffu)/cell. After incubation for 20 h, cells were fixed and permeabilized with methanol. Newly synthesized viral proteins were detected by incubating cells with polyclonal rabbit antireovirus serum, followed by incubation with anti–rabbit immunoglobulin Alexa-546 serum for visualization of infected cells by indirect immunofluorescence. *A,* Representative fields of view are shown. *B,* Reovirus antigen–positive cells were quantitated by enumerating fluorescent cells in 3 random fields of view/well in triplicate. Data are mean fluorescent focus units for 3 wells. Error bars indicate SDs. ffu, Fluorescent-forming units.

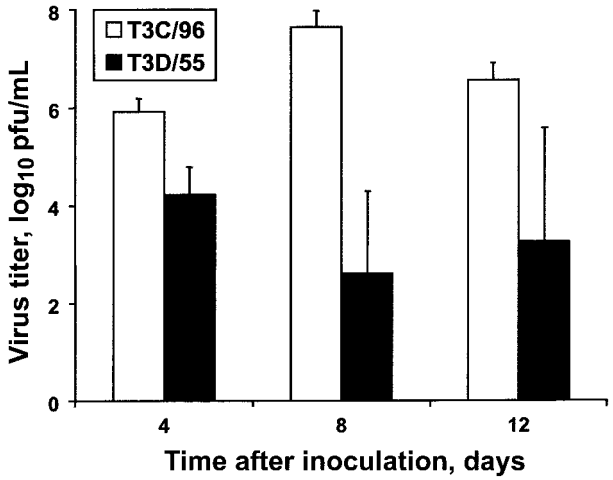

Figure 5. Growth of T3C/96 in mice after intracranial inoculation. ND4 Swiss Webster mice (aged 2–3 days) were inoculated intracranially with 100 plaque-forming units (pfu) of either T3C/96 or T3D/55. At the indicated days after inoculation, mice were killed, and brains were collected. Brain tissue samples were homogenized by sonication, and titers of virus present in homogenates were determined by use of plaque assay. Each data point represents the average virus titer of 2–4 brains. Error bars indicate SD.

pfu of T3C/96 or gelatin saline were examined after staining with hematoxylin-eosin (figure 7*A,* 7*C,* 7*E,* and 7*G;* data not shown). Brain section samples derived from mice infected with T3C/96 demonstrated evidence of meningoencephalitis (figure 7*A* and 7*E*; data not shown). Inflammatory infiltrates were detected primarily in the cerebral cortex, hippocampus, diencephalon, and brain stem. Morphologically, inflammatory cells were mostly lymphocytes and macrophages/microglia, with some plasma cells and neutrophils. The extent of inflammation increased with time after virus inoculation, with the most extensive inflammation observed 6 days after inoculation (data not shown).

To define the extent and location of reovirus antigen in the CNS of T3C/96-infected mice, section samples derived from mice killed 2, 4, and 6 days after inoculation with either 10^4 pfu of T3C/96 or gelatin saline were examined after staining with a reovirus-specific antiserum (figure 7*B,* 7*D,*7*F,* and 7*H;* data not shown). Immunohistochemical staining for reovirus protein demonstrated immunoreactive neurons in brain section samples derived from T3C/96-infected, but not mock-infected, mice. Antigen-positive neurons were detected primarily in the cerebral cortex, hippocampus, diencephalon, and brain stem. Similar to the observed inflammatory changes, the number of antigen-positive cells increased with time after virus inoculation (data not shown). Most cells demonstrating immunohistochemical evidence of reovirus protein were detected in inflamed foci. These observations indicate that intracranial inoculation of T3C/96 leads to encephalitis and reovirus protein expression in newborn mice. Therefore, T3C/96 is capable of neurovirulent infection.

DISCUSSION

The present study is the first molecular characterization of a reovirus strain isolated directly from the CSF of an infant with symptoms and signs consistent with meningitis. The strain isolated, T3C/96, is a novel T3 reovirus, as determined by its HA capacity, neutralization profile, and S1 gene sequence. Molecular analysis of the T3C/96 S1 gene indicates that this strain is the most divergent T3 reovirus isolated to date. Despite this divergence, key functional domains of σ1 are conserved in this strain. T3C/96 encodes an isoleucine at position 249 in σ1, a polymorphism that has been linked to the capacity of T3 reovirus strains to infect the murine intestine and to spread from the intestine to the CNS [28]. In addition, key aa residues in the σ1 head domain implicated in T3 neural tropism and neu-

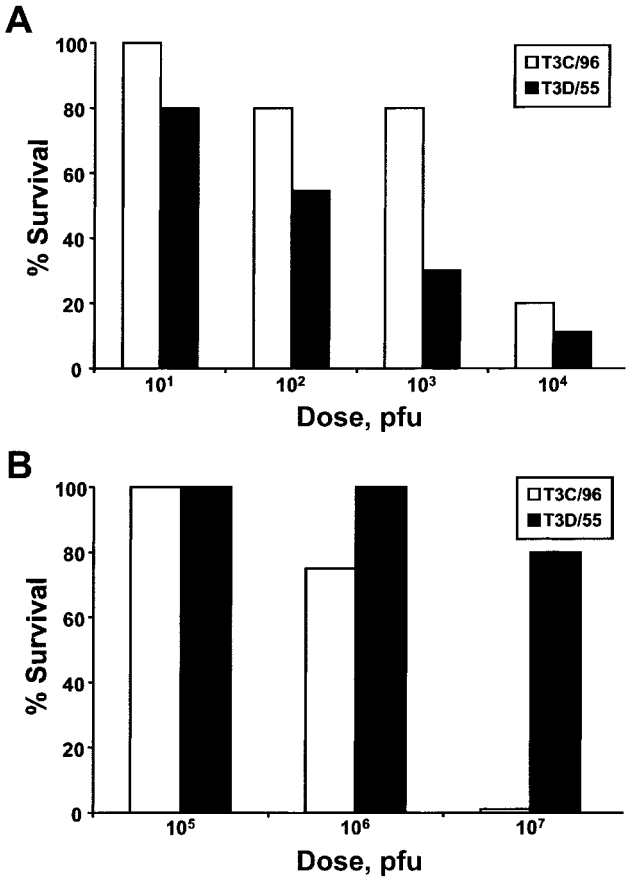

Figure 6. Lethality of T3D/55 and T3C/96 after either intracranial *(A)* or peroral inoculation *(B).* ND4 Swiss Webster mice (2–3 days) were inoculated with various doses of either T3D/55 or T3C/96. Each dose was inoculated into single litters of mice. Survival was monitored daily for 21 days. pfu, Plaque-forming units.

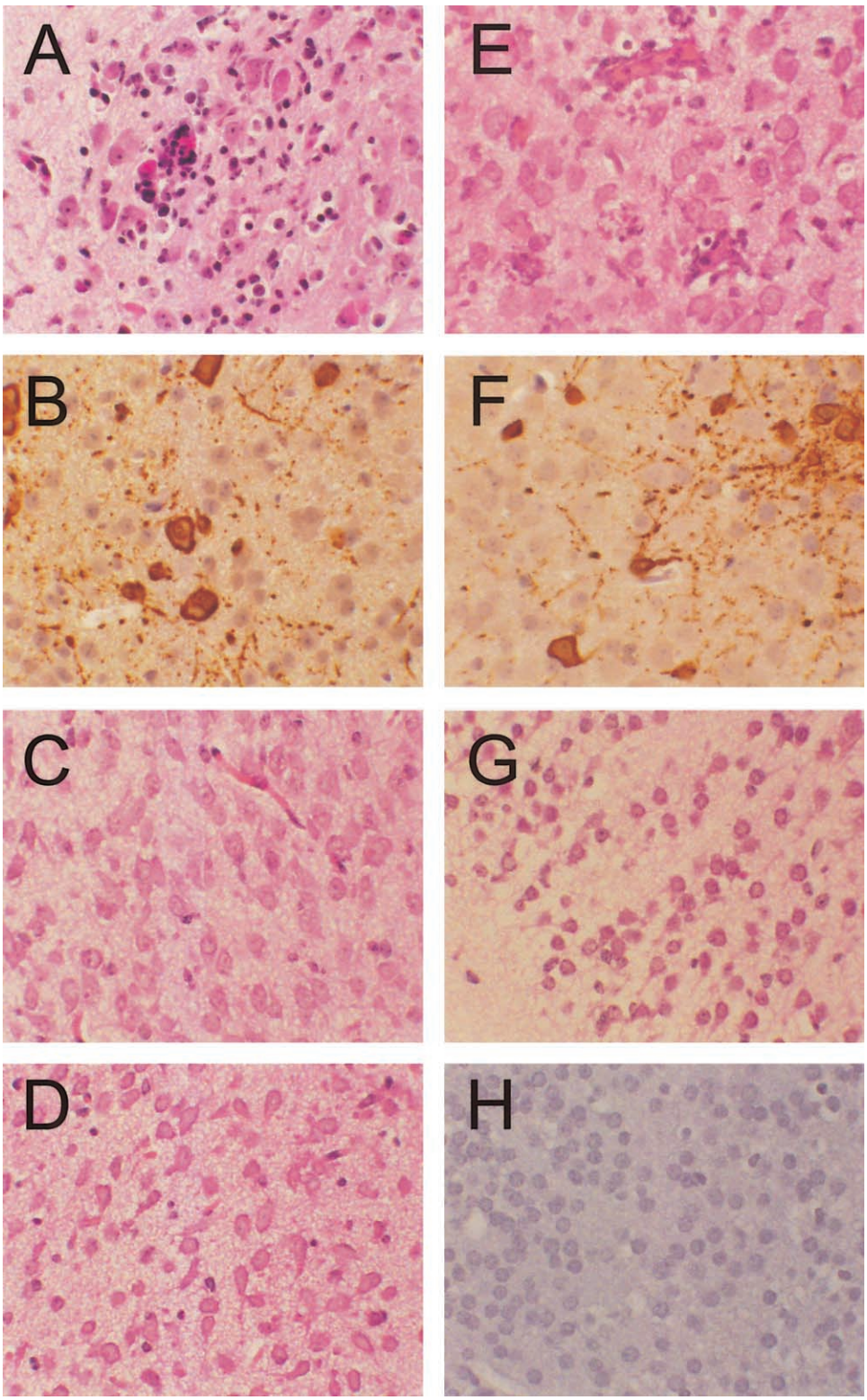

Figure 7. Inflammation and reovirus protein expression in the brain of newborn mice infected with T3C/96. ND4 Swiss Webster mice (2–3 days) were inoculated intracranially with either 10^4 pfu of T3C/96 *(A, B, E,* and *F)* or gelatin saline *(C, D, G,* and *H).* At 6 days after inoculation, brain tissue samples were harvested, paraffin embedded, sectioned, and stained with hematoxylin-eosin *(A, C, E,* and *G)* or stained for reovirus antigen by use of a polyclonal antireovirus serum *(B, D, F,* and *H).* Sections are from the upper brain stem *(A–D)* and the cortex *(E–H).* Brown staining indicates reovirus antigen.

rovirulence [55, 56] are conserved. The conservation of aa residues involved in sialic acid binding [24, 25, 52, 54] in T3C/96 σ1 suggests that binding to this carbohydrate may be important in neurovirulence, a hypothesis supported by the finding that the capacity to bind sialic acid enhances reovirus spread from the murine intestine to the CNS [59].

Experimental infections of mice indicate that T3C/96 is neurotropic and neurovirulent. T3C/96 productively infects the murine CNS, producing lethal infection after direct intracranial inoculation. However, in striking contrast to T3D/55, T3C/96 is also virulent after peroral inoculation, which may be related to a sequence polymorphism in σ1 at aa 249.

Why do reovirus infections of humans rarely produce disease? Analysis of the T3C/96 S1 sequence suggests that the low incidence of serious illness associated with reovirus infection may be caused, in part, by a requirement for a discrete set of viral biochemical characteristics that permit neural spread of enteric reovirus infections. Specifically, a protease-resistant σ1 molecule may be required for both efficient growth in the intestine and spread to secondary sites of replication, including the CNS. In addition, the capacity to bind sialic acid also may function to enhance spread to the CNS in infected humans [59]. Finally, specific sequences may be required in receptor-binding domains of the σ1 head to permit efficient infection of CNS neurons. It is conceivable that viral strains lacking any of these characteristics would be nonpathogenic in humans.

Host factors also play an important role in determining the outcome of reovirus infection. Studies using mice indicate that reovirus virulence strongly correlates with host age. Newborn mice are exquisitely susceptible to reovirus CNS infection, whereas adult mice support limited viral growth and show no histopathological evidence of CNS injury even after intracranial inoculation of large doses of virus [17]. The capacity of reovirus to invade the CNS from a peripheral site of inoculation also declines rapidly with age [60]. In addition to host age, host immune responses can influence susceptibility to reovirus infection. Administration of reovirus-specific antibodies by either transplacental transfer [61] or intraperitoneal inoculation [38, 57, 58] protects newborn mice against fatal reovirus infection of the CNS. The rarity of human neurological infection with reoviruses could reflect the fact that exposure to nonneurovirulent reovirus generates protective immune responses, which, in turn, prevent neurological disease after subsequent exposure to "neurovirulent" strains. Neurological disease would occur only when a nonimmune susceptible individual was exposed to a virus containing the appropriate set of neurovirulence determinants.

In addition to reovirus, other members of the *Reoviridae* family have been associated with CNS disease in humans. Rotavirus, an important cause of gastroenteritis in children (reviewed in [62]) has been implicated in a few cases of encephalitis [63, 64], as has Colorado tick fever virus, a member of the *Coltivirus* genus of the *Reoviridae* [65]. The patient reported in the present study provides evidence that reovirus also can cause human CNS disease.

Acknowledgments

We appreciate the virology skills of Elaine Dowell and the willingness of Gary Mierau to perform electron microscopy on unusual viruses isolated at the Children's Hospital in Denver. We thank Kelly Parman (Vanderbilt Mouse Pathology Core Laboratory) and Sandy Olson (Vanderbilt Pathology Department) for tissue sectioning and staining and Greg Hanley and Joan Richerson for expert veterinary care. We are grateful to Jim Chappell, Tim Peters, and Bryan Youree for review of the manuscript; and Brent Weedman for preparation of the histology figures. We thank Chuck Parkos (Emory University) for providing monoclonal antibody J10.4.

Reference

1. Nibert ML, Schiff LA. Reoviruses and their replication. In: Knipe DM, Howley PM, eds. Fields virology. 4th ed. Philadelphia: Lippincott-Raven, **2001**:1679–728.
2. Sabin AB. Reoviruses: a new group of respiratory and enteric viruses formerly classified as ECHO type 10 is described. Science **1959**; 130: 1387–9.
3. Rosen L. Serologic grouping of reovirus by hemagglutination-inhibition. Am J Hyg **1960**; 71:242–9.
4. Tyler KL. Mammalian reoviruses. In: Knipe DM, Howley PM, eds. Fields virology. 4th ed. Philadelphia: Lippincott-Raven, **2001**:1729–945.
5. Jackson GG, Muldoon RL, Cooper RS. Reovirus type 1 as an etiologic agent of the common cold. J Clin Invest **1961**; 40:1051.
6. Lerner AM, Cherry JD, Klein JO, Finland M. Infections with reoviruses. N Engl J Med **1962**; 267:947–52.
7. Leers WD, Rozee KR. A survey of reovirus antibodies in sera of urban children. Can Med Assoc J **1966**; 94:1040–2.
8. Tyler KL. Pathogenesis of reovirus infections of the central nervous system. Curr Top Microbiol Immunol **1998**; 233:93–124.
9. Krainer L, Aronson BE. Disseminated encephalomyelitis in humans with recovery of hepatoencephalitis virus. J Neuropathol Exp Neurol **1959**; 18:339–42.
10. Joske RA, Keall DD, Leak PJ, Stanley NF, Walters MN. Hepatitis-encephalitis in humans with reovirus infections. Arch Intern Med **1964**; 113:811–6.
11. Johansson PJ, Sveger T, Ahlfors K, Ekstrand J, Svensson L. Reovirus type 1 associated with meningitis. Scand J Infect Dis **1996**; 28:117–20.
12. Wolf JL, Rubin DH, Finberg R, et al. Intestinal M cells: a pathway of entry of reovirus into the host. Science **1981**; 212:471–2.
13. Tyler KL, McPhee DA, Fields BN. Distinct pathways of viral spread in the host determined by reovirus S1 gene segment. Science **1986**; 233: 770–4.
14. Weiner HL, Powers ML, Fields BN. Absolute linkage of virulence and central nervous system tropism of reoviruses to viral hemagglutinin. J Infect Dis **1980**; 141:609–16.
15. Weiner HL, Drayna D, Averill DR Jr, Fields BN. Molecular basis of reovirus virulence: role of the S1 gene. Proc Natl Acad Sci USA **1977**;74: 5744–8.
16. Morrison LA, Sidman RL, Fields BN. Direct spread of reovirus from the intestinal lumen to the central nervous system through vagal autonomic nerve fibers. Proc Natl Acad Sci USA **1991**; 88:3852–6.
17. Tardieu M, Powers ML, Weiner HL. Age-dependent susceptibility to

reovirus type 3 encephalitis: role of viral and host factors. Ann Neurol **1983**; 13:602–7.
18. Dichter MA, Weiner HL. Infection of neuronal cell cultures with reovirus mimics in vitro patterns of neurotropism. Ann Neurol **1984**; 16:603–10.
19. Weiner HL, Ault KA, Fields BN. Interaction of reovirus with cell surface receptors. I. Murine and human lymphocytes have a receptor for the hemagglutinin of reovirus type 3. J Immunol **1980**; 124:2143–8.
20. Lee PW, Hayes EC, Joklik WK. Protein σ1 is the reovirus cell attachment protein. Virology **1981**; 108:156–63.
21. Furlong DB, Nibert ML, Fields BN. Sigma 1 protein of mammalian reoviruses extends from the surfaces of viral particles. J Virol **1988**; 62:246–56.
22. Banerjea AC, Brechling KA, Ray CA, Erikson H, Pickup DJ, Joklik WK. High-level synthesis of biologically active reovirus protein σ1 in a mammalian expression vector system. Virology **1988**; 167:601–12.
23. Fraser RDB, Furlong DB, Trus BL, Nibert ML, Fields BN, Steven AC. Molecular structure of the cell-attachment protein of reovirus: correlation of computer-processed electron micrographs with sequence-based predictions. J Virol **1990**; 64:2990–3000.
24. Chappell JD, Gunn VL, Wetzel JD, Baer GS, Dermody TS. Mutations in type 3 reovirus that determine binding to sialic acid are contained in the fibrous tail domain of viral attachment protein σ1. J Virol **1997**; 71:1834–41.
25. Chappell JD, Duong JL, Wright BW, Dermody TS. Identification of carbohydrate-binding domains in the attachment proteins of type 1 and type 3 reoviruses. J Virol **2000**; 74:8472–9.
26. Barton ES, Forrest JC, Connolly JL, et al. Junction adhesion molecule is a receptor for reovirus. Cell **2001**; 104:441–51.
27. Nibert ML, Chappell JD, Dermody TS. Infectious subvirion particles of reovirus type 3 Dearing exhibit a loss in infectivity and contain a cleaved σ1 protein. J Virol **1995**; 69:5057–67.
28. Chappell JD, Barton ES, Smith TH, et al. Cleavage susceptibility of reovirus attachment protein σ1 during proteolytic disassembly of virions is determined by a sequence polymorphism in the σ1 neck. J Virol **1998**; 72:8205–13.
29. Bodkin DK, Fields BN. Growth and survival of reovirus in intestinal tissue: role of the L2 and S1 genes. J Virol **1989**; 63:1188–93.
30. Tyler KL, Squier MK, Rodgers SE, et al. Differences in the capacity of reovirus strains to induce apoptosis are determined by the viral attachment protein σ1. J Virol **1995**; 69:6972–9.
31. Rodgers SE, Barton ES, Oberhaus SM, et al. Reovirus-induced apoptosis of MDCK cells is not linked to viral yield and is blocked by Bcl-2. J Virol **1997**; 71:2540–6.
32. Connolly JL, Rodgers SE, Clarke P, et al. Reovirus-induced apoptosis requires activation of transcription factor NF-κB. J Virol **2000**; 74: 2981–9.
33. Clarke P, Meintzer SM, Gibson S, et al. Reovirus-induced apoptosis is mediated by TRAIL. J Virol **2000**; 74:8135–9.
34. Richardson-Burns SM, Kominsky DJ, Tyler KL. Reovirus-induced neuronal apoptosis is mediated by caspase 3 and is associated with the activation of death receptors. J Neurovirol **2002**; 8:365–80.
35. Oberhaus SM, Smith RL, Clayton GH, Dermody TS, Tyler KL. Reovirus infection and tissue injury in the mouse central nervous system are associated with apoptosis. J Virol **1997**; 71:2100–6.
36. DeBiasi R, Edelstein C, Sherry B, Tyler K. Calpain inhibition protects against virus-induced apoptotic myocardial injury. J Virol **2001**; 75: 351–61.
37. Connolly JL, Barton ES, Dermody TS. Reovirus binding to cell surface sialic acid potentiates virus-induced apoptosis. J Virol **2001**; 75:4029–39.
38. Virgin HW 4th, Bassel-Duby R, Fields BN, Tyler KL. Antibody protects against lethal infection with the neurally spreading reovirus type 3 (Dearing). J Virol **1988**; 62:4594–604.
39. Smith RE, Zweerink HJ, Joklik WK. Polypeptide components of virions, top component and cores of reovirus type 3. Virology **1969**; 39: 791–810.
40. Virgin HW 4th, Mann MA, Fields BN, Tyler KL. Monoclonal antibodies to reovirus reveal structure/function relationships between capsid proteins and genetics of susceptibility to antibody action. J Virol **1991**; 65:6772–81.
41. Burstin SJ, Spriggs DR, Fields BN. Evidence for functional domains on the reovirus type 3 hemagglutinin. Virology **1982**; 117:146–55.
42. Liu Y, Nusrat A, Schnell FJ, et al. Human junction adhesion molecule regulates tight junction resealing in epithelia. J Cell Sci **2000**; 113: 2363–74.
43. Wilson GJ, Wetzel JD, Puryear W, Bassel-Duby R, Dermody TS. Persistent reovirus infections of L cells select mutations in viral attachment protein σ1 that alter oligomer stability. J Virol **1996**; 70:6598–606.
44. Dermody TS, Nibert ML, Bassel-Duby R, Fields BN. Sequence diversity in S1 genes and S1 translation products of 11 serotype 3 reovirus strains. J Virol **1990**; 64:4842–50.
45. Hsu KH, Lonberg-Holm K, Alstein B, Crowell RL. A monoclonal antibody specific for the cellular receptor for the group B coxsackieviruses. J Virol **1988**; 62:1647–52.
46. Bergelson JM, Cunningham JA, Droguett G, et al. Isolation of a common receptor for coxsackie B viruses and adenoviruses 2 and 5. Science **1997**; 275:1320–3.
47. Wetzel JD, Chappell JD, Fogo AB, Dermody TS. Efficiency of viral entry determines the capacity of murine erythroleukemia cells to support persistent infections by mammalian reoviruses. J Virol **1997**; 71: 299–306.
48. Tyler KL, Bronson RT, Byers KB, Fields BN. Molecular basis of viral neurotropism: experimental reovirus infection. Neurology **1985**; 35:88–92.
49. Rubin DH, Fields BN. Molecular basis of reovirus virulence: role of the M2 gene. J Exp Med **1980**; 152:853–68.
50. Reed LJ, Muench H. A simple method of estimating fifty percent endpoints. Am J Hyg **1938**; 27:493–97.
51. Lerner AM, Cherry JD, Finland M. Haemagglutination with reoviruses. Virology **1963**; 19:58–65.
52. Dermody TS, Nibert ML, Bassel-Duby R, Fields BN. A σ1 region important for hemagglutination by serotype 3 reovirus strains. J Virol **1990**; 64:5173–6.
53. Felsenstein J. PHYLIP 3.2 manual. Berkeley: University of California Herbarium, **1989**.
54. Rubin DH, Weiner DB, Dworkin C, Greene MI, Maul GG, Williams WV. Receptor utilization by reovirus type 3: distinct binding sites on thymoma and fibroblast cell lines result in differential compartmentalization of virions. Microb Pathog **1992**; 12:351–65.
55. Kaye KM, Spriggs DR, Bassel-Duby R, Fields BN, Tyler KL. Genetic basis for altered pathogenesis of an immune-selected antigenic variant of reovirus type 3 Dearing. J Virol **1986**; 59:90–7.
56. Bassel-Duby R, Spriggs DR, Tyler KL, Fields BN. Identification of attenuating mutations on the reovirus type 3 S1 double-stranded RNA segment with a rapid sequencing technique. J Virol **1986**; 60:64–7.
57. Tyler KL, Virgin HW, Bassel-Duby R, Fields BN. Antibody inhibits defined stages in the pathogenesis of reovirus serotype 3 infection of the central nervous system. J Exp Med **1989**; 170:887–900.
58. Tyler KL, Mann MA, Fields BN,Virgin HW 4th. Protective anti-reovirus antibodies and their effects on viral pathogenesis. J Virol **1993**; 67: 3446–53.
59. Barton ES, Youree BE, Ebert DH, et al. Utilization of sialic acid as a coreceptor is required for reovirus-induced biliary disease. J Clin Invest **2003**; 111:1823–33.
60. Mann MA, Knipe DM, Fischbach GD, Fields BN. Type 3 reovirus neuroinvasion after intramuscular inoculation: direct invasion of nerve terminals and age-dependent pathogenesis. Virology **2002**; 303:222–31.
61. Cuff CF, Lavi E, Cebra CK, Rubin DH. Passive immunity to fatal reovirus serotype 3–induced meningoencephalitis mediated by both secretory and transplacental factors in neonatal mice. J Virol **1990**; 64:1256–63.
62. Kapikian A, Hoshino Y, Chanock R. Rotaviruses. In: Knipe DM, Howley PM, eds. Fields virology. 4th ed. Philadelphia: Lippincott-Raven, **2001**:1787–833.
63. Lynch M, Lee B, Azimi P, et al. Rotavirus and central nervous system

symptoms: cause or contaminant? Case reports and review. Clin Infect Dis **2001**; 33:932–8.
64. Wong CJ, Price Z, Bruckner DA. Aseptic meningitis in an infant with rotavirus gastroenteritis. Pediatr Infect Dis **1984**; 3:244–6.
65. Klasco R. Colorado tick fever. Med Clin North Am **2002**; 86:435–40, ix.
66. Ramos-Alvarez M, Sabin AB. Characteristics of poliomyelitis and other enteric viruses recovered in tissue culture from healthy American children. Proc Soc Exp Biol Med **1954**; 87:655–61.
67. Ramos-Alvarez M, Sabin AB. Enteropathogenic viruses and bacteria: role in summer diarrheal diseases of infancy and early childhood. JAMA **1958**; 167:147–58.
68. Hrdy DB, Rosen L, Fields BN. Polymorphism of the migration of double-stranded RNA segments of reovirus isolates from humans, cattle, and mice. J Virol **1979**; 31:104–11.
69. Rosen L, Hovis JF, Mastrota FM, Bell JA, Huebner RJ. Observations on a newly recognized virus (Abney) of the reovirus family. Am J Hyg **1960**; 71:258–65.
70. Goral MI, Mochow-Grundy M, Dermody TS. Sequence diversity within the reovirus S3 gene: reoviruses evolve independently of host species, geographic locale, and date of isolation. Virology **1996**; 216:265–71.

APPENDIX C

STRUCTURE-FUNCTION ANALYSIS OF REOVIRUS BINDING TO JUNCTIONAL ADHESION MOLECULE-A

Forrest JC, Campbell JA, Schelling P, Stehle T, Dermody TS.

Journal of Biological Chemistry. 278(48):48434-44; 2003

THE JOURNAL OF BIOLOGICAL CHEMISTRY
Vol. 278, No. 48, Issue of November 28, pp. 48434–48444, 2003
Printed in U.S.A.

Structure-Function Analysis of Reovirus Binding to Junctional Adhesion Molecule 1

IMPLICATIONS FOR THE MECHANISM OF REOVIRUS ATTACHMENT*

Received for publication, May 30, 2003, and in revised form, August 26, 2003
Published, JBC Papers in Press, September 9, 2003, DOI 10.1074/jbc.M305649200

J. Craig Forrest‡§, Jacquelyn A. Campbell‡§, Pierre Schelling¶, Thilo Stehle¶, and Terence S. Dermody‡§‖**

From the Departments of ‡Microbiology and Immunology and ‖Pediatrics and §Elizabeth B. Lamb Center for Pediatric Research, Vanderbilt University School of Medicine, Nashville, Tennessee 37232 and the ¶Laboratory of Developmental Immunology, Massachusetts General Hospital and Harvard Medical School, Boston, Massachusetts 02114

Mammalian reoviruses are nonenveloped viruses with a long, filamentous attachment protein that dictates disease phenotypes following infection of newborn mice and is a structural homologue of the adenovirus attachment protein. Reoviruses use junctional adhesion molecule 1 (JAM1) as a serotype-independent cellular receptor. JAM1 is a broadly expressed immunoglobulin superfamily protein that forms stable homodimers and regulates tight-junction permeability and lymphocyte trafficking. We employed a series of structure-guided binding and infection experiments to define residues in human JAM1 (hJAM1) important for reovirus-receptor interactions and to gain insight into mechanisms of reovirus attachment. Binding and infection experiments using chimeric and domain deletion mutant receptor molecules indicate that the amino-terminal D1 domain of hJAM1 is required for reovirus attachment, infection, and replication. Reovirus binding to hJAM1 occurs more rapidly than homotypic hJAM1 association and is competed by excess hJAM1 *in vitro* and on cells. Cross-linking hJAM1 diminishes the capacity of reovirus to bind hJAM1 *in vitro* and on cells and negates the competitive effects of soluble hJAM1 on reovirus attachment. Finally, mutagenesis studies demonstrate that residues intimately associated with the hJAM1 dimer interface are critical for reovirus interactions with hJAM1. These results suggest that reovirus attachment disrupts hJAM1 dimers and highlight similarities between the attachment strategies of reovirus and adenovirus.

Mammalian reoviruses are prototype members of the *Reoviridae* family of viruses. They are nonenveloped viruses that contain a genome of 10 double-stranded RNA segments (1). Reoviruses have been isolated from many mammalian species, including humans; however, severe disease is rare and usually restricted to the very young (2). Neonatal mice are exquisitely susceptible to reovirus infection and have been employed for studies of viral pathogenesis with particular emphasis on central nervous system tropism and corollary disease phenotypes. Following oral inoculation of newborn mice, serotype 1 (T1) reovirus strains spread hematogenously from the intestine to the central nervous system and demonstrate tropism for ependymal cells (3–5). In contrast, serotype 3 (T3) reoviruses spread via neural routes to the central nervous system, where they infect neurons (3–6). As a result of these differences in cell tropism, T1 strains cause nonlethal hydrocephalus, whereas T3 strains cause lethal encephalitis. Reassortant genetics defined the viral S1 gene segment as the primary genetic correlate of these tropism and disease phenotypes (3–5).

The S1 gene segment encodes the reovirus attachment protein, σ1 (7, 8). The trimeric σ1 protein exhibits head-and-tail morphology (9–13) and inserts into the virion capsid at the icosahedral 5-fold symmetry axes. The adenovirus attachment protein, fiber, exhibits similar morphology and virion insertion (14). A major portion of the σ1 tail, including residues important for carbohydrate binding (15), folds into a triple β-spiral structural motif (13). This motif consists of repeating units of short β-strands that previously had only been seen in the "shaft" domain of adenovirus fiber (16). Similarities also exist between the "knob" domain of fiber and the σ1 head, which both form globular structures composed of unique eight-stranded β-barrels (13). Evidence gathered from biochemical and genetic studies previously defined the σ1 head as the viral determinant of proteinaceous cellular receptor engagement (3–5, 17). The strong association of the S1 gene segment with serotype-dependent differences in reovirus tropism and disease led to the hypothesis that reovirus serotypes usurp distinct cell surface molecules for attachment and infection.

To better understand the contributions of cellular receptors in reovirus pathogenesis, we used an expression-cloning approach to identify junctional adhesion molecule 1 (JAM1)[1] as a receptor for reovirus and demonstrated that reovirus directly engages JAM1 in a bimolecular interaction via the head domain of σ1 (17). JAM1 is a receptor for both T1 and T3 reovirus strains in culture (17); however, the *in vivo* roles of JAM1 in reovirus tropism and pathogenesis have not been defined.

* This work was supported by Public Health Service awards T32 CA09385 (to J. C. F. and J. A. C.), R01 AI38296 (to T. S. D.), and R01 GM67853 (to T. S. and T. S. D.), the Vanderbilt University Research Council (to J. C. F.), and the Elizabeth B. Lamb Center for Pediatric Research. Additional support was provided by Public Health Service Awards CA68485 (to the Vanderbilt Cancer Center) and DK20593 (to the Vanderbilt Diabetes Research and Training Center). The costs of publication of this article were defrayed in part by the payment of page charges. This article must therefore be hereby marked "*advertisement*" in accordance with 18 U.S.C. Section 1734 solely to indicate this fact.

** To whom correspondence should be addressed: Lamb Center for Pediatric Research, D7235 MCN, Vanderbilt University School of Medicine, Nashville, TN 37232. Tel.: 615-343-9943; Fax: 615-343-9723; E-mail: terry.dermody@vanderbilt.edu.

[1] The abbreviations used are: JAM1, junctional adhesion molecule 1; mJAM1, mouse JAM1; hJAM1, human JAM1; hCAR, human coxsackievirus and adenovirus receptor; CHO, Chinese hamster ovary; T1L, type 1 Lang; Ad 5-GFP, green fluorescent protein-encoding serotype 5 adenovirus; mAb, monoclonal antibody; PBS, phosphate-buffered saline; HRP, horseradish peroxidase; BS^3, bis(sulfosuccinimidyl) suberate; ELISA, enzyme-linked immunosorbent assay.

JAM1 is a type 1 transmembrane protein consisting of two extracellular Ig-like domains, termed D1 and D2, a single transmembrane segment, and a short cytoplasmic tail (18, 19). JAM1 is expressed in a variety of tissues, including epithelial and endothelial barriers (18–20), where it is thought to regulate tight junction permeability and mediate lymphocyte trafficking (18–21). The crystal structures of murine and human homologues of JAM1 (mJAM1 and hJAM1, respectively), both of which are functional reovirus receptors (17), indicate that JAM1 forms homodimers via extensive hydrophobic and ionic contacts between apposing D1 domains (22, 23). Residues that facilitate interdimer interactions are strictly conserved between mJAM1 and hJAM1 (22, 23). JAM1-JAM1 dimers are highly stable and thought to be physiologically relevant, perhaps functioning in tight junction barrier integrity or diapedesis of inflammatory cells (22–24).

The contacts that facilitate JAM1 dimerization are interesting in that they occur via the GFCC′ face of the D1 Ig-like domain (22, 23). The only other molecules demonstrated to form homodimers using similar interdimer contacts are the human coxsackievirus and adenovirus receptor (hCAR) and CD2 (25–27). The structure of hCAR in complex with the adenovirus fiber knob revealed that fiber engages the D1 domain of hCAR using residues involved in hCAR homodimer formation and that knob mimics the hCAR-hCAR interaction (16, 25). Biophysical evidence suggests that fiber-hCAR interactions are thermodynamically favored over hCAR-hCAR interactions, providing support for a model in which residues in the hCAR dimer interface preferentially bind fiber over hCAR (28). The structural similarities between the reovirus and adenovirus attachment proteins and between their cognate receptors, paired with the absolute conservation of residues in mJAM1 and hJAM1 that mediate homodimer formation, suggest that reovirus engages the D1 domain of hJAM1 and that residues involved in hJAM1 dimerization are important for reovirus attachment (23). This hypothesis was formally tested in the current study.

For these experiments, we generated chimeric receptor molecules consisting of reciprocal domain exchanges between hCAR and hJAM1 and single domain hJAM1 deletion mutants and tested the capacity of these constructs to support reovirus binding and infection. We performed complementary *in vitro* and cellular competition binding studies and hJAM1 dimer cross-linking experiments to assess the effects on reovirus attachment. Finally, we generated a series of hJAM1 point mutants to define specific residues important for reovirus-hJAM1 interactions. The results of these structure-guided approaches reveal that residues in the hJAM1 D1 domain within and proximal to the dimer interface are critical for reovirus-hJAM1 interactions. These findings more clearly define the molecular basis of reovirus binding to hJAM1 and highlight potential mechanisms of reovirus attachment. Moreover, they provide biological and biophysical evidence that reovirus and adenovirus use remarkably similar attachment strategies.

EXPERIMENTAL PROCEDURES

Cells, Viruses, and Antibodies—Spinner adapted L929 (L) cells were maintained in Joklik's modified essential medium supplemented to contain 5% fetal bovine serum, 2 mM L-glutamine, 100 units/ml penicillin, 100 μg/ml streptomycin, and 0.25 μg/ml amphotericin B. HeLa cells were maintained in Dulbecco's modified Eagle's medium, and Chinese hamster ovary (CHO) cells were maintained in Ham's F-12 medium, both supplemented to contain 10% fetal bovine serum, 2 mM L-glutamine, 100 units/ml penicillin, and 100 μg/ml streptomycin. Reovirus strain type 1 Lang (T1L) is a laboratory stock. Strain T3SA− is a non-sialic acid-binding monoreassortant virus (29). Reoviruses were purified from infected L cells as previously described (9). Particle concentrations were determined by spectrophotometry at 260 nm using a conversion factor of 2.1×10^{12} particles/ml/A_{260}. Particle/plaque-forming unit ratios for T1L were 100:1. Particle/fluorescent focus unit ratios for T1L were 10,000:1. Green fluorescent protein-encoding serotype 5 adenovirus (Ad 5-GFP) was provided by Dr. Jeffrey Bergelson (University of Pennsylvania). hJAM1-specific monoclonal antibody (mAb) J10.4 and rabbit polyclonal hJAM1 antiserum were provided by Dr. Charles Parkos (Emory University).

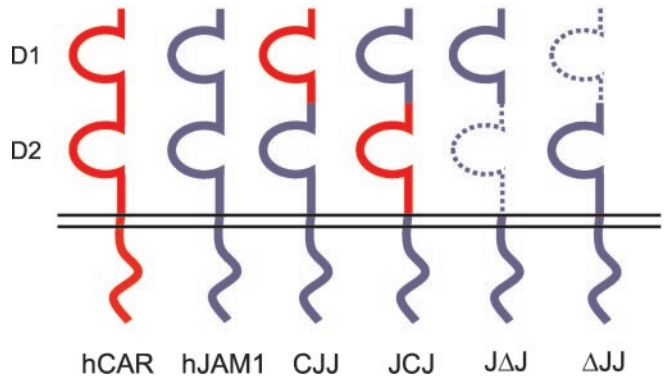

FIG. 1. **Chimeric and deletion mutant receptor constructs for studies of reovirus binding and growth.** Ig superfamily proteins hCAR (*red*) and hJAM1 (*blue*) were used to generate chimeric receptor constructs in which Ig-like domains were reciprocally exchanged. Single Ig-like domains of hJAM1 also were deleted. Nomenclature indicates origin or deletion of domains D1, D2, and cytoplasmic tail (*left* to *right*) relative to wild-type hCAR or hJAM1.

Generation of Chimeric and Mutant Receptor Constructs—Nomenclature of chimeric and deletion mutant constructs indicates exchanged or deleted domains relative to wild-type hCAR or hJAM1 from amino to carboxyl termini. Chimeric receptor CJJ (hCAR residues 1–141; hJAM1 residues 133–299) and deletion mutants JΔJ (hJAM1 residues 133–234 deleted) and ΔJJ (hJAM1 residues 29–132 deleted) were generated using PCR to insert a HindIII endonuclease restriction site at the 3′ or 5′ end of respective amino-terminal or carboxyl-terminal receptor fragments. Chimera JCJ (hJAM1 residues 1–128, hCAR residues 138–227, hJAM1 residues 235–299) and full-length D1 point mutant receptors were generated by overlap extension PCR. All chimeric and mutant receptor PCR products were digested with restriction endonucleases and ligated into plasmid pcDNA3.1+ (Invitrogen). The fidelity of cloning was confirmed by automated sequencing. The PCR primers used to generate chimeric and deletion mutant receptors are shown in Table I. The PCR primers used for point mutant coding changes are shown in Table II.

Transient Transfection and Infection of CHO Cells—CHO cells were transiently transfected with empty vector or plasmids encoding wild-type, chimeric, or deletion mutant receptors using LipofectAMINE and PLUS reagent (Invitrogen) as previously described (23). Cells were incubated for 24 h to allow receptor expression and then infected with reovirus T1L at multiplicities of infection of 1 fluorescent focus unit/cell and 1 plaque-forming unit/cell for fluorescent focus and plaque assays, respectively. For fluorescent focus assays, infected cells were processed for indirect immunofluorescence as previously described (29). Images were captured at ×20 magnification using a Leica DM IRB inverted microscope. For plaque assays, viral titers in cell lysates were determined at 0 and 24 h after adsorption as previously described (30).

Flow Cytometric Analysis of Receptor Expression and Virus Binding—CHO cells were transiently transfected and incubated for 24 h to allow receptor expression. Cells were detached from plates by incubation with 20 mM EDTA in PBS. Cells (1×10^6) were incubated with hCAR- or hJAM1-specific antiserum at dilutions of 1:750 or 1:1000, respectively, or incubated with reovirus T1L or T3SA− (1×10^5 particles/cell) on ice for ~ 60 min. Virus-adsorbed cells were washed with PBS and incubated with clarified, combined T1L/T3D antiserum (31) at 1:1000 dilution on ice for ~60 min. All samples were washed with PBS and incubated with phycoerythrin-conjugated goat anti-rabbit IgG secondary antiserum (Molecular Probes, Inc.) at a 1:1000 dilution on ice for ~30 min. Cells were washed twice with PBS and fixed with 2% paraformaldehyde in PBS. Cells were analyzed using a FACScan flow cytometer (Becton-Dickinson).

Expression and Purification of Soluble Receptor Constructs—Soluble ectodomains of wild-type and point mutant hJAM1 constructs were fused to an amino-terminal glutathione *S*-transferase affinity tag via a thrombin cleavage site and purified as described (23). Nucleotide sequences corresponding to residues 27–233 of wild-type hJAM1 and

TABLE I
PCR primers for chimeric and deletion mutant receptors

T7 and BGH primers were used as 5′ forward and 3′ reverse primers for all constructs. Underlined nucleotides denote HindIII restriction endonuclease site.

Receptor construct (N→C)	Primers	
	Reverse	Forward
CJJ	5′ CGATAAGCTTAGGCTTAACAAG 3′	5′ ATCGAAGCTTTCCAAGCCTACA 3′
JCJ[1]	5′ GCACCTGAAGGCTTAACAAG CACGATGAGCTTGACCTTGA 3′	5′ CTTGTTAAGCCTTCAGGTGC 3′
JCJ[2]	5′ GCCACGATGACCCCCACATT TAGACGCAACAGGCACTGAT 3′	5′ AATGTGGGGGTCATCGTGGC 3′
JΔJ	5′ CGATAAGCTTTGGAGGCACAAG 3′	5′ ATCGAAGCTTAATGTGGGGGTC 3′
ΔJJ	5′ CGATAAGCTTGCCCAATGCCAG 3′	5′ ATCGAAGCTTTCCAAGCCTACA 3′

[1] These primers were used to generate the upstream (5′) J-C junction in chimera JCJ using JCJ[2] PCR product as template.
[2] These primers were used to generate the downstream (3′) C-J junction in chimera JCJ.

hJAM1 point mutants were cloned by PCR, digested with restriction endonucleases, and ligated into pGEX-4T-3 (Amersham Biosciences) for bacterial transformation. Bacteria were cultured in Luria-Bertani broth at 37 °C with shaking, and protein expression was induced with 0.1 mM isopropyl-β-D-thiogalactoside (Amersham Biosciences). Bacteria were harvested by centrifugation and lysed by sonication in the presence of protease inhibitor mixture (Roche Molecular Biochemicals). Glutathione *S*-transferase-hJAM1 constructs were purified from bacterial lysates by glutathione affinity chromatography. Soluble wild-type and point mutant hJAM1 ectodomains were liberated from the glutathione resin by thrombin cleavage (20 units/ml) at room temperature overnight.

In Vitro hJAM1 and Reovirus Binding Analysis—hJAM1 (500 μg/ml) and reovirus T1L (1.1×10^{13} particles/ml) in PBS were biotinylated by incubation in 200 μg/ml EZ-Link Sulfo-NHS-LC-biotin (Pierce) at room temperature for 60 min. Unincorporated biotin was removed by exhaustive dialysis against PBS. ELISA plates were coated with 20 nM solutions of soluble hJAM1, cross-linked hJAM1, point mutant hJAM1, or bovine serum albumin (2 μg/ml) in pH 9.6 carbonate-bicarbonate buffer (Sigma). Plates were blocked by incubation with 2% (w/v) bovine serum albumin, 0.05% Triton X-100, PBS. For kinetic analyses, biotinylated hJAM1 (20, 40, 80, or 160 nM) in blocking buffer was incubated with hJAM1-coated plates for 0, 5, 15, 30, 60, 120, 180, 240, or 300 min, and biotinylated reovirus (2.5×10^{10}, 5.0×10^{10}, 1.0×10^{11}, or 2×10^{11} particles/ml or 0.042, 0.083. 0.16, or 0.33 nM, respectively) in blocking buffer was incubated with hJAM1-coated plates for 0, 5, 15, 30, 60, 120, 180, and 240 min at 37 °C. As controls for specificity, binding of 80 nM biotinylated hJAM1 in the presence of a 100-fold excess of unlabeled hJAM1 at 180 min and binding of 0.33 nM reovirus (2×10^{11} particles/ml) in the presence of 20 μg/ml hJAM1-specific mAb J10.4 or hCAR-specific mAb RmcB (32) were assessed. For competition and equilibrium analyses, biotinylated reovirus (2×10^{11} particles/ml; 0.33 nM) in blocking buffer was incubated with hJAM1-, cross-linked hJAM1-, or point mutant hJAM1-coated plates in the presence or absence of excess soluble hJAM1 or cross-linked hJAM1 at 37 °C for 180 min. Binding in the presence of 20 μg/ml hJAM1-specific mAb J10.4 was tested as a control for specificity. All plates were washed twice with 0.05% Triton X-100/PBS and once with PBS and incubated with 2 μg/ml horseradish peroxidase (HRP)-conjugated streptavidin (Amersham Biosciences) in blocking buffer at room temperature for 30 min. Plate-bound biotinylated hJAM1 or reovirus was detected following incubation with HRP substrate (ABTS (2,2′-azino-bis(3-ethylbenz-thiazoline-6-sulfonic acid), Sigma) and analysis by spectrophotometry at 405 nm. For all conditions tested, no binding to bovine serum albumin-coated plates was detected.

Virus Radioligand Binding Assays—Radioligand binding assays were performed as previously described (29). Reovirus T1L was metabolically labeled with Easy Tag TM EXPRE^{35}S^{35}S (PerkinElmer Life Sciences) and purified as described (9). HeLa cells were detached from plates by incubation with 20 mM EDTA, resuspended in Dulbecco's PBS (Invitrogen) supplemented with metabolic inhibitors (10 mM NaN_3, 5 mM 2-deoxyglucose, and 2 mM NaF), and incubated at 37 °C for 30 min to deplete cellular ATP and block receptor-mediated endocytosis (29, 33). Cells (1×10^6) were incubated with ^{35}S-labeled reovirus T1L (1×10^5 particles/cell) for 180 min in the presence or absence of excess soluble hJAM1. Cells were collected by vacuum filtration, and virus binding was assessed by liquid scintillation.

Cross-linking Analysis—Soluble hJAM1 (500 μg/ml) was incubated with a 50-fold molar excess of the water-soluble cross-linking reagent bis(sulfosuccinimidyl) suberate (BS^3) in PBS at room temperature for 60 min. Unreacted BS^3 was quenched by the addition of 20 mM Tris-HCl (pH 7.5). HeLa cells (1×10^7) were incubated with PBS or 2 mM BS^3 at 4 °C for 120 min, followed by washing with PBS to remove excess BS^3. The efficiency of cross-linking was assessed following lysis of cells in 1% Triton X-100/PBS on ice for 30 min. Lysates were clarified by centrifugation, and hJAM1 was immunoprecipitated using 10 μg/ml hJAM1-specific mAb J10.4. Immunoprecipitates and soluble hJAM1 were resolved by SDS-PAGE. Resolved proteins were transferred to nitrocellulose and immunoblotted with hJAM1-specific antiserum (1:1000). Proteins were detected by ECL. Soluble hJAM1 was tested for the capacity to bind reovirus and compete virus binding *in vitro*, and HeLa cells were tested for the capacity to bind virus in a radioligand binding assay.

RESULTS

Identification of hJAM1 Domains Required for Reovirus Attachment—We previously have shown that JAM1 is a serotype-independent reovirus receptor (17). However, specific sequences in JAM1 required for reovirus attachment are not known. To identify domains in JAM1 required for reovirus binding and infection, we generated receptor chimeras using hJAM1 and Ig superfamily relative hCAR (Fig. 1 and Table I). hCAR is incapable of supporting reovirus binding and infection (17) and was selected as the chimera partner for these studies due to its structural similarities to JAM1 (23). A PCR-based approach was used to reciprocally exchange sequences encoding either the D1 or D2 Ig-like domains of wild-type receptor

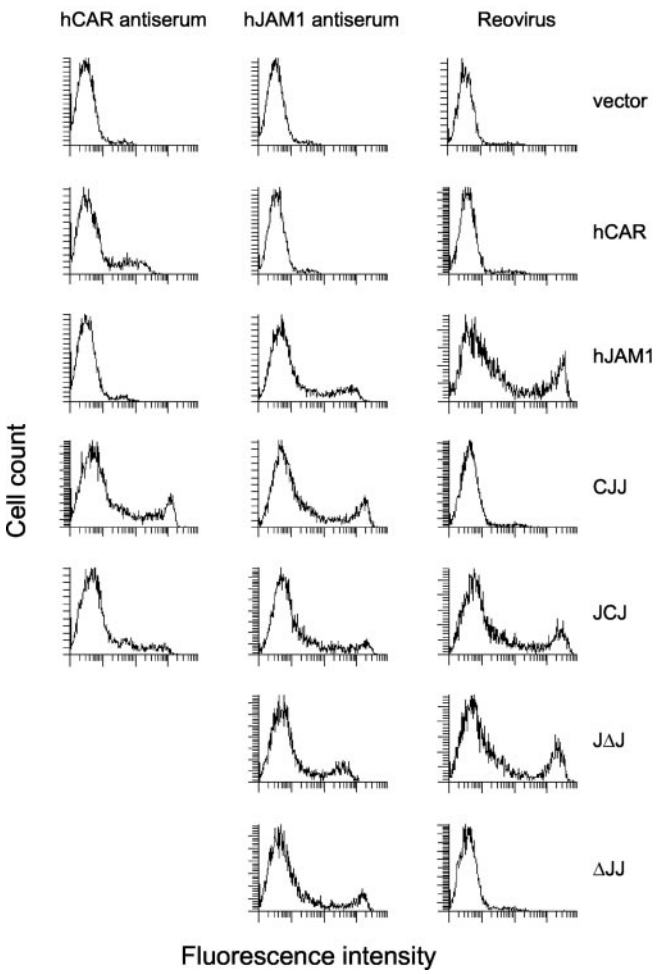

FIG. 2. **Reovirus engages the D1 domain of hJAM1.** CHO cells were transiently transfected with plasmids encoding the indicated receptor constructs. Following incubation for 24 h to permit receptor expression, cells (1×10^6) were stained with hCAR- or hJAM1-specific antisera or adsorbed with reovirus T1L (1×10^{11} particles). Cell surface expression of receptor constructs and virus binding were assessed by flow cytometry.

cDNAs. We also generated single-domain deletion mutants of hJAM1 to complement data obtained using the chimeric receptor molecules. CHO cells, which lack expression of both JAM1 and CAR (see Refs. 19 and 32 and Fig. 2), were transiently transfected with plasmids encoding wild-type hJAM1 and hCAR, chimeric receptor molecules CJJ and JCJ, and hJAM1 deletion mutants JΔJ and ΔJJ. Cell surface expression of each construct and the capacity of reovirus to bind transfected cells were assessed by flow cytometry (Fig. 2). All constructs were detected at the cell surface. Chimera-transfected cells stained with both hJAM1- and hCAR-specific antisera, indicating that the molecules are indeed chimeric (Fig. 2). Prototype reovirus strain T1L bound cells expressing wild-type hJAM1, chimera JCJ, and deletion mutant JΔJ but failed to bind cells expressing hCAR, chimera CJJ, or deletion mutant ΔJJ (Fig. 2). T3 reovirus strain T3SA− also bound cells expressing constructs that contained the D1 domain of hJAM1 (data not shown). These data demonstrate that both T1 and T3 reoviruses engage the membrane-distal D1 domain of hJAM1.

Reovirus Infection and Growth in CHO Cells Expressing Chimeric and Deletion Mutant Receptors—To determine the role of specific JAM1 domains in reovirus infection, CHO cells were transiently transfected with plasmids encoding the hCAR-hJAM1 chimeras or hJAM1 domain-deletion mutants. Transfected cells were adsorbed with T1L, and the capacity of reovirus to infect these cells was assessed by indirect immunofluorescence. Consistent with the binding experiments, reovirus protein expression was detected after infection of cells expressing wild-type hJAM1, chimera JCJ, and deletion mutant JΔJ (Fig. 3*A*). As a control, adenovirus infection also was tested by adsorbing transfected cells with Ad 5-GFP. Cells expressing hCAR and CJJ supported infection by adenovirus (data not shown), demonstrating that these molecules also can serve as functional virus receptors. To provide further support for the role of hJAM1 D1 in reovirus infection, viral replication was assessed 24 h after adsorption by plaque assay. T1L produced substantially higher yields in cells expressing hJAM1, JCJ, and JΔJ compared with cells expressing receptors that lack the hJAM1 D1 domain (Fig. 3*B*). Together, these data indicate that the D1 domain of hJAM1 is required for reovirus attachment, infection, and growth.

Competitive Reovirus-hJAM1 Binding Analysis—To assess the capacity of reovirus and hJAM1 to compete for engagement of hJAM1, a series of complementary *in vitro* and cell binding studies were performed. Due to the apparent high affinity and slow dissociation rate of hJAM1 dimers (23),[2] we first established an experimental system in which equilibrium could be achieved over an extended time course to provide evidence that hJAM1-hJAM1 interactions are saturable and specific and, therefore, support the use of soluble hJAM1 as a competitor for virus binding studies. For these experiments, ELISA plates were coated with 20 nM solutions of soluble hJAM1 ectodomain. This concentration facilitated maximal hJAM1 immobilization (data not shown). Increasing concentrations of biotinylated hJAM1 were then tested for the capacity to bind immobilized hJAM1 in a kinetic binding assay (Fig. 4*A*). Homophilic hJAM1 interactions occurred in a concentration- and time-dependent manner, approaching equilibrium following incubation for intervals greater than 240 min at 80 and 160 nM concentrations. Furthermore, hJAM1-hJAM1 interactions are specific, since incubation in the presence of 100-fold excess concentrations of unlabeled hJAM1 resulted in no detectable binding following incubation for 180 min (data not shown).

To gather further evidence for the validity of *in vitro* binding assays for studies of reovirus-hJAM1 interactions, we performed kinetic virus-binding analyses. Binding of biotinylated reovirus T1L to immobilized hJAM1 was assessed over time (Fig. 4*B*). Reovirus exhibited concentration- and time-dependent binding to hJAM1-coated plates, achieving equilibrium more rapidly than hJAM1 (~180 min) and at lower concentrations (particle concentrations of 1.0×10^{11}/ml (6.2 nM σ1) and 2.0×10^{11}/ml (12 nM σ1)). Reovirus binding to immobilized hJAM1 was abolished in the presence of 20 μg/ml hJAM1-specific mAb J10.4 but not affected by 20 μg/ml hCAR-specific mAb RmcB at the highest virus concentration tested, indicating the specificity of the reovirus-hJAM1 interaction (data not shown). Together, these results demonstrate that hJAM1 and reovirus specifically engage immobilized hJAM1 and provide confidence that this *in vitro* binding assay is a valid method for assessing whether hJAM1 and reovirus compete for overlapping binding sites.

We next used the *in vitro* binding assay to test the capacity of soluble hJAM1 to compete for reovirus binding to immobilized hJAM1 (Fig. 4*C*). Biotinylated reovirus T1L particles (2×10^{11}/ml) were mixed with fold molar excess concentrations of soluble hJAM1, calculated to account for 36 copies of σ1 per virion particle, and tested for the capacity to bind immobilized hJAM1. Reovirus binding was inhibited in a dose-dependent fashion, with a 50% inhibitory concentration (IC_{50}) between 20-

[2] J. C. Forrest and T. S. Dermody, unpublished results.

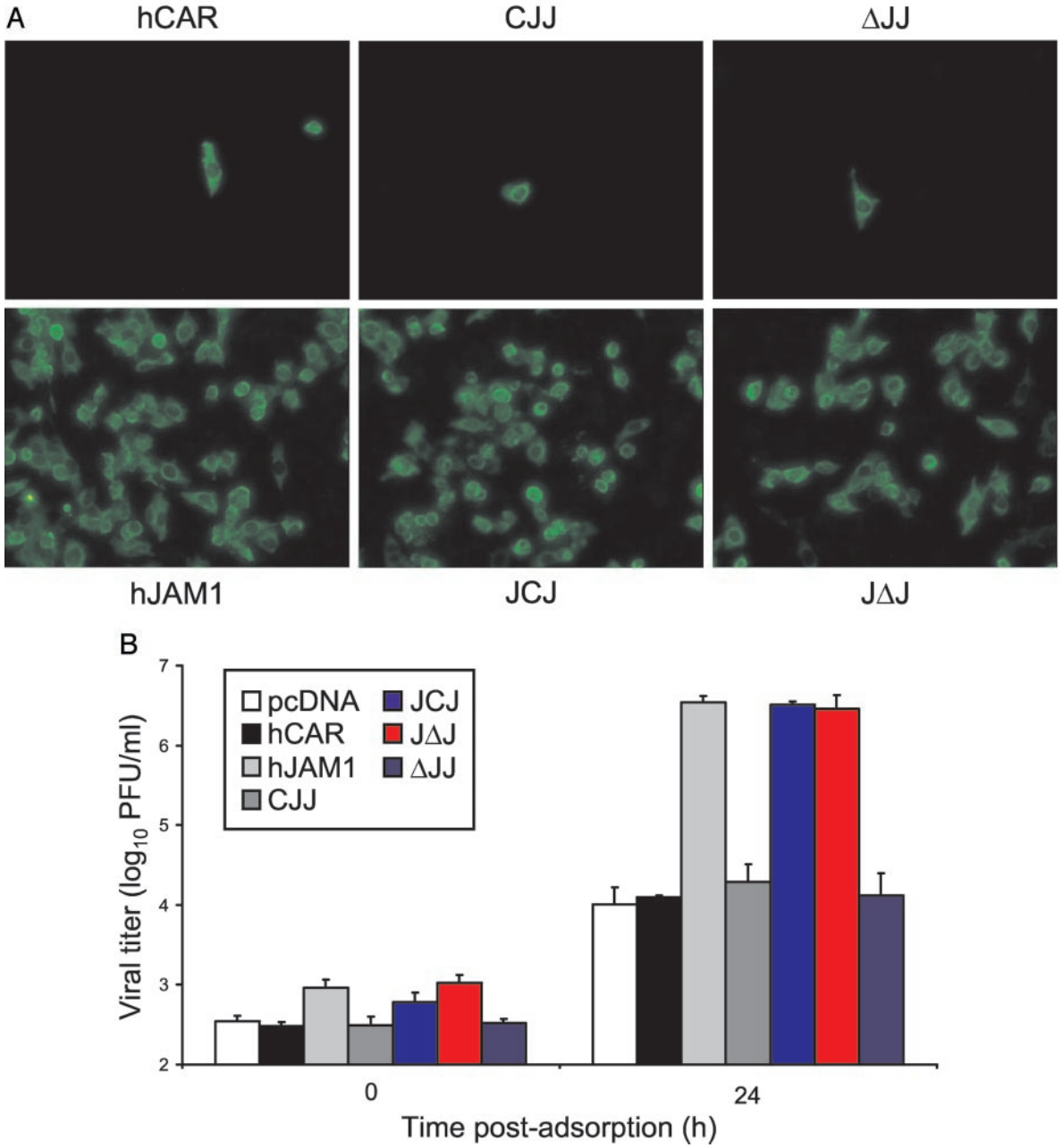

FIG. 3. **The D1 domain of hJAM1 is required for reovirus infection and replication.** CHO cells were transiently transfected with plasmids encoding the indicated receptor constructs and incubated for 24 h to permit receptor expression. *A*, transfected cells (4×10^5) were infected with reovirus T1L at a multiplicity of infection of 1 fluorescent focus unit/cell and incubated at 37 °C for 20 h. Cells were fixed and stained for reovirus protein, and infected cells were identified by indirect immunofluorescence. Representative images are shown. *B*, transfected cells (2×10^5) were adsorbed with reovirus T1L at a multiplicity of infection of 1 plaque-forming unit (*PFU*)/cell. Reovirus growth was assessed by plaque assay at 0 and 24 h postadsorption. Shown are mean viral titers for three independent experiments. The *error bars* indicate S.D.

and 50-fold molar excess soluble hJAM1. At 100-fold molar excess hJAM1, virus binding was reduced to near background levels, which were determined by assessing virus binding in the presence of hJAM1-specific mAb J10.4.

To provide a more complete assessment of reovirus-hJAM1 interactions, we tested the capacity of soluble hJAM1 to compete for reovirus binding to HeLa cells (Fig. 4*D*). HeLa cells were incubated with radiolabeled T1L virions in the presence of increasing fold molar excess of soluble hJAM1. Similar to results obtained using the *in vitro* binding assay, reovirus binding to HeLa cells was inhibited by soluble hJAM1 in a dose-dependent fashion, with an IC_{50} between 20- and 50-fold molar excess hJAM1 and nearly complete inhibition by 100-fold molar excess. These data provide additional support for the primary role of hJAM1 in reovirus attachment to cells. Moreover, the large excess of hJAM1 required for competition suggests a higher affinity for reovirus-hJAM1 interactions than those of hJAM1-hJAM1 (35).

Effect of Cross-linking on Reovirus Binding to hJAM1—To more directly assess the importance of residues involved in hJAM1 dimerization for reovirus attachment, we tested the effect of hJAM1 cross-linking on reovirus binding. Soluble hJAM1 was cross-linked by incubation with the water-soluble cross-linking agent BS^3. This treatment resulted in the formation of higher order oligomers whose M_r values correspond to hJAM1 dimers (Fig. 5*A*). Similar results were observed previously for cross-linked mJAM1 (24), suggesting that cross-linking hJAM1 and mJAM1 covalently join the dimeric structures

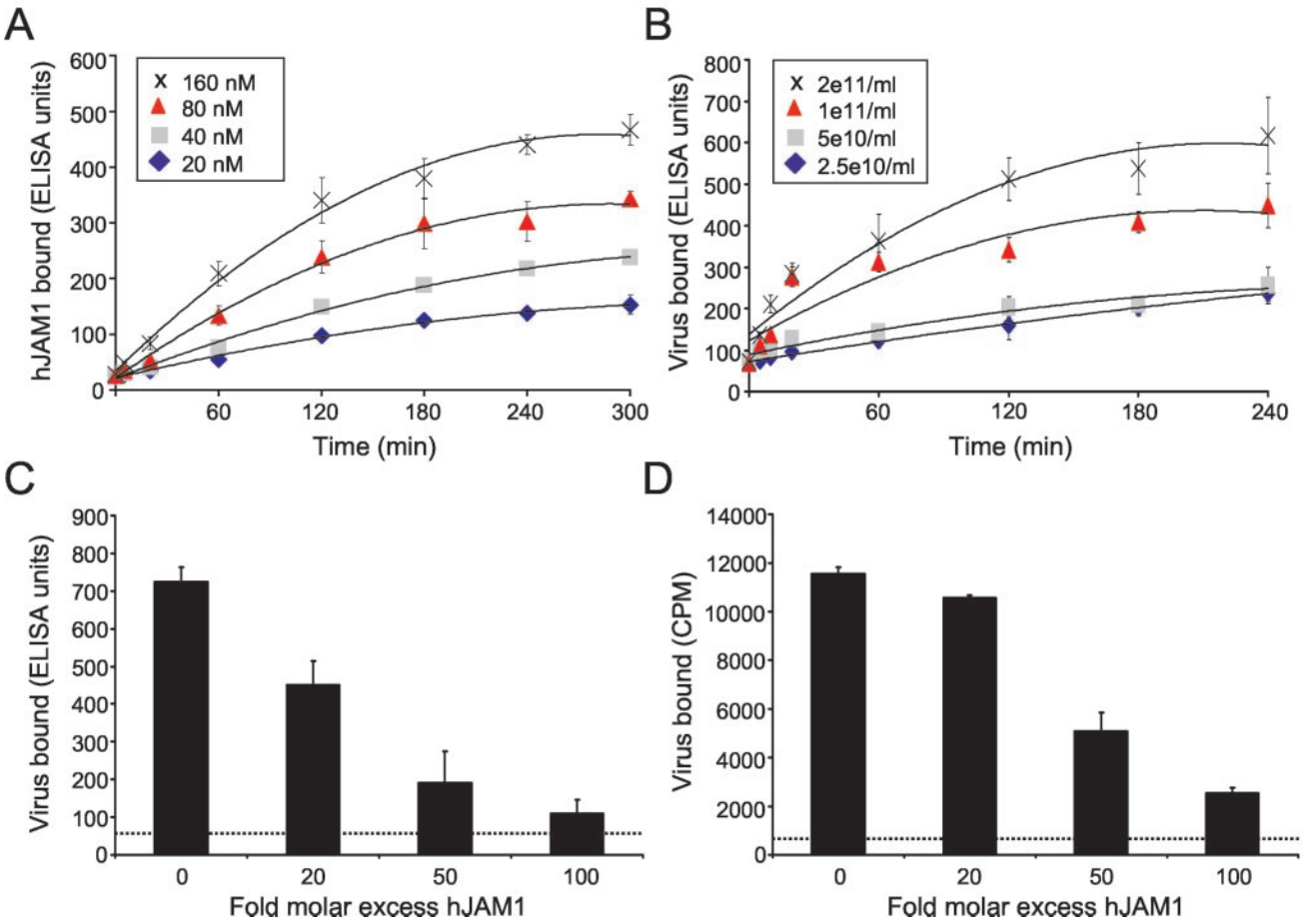

FIG. 4. **Soluble hJAM1 competes for reovirus binding to hJAM1.** *A*, kinetic analysis of hJAM1-hJAM1 interactions. ELISA plates were coated with 20 nM solutions of soluble hJAM1. Increasing concentrations of biotinylated soluble hJAM1 were incubated with immobilized hJAM1 at 37 °C for the indicated times. Binding was detected by spectrophotometry at 405 nm following incubation with streptavidin-HRP. Results are the means of quadruplicate experiments. The *error bars* indicate S.D. *B*, kinetic analysis of reovirus-hJAM1 interactions. Increasing concentrations of biotinylated reovirus T1L particles were incubated with immobilized hJAM1 at 37 °C for the indicated times. Binding was detected following incubation with streptavidin-HRP. Results are the means of quadruplicate experiments. The *error bars* indicate S.D. *C*, competition by hJAM1 for reovirus binding *in vitro*. The binding of biotinylated T1L reovirus (2×10^{11} particles/ml) to immobilized hJAM1 was assessed in the presence of the indicated fold molar excess of hJAM1. After incubation at 37 °C for 180 min, binding was detected following incubation with streptavidin-HRP. The *dashed line* indicates background binding in the presence of 20 μg/ml hJAM1-specific mAb J10.4. Results are the means of quadruplicate experiments. The *error bars* indicate S.D. *D*, competition by hJAM1 for reovirus binding to cells. HeLa cells (1×10^6) were incubated with ^{35}S-labeled reovirus T1L particles (1×10^{11}) at 37 °C for 180 min in the presence of the indicated fold molar excess of hJAM1. Virus binding was detected by liquid scintillation. The *dashed line* indicates background binding in the presence of 20 μg/ml hJAM1-specific mAb J10.4. Results are the means of duplicate experiments. The *error bars* indicate the range of data.

elucidated for both molecules. To assess the effects of cross-linking on reovirus attachment, ELISA plates were coated with 20 nM solutions of either untreated or BS^3-treated hJAM1 and tested for the capacity to bind biotinylated T1L virions (Fig. 5*B*). Cross-linking resulted in a reduction of reovirus binding to immobilized hJAM1 to near background levels, suggesting that reovirus binds a monomeric form of hJAM1 via residues in the dimer interface. To corroborate these results, we tested the capacity of 100-fold excess BS^3-treated hJAM1 to compete for reovirus binding to untreated hJAM1 (Fig. 5*B*). In sharp contrast to untreated hJAM1 at 100-fold molar excess, 100-fold molar excess cross-linked hJAM1 was an inefficient competitor of reovirus binding. These data strongly suggest that the hJAM1 dimer interface is involved in reovirus attachment.

To define the effect of hJAM1 cross-linking on reovirus binding to cells, HeLa cell surface proteins were cross-linked by incubation with BS^3. Cross-linked hJAM1 was captured by immunoprecipitation using hJAM1-specific mAb J10.4 and detected by immunoblotting using hJAM1-specific antiserum (Fig. 5*C*). BS^3 treatment of cells resulted in the formation of a very large M_r species (>97 kDa). Following BS^3 treatment, the binding capacity of radiolabeled T1L was diminished, with cross-linking resulting in >50% reduction in virus binding (Fig. 5*D*). Virus binding in the presence of 20 μg/ml hJAM1-specific mAb J10.4 was completely abolished *in vitro* (Fig. 5*B*) and on cells (Fig. 5*D*), indicating that residual binding following BS^3 is dependent on hJAM1. Therefore, the consistent reduction in reovirus binding due to cross-linking and the failure of BS^3-treated hJAM1 to compete for viral attachment to untreated hJAM1 suggest that reovirus engages hJAM1 using residues within the hJAM1 dimer interface. However, it is also possible that cross-linking alters the conformation of hJAM1 in such a manner to prevent efficient reovirus binding or the cross-linking agent covers a region in the hJAM1 dimer that otherwise would be engaged by reovirus. The apparent inefficiency of cross-linking relative to the effects on virus binding may reflect a loss of antibody-binding epitopes due to BS^3 treatment, with resultant diminished band intensity by immunoblotting relative to the untreated species.

Mutational Analysis of Reovirus Binding to hJAM1—To precisely define the region of hJAM1 bound by σ1 and to identify residues critical for reovirus attachment, we used a PCR-based approach to generate mutant forms of hJAM1 containing single amino acid substitutions. Guided by the hJAM1 crystal struc-

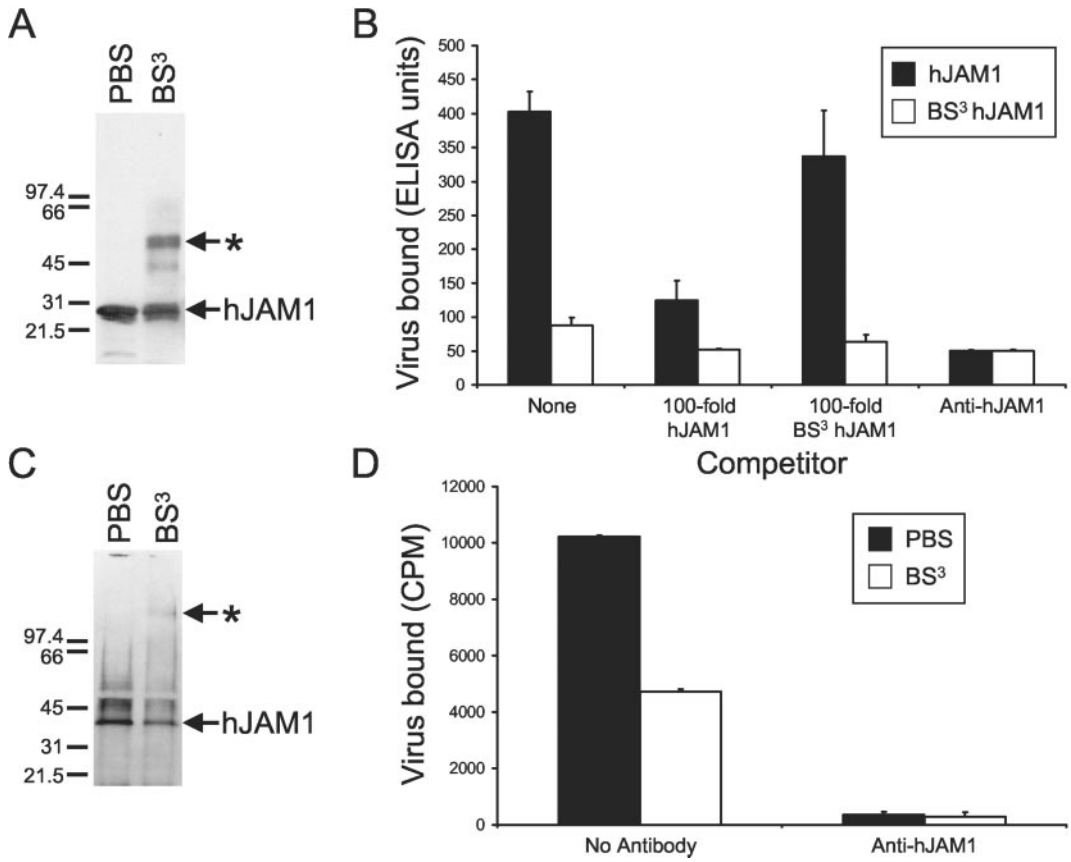

FIG. 5. **Cross-linking hJAM1 inhibits reovirus binding.** *A*, soluble hJAM1 (500 μg/ml) was cross-linked by incubation with 50-fold molar excess BS^3 at room temperature for 1 h. Untreated hJAM1 (PBS) and BS^3-treated hJAM1 were resolved by SDS-PAGE and detected by immunoblotting using hJAM1-specific antiserum. Monomeric hJAM1 is indicated by an *arrow*. A larger M_r hJAM1 species is indicated by an *asterisk*. *B*, ELISA plates were coated with 20 nM solutions of untreated or BS^3-treated hJAM1. The capacity of biotinylated reovirus T1L (2×10^{11} particles/ml) to bind hJAM1 and BS^3-treated hJAM1 was assessed in the presence or absence of the competitors shown. Samples were incubated at 37 °C for 180 min, and binding was detected by spectrophotometry at 405 nM following incubation with streptavidin-HRP. Results are the means of quadruplicate experiments. The *error bars* indicate S.D. *C*, HeLa cells were treated with PBS or 2 mM BS^3 on ice for 2 h. Cells were lysed using 1% Triton X-100/PBS, and hJAM1 was immunoprecipitated using hJAM1-specific mAb J10.4. Immunoprecipitates were resolved by SDS-PAGE and immunoblotted using hJAM1-specific antiserum. Monomeric hJAM1 is indicated by an *arrow*. A larger M_r hJAM1 species is indicated by an *asterisk*. *D*, untreated or BS^3-treated HeLa cells (1×10^6) were incubated with ^{35}S-labeled reovirus T1L virions (1×10^{11}) at 37 °C for 180 min in the presence or absence of 20 μg/ml hJAM1-specific mAb J10.4. Virus binding was detected by liquid scintillation. Results are the means of duplicate experiments. The *error bars* indicate the range of data.

ture (23), mutations were targeted to solvent-exposed residues in regions of the molecule that are highly conserved between hJAM1 and mJAM1 (Fig. 6 and Table II). Soluble ectodomains of hJAM1 mutants were liberated from glutathione *S*-transferase-hJAM1 fusion proteins via treatment with thrombin, and 20 nM solutions of the cleavage products were immobilized onto ELISA plates. Biotinylated T1L virions (2.0×10^{11} particles/ml) were then tested for the capacity to bind the immobilized hJAM1 mutants (Fig. 7). Virus-binding data were normalized for hJAM1 immobilization efficiency, and binding was not detected for any constructs in the presence of 20 μg/ml hJAM1-specific mAb J10.4 (data not shown). Most of the mutations resulted in only minor or modest reductions in virus binding. However, substitution of Ser^{57} with lysine or Tyr^{75} with alanine substantially reduced the efficiency of reovirus binding. Ser^{57} is a solvent-accessible residue at the apex of hJAM1 adjacent to the dimer interface, and Tyr^{75} is a core residue at the top of the dimer interface (Fig. 6). Neither of these mutations alters the dimeric nature of the molecule in solution (data not shown), indicating that the observed effects of these mutations on reovirus binding are not attributable to alterations in the capacity of the mutant proteins to form dimers. Thus, these findings suggest that Ser^{57} and Tyr^{75} play critical roles in reovirus attachment and highlight the importance of a region at the top of the homodimer interface in reovirus binding to hJAM1.

DISCUSSION

Experiments reported here were performed to define the molecular basis of reovirus attachment to hJAM1. The capacity of reovirus to bind, infect, and replicate to high titers in cells expressing chimeric hCAR-hJAM1 receptor constructs and single domain deletion mutants demonstrates that the membrane-distal D1 domain of hJAM1 is an essential component of the reovirus receptor function of hJAM1 (Figs. 2 and 3). Several viruses have been demonstrated to engage cellular receptors via the most distal domain of an Ig superfamily receptor, including adenovirus (hCAR) (16, 36), coxsackievirus (hCAR) (37), human immunodeficiency virus (CD4) (38), measles virus (SLAM) (39), poliovirus (PVR) (40), and rhinovirus (ICAM-1) (41). Thus, utilization of the membrane-distal D1 domain of hJAM1 by reovirus provides additional evidence for a common theme in viral attachment.

Of the virus receptors whose structures have been solved, only adenovirus receptor hCAR and reovirus receptor JAM1 have been demonstrated to form homodimers by contacts between the GFCC′ β-strands of apposing D1 domains (22, 23, 25). Moreover, there are numerous similarities in the attach-

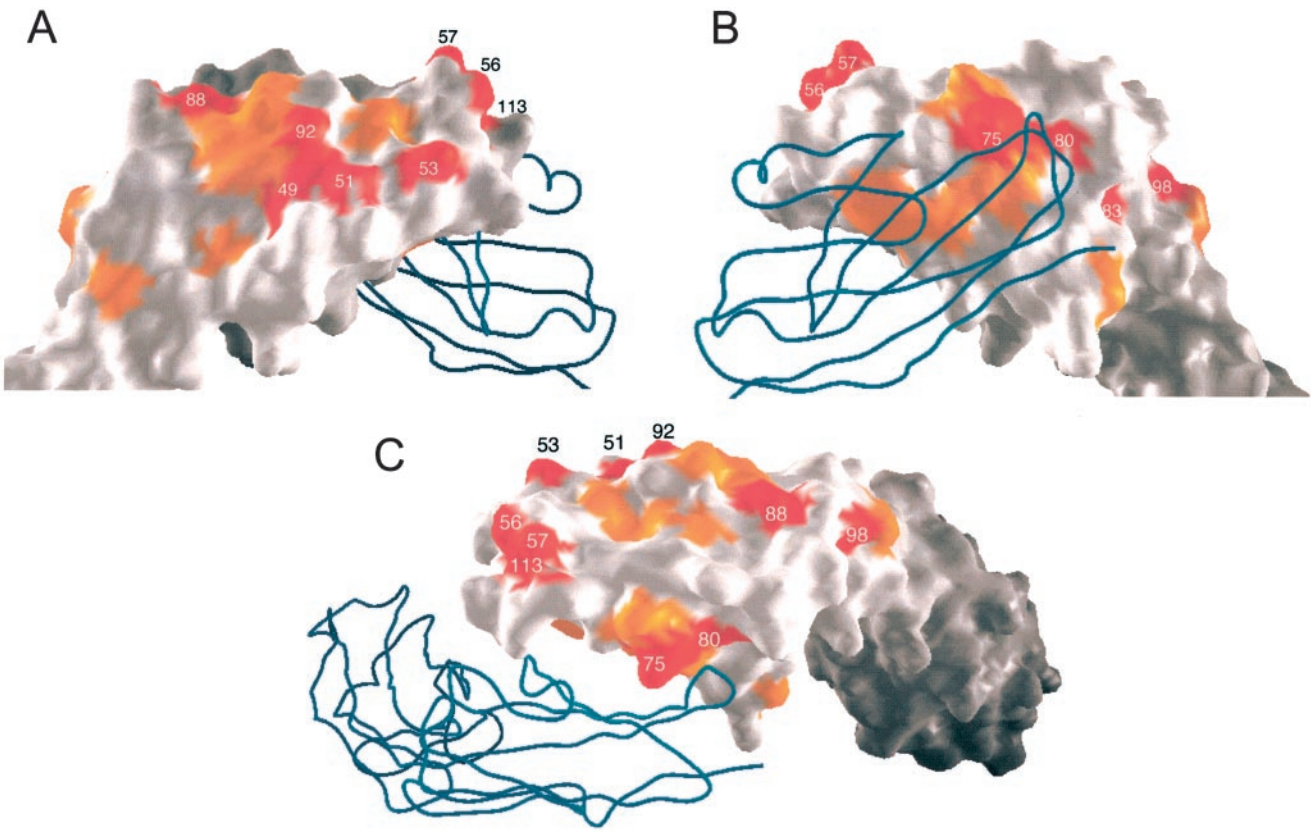

FIG. 6. **Orientation of mutagenized hJAM1 residues.** The structure of the hJAM1 dimer is shown in three orientations: back (*A*), dimer interface or front (*B*), and top (*C*). In each image, one monomer is depicted as a space-filling model and the other as an α-carbon tracing. Conserved residues selected for mutagenesis are shown in *red*. Other conserved residues in hJAM1 and mJAM1 are shown in *orange*. Mutations are summarized in Table II. This *figure* was prepared with GRASP (47).

TABLE II
PCR primers for point mutant hJAM1 constructs

T7 and BGH primers were used as 5′ forward and 3′ reverse primers for all constructs.

Point mutation	Primer	
	Forward	Reverse
S49A	5′-GTGAAGTTGGCATGTGCCTAC-3′	5′-GTAGGCACATGCCAACTTCAC-3′
A51K	5′-TTGTCCTGTAAATACTCGGGC-3′	5′-GCCCGAGTATTTACAGGACAA-3′
S53A	5′-TGTGCCTACGCCGGCTTTTCT-3′	5′-AGAAAAGCCGGCGTAGGCACA-3′
S56K	5′-TCGGGCTTTAAATCTCCCCGT-3′	5′-ACGGGGAGATTTAAAGCCCGA-3′
S57K	5′-GGCTTTTCTAAACCCCGTGTG-3′	5′-CACACGGGGTTTAGAAAAGCC-3′
Y75A	5′-CTCGTTTGCGCCAATAACAAG-3′	5′-CTTGTTATTGGCGCAAACGAG-3′
T80A	5′-AACAAGATCGCCGCTTCCTAT-3′	5′-ATAGGAAGCGGCGATCTTGTT-3′
Y83A	5′-ACAGCTTCCGCCGAGGACCGG-3′	5′-CCGGTCCTCGGCGGAAGCTGT-3′
T88A	5′-GACCGGGTGGCATTCTTGCCA-3′	5′-TGGCAAGAATGCCACCCGGTC-3′
T92A	5′-TTCTTGCCAGCGGGTATCACC-3′	5′-GGTGATACCCGCTGGCAAGAA-3′
S98A	5′-ACCTTCAAGGCAGTGACACGG-3′	5′-CCGTGTCACTGCCTTGAAGGT-3′
E113K	5′-ATGGTCTCTAAAGAAGGCGGC-3′	5′-GCCGCCTTCTTTAGAGACCAT-3′

ment proteins of adenovirus and reovirus: 1) both form trimers; 2) both insert into pentamers of capsid proteins at the virion 5-fold symmetry axes; 3) both have fibrous domains formed by unique triple β-spiral structural motifs; and 4) both have globular, virion-distal domains formed by β-barrel structures with unique and identical β-strand connectivity. These similarities suggest functionally convergent evolution of two large, nonenveloped viruses (14). Additionally, the observation that hJAM1 and hCAR share numerous structural and functional similarities leads to the hypothesis that adenovirus and reovirus engage their receptors using similar mechanisms.

Structural and biophysical evidence indicates that adenovirus engages the D1 domain of hCAR using sequences involved in hCAR homodimerization. Specifically, adenovirus fiber knob engages the GFCC′ face of hCAR (16) in a manner thermodynamically favored over hCAR-hCAR interactions (28). To test the hypothesis that reovirus engages hJAM1 using residues involved in hJAM1 homodimerization, we developed an *in vitro* binding assay and tested the capacity of hJAM1 to compete for reovirus binding to hJAM1. We first established that hJAM1-hJAM1 and reovirus-hJAM1 interactions are saturable and specific (Fig. 4, *A* and *B*). Interestingly, reovirus achieved equilibrium more rapidly in these experiments and at molarities much lower than those of hJAM1 (equilibrium in ~180 min at 0.16 nM for reovirus *versus* ~300 min at 80 nM for hJAM1). Limitations of the experimental system do not permit accurate calculations of equilibrium binding constants. Nonetheless, it is likely that reovirus-hJAM1 interactions are thermodynamically favored over hJAM1-hJAM1 interactions.

The calculated K_D of mJAM1 for mJAM1 (~15 nM) (24) approximates that of the purified T3D σ1 head domain for hJAM1 (~60 nM) (17). However, the multivalent nature of σ1

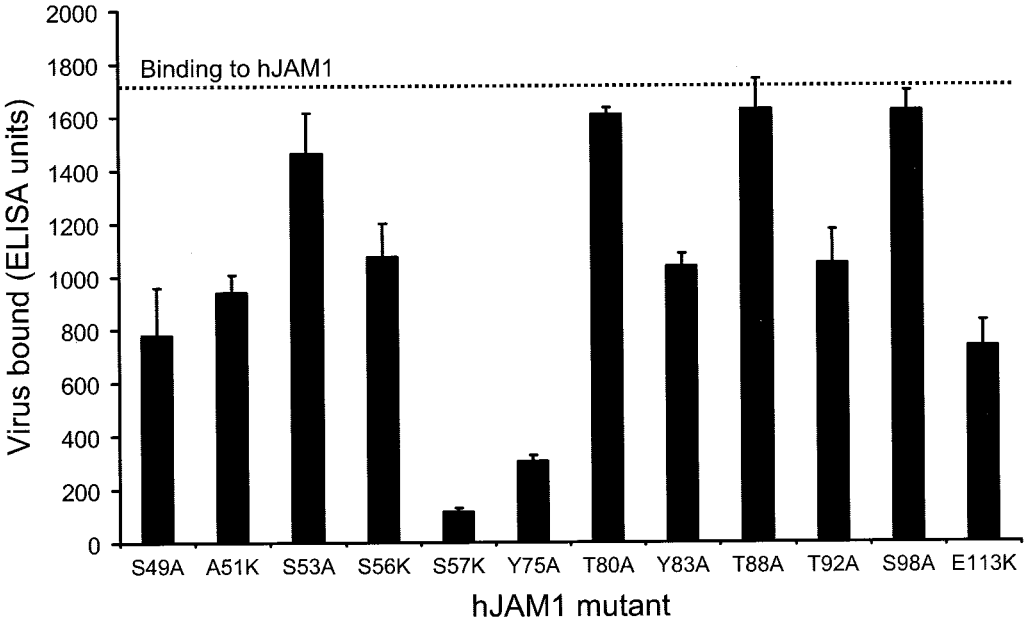

FIG. 7. **Ser[57] and Tyr[75] facilitate efficient reovirus attachment to hJAM1.** ELISA plates were coated with 20 nM solutions of wild-type or point mutant forms of soluble hJAM1. Binding of biotinylated reovirus T1L (2×10^{11} particles/ml) to immobilized hJAM1 constructs was assessed after incubation at 37 °C for 180 min. Virus binding was detected following incubation with streptavidin-HRP. The *dashed line* indicates reovirus binding to wild-type hJAM1. Results are the means of quadruplicate experiments. The *error bars* indicate S.D. Data are normalized for immobilization efficiency.

on reovirus particles probably mediates cooperative binding effects that enhance the on rate and stability of reovirus binding to hJAM1. Additionally, soluble hJAM1 competes for reovirus binding to hJAM1 *in vitro* and on cells with comparable IC_{50} values between 20- and 50-fold molar excess hJAM1 relative to particle-associated σ1 and nearly complete inhibition at 100-fold excess concentrations (Fig. 4, *C* and *D*). The relatively high concentration of hJAM1 necessary to detect soluble hJAM1 binding to immobilized hJAM1 precludes the converse competition experiment using reovirus as competitor (100-fold molar excess = 1.3×10^{14} particles/ml or 4.8×10^{15} copies of σ1/ml). Nonetheless, these data further establish the specificity of reovirus binding to hJAM1 and suggest that reovirus and hJAM1 utilize identical or overlapping sites for attachment and dimerization, respectively. Moreover, the high concentration of hJAM1 necessary to compete reovirus binding provides additional support for virus-hJAM1 associations being thermodynamically favored over homotypic hJAM1 interactions.

To further assess the role of the hJAM1 dimer interface in reovirus binding, we tested the effect of chemically cross-linking hJAM1 on reovirus binding to hJAM1 *in vitro* and on cells. We found that cross-linking substantially reduced the efficiency of reovirus binding (Fig. 5). Furthermore, cross-linked hJAM1 exhibited only minimal competition for reovirus binding to hJAM1 (Fig. 5*B*). The most likely interpretation of these data is that access to the hJAM1 dimer interface is required for efficient reovirus binding, although it is also possible that cross-linking induces structural changes in hJAM1 that inhibit viral attachment or that the bound cross-linking reagent prevents access to the hJAM1 dimer. In these experiments, cross-linking HeLa cell surface proteins induced the formation of a very large M_r band recognized by antiserum specific for hJAM1 following immunoprecipitation with an hJAM1-specific mAb (Fig. 5*C*). It is possible that formation of a large M_r hJAM1-containing species following cross-linking indicates the tight association of hJAM1 with additional cellular proteins that facilitate reovirus entry following attachment to hJAM1 in a manner analogous to the attachment and entry strategy of adenovirus (42). The presence of such proteins also might offer an explanation for the inefficient viral growth in CHO cells observed in the absence of hJAM1 D1 expression (Fig. 3*B*).

We previously demonstrated that both hJAM1 and mJAM1 function as reovirus receptors (17). Since this observation, two additional human and murine JAM proteins (JAM2 and JAM3) have been identified. However, only JAM1 is capable of supporting reovirus infection (23). Comparative sequence and structural analysis identified regions of conserved residues in hJAM1 and mJAM1, but not hJAM2 or hJAM3, which suggested roles for these conserved regions in reovirus attachment (23). To define residues critical for reovirus binding, mutations were introduced in several solvent-accessible residues covering most of the hJAM1 D1 surface (Fig. 6), and these mutant constructs were tested for the capacity to bind reovirus *in vitro*. Using this approach, we found that residues Ser[57] and Tyr[75] are important for efficient reovirus binding (Fig. 7). Interestingly, these residues localize to a region at the very top of the hJAM1 dimer interface (Figs. 6 and 8). Mutagenesis of Glu[113], another residue localized to the top of the dimer interface (Figs. 6 and 8), also diminished reovirus binding, but to a lesser extent than mutations at Ser[57] or Tyr[75] (Fig. 7). In contrast, mutation of the other residues chosen for study had little effect on binding, suggesting that the surface opposite to the dimer interface (the exposed "back" of hJAM1) does not participate in interactions with reovirus.

Of the hJAM1 residues important for reovirus attachment, Ser[57] presents the most accessible potential contact point, and as such, the exposed serine hydroxyl group may provide a hydrogen bond donor for σ1 binding. It is also possible that the S57K mutation introduces a structural change at the top of hJAM1. A lysine side chain could potentially interact with nearby acidic residues Glu[113] and Glu[114], thereby distorting the reovirus-binding surface. However, this possibility is unlikely, given that mutagenesis of Ser[56] to lysine does not elicit a similar inhibitory effect on reovirus binding. We note that several mutations in a region adjacent to or in the dimer interface (S49A, A51K, S56K, Y83A, and T92A) modestly inhibit binding (Fig. 7). Most of these mutations (Ser[49], Ala[51], and Ser[56]) are in close proximity to and form part of the

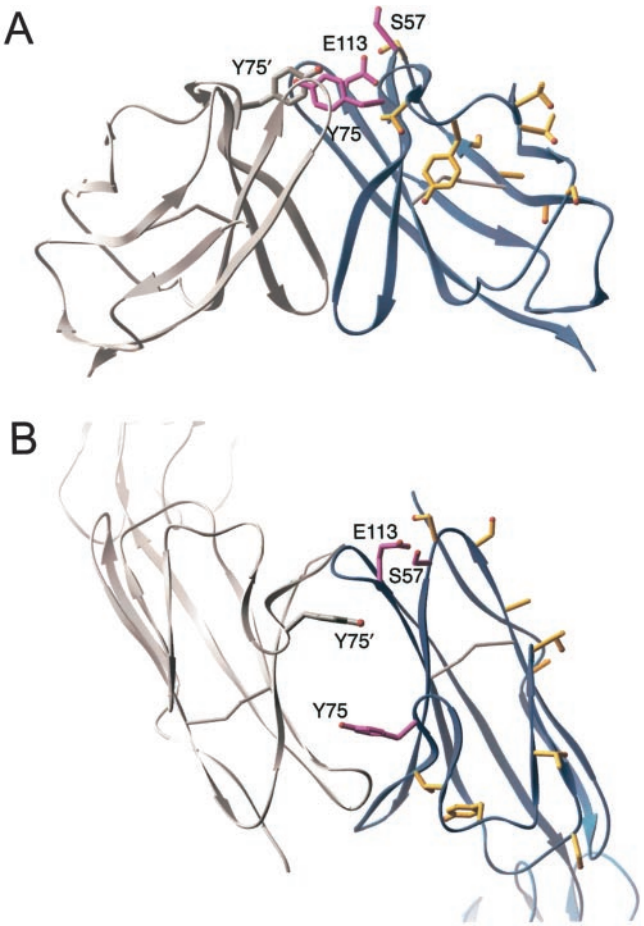

FIG. 8. **Location of residues implicated in reovirus binding.** Shown are *ribbon diagrams* of an hJAM1 D1 dimer with mutated residues shown in *ball-and-stick representations*. Residues Ser^{57}, Tyr^{75}, and Glu^{113} (*magenta*) form likely interaction sites for reovirus. The Tyr^{75} side chain of the symmetry-related D1 domain, which also is close to this site, is shown in *gray* (*Y75′*). Other conserved residues are shown in *yellow*. The two views differ by 90° along the 2-fold symmetry axis. This *figure* was prepared with Ribbons (34).

contiguous β-strand leading to Ser^{57}. It is conceivable that mutagenesis of some of these residues slightly alters the orientation of the Ser^{57} side chain in a manner that diminishes the efficiency of reovirus attachment. Residue Tyr^{75} is buried in the dimer interface. The drastic effect of Y75A on reovirus attachment suggests that disruption of hJAM1 homodimers is required for efficient reovirus binding and, furthermore, that reovirus interacts with residues at the hJAM1 dimer interface. An alternative explanation, given the location of Tyr^{75} at the hJAM1-hJAM1 interface, might be that the Y75A mutation adversely affects the dimeric structure, thereby preventing reovirus binding to dimeric hJAM1. However, mutant Y75A maintains its dimeric nature in solution (data not shown), making this explanation less likely. Moreover, our competitive binding and cross-linking experiments (Figs. 4 and 5, respectively) strengthen the argument against this second possibility.

Our experiments preclude an exact determination of the mechanism by which Y75A diminishes reovirus binding. Mutagenesis of Tyr^{75} may alter the dissociation capacity of hJAM1 dimers or remove a potential reovirus contact point. We also consider it possible that reovirus engages hJAM1 using a two-step mechanism that facilitates dimer dissolution and efficient reovirus binding. If so, initial contact with Ser^{57} may induce a conformational change in reovirus particles, hJAM1, or both molecules to promote the formation of a higher affinity binding state, perhaps by exposing Tyr^{75}. We note that, in the hJAM1 dimer structure, Ser^{57} is very close to Tyr^{75} of the apposed hJAM1 monomer (*Y75′* in Fig. 8); thus, interaction with Ser^{57} could easily trigger rearrangements at the JAM1-JAM1 interface. Several lines of evidence lend support to this hypothesis. First, the localization of closely apposed aspartic acid residues in the interior of the σ1 head trimer interface suggests that σ1 is a metastable protein primed for structural rearrangements (13). Second, although homotypic hJAM1 association cannot be detected in real time by surface plasmon resonance (data not shown), in similar experiments reovirus engages hJAM1 with rapid and saturable kinetics to form a highly stable complex (17). Third, reovirus binding to cell surfaces or cell membrane preparations alters the sensitivity of the virus to proteolysis in a σ1-dependent fashion (43), suggesting a role for σ1 in particle-associated structural changes. Ongoing biophysical and structural approaches will facilitate a further understanding of the mechanism of reovirus-hJAM1 interactions.

Studies reported in this manuscript provide evidence for possible mechanisms of reovirus binding to hJAM1. They also highlight common mechanisms of attachment for reovirus and adenovirus in which structurally analogous attachment proteins disrupt dimers of structurally analogous receptors to engage and infect target cells. Intriguingly, hJAM1 and hCAR, as well as several other viral receptors, localize to epithelial barriers (44), suggesting that aspects of these physiologic locations provide permissive sites for viral infection. Both hJAM1 and hCAR have been reported to regulate tight junction barrier function (18–20, 45), and adenovirus may usurp this property to facilitate release and spread of progeny virions into the environment (46). Whether reovirus disregulates hJAM1 in a similar manner is not known. It is also possible that hJAM1 and hCAR were simply selected as abundant and convenient attachment moieties that are readily accessible by natural routes of inoculation, which raises the question of why these particular molecules were chosen. An interesting explanation would be that particular receptors associate with additional cellular molecules that contribute to viral replication by facilitating cell entry or activating intracellular signaling to induce a virus-permissive state. Differential requirements for entry or replication may offer an explanation for why reoviruses and adenoviruses have selected distinct molecules for amazingly similar mechanisms of attachment.

Acknowledgments—We thank members of our laboratory for many useful discussions and Jim Chappell and Tim Peters for review of the manuscript. We acknowledge the Nashville Veterans Affairs Hospital Flow Cytometry Facility for assistance and data analysis.

REFERENCES

1. Nibert, M. L., and Schiff, L. A. (2001) in *Fields Virology* (Knipe, D. M., and Howley, P. M., eds) 4th Ed., pp. 1679–1728, Lippincott-Raven, Philadelphia
2. Tyler, K. L. (2001) in *Fields Virology* (Knipe, D. M., and Howley, P. M., eds), 4th Ed., pp. 1729–1945, Lippincott-Raven, Philadelphia
3. Weiner, H. L., Drayna, D., Averill, D. R., Jr., and Fields, B. N. (1977) *Proc. Natl. Acad. Sci. U. S. A.* **74,** 5744–5748
4. Weiner, H. L., Powers, M. L., and Fields, B. N. (1980) *J. Infect. Dis.* **141,** 609–616
5. Tyler, K. L., McPhee, D. A., and Fields, B. N. (1986) *Science* **233,** 770–774
6. Morrison, L. A., Sidman, R. L., and Fields, B. N. (1991) *Proc. Natl. Acad. Sci. U. S. A.* **88,** 3852–3856
7. Weiner, H. L., Ault, K. A., and Fields, B. N. (1980) *J. Immunol.* **124,** 2143–2148
8. Lee, P. W., Hayes, E. C., and Joklik, W. K. (1981) *Virology* **108,** 156–163
9. Furlong, D. B., Nibert, M. L., and Fields, B. N. (1988) *J. Virol.* **62,** 246–256
10. Banerjea, A. C., Brechling, K. A., Ray, C. A., Erikson, H., Pickup, D. J., and Joklik, W. K. (1988) *Virology* **167,** 601–612
11. Fraser, R. D. B., Furlong, D. B., Trus, B. L., Nibert, M. L., Fields, B. N., and Steven, A. C. (1990) *J. Virol.* **64,** 2990–3000
12. Strong, J. E., Leone, G., Duncan, R., Sharma, R. K., and Lee, P. W. (1991) *Virology* **184,** 23–32
13. Chappell, J. D., Prota, A., Dermody, T. S., and Stehle, T. (2002) *EMBO J.* **21,** 1–11
14. Stehle, T., and Dermody, T. S. (2003) *Rev. Med. Virol.* **13,** 123–132
15. Chappell, J. D., Duong, J. L., Wright, B. W., and Dermody, T. S. (2000) *J. Virol.* **74,** 8472–8479
16. Bewley, M. C., Springer, K., Zhang, Y. B., Freimuth, P., and Flanagan, J. M. (1999) *Science* **286,** 1579–1583

17. Barton, E. S., Forrest, J. C., Connolly, J. L., Chappell, J. D., Liu, Y., Schnell, F., Nusrat, A., Parkos, C. A., and Dermody, T. S. (2001) *Cell* **104,** 441–451
18. Liu, Y., Nusrat, A., Schnell, F. J., Reaves, T. A., Walsh, S., Ponchet, M., and Parkos, C. A. (2000) *J. Cell Sci.* **113,** 1–11
19. Martin-Padura, I., Lostaglio, S., Schneemann, M., Williams, L., Romano, M., Fruscella, P., Panzeri, C., Stoppacciaro, A., Ruco, L., Villa, A., Simmons, D., and Dejana, E. (1998) *J. Cell Biol.* **142,** 117–127
20. Ozaki, H., Ishii, K., Horiuchi, H., Arai, H., Kawamoto, T., Okawa, K., Iwamatsu, A., and Kita, T. (1999) *J. Immunol.* **163,** 553–557
21. Del Maschio, A., De Luigi, A., Martin-Padura, I., Brockhaus, M., Bartfai, T., Fruscella, P., Adorini, L., Martino, G., Furlan, R., De Simoni, M. G., and Dejana, E. (1999) *J. Exp. Med.* **190,** 1351–1356
22. Kostrewa, D., Brockhaus, M., D'Arcy, A., Dale, G. E., Nelboeck, P., Schmid, G., Mueller, F., Bazzoni, G., Dejana, E., Bartfai, T., Winkler, F. K., and Hennig, M. (2001) *EMBO J.* **20,** 4391–4398
23. Prota, A. E., Campbell, J. A., Schelling, P., Forrest, J. C., Peters, T. R., Watson, M. J., Aurrand-Lions, M., Imhof, B., Dermody, T. S., and Stehle, T. (2003) *Proc. Natl. Acad. Sci. U. S. A.* **100,** 5366–5371
24. Bazzoni, G., Martinez-Estrada, O. M., Mueller, F., Nelboeck, P., Schmid, G., Bartfai, T., Dejana, E., and Brockhaus, M. (2000) *J. Biol. Chem.* **275,** 30970–30976
25. van Raaij, M. J., Chouin, E., van der Zandt, H., Bergelson, J. M., and Cusack, S. (2000) *Struct. Fold. Des.* **8,** 1147–1155
26. Bodian, D. L., Jones, E. Y., Harlos, K., Stuart, D. I., and Davis, S. J. (1994) *Structure* **2,** 755–766
27. Jones, E. Y., Davis, S. J., Williams, A. F., Harlos, K., and Stuart, D. I. (1992) *Nature* **360,** 232–239
28. Lortat-Jacob, H., Chouin, E., Cusack, S., and van Raaij, M. J. (2001) *J. Biol. Chem.* **276,** 9009–9015
29. Barton, E. S., Connolly, J. L., Forrest, J. C., Chappell, J. D., and Dermody, T. S. (2001) *J. Biol. Chem.* **276,** 2200–2211
30. Virgin, H. W., IV, Bassel-Duby, R., Fields, B. N., and Tyler, K. L. (1988) *J. Virol.* **62,** 4594–4604
31. Becker, M. M., Goral, M. I., Hazelton, P. R., Baer, G. S., Rodgers, S. E., Brown, E. G., Coombs, K. M., and Dermody, T. S. (2001) *J. Virol.* **75,** 1459–1475
32. Bergelson, J. M., Cunningham, J. A., Droguett, G., Kurt-Jones, E. A., Krithivas, A., Hong, J. S., Horwitz, M. S., Crowell, R. L., and Finberg, R. W. (1997) *Science* **275,** 1320–1323
33. Schmid, S. L., and Carter, L. L. (1990) *J. Cell Biol.* **111,** 2307–2318
34. Carson, M. (1987) *J. Mol. Graph.* **5,** 103–106
35. Limbird, L. E. (1996) *Cell Surface Receptors: A Short Course on Theory and Methods*, 2nd Ed., Kluwer Academic Publishers, Boston
36. Freimuth, P., Springer, K., Berard, C., Hainfeld, J., Bewley, M., and Flanagan, J. (1999) *J. Virol.* **73,** 1392–1398
37. He, Y., Chipman, P. R., Howitt, J., Bator, C. M., Whitt, M. A., Baker, T. S., Kuhn, R. J., Anderson, C. W., Freimuth, P., and Rossmann, M. G. (2001) *Nat. Struct. Biol.* **8,** 874–878
38. Kwong, P., Wyatt, R., Robinson, J., Sweet, R., Sodroski, J., and Hendrickson, W. (1998) *Nature* **393,** 648–659
39. Ono, N., Tatsuo, H., Tanaka, K., Minagawa, H., and Yanagi, Y. (2001) *J. Virol.* **75,** 1594–1600
40. Belnap, D. M., McDermott, B. M., Jr., Filman, D. J., Cheng, N., Trus, B. L., Zuccola, H. J., Racaniello, V. R., Hogle, J. M., and Steven, A. C. (2000) *Proc. Natl. Acad. Sci. U. S. A.* **97,** 73–78
41. Kolatkar, P. R., Bella, J., Olson, N. H., Bator, C. M., Baker, T. S., and Rossmann, M. G. (1999) *EMBO J.* **18,** 6249–6259
42. Nemerow, G. R., and Stewart, P. L. (1999) *Microbiol. Mol. Biol. Rev.* **63,** 725–734
43. Fernandes, J., Tang, D., Leone, G., and Lee, P. W. (1994) *J. Biol. Chem.* **269,** 17043–17047
44. Spear, P. G. (2002) *Dev. Cell* **3,** 462–464
45. Cohen, C. J., Shieh, J. T., Pickles, R. J., Okegawa, T., Hsieh, J. T., and Bergelson, J. M. (2001) *Proc. Natl. Acad. Sci. U. S. A.* **98,** 15191–15196
46. Walters, R. W., Freimuth, P., Moninger, T. O., Ganske, I., Zabner, J., and Welsh, M. J. (2002) *Cell* **110,** 789–799
47. Nicholls, A., Sharp, K. A., and Honig, B. (1991) *Proteins* **11,** 281–296

APPENDIX D

CRYSTAL STRUCTURE OF HUMAN JUNCTIONAL ADHESION MOLECULE-A: IMPLICATIONS FOR REOVIRUS BINDING

Prota AE, Campbell JA, Schelling P, Forrest JC, Watson MJ, Peters TR, Aurrand-Lions M,

Imhof BA, Dermody TS, Stehle T.

Proceedings of the National Academy of Science. 100(9):5366-71;2003

Crystal structure of human junctional adhesion molecule 1: Implications for reovirus binding

Andrea E. Prota*[†‡], Jacquelyn A. Campbell[†§¶], Pierre Schelling*, J. Craig Forrest[§¶], Melissa J. Watson[¶‖], Timothy R. Peters[¶‖], Michel Aurrand-Lions**, Beat A. Imhof**, Terence S. Dermody[§¶‖††], and Thilo Stehle*[††]

*Laboratory of Developmental Immunology, Massachusetts General Hospital and Harvard Medical School, Boston, MA 02114; Departments of [§]Microbiology and Immunology and [‖]Pediatrics and [¶]Elizabeth B. Lamb Center for Pediatric Research, Vanderbilt University School of Medicine, Nashville, TN 37232; and **Department of Pathology, Centre Medical Universitaire, 1211 Geneva, Switzerland

Edited by Stephen C. Harrison, Children's Hospital, Boston, MA, and approved March 10, 2003 (received for review December 18, 2002)

Reovirus attachment to cells is mediated by the binding of viral attachment protein σ1 to junctional adhesion molecule 1 (JAM1). The crystal structure of the extracellular region of human JAM1 (hJAM1) reveals two concatenated Ig-type domains with a pronounced bend at the domain interface. Two hJAM1 molecules form a dimer that is stabilized by extensive ionic and hydrophobic contacts between the N-terminal domains. This dimeric arrangement is similar to that observed previously in the murine homolog of JAM1, indicating physiologic relevance. However, differences in the dimeric structures of hJAM1 and murine JAM1 suggest that the interface is dynamic, perhaps as a result of its ionic nature. We demonstrate that hJAM1, but not the related proteins hJAM2 and hJAM3, serves as a reovirus receptor, which provides insight into sites in hJAM1 that likely interact with σ1. In addition, we present evidence that the previously reported structural homology between σ1 and the adenovirus attachment protein, fiber, also extends to their respective receptors, which form similar dimeric structures. Because both receptors are located at regions of cell–cell contact, this similarity suggests that reovirus and adenovirus use conserved mechanisms of entry and pathways of infection.

Attachment to specific host molecules is the initial step in viral infection and plays a key role in target-cell selection in the infected host. In the case of mammalian reoviruses, this is accomplished by interactions between the viral attachment protein, σ1, and junctional adhesion molecule 1 (JAM1) (1). Reoviruses are nonenveloped, icosahedral viruses that infect most mammalian species, including humans. The capacity of reovirus strains to engage distinct types of receptors in the host strongly influences tissue tropism and disease after reovirus infection (2). JAM1 is a member of the Ig superfamily with two extracellular Ig-like domains, a single transmembrane region, and a short cytosolic tail. The crystal structure of the extracellular region of murine JAM1 (mJAM1) revealed a dimer stabilized by interactions involving the membrane-distal Ig-like domain (3). The protein is expressed in a variety of tissues and cell types, including circulating platelets and lymphocytes, and it has been postulated to function as a regulator of endothelial and epithelial tight junction formation (4–6). The human homolog of JAM1 (hJAM1) serves as a ligand for the integrin αLβ2 (LFA-1) (7), an interaction that likely plays an important role in host inflammatory responses by mediating transmigration of leukocytes. Two hJAM1 homologs, hJAM2 and hJAM3, have been recently identified (8–13). Additional evidence that JAM family members are involved in the inflammatory response is provided by the observations that hJAM2 interacts with α4β1 integrins (14), and hJAM3 interacts with αMβ2 (MAC-1) integrins (15).

Reovirus attachment protein σ1 is a long, fibrous molecule with head-and-tail morphology and several defined regions of flexibility within its tail (16, 17). The σ1 tail inserts into the 12 vertices of the icosahedral virion, whereas the JAM-binding σ1 head extends away from the particle surface (18, 19). Laboratory-adapted and field-isolate strains of all three reovirus serotypes bind JAM1 (ref. 1; J.A.C. and T.S.D., unpublished observations). Some reoviruses also use additional carbohydrate-based coreceptors for cell attachment (20, 21). For type 3 reoviruses, this coreceptor is α-linked sialic acid (22), and its binding site has been mapped to a region close to the midpoint of the σ1 tail (20, 23). The finding that reoviruses bind to different receptors by using distinct domains within the σ1 protein has led to the suggestion that reoviruses use a multiple-step adhesion-strengthening mechanism to engage the cell surface (21). In this scenario, reovirus binding to carbohydrate facilitates viral attachment through low-affinity adhesion. This interaction places the virus on the cell surface where access to the higher affinity, but lower abundance, JAM1 protein is thermodynamically favored.

The recently determined crystal structure of a JAM1-binding fragment of σ1 revealed numerous structural and functional similarities to the adenovirus attachment protein, fiber, suggesting an evolutionary link in the receptor-binding strategies of reoviruses and adenoviruses (17). Most adenovirus serotypes initiate infection by binding to the coxsackievirus and adenovirus receptor (CAR) (24). The crystal structure of the adenovirus fiber knob in complex with CAR is known (25). Although no structural information is currently available for a reovirus-receptor complex, analysis of the crystallized σ1 fragment revealed a region that is likely involved in the interaction with JAM1 (17). This putative JAM1-binding site forms a recessed groove at the lower edge of the σ1 head that contains many of the residues conserved in prototype strains of the three reovirus serotypes. The location of this site suggests that each σ1 monomer can independently interact with a JAM1 molecule.

To enhance an understanding of how reovirus mediates cell tropism and initiates organ-specific disease, we determined the crystal structure of the hJAM1 ectodomain. Analysis of this structure allows us to identify regions of the receptor that are most likely involved in the binding of σ1. Moreover, comparison of the structures of hJAM1 and mJAM1 reveals differences in the dimeric arrangements of the molecules despite absolute conservation of residues at the interface, suggesting that the JAM1 dimer is dynamic and can undergo rearrangement and perhaps dissociation. Finally, we show that the structure of the JAM1 dimer closely resembles that of the CAR dimer, mirroring the close resemblance of the reovirus and adenovirus attachment proteins and suggesting that the similarities extend beyond conservation of structure toward conserved strategies of attachment and entry.

This paper was submitted directly (Track II) to the PNAS office.

Abbreviations: CAR, coxsackievirus and adenovirus receptor; JAM, junctional adhesion molecule; mJAM, murine JAM; hJAM, human JAM; CHO, Chinese hamster ovary.

Data deposition: The atomic coordinates have been deposited in the Protein Data Bank, www.rcsb.org (PDB ID code 1NBQ).

[†]A.E.P. and J.A.C. contributed equally to this work.

[‡]Present address: Paul Scherrer Institute, Life Sciences, 5232 Villigen PSI, Switzerland.

[††]To whom correspondence should be addressed. E-mail: terry.dermody@vanderbilt.edu or tstehle@partners.org.

 www.pnas.org/cgi/doi/10.1073/pnas.0937718100

Table 1. Data collection and refinement statistics

Data set	Native
Diffraction data*	
Resolution range, Å	30–2.9
Completeness, %	85.1 (51.0)
Total reflections	27,850
Unique reflections	9,736
R_{merge},† %	11.4 (13.5)
I/σ	8.8 (3.7)
Refinement statistics	
R_{cryst}, %; work set‡	22.0 (no $I/\sigma I$ cutoff)
R_{cryst}, %; free set‡	30.5 (no $I/\sigma I$ cutoff)
rms deviation bond lengths, Å	0.02
rms deviation bond angles, °	2.7
Number of waters	124

*Data sets were collected at 100 K and a wavelength of 1.1 Å. Values in parentheses refer to the outermost resolution shell.

†$R_{merge} = \Sigma_{hkl}|I - \langle I\rangle|/\Sigma_{hkl}I$, where I is the intensity of a reflection hkl, and $\langle I\rangle$ is the average over symmetry-related observations of hkl.

‡$R_{cryst} = \Sigma_{hkl}|F_{obs} - F_{calc}|/\Sigma_{hkl}F_{obs}$, where F_{obs} and F_{calc} are observed and calculated structure factors, respectively. Free set (28) contains 10% of the data.

Methods

Protein Expression, Purification, and Crystallization. A cDNA corresponding to the extracellular region of hJAM1 (residues 27–233) was cloned into the pGEX-4T-3 expression vector (Amersham Pharmacia), which encodes N-terminal GST followed by a thrombin cleavage site. GST–hJAM1 fusion protein was expressed in *Escherichia coli* and purified by affinity chromatography using glutathione beads. hJAM1 was released from the beads by thrombin cleavage and further purified by anion-exchange chromatography. The cleaved protein contains three additional non-native amino acids (Gly-24, Ser-25, and Met-26) at the N terminus. A final gel filtration step resulted in a homogenous peak that corresponded to a dimer of 48 kDa. Higher-order oligomers were not observed. Crystals were obtained by using 8 mg/ml protein and 16% PEG 6K, 18% isopropanol, 0.1 M sodium citrate as precipitant. The final pH of the mixture was 6.0.

Structure Determination. The crystals belong to space group C2 (a = 116.8 Å, b = 61.8 Å, c = 82.9 Å, β = 120.01°) and contain two molecules in their asymmetric unit. Before data collection, crystals were cryoprotected with 15% glycerol and then flash-frozen in liquid nitrogen. Diffraction data were collected at NSLS beamline X25 and processed with HKL (26). The structure was determined by molecular replacement using the structure of mJAM1 (3). Rotation and translation searches were performed separately with the N- and C-terminal domains of mJAM1 in AMORE (27), which yielded two clear solutions for each domain. The free R factor (28) for the combined solutions was 45.1% (8–3.5 Å) after rigid body refinement. Alternating rounds of model building in O (29) and refinement in X-PLOR (30) produced a model with good refinement statistics (Table 1). Bulk solvent correction and noncrystallographic symmetry constraints were used throughout the refinement. The final model contains residues 25–233 of both chains and 124 water molecules. PROCHECK (27) analysis shows no residues in disallowed regions in the Ramachandran plot.

Infectivity Assay. Chinese hamster ovary (CHO) cells (60–80% confluence) were transfected with 0.4 μg of plasmid encoding hJAM1, hJAM2, hJAM3, or pEGFP-N1 (transfection control) by using Lipofectamine Plus (GIBCO/BRL). Surface expression was confirmed by flow cytometry using antibodies specific for hJAM1 (31), hJAM2 (M.A.L. and B.A.I., unpublished observations), or hJAM3 (32). Transfected cells were infected with reovirus type 1 Lang (T1L) at a multiplicity of infection of 1 fluorescent focus unit per cell in a total volume of 150 μl. Adsorptions were terminated after incubation at room temperature for 1 h by washing with PBS. Infected cells were identified 18 h after adsorption by indirect immunofluorescence using rabbit antireovirus sera (1).

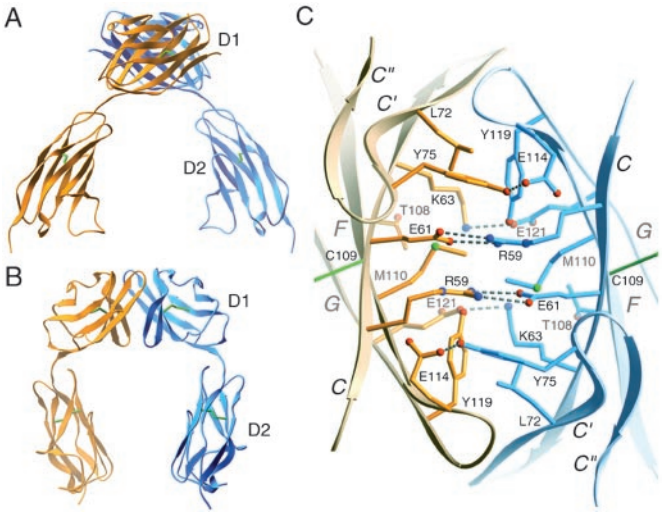

Fig. 1. Structure of hJAM1 D1D2. (*A* and *B*) Ribbon drawings of the hJAM1 dimer, with one monomer shown in orange and the other in blue. Two orthogonal views are displayed. Disulfide bonds are shown in green. (*C*) View of the interface between two hJAM1 monomers. The interface is formed by residues on the GFCC′ faces of two D1 domains. The view is along a crystallographic dyad. Hydrogen bonds and salt bridges are represented by broken cylinders. Amino acids are labeled in single-letter code.

Results and Discussion

Overall Structure. The polypeptide chain of the extracellular region of hJAM1 folds into two concatenated Ig-like domains, termed D1 and D2 (Fig. 1 *A* and *B*). The N-terminal D1 domain contains two antiparallel β-sheets (strands ABED and GFCC′C″), which classifies it as an Ig-like domain of the variable type (V-set). Although the fold of D2 is very similar to that of D1, this domain has a much shorter C′ strand, and it lacks the C″ strand. These differences indicate that D2 is an intermediate type (I-set) Ig-like domain (33) and not a V-set Ig-like domain, as reported for mJAM1 D2 (3). Analysis with DALI (34) shows that the prototypical I-set domain, telokin (33), is among the closest structural homologs of hJAM1 D2. Both D1 and D2 of hJAM1 have the classical disulfide bond between β-strands B and F. The hJAM1 structure exhibits a pronounced elbow angle of ≈125° between the two domains. As expected, the overall structure of each hJAM1 D1D2 monomer resembles that of mJAM1 D1D2 (3), although there are conformational differences between the two proteins in surface loops and at the interdomain interface. Our structure also allows us to trace a long loop between β-strands C′ and D (C′D loop) in D2 that was disordered in the model for mJAM1 D1D2.

The asymmetric unit of the hJAM1 crystals contains two independent but virtually identical chains (termed A and B). Each chain assembles into a U-shaped homodimer with crystallographic 2-fold symmetry. The dimer interface features an extensive contact between the D1 domains and is reminiscent of an arm-wrestling grip, with the GFCC′ faces of the two N-terminal domains interlocking at an angle of ≈90° (Fig. 1 *A* and *B*). Two crystallographically independent dimers are observed. One is formed by chain A and its symmetry mate A, and the other

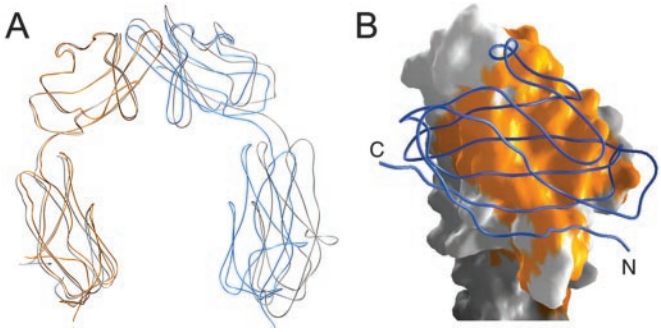

Fig. 2. Comparison of dimeric arrangements in hJAM1 and mJAM1 (3). (*A*) Superposition of dimeric structures of hJAM1 D1D2 (colored as in Fig. 1) and mJAM1 D1D2 (gray). The superposition is based on D1 residues of one monomer only (the orange monomer of hJAM1), which yielded a rms deviation of 0.55 Å for 2 × 90 Cα atoms. The matrix derived from this superposition was applied to the entire dimer. (*B*) Conservation of residues at the mJAM1 and hJAM1 D1 domain dimer interfaces. One hJAM1 monomer is shown in surface representation, and the other is shown as a blue ribbon. Residues that are strictly conserved in mJAM1 are shown in orange and cover the entire dimer interface.

is formed by chains B and B. Two observations suggest that the hJAM1 dimer is physiologically relevant: (*i*) the purified protein elutes at the expected molecular mass for a dimer (48 kDa) by size-exclusion chromatography and (*ii*) a similar dimeric structure was seen in the crystals of mJAM1 (3). With the exception of the dimeric interaction, the arrangements of the molecules in the hJAM1 and mJAM1 crystals are not related.

Structure of the Dimer. Residues involved in hJAM1 homodimer formation are exclusively located on the concave GFCC′ face of D1. The dimer interface includes four buried salt bridges (Arg-59–Glu-61, Glu-61–Arg-59, Lys-63–Glu-121, and Glu-121–Lys-63) as well as several hydrophobic contacts (Leu-72–Tyr-119, Met-110–Met-110, and Tyr-119–Leu-72) (Fig. 1*C*). Hydrogen bonds exist between the Tyr-75 and Glu-114 side chains.

Although the GFCC′ face of D1 also mediates homodimer formation in the mJAM1 D1D2 structure (3), the relative arrangements of the D1 domains in the two dimers are noticeably different (Fig. 2*A*). The mJAM1 interdomain interface contains only two salt bridges and fewer additional contacts (3). The Lys-63–Glu-121 and Met-110–Met-110 interactions at the center of the hJAM1 interface are absent in mJAM1, as are the hydrogen bonds involving Tyr-75, Glu-114, and their symmetry-related counterparts. These differences result in a smaller interface in mJAM1 (Fig. 2*A*). Using the program SURFACE (27) and a standard probe radius of 1.4 Å, we calculate buried surface areas of 1,380 and 1,200 Å^2 for the hJAM1 and mJAM1 dimers, respectively.

The observed differences in the hJAM1 and mJAM1 dimers are noteworthy given the near absolute conservation of residues at the dimer interfaces (Fig. 2*B*). The GFCC′ faces of hJAM1 and mJAM1 (residues 58–75 and 105–122 of hJAM1) can be superimposed onto each other with an rms deviation of 0.4 Å for the 36 Cα atoms. There are only six substitutions among these 36 aa, and none of the substituted residues engage in dimer contacts (distances >4 Å). Thus, differences in the arrangement of the hJAM1 and mJAM1 dimer interfaces cannot be explained by altered contacts mediated by substituted residues. Instead, these differences are likely caused by crystal packing forces involving other regions of the molecules, and they indicate that small movements of one monomer with respect to the other can occur.

The dynamic nature of the JAM1 dimer interface may result in part from its dependence on ionic interactions, which is unusual for protein–protein interfaces. Low pH and moderately high ionic strength lead to dissociation of the mJAM1 dimer (35), indicating that ionic interactions represent the principal means of association. We note that both structures were obtained by using conditions of low ionic strength and at pH values at which acidic side chains are expected to be deprotonated. Thus, salt bridges are expected to exist in both cases. However, the free energy contribution of salt bridges in an aqueous environment is small (36). The JAM1 dimer interface, which is stabilized primarily by salt bridges and contains several solvent molecules, is therefore especially likely to undergo rearrangement or dissociation.

Implications for the Structures of hJAM2 and hJAM3. The conservation of key features of the dimer interface in hJAM1 and mJAM1 strongly suggests that this interface is responsible for the dimeric structure of the protein in solution, as suggested (3). Thus, it offers a framework for predicting the oligomeric state of other JAM family members. Sequence alignments show that most of the residues mediating dimer formation are conserved in the two additional hJAM family members, hJAM2 and hJAM3, which has led to the suggestion that these two molecules form similar dimeric structures (3). Analysis of conserved residues at the dimer interface, however, shows that several key residues are not conserved in hJAM2 or hJAM3. Met-110, which is located at the center of the hJAM1 interface (Fig. 1*C*) and conserved in mJAM1, is replaced with a glutamic acid in both hJAM2 and hJAM3. The nearby residue Thr-108 (Fig. 1*C*), which also is conserved in hJAM1 and mJAM1, is replaced with an arginine in hJAM2 and hJAM3. The presence of two additional charged residues is almost certain to impart different characteristics to the structure and stability of hJAM2 and hJAM3 dimers. hJAM2 and hJAM3 have been shown to engage in heterophilic interactions, with hJAM2 serving as a counter-receptor for hJAM3 (12, 13). The precise distribution of residues at the respective GFCC′ faces and secondary interactions may favor heterodimeric contacts rather than homodimeric interactions between these proteins. It is also possible that formation of an hJAM2–hJAM3 dimer uses molecular regions other than those described, although the D1 domain of hJAM2 is clearly involved in facilitating this arrangement (14).

The hJAM1 residues involved in salt bridge formation (Arg-59, Glu-61, Lys-63, Glu-121) and hydrophobic contacts (Leu-72, Tyr-119) are highly conserved not only in the JAM1 sequences of other mammals but also in those of nonmammalian vertebrates such as zebrafish and the African clawed frog (data not shown). This observation suggests that the dimeric structure of JAM1 is present throughout vertebrates. We note that some nonmammalian sequences have features that render them more similar to JAM2 or JAM3 (e.g., substitution of Met-110 with Glu), suggesting that versions of all three JAM variants exist in vertebrates.

Implications for Homophilic Interaction at Tight Junctions. Analysis of the crystal-packing arrangement of the mJAM1 molecules has led to a model of JAM1 interactions at tight junctions (3). In this model, a JAM1 dimer located at the surface of one cell engages a dimer on the opposing cell via contacts in D1, producing an extensive network of contacts between dimers. Although our crystals contain two crystallographically nonequivalent copies of hJAM1, we do not observe a similar contact involving either of these molecules in our crystals, and thus our structural analysis does not provide supporting evidence for the model presented by Kostrewa *et al.* (3). In the hJAM1 crystals, two alternative contacts between hJAM1 dimers that could form the basis for interactions in tight junctions exist. However, neither of these contacts is observed in the mJAM1 crystal lattice. One interpretation of the available crystallographic data is that contacts between JAM1 dimers in tight junctions involve low-affinity

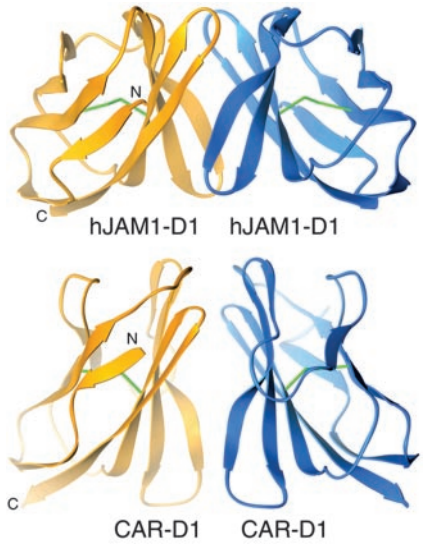

Fig. 3. Dimeric structures of virus receptors hJAM1 and CAR. The D1 domains of hJAM1 (*Upper*) and CAR (*Lower*) engage in a conserved mode of dimerization based on interactions between the concave GFCC′ β-sheets. Disulfide bonds are in green.

interactions that depend on the presence of additional proteins, and these interactions cannot be easily reproduced by using conditions that promote crystallization. Another interpretation is that the JAM1 dimer itself, which is observed in the crystals of hJAM1 and mJAM1, represents a physiologic contact present in tight junctions. In this interpretation, JAM1 monomers would engage JAM1 monomers on apposing cells to help mediate homophilic cell–cell interactions. The dimensions for such a model suggest that it deserves consideration, because it would lead to a separation of cells of ≈85 Å, similar to the observed distances at tight junctions of ≈100 Å. CAR is also thought to mediate homophilic interactions between cells (37–39), and the homodimeric structure of CAR has been interpreted to depict an interaction between CAR monomers from apposing cells (40).

Similarities to CAR. The attachment proteins of adenovirus and reovirus share structural and functional properties, which has led to speculation that they have a common ancestor (17). Remarkably, the receptors for both viruses, CAR and JAM1, respectively, also share key structural properties. CAR forms a homodimer (40) that is structurally similar to the hJAM1 homodimer and also is formed by interactions between the GFCC′ β-sheets of the N-terminal D1 domains (Fig. 3). Although the contacts between CAR monomers are somewhat more hydrophobic and do not directly involve salt bridges (40), several charged residues are present at the CAR–CAR interface (Glu-56, Asp-68, Lys-121). It is possible that these side chains interact via water molecules. Moreover, the relative arrangement of the two CAR monomers is highly similar to that observed for the two hJAM1 monomers (Fig. 3). Both contacts involve concave GFCC′ β-sheets that face each other at an angle of ≈90° and bury an almost identical amount of solvent [1,300 $Å^2$ for the CAR–CAR dimer (40) and 1,380 $Å^2$ for hJAM1–hJAM1].

Homodimeric structures have been observed in a number of other Ig superfamily proteins (41–45), but only one of these proteins, CD2, forms dimers via the GFCC′ β-sheet of D1 (45, 46). However, it is noteworthy that several Ig superfamily receptors engage viral ligands via the GFCC′ β-sheet. The HIV glycoprotein gp120 binds to residues on the GFCC′ face of its receptor CD4 (47), and the same region of CD4 also interacts with its natural ligand MHC class II (48). Complexes of rhinoviruses and coxsackievirus A21 with their receptor intercellular adhesion molecule-1 (ICAM-1) also show that the interactions involve residues at the top of ICAM-1 D1, a region that includes part of the GFCC′ face (49, 50). Moreover, the adenovirus fiber knob engages the same area of the GFCC′ face that mediates formation of the CAR–CAR dimer (25, 40). The structure of the complex between fiber knob and CAR shows a trimeric knob decorated with three copies of monomeric CAR (25, 40).

Interaction of hJAM1 with the Reovirus Attachment Protein σ1. The crystal structure of the reovirus attachment protein σ1 revealed a putative binding site for JAM1 at the lower edge of the σ1 head domain (17). To investigate whether other JAM family members serve as reovirus receptors, we transiently transfected CHO cells with hJAM1, hJAM2, or hJAM3 and assayed transfected cells for the capacity to support reovirus infection. Expression of JAM proteins at the cell surface was confirmed by flow cytometry (Fig. 4*A*). In contrast to cells transfected with hJAM1, cells transfected with hJAM2 or hJAM3 were not infected by reovirus (Fig. 4*B*). Our findings clearly demonstrate that reovirus recognizes structural features that are present in hJAM1 but not in hJAM2 or hJAM3.

To define structural features unique to JAM1 and potentially involved in contacting σ1, we identified conserved sequences in hJAM1 and mJAM1 that are not conserved in the other two JAM family members (Fig. 4*C*). Both hJAM1 and mJAM1 serve as reovirus receptors (1), whereas hJAM2 and hJAM3 do not. Because the D1 domain of hJAM1 is necessary and sufficient for interaction with σ1 (J.C.F. and T.S.D., unpublished observations), our analysis was restricted to that domain. Residues unique to hJAM1 D1 and mJAM1 D1, and therefore likely to participate in σ1 binding, cluster in three main areas (Fig. 4*D*): a region at the dimer interface (shown in orange) and two surface-exposed regions at the "back" of the molecule, opposite the dimer interface (shown in green and magenta, respectively). All three areas are candidates for interaction with σ1.

Interestingly, the "top" of the hJAM1 dimer does not contain conserved residues, and therefore we hypothesize that σ1 either engages the side of the hJAM1 dimer (via the magenta or green surfaces) or the JAM1 dimer interface (via the orange surface). The green surface near the top of D1 comprises the BC loop and the beginning of strand C. This surface is most complementary in shape and size to the proposed JAM1-binding region of σ1 (17) and, thus, it is a good candidate for σ1–JAM1 interactions. The equivalent regions in JAM2 and JAM3 likely have a different structure because of two-residue insertions (Fig. 4*C*), perhaps explaining the inability of these proteins to serve as reovirus receptors. The magenta-colored regions at the "back" of the protein contain three solvent-exposed side chains, Lys-47, Thr-88, and Thr-95, which also could participate in the interaction with σ1.

The interdimer interface of JAM1 (the orange surface in Fig. 4*D*) is not accessible to σ1 in the context of a JAM1–JAM1 dimer. However, σ1 might engage this surface in monomeric forms of JAM1. Such a mechanism of binding is identical to the strategy used by the adenovirus fiber knob to bind the monomeric form of CAR (25). Indeed, comparison of the sequences of JAM1 and CAR shows that JAM1 residues highlighted in orange cluster in the same region as the CAR residues known to bind fiber (Fig. 4*C*). Although we have no evidence to suggest that σ1 binds to JAM1 in a similar manner, the similarities exhibited by σ1 and fiber, and between JAM1 and CAR, indicate that such an interaction might occur. The affinity of the σ1 head domain for hJAM1 is in the nanomolar range (6×10^{-8} M) (1). Although the affinity of JAM1 for itself is not known, studies using recombinant mJAM1 demonstrated that a significant portion of this protein is monomeric under physiologic conditions (35). This finding suggests that JAM1–JAM1 interactions

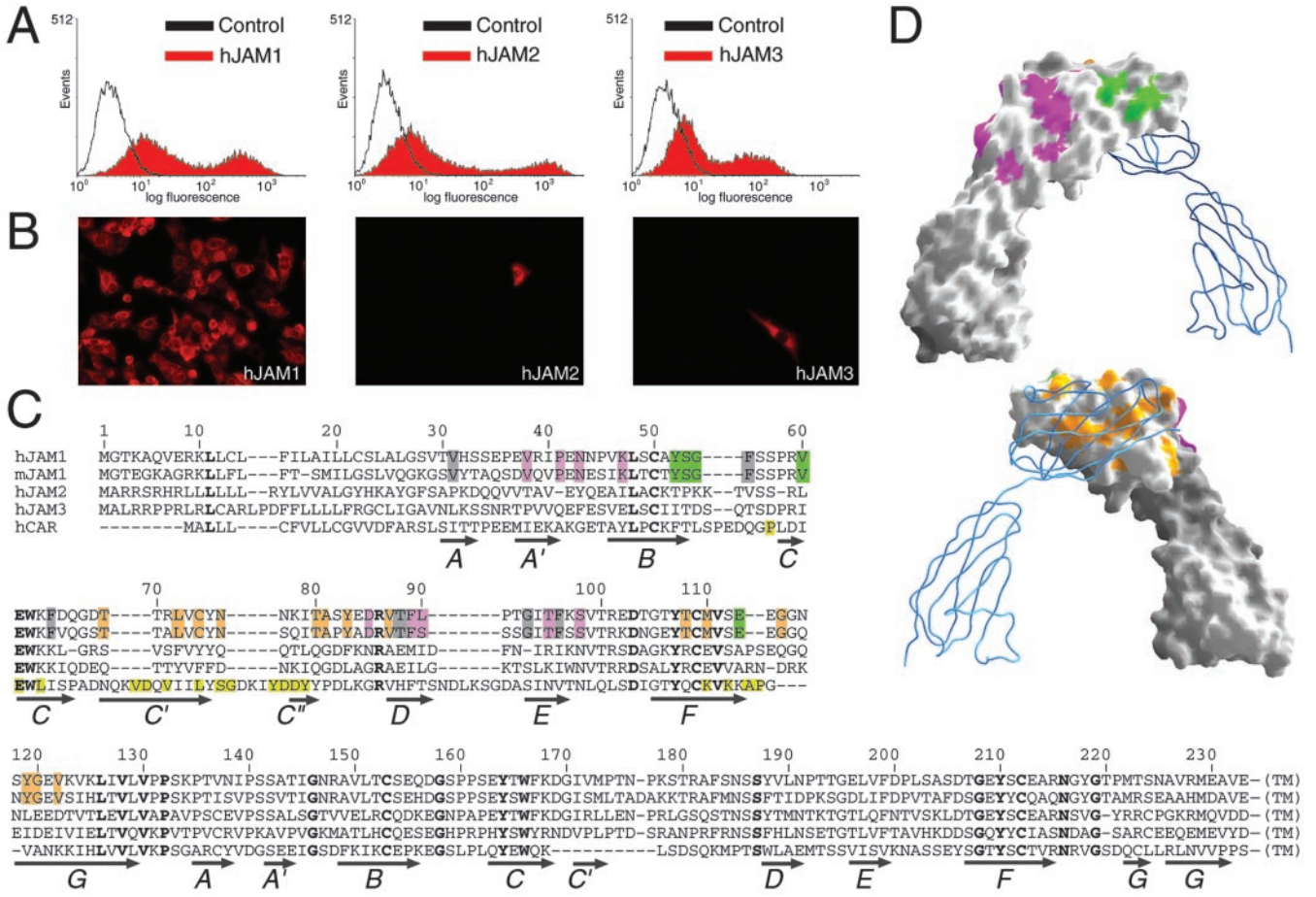

Fig. 4. Interaction of reovirus with hJAM1. (*A*) Transiently transfected CHO cells display surface expression of JAM family members. CHO cells were transiently transfected with hJAM1, hJAM2, or hJAM3 and screened for surface expression of JAM proteins by flow cytometry. (*B*) Transfection of CHO cells with hJAM1, but not hJAM2 or hJAM3, rescues infection by reovirus strain T1L. Shown are infected cells as detected by indirect immunofluorescence using rabbit antireovirus sera. (*C*) Sequence alignment, with residues conserved in hJAM1 and mJAM1, but not in hJAM2 or hJAM3, highlighted in orange, magenta, and green. Arrows indicate β-strands. The sequence of CAR was aligned with the JAM sequences using CLUSTALW (www.ebi.ac.uk/clustalw). CAR residues contacting the adenovirus fiber knob (distance <4 Å) in the complex (25) are highlighted in yellow. Residues conserved in all sequences are shown in bold. (*D*) The hJAM1 D1D2 dimer viewed from opposite angles, with one monomer shown in surface representation and the other shown as a blue ribbon. The side chains of conserved residues from *C* were mapped onto the hJAM1 D1D2 surface by using the same color code. Residues colored in orange, green, or magenta cluster in three different surface areas. Residues shaded gray in *C* are buried and not visible in this representation.

are weak. Therefore, it seems plausible that σ1 binds to monomeric JAM1, perhaps by engaging residues that form the JAM1–JAM1 interface.

Conclusions

The crystal structure of the hJAM1 ectodomain provides insights into how JAM1 functions in tight junction formation and viral attachment. A key feature of JAM1 is its capacity to form dimers via an extensive interface in its N-terminal domain. This interface is distinguished from traditional protein–protein interfaces by its highly polar character and its capacity to accommodate substantial rearrangements. The latter is evidenced by the different dimeric structures of hJAM1 and mJAM1 despite absolute conservation of residues at the interface. We think it possible that the dynamic nature of the interface plays a role in mediating and perhaps facilitating transitions between monomeric and dimeric forms of JAM1. Moreover, the dynamic nature of the interface likely distinguishes JAM1 from the other JAM family members, JAM2 and JAM3, both of which contain substitutions that are predicted to alter the stability of the interface.

Previous work from our laboratories has shown that the adenovirus and reovirus attachment proteins share many structural and functional features (17). Here we show that the similarities also extend to their receptors. The crystal structure of hJAM1 features a dimeric arrangement that closely resembles that seen in the adenovirus receptor, CAR. Parallels in the structures of these molecules are especially intriguing in light of the recent observation that CAR, like JAM1, is a component of cell–cell junctions (37–39). Thus, both viral and cellular determinants of adenovirus and reovirus binding exhibit striking structural similarities, which suggest conserved strategies of attachment among these viruses.

We thank members of our laboratories for review of the manuscript. This research was supported by Public Health Service Awards T32 CA09385 (to J.A.C. and J.C.F.), R01 AI38296 (to T.S.D.), R01 AI45716 (to T.S.), and R01 GM67853 (to T.S.D. and T.S.), the Vanderbilt University Research Council (to J.C.F.), the Swiss National Science Foundation (to P.S.), the Vanderbilt Medical Scholar's Program (to M.J.W.), the Howard Hughes Medical Institute (to T.R.P.), the Milton Foundation (to A.E.P.), and the Elizabeth B. Lamb Center for Pediatric Research. Additional support was provided by Public Health Service Awards CA68485 for the Vanderbilt Cancer Center and DK20593 for the Vanderbilt Diabetes Research and Training Center.

1. Barton, E. S., Forrest, J. C., Connolly, J. L., Chappell, J. D., Liu, Y., Schnell, F. J., Nusrat, A., Parkos, C. A. & Dermody, T. S. (2001) *Cell* **104,** 441–451.
2. Tyler, K. L. (2001) in *Fields Virology*, eds. Fields, B. N., Knipe, D. M. & Howley, P. M. (Lippincott–Raven, Philadelphia), 4th Ed., pp. 1729–1745.
3. Kostrewa, D., Brockhaus, M., D'Arcy, A., Dale, G. E., Nelboeck, P., Schmid, G., Mueller, F., Bazzoni, G., Dejana, E., Bartfai, T., *et al*. (2001) *EMBO J.* **20,** 4391–4398.
4. Martin-Padura, I., Lostaglio, S., Schneemann, M., Williams, L., Romano, M., Fruscella, P., Panzeri, Stoppacciaro, A., Ruco, L., Villa, A., *et al*. (1998) *J. Cell Biol.* **142,** 117–127.
5. Malergue, F., Galland, F., Martin, F., Mansuelle, P., Aurrand-Lions, M. & Naquet, P. (1998) *Mol. Immunol.* **35,** 1111–1119.
6. Williams, L. A., Martin-Padura, I., Dejana, E., Hogg, N. & Simmons, D. L. (1999) *Mol. Immunol.* **36,** 1175–1188.
7. Ostermann, G., Weber, K. S., Zernecke, A., Schroder, A. & Weber, C. (2002) *Nat. Immunol.* **3,** 151–158.
8. Cunningham, S. A., Arrate, M. P., Rodriguez, J. M., Bjercke, R. J., Vanderslice, P., Morris, A. P. & Brock, T. A. (2000) *J. Biol. Chem.* **275,** 34750–34756.
9. Naik, U. P., Naik, M. U., Eckfeld, K., Martin-DeLeon, P. & Spychala, J. (2001) *J. Cell Sci.* **114,** 539–547.
10. Aurrand-Lions, M., Duncan, L., Ballestrem, C. & Imhof, B. A. (2001) *J. Biol. Chem.* **276,** 2733–2741.
11. Aurrand-Lions, M., Johnson-Leger, C., Wong, C., Du Pasquier, L. & Imhof, B. A. (2001) *Blood* **98,** 3699–3707.
12. Arrate, M. P., Rodriguez, J. M., Tran, T. M., Brock, T. A. & Cunningham, S. A. (2001) *J. Biol. Chem.* **276,** 45826–45832.
13. Liang, T. W., Chiu, H. H., Gurney, A., Sidle, A., Tumas, D. B., Schow, P., Foster, J., Klassen, T., Dennis, K., DeMarco, R. A., *et al*. (2002) *J. Immunol.* **168,** 1618–1626.
14. Cunningham, S. A., Rodriguez, J. M., Arrate, M. P., Tran, T. M. & Brock, T. A. (2002) *J. Biol. Chem.* **277,** 27589–27592.
15. Santoso, S., Sachs, U. J., Kroll, H., Linder, M., Ruf, A., Preissner, K. T. & Chavakis, T. (2002) *J. Exp. Med.* **196,** 679–691.
16. Fraser, R. D., Furlong, D. B., Trus, B. L., Nibert, M. L., Fields, B. N. & Steven, A. C. (1990) *J. Virol.* **64,** 2990–3000.
17. Chappell, J. D., Prota, A. E., Dermody, T. S. & Stehle, T. (2002) *EMBO J.* **21,** 1–11.
18. Furlong, D. B., Nibert, M. L. & Fields, B. N. (1988) *J. Virol.* **62,** 246–256.
19. Dryden, K. A., Wang, G., Yeager, M., Nibert, M. L., Coombs, K. M., Furlong, D. B., Fields, B. N. & Baker, T. S. (1993) *J. Cell Biol.* **122,** 1023–1041.
20. Chappell, J. D., Duong, J. L., Wright, B. W. & Dermody, T. S. (2000) *J. Virol.* **74,** 8472–8479.
21. Barton, E. S., Connolly, J. L., Forrest, J. C., Chappell, J. D. & Dermody, T. S. (2001) *J. Biol. Chem.* **276,** 2200–2211.
22. Paul, R. W., Choi, A. H. & Lee, P. W. (1989) *Virology* **172,** 382–385.
23. Chappell, J. D., Gunn, V. L., Wetzel, J. D., Baer, G. S. & Dermody, T. S. (1997) *J. Virol.* **71,** 1834–1841.
24. Bergelson, J. M., Cunningham, J. A., Droguett, G., Kurt-Jones, E. A., Krithivas, A., Hong, J. S., Horwitz, M. S., Crowell, R. L. & Finberg, R. W. (1997) *Science* **275,** 1320–1323.
25. Bewley, M. C., Springer, K., Zhang, Y. B., Freimuth, P. & Flanagan, J. M. (1999) *Science* **286,** 1579–1583.
26. Otwinowski, Z. & Minor, W. (1997) *Methods Enzymol.* **276,** 307–326.
27. Collaborative Computing Project No. 4 (1994) *Acta Crystallogr. D* **50,** 760–763.
28. Brünger, A. T. (1992) *Nature* **355,** 472–475.
29. Jones, T. A., Zhou, J. Y., Cowan, S. W. & Kjeldgaard, M. (1991) *Acta Crystallogr. A* **47,** 110–119.
30. Brünger, A. T., Kuriyan, J. & Karplus, M. (1987) *Science* **235,** 458–460.
31. Liu, J. H., Nusrat, A., Schnell, F. J., Reaves, T. A., Walsh, S., Pochet, M. & Parkos, C. A. (2000) *J. Cell Sci.* **113,** 2363–2374.
32. Palmeri, D., van Zante, A., Huang, C. C., Hemmerich, S. & Rosen, S. D. (2000) *J. Biol. Chem.* **275,** 19139–19145.
33. Harpaz, Y. & Chothia, C. (1994) *J. Mol. Biol.* **238,** 528–539.
34. Holm, L. & Sander, C. (1993) *J. Mol. Biol.* **233,** 123–138.
35. Bazzoni, G., Martinez-Estrada, O. M., Mueller, F., Nelboeck, P., Schmid, G., Bartfai, T., Dejana, E. & Brockhaus, M. (2000) *J. Biol. Chem.* **275,** 30970–30976.
36. Schulz, G. E. & Schirmer, R. H. (1976) *Principles of Protein Structure* (Springer, New York).
37. Honda, T., Saitoh, H., Masuko, M., Katagiri-Abe, T., Tominaga, K., Kozakai, I., Kobayashi, K., Kumanishi, T., Watanabe, Y. G., Odani, S. & Kuwano, R. (2000) *Brain Res. Mol. Brain Res.* **77,** 19–28.
38. Cohen, C. J., Shieh, J. T., Pickles, R. J., Okegawa, T., Hsieh, J. T. & Bergelson, J. M. (2001) *Proc. Natl. Acad. Sci. USA* **98,** 15191–15196.
39. Walters, R., Freimuth, P., Moninger, T., Ganske, I., Zabner, J. & Welsh, M. (2002) *Cell* **110,** 789–799.
40. van Raaij, M. J., Chouin, E., van der Zandt, H., Bergelson, J. M. & Cusack, S. (2000) *Structure (London)* **8,** 1147–1155.
41. Ostrov, D. A., Shi, W., Schwartz, J. C., Almo, S. C. & Nathenson, S. G. (2000) *Science* **290,** 816–819.
42. Kasper, C., Rasmussen, H., Kastrup, J. S., Ikemizu, S., Jones, E. Y., Berezin, V., Bock, E. & Larsen, I. K. (2000) *Nat. Struct. Biol.* **7,** 389–393.
43. Casasnovas, J. M., Stehle, T., Liu, J., Wang, J. & Springer, T. (1998) *Proc. Natl. Acad. Sci. USA* **95,** 4134–4139.
44. Wu, H., Kwong, P. D. & Hendrickson, W. A. (1997) *Nature* **387,** 527–530.
45. Jones, E. Y., Davis, S. J., Williams, A. F., Harlos, K. & Stuart, D. I. (1992) *Nature* **360,** 232–239.
46. Bodian, D. L., Jones, E. Y., Harlos, K., Stuart, D. I. & Davis, J. P. (1994) *Structure (London)* **2,** 755–766.
47. Kwong, P. D., Wyatt, R., Robinson, J., Sweet, R. W., Sodroski, J. & Hendrickson, W. A. (1998) *Nature* **393,** 648–659.
48. Wang, J. H., Meijers, R., Xiong, Y., Liu, J. H., Sakihama, T., Zhang, R., Joachimiak, A. & Reinherz, E. L. (2001) *Proc. Natl. Acad. Sci. USA* **98,** 10799–10804.
49. Bella, J., Kolatkar, P. R., Marlor, C. W., Greve, J. M. & Rossmann, M. G. (1998) *Proc. Natl. Acad. Sci. USA* **95,** 4140–4145.
50. Xiao, C., Bator, C. M., Bowman, V. D., Rieder, E., He, Y., Hebert, B., Bella, J., Baker, T. S., Wimmer, E., Kuhn, R. J. & Rossmann, M. G. (2001) *J. Virol.* **75,** 2444–2451.

APPENDIX E

A CHIMERIC ADENOVIRUS ENCODING REOVIRUS ATTACHMENT PROTEIN σ1 TARGETS CELLS EXPRESSING JAM-A

Prota AE, Campbell JA, Schelling P, Forrest JC, Watson MJ, Peters TR, Aurrand-Lions M,

Imhof BA, Dermody TS, Stehle T.

Proceedings of the National Academy of Science. 101(16):6188-93;2004

A chimeric adenovirus vector encoding reovirus attachment protein σ1 targets cells expressing junctional adhesion molecule 1

George T. Mercier*, Jacquelyn A. Campbell[†‡], James D. Chappell[‡§], Thilo Stehle[¶], Terence S. Dermody[†‡‖]**, and Michael A. Barry*,**[††‡‡§§]

*Department of Bioengineering, Rice University, Houston, TX 77005; Departments of [†]Microbiology and Immunology, [§]Pathology, and [‖]Pediatrics and [‡]Elizabeth B. Lamb Center for Pediatric Research, Vanderbilt University School of Medicine, Nashville, TN 37232; [¶]Laboratory of Developmental Immunology, Massachusetts General Hospital and Harvard Medical School, Boston, MA 02114; and Departments of [††]Molecular and Human Genetics and [‡‡]Immunology and [§§]Center for Cell and Gene Therapy, Baylor College of Medicine, Houston, TX 77030

Edited by Peter Palese, Mount Sinai School of Medicine, New York, NY, and approved February 23, 2004 (received for review January 23, 2004)

The utility of adenovirus (Ad) vectors for gene transduction can be limited by receptor specificity. We developed a gene-delivery vehicle in which the potent Ad5 vector was genetically reengineered to display the mucosal-targeting σ1 protein of reovirus type 3 Dearing (T3D). A σ1 construct containing all but a small virion-anchoring domain was fused to the N-terminal 44 aa of Ad5 fiber. This chimeric attachment protein Fibtail-T3Dσ1 forms trimers and assembles onto Ad virions. Fibtail-T3Dσ1 was recombined into the Ad5 genome, replacing sequences encoding wild-type fiber. The resulting vector, Ad5-T3Dσ1, expresses Fibtail-T3Dσ1 and infects Chinese hamster ovary cells transfected with human or mouse homologs of the reovirus receptor, junctional adhesion molecule 1 (JAM1), but not the coxsackievirus and Ad receptor. Treatment of Caco-2 intestinal epithelial cells with either JAM1-specific antibody or neuraminidase reduced transduction by Ad5-T3Dσ1, and their combined effect decreased transduction by 95%. Ad5-T3Dσ1 transduces primary cultures of human dendritic cells substantially more efficiently than does Ad5, and this transduction depends on expression of JAM1. These data provide strong evidence that Ad5-T3Dσ1 can be redirected to cells expressing JAM1 and sialic acid for application as a vaccine vector.

Adenovirus (Ad) vectors are potent gene-delivery vehicles capable of eliciting both mucosal and systemic immune responses (1). Human Ad serotypes 2 and 5 (Ad2 and Ad5) bind and enter cells by using the combined interactions of the fiber and penton base proteins with cellular receptors. The fiber protein is an elongated trimer with an N-terminal fibrous tail domain (shaft) and a C-terminal globular head domain (knob). Ad2 and Ad5 engage the coxsackievirus and Ad receptor (CAR) (2, 3) via a binding site located in the knob (4). CAR is a member of the Ig superfamily (2, 3) expressed at regions of cell–cell contact (5). After fiber-mediated attachment, the penton base binds to cell surface α_v integrins, which mediate internalization (6).

Although Ad5 vectors transduce many types of cells, the efficiency of these vectors is limited if cells lack one or more of its receptors (7). For example, dendritic cells (DCs) do not express CAR and are poorly transduced by Ad5 (8). This relatively poor transduction of DCs can be enhanced by reengineering the vector to target alternative receptors (9, 10). Ad serotypes that bind to other receptors [e.g., CD46 (11)] mediate increased transduction of immunologically relevant cells (12), but these vectors are more promiscuous than Ad5 and deliver genes into cells that may not contribute to vaccination and thus may increase toxicity. Therefore, although potent, current Ad vectors lack sufficient specificity to function in some applications.

Mammalian reoviruses are nonenveloped, double-stranded RNA viruses with a broad host range (13). Reovirus infections are common, but most are asymptomatic. Reovirus enters the host by either the respiratory or enteric routes and infects epithelium and associated lymphoid tissue (14). The reovirus attachment protein, σ1, plays a key role in targeting the virus to distinct cell types, including those at mucosal surfaces (15–18). Similar to the Ad fiber, reovirus σ1 is an elongated trimer with head-and-tail morphology (19–21). A domain in the fibrous tail of serotype 3 Dearing (T3D) σ1 binds to α-linked sialic acid (22–25), whereas the head binds to junctional adhesion molecule 1 (JAM1) (26). JAM1 is an Ig-superfamily member expressed by a variety of cells including DCs (27) and epithelial and endothelial barriers (28–30).

The structures of the Ad fiber (31) and reovirus σ1 (32) proteins are strikingly similar (Fig. 1). The two proteins are the only structures known to date to form trimers by using triple β-spiral motifs. The fiber shaft most likely is composed entirely of β-spiral repeats (31), whereas the σ1 tail is predicted to also contain an α-helical coiled-coil N-terminal to the β-spiral region (32). The head domains of both proteins are formed by eight antiparallel β-strands with identical interstrand connectivity. Therefore, although Ad and reovirus belong to different virus families and have few overall properties in common, the observed similarities between the attachment proteins and receptors of these viruses suggest a conserved mechanism of binding.

Based on the structural similarities between Ad fiber and reovirus σ1, we engineered chimeric fiber-σ1 attachment proteins to exploit the JAM1- and sialic acid-binding properties of σ1. Of those tested, only a near-full-length version of σ1 grafted onto the virion-insertion domain of Ad fiber (Fibtail-T3Dσ1) formed trimers and assembled onto Ad particles. We show here that when the fiber gene in the Ad5 genome is replaced with Fibtail-T3Dσ1, the resulting virus, Ad5-T3Dσ1, is capable of infecting intestinal epithelial cells expressing JAM1 and sialic acid and primary human DCs expressing JAM1. These data provide proof of principle for the development of chimeric Ad vectors encoding reovirus σ1 for gene delivery to mucosal surfaces. This work also establishes a foundation for the use of Ad-σ1 chimeric viruses as a template to enable facile reverse genetic manipulation of the reovirus attachment protein for studies of virus–cell and virus–host interactions.

Methods

Cells, Antibodies, and Viruses. 293A (Q-BIOgene, Carlsbad, CA) and Chinese hamster ovary (CHO) cells (American Type Culture Collection) were maintained as described (10). 633 cells, a

This paper was submitted directly (Track II) to the PNAS office.

Abbreviations: Ad, adenovirus; CAR, coxsackievirus and Ad receptor; DC, dendritic cell; T3D, type 3 Dearing; JAM1, junctional adhesion molecule 1; CHO, Chinese hamster ovary; h, human; CMV, cytomegalovirus; m, murine.

**To whom correspondence may be addressed. E-mail: terry.dermody@vanderbilt.edu or mab@bcm.tmc.edu.

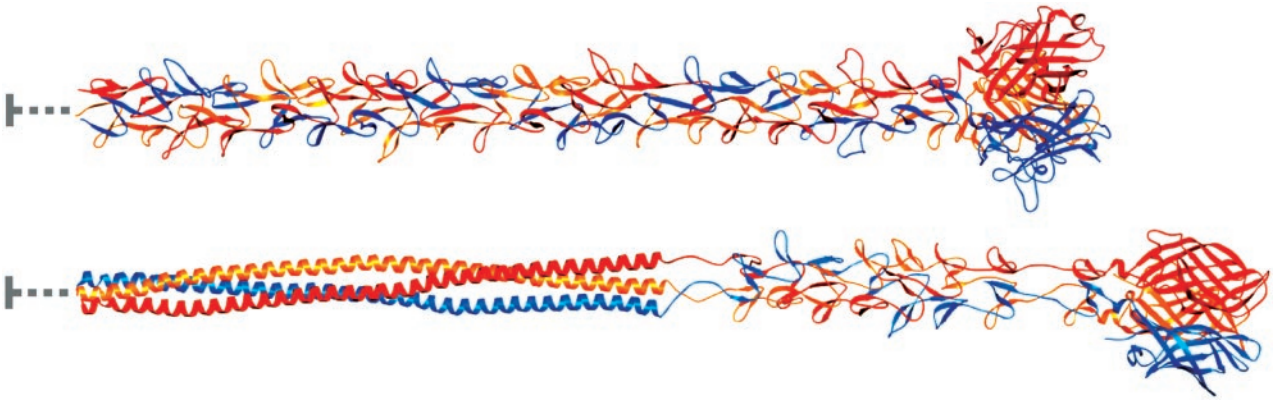

Fig. 1. Full-length models of Ad5 fiber (*Upper*) and reovirus σ1 (*Lower*). The three monomers within each trimer are shown in red, orange, and blue. Both proteins have head-and-tail morphology, with an eight-stranded β-barrel domain forming the head. The Ad5 fiber shaft is predicted to consist of 21 β-spiral repeats (31). The Ad5 fiber model was generated by adding 17 β-spiral repeats to the four present in the crystal structure of an Ad2 fragment, which also has 21 β-spiral repeats (31). Sequence predictions suggest that σ1 contains an N-terminal $\approx$135-residue α-helical coiled coil followed by eight β-spiral repeats and the globular head domain (32, 49). The σ1 model was generated by first adding five β-spiral repeats to the N terminus of the crystallized fragment (32). This model then was joined with a 135-residue trimeric coiled coil formed by elongating an existing coiled-coil structure (50). The N-terminal 45 and 39 residues of fiber and σ1, respectively, are not included in the model, because they form a virion-anchoring structure (indicated by gray lines). The overall lengths of the fiber and σ1 models are $\approx$325 and 385 Å, respectively, which is consistent with data from electron microscopy studies. This figure was prepared by using RIBBONS (51).

derivative of A549 cells expressing E1, E2A, and Ad5 fiber, were provided by D. Von Seggern (The Scripps Research Institute, La Jolla, CA) and maintained as described (33). Caco-2 cells (American Type Culture Collection) were maintained in Alpha minimum essential medium (GIBCO) with 20% FBS. Primary human DCs (NHDC, Cambrex, Baltimore) were maintained according to vendor protocol.

The human (h)CAR-specific mAb RmcB was purified from CRL-2379 hybridoma cells (American Type Culture Collection). The hJAM1-specific mAb J10.4 was provided by Chuck Parkos (Emory University School of Medicine, Atlanta). Rabbit polyclonal serum 1561 was raised against the N-terminal region of Ad5 fiber (peptide ARPSEDTFNPVY). The c-Myc-specific mAb was purchased from PharMingen.

Ad vectors used in this study are based on the AdEasy system (Q-BIOgene) and carry the full E1- and E3-deleted Ad5 genome with the firefly luciferase gene, an internal ribosome entry site, and the humanized *Renilla* GFP expressed from a cytomegalovirus (CMV) immediate-early promoter in the E1 region.

Generation of Chimeric Fiber-σ1 Attachment Proteins. Fiber-σ1 fusion constructs were generated by using λ phage red recombinase (34) expressed in *Escherichia coli* strain BW25113/pKD46 (35) obtained from the *E. coli* Genetic Stock Center (http://cgsc.biology.yale.edu) as follows: Fibshaft-T3Dσ1, consisting of the N-terminal 396 aa of Ad5 fiber fused to amino acid 292 of T3D σ1; Fib8-T3Dσ1, consisting of the N-terminal 170 aa of Ad5 fiber fused to amino acid 167 of T3D σ1; and Fibtail-T3Dσ1, consisting of the N-terminal 44 aa of Ad5 fiber fused to amino acid 18 of T3D σ1. Sequences encoding the reovirus T3D σ1 protein flanked by a bovine growth hormone polyadenylation signal and a zeocin-resistance gene were amplified by using *Pfu* polymerase (Stratagene) and primers containing 39-nt overhangs homologous to the pCMVfiber plasmid. The pCMVfiber plasmid, containing the Ad5 fiber gene expressed from a CMV immediate-early promoter, was cotransformed with the PCR product into the λ phage red strain BW25113/pKD46. Recombinants were selected by using zeocin-containing agar plates.

Fibtail-T3Dσ1 was subcloned into a plasmid containing sequences homologous to E4 and then recombined into the Ad5 genome to replace the fiber gene using red recombinase. To aid in detection of the chimeric protein, two c-Myc tags (C2), and one hexahistidine tag (H6) were added to the C terminus of the chimera (Fibtail-T3Dσ1C2H6) before recombination. The recombinants were screened for loss of the fiber gene by restriction endonuclease mapping and sequencing.

Protein Expression and Characterization. CHO cells were transfected with plasmids encoding fiber-σ1 chimeras by using Lipofectamine-PLUS (Invitrogen), and cell extracts were harvested for SDS/PAGE. Immunoblots were performed as described (10).

Generation of a Chimeric Ad Vector. Linearized Ad genome encoding the Fibtail-T3Dσ1C2H6 chimera was transfected into 633 cells and maintained in the presence of 0.3 μM dexamethasone and 4 μg/ml polybrene. Virus was propagated, purified by CsCl gradient centrifugation, and quantitated as described (36). The resultant recombinant virus, Ad5-T3Dσ1, was amplified for a final round by using 293A cells to remove any residual fiber from newly assembled virions.

CsCl-banded Ad5, CAR-ablated biotinylated Ad [Ad5-BAP-TR (10)], and Ad5-T3Dσ1 were precipitated with trichloroacetic acid. Pellets were resuspended in loading buffer, and 4×10^{10} particles per lane were resolved by SDS/PAGE and immunoblotting. For total protein analysis, precipitated virus (1.5×10^{11} particles per lane) was resolved by SDS/PAGE, and gels were stained with Coomassie blue.

Transduction of CHO Cells Transfected with Receptor Constructs. CHO cells were transfected with plasmids expressing hCAR, hJAM1, or murine (m)JAM1 (37, 38). After 48 h, the cells were washed once with Hanks' balanced salt solution (GIBCO) with 1% BSA (HBSS-BSA) and adsorbed with 5,000 particles per cell of Ad5-T3Dσ1 at 4°C for 30 min. Cells were washed twice with HBSS-BSA, and fresh medium was added. After incubation at 37°C for 24 h, cells were lysed, and luciferase activity (in lumens) was measured as described (10).

Transduction of Caco-2 Cells and Primary DCs After Receptor Blockade. Cells were harvested, washed with HBSS-BSA, and incubated in suspension with 10 μg/ml of either hCAR-specific mAb RmcB or hJAM1-specific mAb J10.4 at 4°C for 30 min. Alternatively, cells were treated with 333 milliunits/ml of *Clostridium perfringens* neuraminidase type X (Sigma) at 37°C for 30 min to remove cell-surface sialic acid, followed by two washes with HBSS-BSA. Cells then were adsorbed with 5,000 particles per cell of Ad5-

MICROBIOLOGY

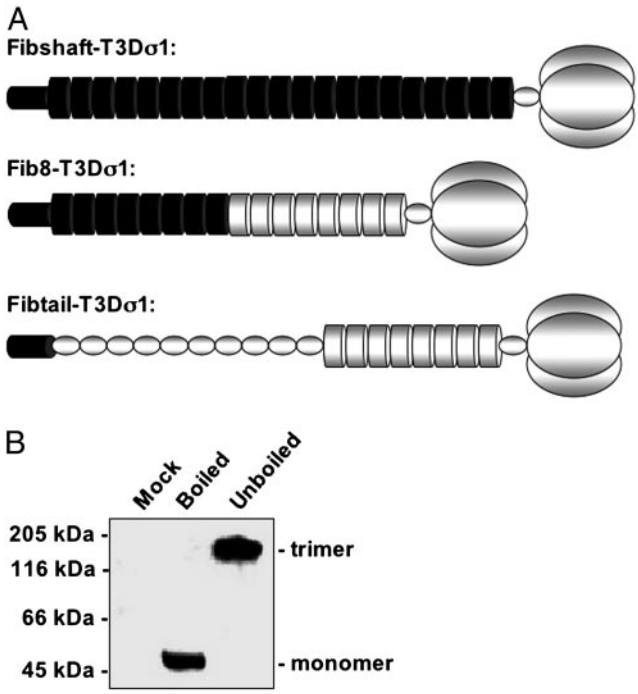

Fig. 2. Design and expression of chimeric fiber-σ1 attachment proteins. (*A*) Schematic diagram of the chimeric fiber-σ1 attachment proteins described in the text. Regions corresponding to fiber and σ1 in the diagrams are shaded black and gray, respectively (not drawn to scale). Fiber tail, which mediates virion anchoring, is represented as a small cylinder, the α-helical coiled coils as small ovals, the β-spiral repeats as large cylinders, and the head domain as three large ovals. (*B*) Immunoblots of denatured (boiled) and native (unboiled) lysates of CHO cells transfected with plasmid expressing Fibtail-T3Dσ1 probed with a serum (1561) that recognizes the N-terminal region of Ad5 fiber.

T3Dσ1 at 4°C for an additional 30 min, washed twice, and seeded onto 24-well plates in fresh medium. After incubation at 37°C for 24 h, cells were harvested for determination of luciferase activity.

Results

Design and Characterization of a Functional Fiber-σ1 Chimera. Based on the structural similarities between Ad5 fiber and reovirus σ1 (Fig. 1), we engineered three Ad fiber-reovirus σ1 chimeras with increasingly larger portions of σ1 protein replacing structurally homologous regions of fiber (Fig. 2*A*). Fibshaft-T3Dσ1 contains the N-terminal 21 β-spiral repeats of fiber fused to the head domain of T3D σ1. Fib8-T3Dσ1 contains the N-terminal eight β-spiral repeats of fiber fused to the T3D σ1 β-spiral and head domains. Fibtail-T3Dσ1 contains the N-terminal 44 aa virion-anchoring domain (39) fused to T3D σ1 lacking only the N-terminal 17 amino acids. After transfection of CHO cells, each of the chimeric attachment proteins was expressed, but only Fibtail-T3Dσ1 formed trimers (Fig. 2*B* and data not shown), suggesting that only this chimera maintains native folding.

Production and Characterization of an Ad Vector Expressing a Chimeric Fiber-σ1 Attachment Protein. The Fibtail-T3Dσ1 gene was recombined into an Ad5 genome lacking E1 and E3 to replace the fiber gene by using λ phage red recombinase (34). During the cloning process, two c-Myc tags (C2) and one hexahistidine tag (H6) were added to the C terminus of Fibtail-T3Dσ1 (Fibtail-T3Dσ1C2H6) to facilitate protein detection. The resulting virus, Ad5-T3Dσ1, was rescued by transfection and production in 633 fiber-expressing cells (33). After amplification in 633 cells, the virus was passaged in 293A cells to eliminate fiber from the virions and allow only Fibtail-T3Dσ1C2H6 to be encapsidated.

To determine whether Fibtail-T3Dσ1C2H6 was encapsidated onto Ad5 virions, CsCl-purified Ad5, Ad5-BAP-TR, which displays biotinylated fibers (10), and Ad5-T3Dσ1 were analyzed by immunoblotting with antibodies specific for either the fiber N terminus or the c-Myc epitope tag (Fig. 3*A*). Comparison of the immunoblots demonstrated that Fibtail-T3Dσ1C2H6 was encapsidated onto Ad5 virions at levels similar to those of fiber on Ad5 and Ad5-BAP-TR. As anticipated, the anti-c-Myc antibody recognized both Ad5-BAP-TR and Ad5-T3Dσ1, which contain c-Myc tags but not wild-type fiber. Coomassie blue staining demonstrated that relative amounts of the capsid proteins of wild-type Ad5 and Ad5-T3Dσ1 were indistinguishable (Fig. 3*B*). Thus, Fibtail-T3Dσ1C2H6 is encapsidated onto Ad virions and enables normal virion maturation.

Transient Transfection of CHO Cells with JAM1 Rescues Infection by Ad5-T3Dσ1. To determine whether the chimeric Fibtail-T3Dσ1 attachment protein could bind to JAM1, CHO cells were transfected with plasmids expressing hCAR, hJAM1, and mJAM1 and tested for infection by luciferase-expressing Ad5-T3Dσ1. CHO cells were chosen for these studies, because they lack both CAR and JAM1 and are poorly infected by both Ad and reovirus (38). Transduction of CHO cells by Ad5-T3Dσ1 was increased substantially by expression of either hJAM1 or mJAM1 but not by expression of hCAR (Fig. 4*A*), the receptor for Ad5 (2, 3). These data indicate that the JAM1-binding domain of Ad5-T3Dσ1 is functional and can target JAM1-expressing cells in a species-independent fashion.

Inhibition of Binding to JAM1 and Sialic Acid Blocks Ad5-T3Dσ1 Infection of Caco-2 Cells. We next tested the capacity of hJAM1-specific mAb J10.4 and *C. perfringens* neuraminidase to inhibit transduction by Ad5-T3Dσ1. Caco-2 intestinal epithelial cells, a model for enteric mucosal surfaces (40, 41), were used for these experiments, because these cells express CAR, JAM1, and sialic acid (26, 42). Transduction by Ad5-T3Dσ1 was inhibited 50% by JAM1-specific mAb J10.4 and 80% by neuraminidase (Fig. 4*B*). Combined treatment with both mAb J10.4 and neuraminidase reduced transduction nearly 95%. In contrast, isotype-matched hCAR-specific mAb RmcB, used as a negative control, did not diminish luciferase transduction (Fig. 4*B*).

To ensure that JAM1-dependent transduction by Ad5-T3Dσ1 depends on σ1 and not another Ad protein, we tested the capacity of the T3D σ1-specific mAb 9BG5 (24) to block infection of Caco-2 cells. In contrast to T1L σ1-specific mAb 5C6 (24), mAb 9BG5 inhibited transduction in a dose-dependent fashion (data not shown). We noted a similar decrease in transduction efficiency after incubation of Ad5-T3Dσ1 with sialoglycophorin, which is known to interact with reovirus T3D σ1 (22), before infection (data not shown). These results demonstrate that transduction by Ad5-T3Dσ1 requires σ1 and its receptors, JAM1 and sialic acid.

Ad5-T3Dσ1 Transduces Primary Human DCs. DCs play important roles in induction of adaptive immune responses (43). To determine whether Ad5-T3Dσ1 is capable of transducing DCs, we infected primary cultures of human DCs with Ad5 and Ad5-T3Dσ1. DCs express JAM1 but not CAR (Fig. 5*A*), which is consistent with previous observations (27). Transduction of DCs by Ad5-T3Dσ1 was substantially more efficient than by Ad5 (Fig. 5*B*). Moreover, transduction was eliminated almost completely by treatment with hJAM1-specific mAb J10.4 (Fig. 5*B*). These findings suggest that Ad5-T3Dσ1 may have utility for transducing CAR-negative DCs at mucosal and other sites.

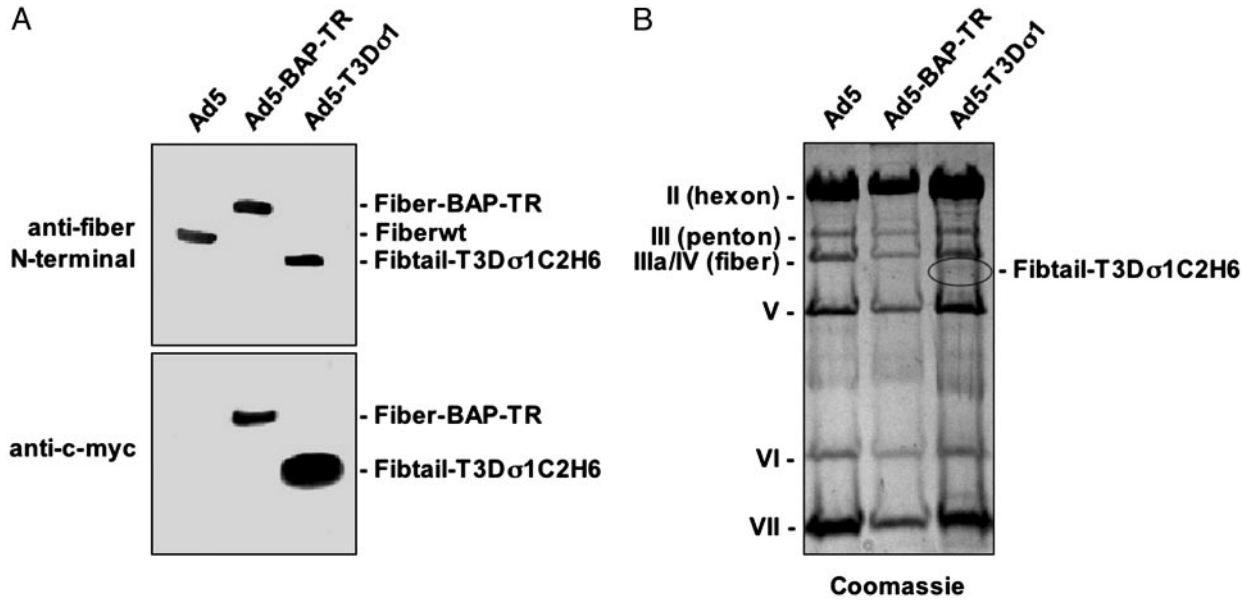

Fig. 3. Characterization of Ad5-T3Dσ1. Ad5 virions expressing wild-type fiber (Fiberwt), CAR-ablated biotinylated fiber (Fiber-BAP-TR) (10), and Fibtail-T3Dσ1C2H6 were precipitated with trichloroacetic acid. (*A*) Precipitated particles (4×10^{10} per lane) were resolved by SDS/PAGE and immunoblotted with anti-c-Myc mAb 9E10 or antiserum 1561, which recognizes the N-terminal region of Ad5 fiber. (*B*) Precipitated particles (1.5×10^{11} per lane) were resolved by SDS/PAGE and stained with Coomassie blue.

Discussion

In this study, we fused two structurally homologous viral attachment proteins, Ad fiber and reovirus σ1, to produce a functional chimeric virus, Ad5-T3Dσ1. Of the three fiber-σ1 chimeras tested, only Fibtail-T3Dσ1 bearing the Ad5 fiber virion-insertion domain fused to an almost-full-length version of T3D σ1 protein formed trimers and assembled onto Ad virions. The lack of trimerization of Fib8-T3Dσ1 and Fibshaft-T3Dσ1 was surprising, because both the head and tail regions of σ1 contain trimerization domains (44), whereas the fiber knob domain initiates and maintains trimerization (45). Because only Fibtail-T3Dσ1 formed trimers, it is likely that the C-terminal trimerization domain of σ1 is insufficient for trimerization of the fiber shaft. Alternatively, it is possible that the chimeric Fib8-T3Dσ1 and Fibshaft-T3Dσ1 proteins do not form trimers, because the fused β-spiral junctions are imperfectly matched.

In Ad5-T3Dσ1 virions, Fibtail-T3Dσ1 was encapsidated at levels comparable with wild-type fiber. Furthermore, the capsid protein profile of Ad5-T3Dσ1 is identical to that of wild-type Ad5. Most importantly, experiments using receptor-transfected cells, antibodies, and reagents that block σ1–sialic acid interactions provide

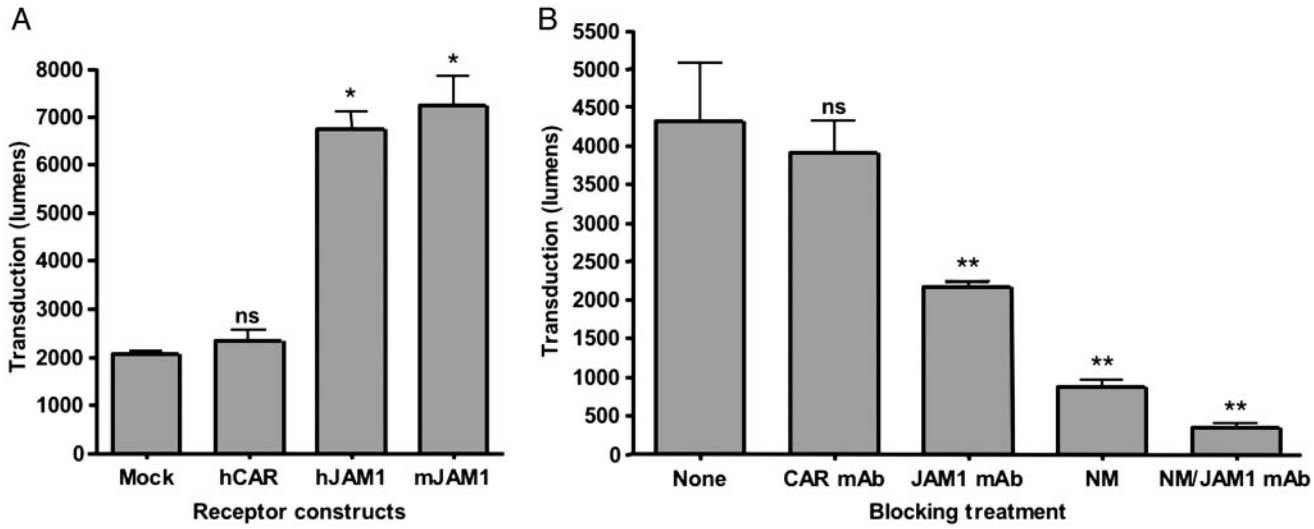

Fig. 4. Ad5-T3Dσ1 transduction is mediated by JAM1 and sialic acid. (*A*) CHO cells were transiently transfected with plasmids encoding hCAR, hJAM1, or mJAM1. After 48 h of incubation to permit receptor expression, cells were adsorbed with 5,000 particles per cell of Ad5-T3Dσ1 and harvested 24 h later for luciferase assay. Transduction was measured in lumens. (*B*) Caco-2 cells were either untreated or treated with 10 μg/ml hCAR-specific mAb RmcB (CAR mAb), 10 μg/ml hJAM1-specific mAb J10.4 (JAM1 mAb), 333 milliunits/ml *C. perfringens* neuraminidase (NM), or both JAM1 mAb and neuraminidase. Cells were adsorbed with 5,000 particles per cell of Ad5-T3Dσ1 and harvested 24 h later for luciferase assay. Transduction was measured in lumens. The results are presented as the means for three independent experiments. Error bars indicate SD. A paired Student's *t* test was performed to compare transduction of transfected or treated cells versus mock or untreated cells (*, $P < 0.01$; **, $P < 0.05$; ns, not significant).

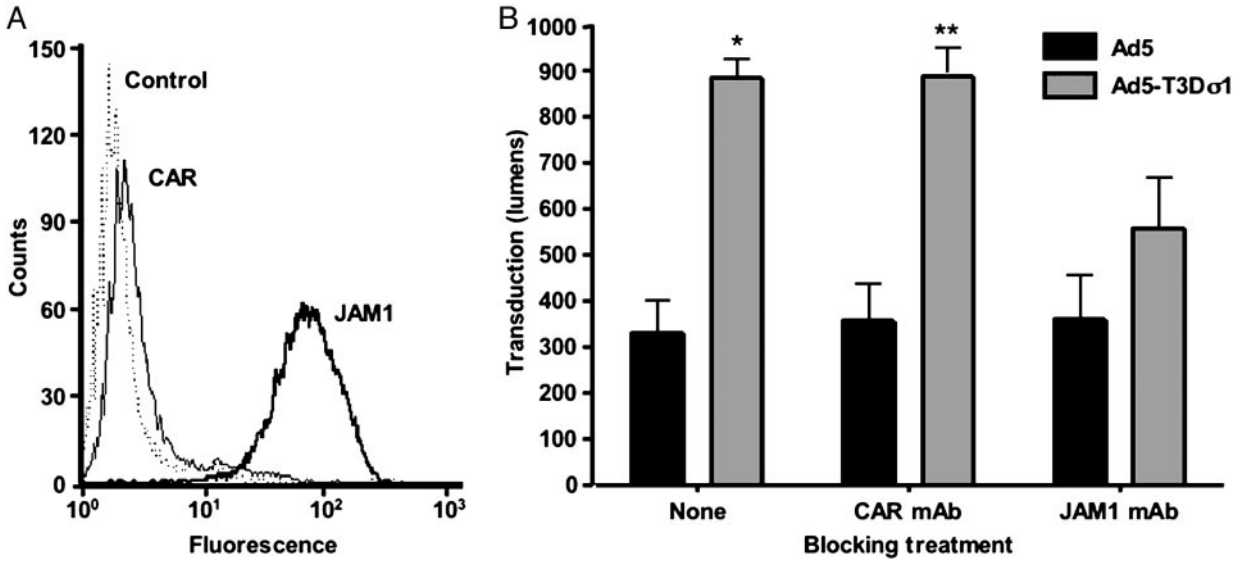

Fig. 5. Ad5 and Ad5-T3Dσ1 transduction of primary human DCs. (*A*) DCs were assessed for surface expression of CAR and JAM1 by flow cytometry by using hCAR-specific mAb RmcB and hJAM1-specific mAb J10.4, respectively (38). (*B*) DCs were either untreated or treated with 10 μg/ml hCAR-specific mAb RmcB (CAR mAb) or hJAM1-specific mAb J10.4 (JAM1 mAb) before adsorption with 5,000 particles per cell of either Ad5 or Ad5-T3Dσ1. Cells were harvested 24 h later for luciferase assay. Transduction was measured in lumens. The results are presented as the means for three independent experiments. Error bars indicate SD. A paired Student's *t* test was performed to compare transduction by Ad5 versus Ad5-T3Dσ1 (*, $P < 0.01$; **, $P < 0.05$).

compelling evidence that Ad5-T3Dσ1 displaying Fibtail-T3Dσ1 retains both the JAM1- and sialic acid-binding functions of the T3D σ1 protein.

We envision at least four applications for chimeric Ad vectors in which the CAR-binding functions of fiber have been replaced with the JAM1- and sialic acid-binding functions of σ1. First, Ad vectors based on fiber-σ1 chimeras may serve to efficiently target mucosal sites for enhanced induction of immune responses at mucosal surfaces. Second, because JAM1 and sialic acid are expressed on a variety of cells, Ad5-T3Dσ1 and its derivatives may have utility for transducing cells deficient in CAR (e.g., DCs and certain types of cancer cells). Third, because σ1 incorporates its own trimerization motifs, fiber-σ1 fusions may provide a trimeric scaffold for the display of other cell-targeting ligands in a manner analogous to fiber-fibritin chimeras (46). In support of this approach, we recently appended single-chain antibodies onto truncated forms of Fibtail-T3Dσ1 (unpublished data). Fourth, Ad vectors based on Ad5-T3Dσ1 can be used as a simple genetic platform for directed mutagenesis of σ1 for studies of reovirus tropism and receptor-linked signaling.

The opportunity to use Ad vectors encoding fiber-σ1 chimeras for mucosal targeting is especially appealing. Increased delivery of antigens to intestinal epithelial cells and Peyer's patch lymphocytes by such vectors might result in more potent and less toxic gene-based vaccines. Reovirus binds to murine microfold cells (15, 16, 18), and the σ1 protein plays an important role in conferring this tropism (18, 47). Interactions of Ad5-σ1 vectors with microfold cells may facilitate efficient delivery to underlying Peyer's patches for induction of immune responses in the gut. Alternatively, σ1-bearing Ad vectors may directly infect DCs at the luminal surface, which are known to shuttle bacteria across epithelial monolayers by opening tight junctions and sampling the intestinal lumen (48). DCs express tight junction proteins, including JAM1 (27), which are hypothesized to facilitate epithelial barrier penetration. Our finding that Ad5-T3Dσ1 transduces primary DCs more efficiently than wild-type Ad5 suggests that Ad5-σ1 vectors may be useful for antigen gene delivery to DCs in the intestine and other sites.

Findings described in this report indicate that Ad vectors can be efficiently retargeted to cells expressing JAM1 and sialic acid by the reovirus attachment protein σ1. By virtue of the capacity to infect both intestinal epithelial cells and DCs, Ad5-σ1 vectors may have utility in the induction of immune responses at mucosal surfaces and thus prevention of infection at the site of pathogen entry. These vectors also will allow a precise determination of the contribution of the JAM1- and sialic acid-binding properties of σ1 to interactions of σ1 with cells *in vivo*. This approach should lead to improved Ad vectors for gene delivery and enhance an understanding of σ1 biology.

We thank Mary E. Barry and Jared Abramian for excellent technical assistance; members of the Barry and Dermody laboratories for many useful discussions; Chuck Parkos for providing hJAM1-specific mAb J10.4; and Dan Von Seggern for providing the 633 cells. This work was supported by National Science Foundation IGERT Award DGE-0114264 (to G.T.M.), Public Health Service Awards T32 CA09385 (to J.A.C.), T32 HL07751 (to J.D.C.), R01 GM67853 (to T.S. and T.S.D.), R01 AI38296 (to T.S.D.), and R01 AI42588 (to M.A.B.), and the Elizabeth B. Lamb Center for Pediatric Research. Additional support was provided by Public Health Service Awards AI36211 for the Center for AIDS Research at Baylor College of Medicine, DK056338 for the Texas Gulf Coast Digestive Diseases Center (Baylor College of Medicine), CA68485 for the Vanderbilt Cancer Center, and DK20593 for the Vanderbilt Diabetes Research and Training Center.

1. Shiver, J. W. & Emini, E. A. (2004) *Annu. Rev. Med.* **55,** 355–372.
2. Bergelson, J. M., Cunningham, J. A., Droguett, G., Kurt-Jones, E. A., Krithivas, A., Hong, J. S., Horwitz, M. S., Crowell, R. L. & Finberg, R. W. (1997) *Science* **275,** 1320–1323.
3. Tomko, R. P., Xu, R. & Philipson, L. (1997) *Proc. Natl. Acad. Sci. USA* **94,** 3352–3356.
4. Roelvink, P. W., Lizonova, A., Lee, J. G., Li, Y., Bergelson, J. M., Finberg, R. W., Brough, D. E., Kovesdi, I. & Wickham, T. J. (1998) *J. Virol.* **72,** 7909–7915.
5. Cohen, C. J., Shieh, J. T., Pickles, R. J., Okegawa, T., Hsieh, J. T. & Bergelson, J. M. (2001) *Proc. Natl. Acad. Sci. USA* **98,** 15191–15196.
6. Wickham, T. J., Mathias, P., Cheresh, D. A. & Nemerow, G. R. (1993) *Cell* **73,** 309–319.
7. Huang, S., Kamata, T., Takada, Y., Ruggeri, Z. M. & Nemerow, G. R. (1996) *J. Virol.* **70,** 4502–4508.
8. Tillman, B. W., de Gruijl, T. D., Luykx-de Bakker, S. A., Scheper, R. J., Pinedo, H. M., Curiel, T. J., Gerritsen, W. R. & Curiel, D. T. (1999) *J. Immunol.* **162,** 6378–6383.

9. Belousova, N., Korokhov, N., Krendelshchikova, V., Simonenko, V., Mikheeva, G., Triozzi, P. L., Aldrich, W. A., Banerjee, P. T., Gillies, S. D., Curiel, D. T. & Krasnykh, V. (2003) *J. Virol.* **77,** 11367–11377.
10. Parrott, M. B., Adams, K. E., Mercier, G. T., Mok, H., Campos, S. K. & Barry, M. A. (2003) *Mol. Ther.* **8,** 689–702.
11. Gaggar, A., Shayakhmetov, D. M. & Lieber, A. (2003) *Nat. Med.* **9,** 1408–1412.
12. Vogels, R., Zuijdgeest, D., van Rijnsoever, R., Hartkoorn, E., Damen, I., de Bethune, M. P., Kostense, S., Penders, G., Helmus, N., Koudstaal, W., *et al.* (2003) *J. Virol.* **77,** 8263–8271.
13. Nibert, M. L. & Schiff, L. A. (2001) in *Fields Virology*, eds. Knipe, D. M. & Howley, P. M. (Lippincott-Raven, Philadelphia), pp. 1679–1728.
14. Tyler, K. L. (2001) in *Fields Virology*, eds. Knipe, D. M. & Howley, P. M. (Lippincott-Raven, Philadelphia), pp. 1729–1945.
15. Wolf, J. L., Rubin, D. H., Finberg, R., Kauffman, R. S., Sharpe, A. H., Trier, J. S. & Fields, B. N. (1981) *Science* **212,** 471–472.
16. Wolf, J. L., Kauffman, R. S., Finberg, R., Dambrauskas, R., Fields, B. N. & Trier, J. S. (1983) *Gastroenterology* **85,** 291–300.
17. Bodkin, D. K., Nibert, M. L. & Fields, B. N. (1989) *J. Virol.* **63,** 4676–4681.
18. Amerongen, H. M., Wilson, G. A., Fields, B. N. & Neutra, M. R. (1994) *J. Virol.* **68,** 8428–8432.
19. Furlong, D. B., Nibert, M. L. & Fields, B. N. (1988) *J. Virol.* **62,** 246–256.
20. Banerjea, A. C., Brechling, K. A., Ray, C. A., Erikson, H., Pickup, D. J. & Joklik, W. K. (1988) *Virology* **167,** 601–612.
21. Fraser, R. D., Furlong, D. B., Trus, B. L., Nibert, M. L., Fields, B. N. & Steven, A. C. (1990) *J. Virol.* **64,** 2990–3000.
22. Dermody, T. S., Nibert, M. L., Bassel-Duby, R. & Fields, B. N. (1990) *J. Virol.* **64,** 5173–5176.
23. Chappell, J. D., Gunn, V. L., Wetzel, J. D., Baer, G. S. & Dermody, T. S. (1997) *J. Virol.* **71,** 1834–1841.
24. Chappell, J. D., Duong, J. L., Wright, B. W. & Dermody, T. S. (2000) *J. Virol.* **74,** 8472–8479.
25. Barton, E. S., Connolly, J. L., Forrest, J. C., Chappell, J. D. & Dermody, T. S. (2001) *J. Biol. Chem.* **276,** 2200–2211.
26. Barton, E. S., Forrest, J. C., Connolly, J. L., Chappell, J. D., Liu, Y., Schnell, F. J., Nusrat, A., Parkos, C. A. & Dermody, T. S. (2001) *Cell* **104,** 441–451.
27. Rescigno, M., Rotta, G., Valzasina, B. & Ricciardi-Castagnoli, P. (2001) *Immunobiology* **204,** 572–581.
28. Martin-Padura, I., Lostaglio, S., Schneemann, M., Williams, L., Romano, M., Fruscella, P., Panzeri, C., Stoppacciaro, A., Ruco, L., Villa, A., *et al.* (1998) *J. Cell Biol.* **142,** 117–127.
29. Ozaki, H., Ishii, K., Horiuchi, H., Arai, H., Kawamoto, T., Okawa, K., Iwamatsu, A. & Kita, T. (1999) *J. Immunol.* **163,** 553–557.
30. Liu, Y., Nusrat, A., Schnell, F. J., Reaves, T. A., Walsh, S., Pochet, M. & Parkos, C. A. (2000) *J. Cell Sci.* **113,** 2363–2374.
31. van Raaij, M. J., Mitraki, A., Lavigne, G. & Cusack, S. (1999) *Nature* **401,** 935–938.
32. Chappell, J. D., Prota, A. E., Dermody, T. S. & Stehle, T. (2002) *EMBO J.* **21,** 1–11.
33. Von Seggern, D. J., Huang, S., Fleck, S. K., Stevenson, S. C. & Nemerow, G. R. (2000) *J. Virol.* **74,** 354–362.
34. Poteete, A. R. (2001) *FEMS Microbiol. Lett.* **201,** 9–14.
35. Datsenko, K. A. & Wanner, B. L. (2000) *Proc. Natl. Acad. Sci. USA* **97,** 6640–6645.
36. Davis, A. R., Wivel, N. A., Palladino, J. L., Tao, L. & Wilson, J. M. (2000) *Methods Mol. Biol.* **135,** 515–523.
37. Bewley, M. C., Springer, K., Zhang, Y. B., Freimuth, P. & Flanagan, J. M. (1999) *Science* **286,** 1579–1582.
38. Forrest, J. C., Campbell, J. A., Schelling, P., Stehle, T. & Dermody, T. S. (2003) *J. Biol. Chem.* **278,** 48434–48444.
39. Chroboczek, J., Ruigrok, R. W. & Cusack, S. (1995) *Curr. Top. Microbiol. Immunol.* **199,** 163–200.
40. Kerneis, S., Bogdanova, A., Kraehenbuhl, J. P. & Pringault, E. (1997) *Science* **277,** 949–952.
41. van der Lubben, I. M., van Opdorp, F. A., Hengeveld, M. R., Onderwater, J. J., Koerten, H. K., Verhoef, J. C., Borchard, G. & Junginger, H. E. (2002) *J. Drug Target.* **10,** 449–456.
42. Cheng, X., Ming, X. & Croyle, M. A. (2003) *Pharm. Res.* **20,** 1444–1451.
43. Banchereau, J., Briere, F., Caux, C., Davoust, J., Lebecque, S., Liu, Y. J., Pulendran, B. & Palucka, K. (2000) *Annu. Rev. Immunol.* **18,** 767–811.
44. Gilmore, R., Coffey, M. C., Leone, G., McLure, K. & Lee, P. W. (1996) *EMBO J.* **15,** 2651–2658.
45. Hong, J. S. & Engler, J. A. (1996) *J. Virol.* **70,** 7071–7078.
46. Krasnykh, V., Belousova, N., Korokhov, N., Mikheeva, G. & Curiel, D. T. (2001) *J. Virol.* **75,** 4176–4183.
47. Helander, A., Silvey, K. J., Mantis, N. J., Hutchings, A. B., Chandran, K., Lucas, W. T., Nibert, M. L. & Neutra, M. R. (2003) *J. Virol.* **77,** 7964–7977.
48. Rescigno, M., Urbano, M., Valzasina, B., Francolini, M., Rotta, G., Bonasio, R., Granucci, F., Kraehenbuhl, J. P. & Ricciardi-Castagnoli, P. (2001) *Nat. Immunol.* **2,** 361–367.
49. Bassel-Duby, R., Jayasuriya, A., Chatterjee, D., Sonenberg, N., Maizel, J. V., Jr., & Fields, B. N. (1985) *Nature* **315,** 421–423.
50. Weis, W., Brown, J. H., Cusack, S., Paulson, J. C., Skehel, J. J. & Wiley, D. C. (1988) *Nature* **333,** 426–431.
51. Carson, M. (1987) *J. Mol. Graphics* **5,** 103–106.

REFERENCES

1. **Amerongen, H. M., G. A. R. Wilson, B. N. Fields, and M. R. Neutra.** 1994. Proteolytic processing of reovirus is required for adherence to intestinal M cells. Journal of Virology **68:**8428-8432.

2. **Armstrong, G. D., R. W. Paul, and P. W. Lee.** 1984. Studies on reovirus receptors of L cells: virus binding characteristics and comparison with reovirus receptors of erythrocytes. Virology **138:**37-48.

3. **Arrate, M. P., J. M. Rodriguez, T. M. Tran, T. A. Brock, and S. A. Cunningham.** 2001. Cloning of human junctional adhesion molecule 3 (JAM3) and its identification as the JAM2 counter-receptor. Journal of Biological Chemistry **276:**45826-45832.

4. **Aurrand-Lions, M., C. Johnson-Leger, C. Wong, L. Du Pasquier, and B. A. Imhof.** 2001. Heterogeneity of endothelial junctions is reflected by differential expression and specific subcellular localization of the three JAM family members. Blood **98:**3699-707.

5. **Baer, G. S., and T. S. Dermody.** 1997. Mutations in reovirus outer-capsid protein σ3 selected during persistent infections of L cells confer resistance to protease inhibitor E64. Journal of Virology **71:**4921-4928.

6. **Balda, M. S., M. D. Garrett, and K. Matter.** 2003. The ZO-1-associated Y-box factor ZONAB regulates epithelial cell proliferation and cell density. J Cell Biol **160:**423-32.

7. **Balda, M. S., and K. Matter.** 2000. Transmembrane proteins of tight junctions. Seminars in Cell and Developmental Biology **11:**281-289.

8. **Banchereau, J., F. Briere, C. Caux, J. Davoust, S. Lebecque, Y. J. Liu, B. Pulendran, and K. Palucka.** 2000. Immunobiology of dendritic cells. Annu Rev Immunol **18:**767-811.

9. **Barton, E. S., J. L. Connolly, J. C. Forrest, J. D. Chappell, and T. S. Dermody.** 2001. Utilization of sialic acid as a coreceptor enhances reovirus attachment by multistep adhesion strengthening. Journal of Biological Chemistry **276:**2200-2211.

10. **Barton, E. S., J. C. Forrest, J. L. Connolly, J. D. Chappell, Y. Liu, F. Schnell, A. Nusrat, C. A. Parkos, and T. S. Dermody.** 2001. Junction adhesion molecule is a receptor for reovirus. Cell **104:**441-451.

11. **Barton, E. S., B. E. Youree, D. H. Ebert, J. C. Forrest, J. L. Connolly, T. Valyi-Nagy, K. Washington, J. D. Wetzel, and T. S. Dermody.** 2003. Utilization of sialic acid as a coreceptor is required for reovirus-induced biliary disease. Journal of Clinical Investigation **111:**1823-1833.
12. **Barton, G. J.** 1993. ALSCRIPT: a tool to format multiple sequence alignments. Protein Eng **6:**37-40.

13. **Bassel-Duby, R., A. Jayasuriya, D. Chatterjee, N. Sonenberg, J. V. Maizel, Jr, and B. N. Fields.** 1985. Sequence of reovirus haemagglutinin predicts a coiled-coil structure. Nature **315:**421-423.

14. **Bassel-Duby, R., M. Nibert, C. Homcy, B. Fields, and D. Sawutz.** 1987. Evidence that the sigma 1 protein of reovirus serotype 3 is a multimer. Journal of Virology **61:**1834-1841.

15. **Bassel-Duby, R., D. R. Spriggs, K. L. Tyler, and B. N. Fields.** 1986. Identification of attenuating mutations on the reovirus type 3 S1 double-stranded RNA segment with a rapid sequencing technique. Journal of Virology **60:**64-67.

16. **Bauer, P. H., R. T. Bronson, S. C. Fung, R. Freund, T. Stehle, S. C. Harrison, and T. L. Benjamin.** 1995. Genetic and structural analysis of a virulence determinant in polyomavirus VP1. Journal of Virology **69:**7925-31.

17. **Bazzoni, G., O. Martinez Estrada, and E. Dejana.** 1999. Molecular structure and functional role of vascular tight junctions. Trends in Cardiovascular Medicine **9:**147-52.

18. **Bazzoni, G., O. M. Martinez-Estrada, F. Mueller, P. Nelboeck, G. Schmid, T. Bartfai, E. Dejana, and M. Brockhaus.** 2000. Homophilic interaction of junctional adhesion molecule. Journal of Biological Chemistry **275:**30970-30976.

19. **Bazzoni, G., O. M. Martinez-Estrada, F. Orsenigo, M. Cordenonsi, S. Citi, and E. Dejana.** 2000. Interaction of junctional adhesion molecule with the tight junction components ZO-1, cingulin, and occludin. Journal of Biological Chemistry **275:**20520-20526.

20. **Bella, J., P. R. Kolatkar, C. W. Marlor, J. M. Greve, and M. G. Rossmann.** 1998. The structure of the two amino-terminal domains of human ICAM-1 suggests how it functions as a rhinovirus receptor and as an LFA-1 integrin ligand. Proceedings of the National Academy of Sciences **95:**4140-4145.

21. **Belnap, D. M., B. M. McDermott, Jr., D. J. Filman, N. Cheng, B. L. Trus, H. J. Zuccola, V. R. Racaniello, J. M. Hogle, and A. C. Steven.** 2000. Three-dimensional structure of poliovirus receptor bound to poliovirus. Proc Natl Acad Sci USA **97:**73-8.

22. **Belousova, N., N. Korokhov, V. Krendelshchikova, V. Simonenko, G. Mikheeva, P. L. Triozzi, W. A. Aldrich, P. T. Banerjee, S. D. Gillies, D. T. Curiel, and V. Krasnykh.** 2003. Genetically targeted adenovirus vector directed to CD40-expressing cells. J Virol **77:**11367-77.

23. **Bergelson, J. M., J. A. Cunningham, G. Droguett, E. A. Kurt-Jones, A. Krithivas, J. S. Hong, M. S. Horwitz, R. L. Crowell, and R. W. Finberg.** 1997. Isolation of a common receptor for Coxsackie B viruses and adenoviruses 2 and 5. Science **275:**1320-1323.

24. **Bewley, M. C., K. Springer, Y. B. Zhang, P. Freimuth, and J. M. Flanagan.** 1999. Structural analysis of the mechanism of adenovirus binding to its human cellular receptor, CAR. Science **286:**1579-1583.

25. **Bisaillon, M., S. Senechal, L. Bernier, and G. Lemay.** 1999. A glycosyl hydrolase activity of mammalian reovirus sigma1 protein can contribute to viral infection through a mucus layer. J Mol Biol **286:**759-73.

26. **Bodian, D. L., E. Y. Jones, K. Harlos, D. I. Stuart, and S. J. Davis.** 1994. Crystal structure of the extracellular region of the human cell adhesion molecule CD2 at 2.5 A resolution. Structure **2:**755-66.

27. **Bodkin, D. K., and B. N. Fields.** 1989. Growth and survival of reovirus in intestinal tissue: role of the L2 and S1 genes. Journal of Virology **63:**1188-1193.

28. **Brünger, A. T.** 1992. Free *R* value: a novel statistical quantity for assessing the accuracy of crystal structures. Nature **355:**472-475.

29. **Campbell, J. A., P. Schelling, J. D. Wetzel, E. M. Johnson, J. C. Forrest, G. A. Wilson, M. Aurrand-Lions, B. A. Imhof, T. Stehle, and T. S. Dermody.** 2005. Junctional adhesion molecule-A serves as a receptor for prototype and field-isolate strains of mammalian reovirus. J Virol **79:**7967-7978.

30. **Cao, W., M. D. Henry, P. Borrow, H. Yamada, J. H. Elder, E. V. Ravkov, S. T. Nichol, R. W. Compans, K. P. Campbell, and M. B. Oldstone.** 1998. Identification of alpha-dystroglycan as a receptor for lymphocytic choriomeningitis virus and Lassa fever virus. Science **282:**2079-81.

31. **Casasnovas, J. M., T. Stehle, J. H. Liu, J. H. Wang, and T. A. Springer.** 1998. A dimeric crystal structure for the N-terminal two domains of intercellular adhesion molecule-1. Proc Natl Acad Sci U S A **95:**4134-9.

32. **Cera, M. R., A. Del Prete, A. Vecchi, M. Corada, I. Martin-Padura, T. Motoike, P. Tonetti, G. Bazzoni, W. Vermi, F. Gentili, S. Bernasconi, T. N. Sato, A. Mantovani, and E. Dejana.** 2004. Increased DC trafficking to lymph

nodes and contact hypersensitivity in junctional adhesion molecule-A-deficient mice. Journal of Clinical Investigation **114:**729-738.

33. **Chandran, K., X. Zhang, N. H. Olson, S. B. Walker, J. D. Chappell, T. S. Dermody, T. S. Baker, and M. L. Nibert.** 2001. Complete in vitro assembly of the reovirus outer capsid produces highly infectious particles suitable for genetic studies of the receptor-binding protein. Journal of Virology **75:**5335-5342.

34. **Chappell, J. D., E. S. Barton, T. H. Smith, G. S. Baer, D. T. Duong, M. L. Nibert, and T. S. Dermody.** 1998. Cleavage susceptibility of reovirus attachment protein σ1 during proteolytic disassembly of virions is determined by a sequence polymorphism in the σ1 neck. Journal of Virology **72:**8205-8213.

35. **Chappell, J. D., J. L. Duong, B. W. Wright, and T. S. Dermody.** 2000. Identification of carbohydrate-binding domains in the attachment proteins of type 1 and type 3 reoviruses. Journal of Virology **74:**8472-8479.

36. **Chappell, J. D., V. L. Gunn, J. D. Wetzel, G. S. Baer, and T. S. Dermody.** 1997. Mutations in type 3 reovirus that determine binding to sialic acid are contained in the fibrous tail domain of viral attachment protein σ1. Journal of Virology **71:**1834-1841.

37. **Chappell, J. D., A. Prota, T. S. Dermody, and T. Stehle.** 2002. Crystal structure of reovirus attachment protein σ1 reveals evolutionary relationship to adenovirus fiber. EMBO Journal **21:**1-11.

38. **Chen, S. H., M. F. Stins, S. H. Huang, Y. H. Chen, K. J. Kwon-Chung, Y. Chang, K. S. Kim, K. Suzuki, and A. Y. Jong.** 2003. Cryptococcus neoformans induces alterations in the cytoskeleton of human brain microvascular endothelial cells. J Med Microbiol **52:**961-70.

39. **Cheng, X., X. Ming, and M. A. Croyle.** 2003. PEGylated adenoviruses for gene delivery to the intestinal epithelium by the oral route. Pharm Res **20:**1444-51.

40. **Chesebro, B., R. Buller, J. Portis, and K. Wehrly.** 1990. Failure of human immunodeficiency virus entry and infection in CD4-positive human brain and skin cells. J Virol **64:**215-21.

41. **Chroboczek, J., R. W. Ruigrok, and S. Cusack.** 1995. Adenovirus fiber. Curr Top Microbiol Immunol **199 (Pt 1):**163-200.

42. **Co, M. S., G. N. Gaulton, A. Tominaga, C. J. Homcy, B. N. Fields, and M. I. Greene.** 1985. Structural similarities between the mammalian beta-adrenergic and reovirus type 3 receptors. Proceedings of the National Academy of Sciences USA **82:**5315-5318.

43. **Cohen, C. J., J. T. Shieh, R. J. Pickles, T. Okegawa, J. T. Hsieh, and J. M. Bergelson.** 2001. The coxsackievirus and adenovirus receptor is a transmembrane component of the tight junction. Proceedings of the National Academy of Sciences of the United States of America **98:**15191-15196.

44. **Cunningham, S. A., M. P. Arrate, J. M. Rodriguez, R. J. Bjercke, P. Vanderslice, A. P. Morris, and T. A. Brock.** 2000. A novel protein with homology to the junctional adhesion molecule. Characterization of leukocyte interactions. Journal of Biological Chemistry **275:**34750-34756.

45. **Dalgleish, A. G., P. C. L. Beverley, P. R. Clapham, D. H. Crawford, M. F. Greaves, and R. A. Weiss.** 1984. The CD4 (T4) antigen is an essential component of the receptor for the AIDS retrovirus. Nature **312:**763-767.

46. **Datsenko, K. A., and B. L. Wanner.** 2000. One-step inactivation of chromosomal genes in Escherichia coli K-12 using PCR products. Proc Natl Acad Sci U S A **97:**6640-5.

47. **Davis, A. R., N. A. Wivel, J. L. Palladino, L. Tao, and J. M. Wilson.** 2000. Construction of adenoviral vectors. Methods Mol Biol **135:**515-23.

48. **Del Maschio, A., A. De Luigi, I. Martin-Padura, M. Brockhaus, T. Bartfai, P. Fruscella, L. Adorini, G. Martino, R. Furlan, M. G. De Simoni, and E. Dejana.** 1999. Leukocyte recruitment in the cerebrospinal fluid of mice with experimental meningitis is inhibited by an antibody to junctional adhesion molecule (JAM). Journal of Experimental Medicine **190:**1351-1356.

49. **Dermody, T. S., M. L. Nibert, R. Bassel-Duby, and B. N. Fields.** 1990. A σ1 region important for hemagglutination by serotype 3 reovirus strains. Journal of Virology **64:**5173-5176.

50. **Dermody, T. S., M. L. Nibert, R. Bassel-Duby, and B. N. Fields.** 1990. Sequence diversity in S1 genes and S1 translation products of 11 serotype 3 reovirus strains. Journal of Virology **64:**4842-4850.

51. **Dermody, T. S., M. L. Nibert, J. D. Wetzel, X. Tong, and B. N. Fields.** 1993. Cells and viruses with mutations affecting viral entry are selected during persistent infections of L cells with mammalian reoviruses. Journal of Virology **67:**2055-2063.

52. **Dermody, T. S., and K. L. Tyler.** 2005. Introduction to viruses and viral diseases., p. 1729-1742. *In* G. L. Mandell, J. E. Bennett, and R. Dolin (ed.), Mandell, Douglas, and Bennett's Principles and Practice of Infectious Diseases., Sixth Edition ed, vol. 2. Churchill Livingstone, New York.

53. **Dichter, M. A., and H. L. Weiner.** 1984. Infection of neuronal cell cultures with reovirus mimics in vitro patterns of neurotropism. Annals of Neurology **16:**603-610.

54. **Doranz, B. J., J. F. Berson, J. Rucker, and R. W. Doms.** 1997. Chemokine receptors as fusion cofactors for human immunodeficiency virus type 1 (HIV-1). Immunologic Research **16:**15-28.

55. **Dörig, R. E., A. Marcil, A. Chopra, and C. D. Richardson.** 1993. The human CD46 molecule is a receptor for measles virus (Edmonston strain). Cell **75:**295-305.

56. **Duncan, R., D. Horne, L. W. Cashdollar, W. K. Joklik, and P. W. K. Lee.** 1990. Identification of conserved domains in the cell attachment proteins of the three serotypes of reovirus. Virology **174:**399-409.

57. **Duncan, R., D. Horne, J. E. Strong, G. Leone, R. T. Pon, M. C. Yeung, and P. W. K. Lee.** 1991. Conformational and functional analysis of the C-terminal globular head of the reovirus cell attachment protein. Virology **182:**810-819.

58. **Duncan, R., and P. W. K. Lee.** 1994. Localization of two protease-sensitive regions separating distinct domains in the reovirus cell-attachment protein sigma 1. Virology **203:**149-152.

59. **Ebnet, K., C. U. Schulz, M. K. Meyer Zu Brickwedde, G. G. Pendl, and D. Vestweber.** 2000. Junctional adhesion molecule interacts with the PDZ domain-containing proteins AF-6 and ZO-1. Journal of Biological Chemistry **275:**27979-27988.

60. **Ebnet, K., A. Suzuki, Y. Horikoshi, T. Hirose, M. K. Meyer Zu Brickwedde, S. Ohno, and D. Vestweber.** 2001. The cell polarity protein ASIP/PAR-3 directly associates with junctional adhesion molecule (JAM). EMBO Journal **20:**3738-3748.

61. **Fanning, A. S., B. J. Jameson, L. A. Jesaitis, and J. M. Anderson.** 1998. The tight junction protein ZO-1 establishes a link between the transmembrane protein occludin and the actin cytoskeleton. J Biol Chem **273:**29745-53.

62. **Fanning, A. S., T. Y. Ma, and J. M. Anderson.** 2002. Isolation and functional characterization of the actin binding region in the tight junction protein ZO-1. Faseb J **16:**1835-7.

63. **Forrest, J. C., J. A. Campbell, P. Schelling, T. Stehle, and T. S. Dermody.** 2003. Structure-function analysis of reovirus binding to junctional adhesion molecule 1. Implications for the mechanism of reovirus attachment. The Journal of Biological Chemistry **278:**48434-48444.

64. **Fraser, R. D. B., D. B. Furlong, B. L. Trus, M. L. Nibert, B. N. Fields, and A. C. Steven.** 1990. Molecular structure of the cell-attachment protein of reovirus: correlation of computer-processed electron micrographs with sequence-based predictions. Journal of Virology **64:**2990-3000.

65. **Freimuth, P., K. Springer, C. Berard, J. Hainfeld, M. Bewley, and J. Flanagan.** 1999. Coxsackievirus and adenovirus receptor amino-terminal immunoglobulin V-related domain binds adenovirus type 2 and fiber knob from adenovirus type 12. J Virol **73:**1392-8.

66. **Furlong, D. B., M. L. Nibert, and B. N. Fields.** 1988. Sigma 1 protein of mammalian reoviruses extends from the surfaces of viral particles. Journal of Virology **62:**246-256.

67. **Gaggar, A., D. M. Shayakhmetov, and A. Lieber.** 2003. CD46 is a cellular receptor for group B adenoviruses. Nature Medicine **9:**1408-1412.

68. **Gentsch, J. R., and A. F. Pacitti.** 1985. Effect of neuraminidase treatment of cells and effect of soluble glycoproteins on type 3 reovirus attachment to murine L cells. Journal of Virology **56:**356-364.

69. **Gilmore, R., M. C. Coffey, G. Leone, K. McLure, and P. W. Lee.** 1996. Co-translational trimerization of the reovirus cell attachment protein. Embo J **15:**2651-8.

70. **Gliki, G., K. Ebnet, M. Aurrand-Lions, B. A. Imhof, and R. H. Adams.** 2004. Spermatid differentiation requires the assembly of a cell polarity complex downstream of junctional adhesion molecule-C. Nature **431:**320-324.

71. **Gomatos, P. J., and W. Stoeckenius.** 1964. Electron microscope studies on reovirus RNA. Proceedings of the National Academy of Sciences USA **52:**1449-1455.

72. **Gonzalez-Mariscal, L., A. Betanzos, and A. Avila-Flores.** 2000. MAGUK proteins: structure and role in the tight junction. Semin Cell Dev Biol **11:**315-24.

73. **Goral, M. I., M. Mochow-Grundy, and T. S. Dermody.** 1996. Sequence diversity within the reovirus S3 gene: reoviruses evolve independently of host species, geographic locale, and date of isolation. Virology **216:**265-271.

74. **Gottardi, C. J., M. Arpin, A. S. Fanning, and D. Louvard.** 1996. The junction-associated protein, zonula occludens-1, localizes to the nucleus before the maturation and during the remodeling of cell-cell contacts. Proc Natl Acad Sci U S A **93:**10779-84.

75. **Gottschalk, A.** 1958. The influenza virus neuraminidase. Nature **181:**377-8.

76. **Greve, J. M., G. Davis, A. M. Meyer, C. P. Forte, S. C. Yost, C. W. Marlor, M. E. Kamarck, and A. McClelland.** 1989. The major human rhinovirus receptor is ICAM-1. Cell **56:**839-847.

77. **Hamazaki, Y., M. Itoh, H. Sasaki, M. Furuse, and S. Tsukita.** 2002. Multi-PDZ domain protein 1 (MUPP1) is concentrated at tight junctions through its possible interaction with claudin-1 and junctional adhesion molecule. Journal of Biological Chemistry **277:**455-461.

78. **Harpaz, Y., and C. Chothia.** 1994. Many of the immunoglobulin superfamily domains in cell adhesion molecules and surface receptors belong to a new structural set which is close to that containing variable domains. J Mol Biol **238:**528-39.

79. **He, Y., P. R. Chipman, J. Howitt, C. M. Bator, M. A. Whitt, T. S. Baker, R. J. Kuhn, C. W. Anderson, P. Freimuth, and M. G. Rossmann.** 2001. Interaction of coxsackievirus B3 with the full length coxsackievirus-adenovirus receptor. Nat Struct Biol **8:**874-8.

80. **Helander, A., K. J. Silvey, N. J. Mantis, A. B. Hutchings, K. Chandran, W. T. Lucas, M. L. Nibert, and M. R. Neutra.** 2003. The viral sigma1 protein and glycoconjugates containing alpha2-3-linked sialic acid are involved in type 1 reovirus adherence to M cell apical surfaces. Journal of Virology **77:**7964-7977.

81. **Hendrie, P. C., and D. W. Russell.** 2005. Gene targeting with viral vectors. Mol Ther **12:**9-17.

82. **Holm, L., and C. Sander.** 1993. Protein structure comparison by alignment of distance matrices. Journal of Molecular Biology **233:**123-138.

83. **Honda, T., H. Saitoh, M. Masuko, T. Katagiri-Abe, K. Tominaga, I. Kozakai, K. Kobayashi, T. Kumanishi, Y. G. Watanabe, S. Odani, and R. Kuwano.** 2000. The coxsackievirus-adenovirus receptor protein as a cell adhesion molecule in the developing mouse brain. Brain Res Mol Brain Res **77:**19-28.

84. **Hong, J. S., and J. A. Engler.** 1996. Domains required for assembly of adenovirus type 2 fiber trimers. J Virol **70:**7071-8.

85. **Hrdy, D. B., L. Rosen, and B. N. Fields.** 1979. Polymorphism of the migration of double-stranded RNA segments of reovirus isolates from humans, cattle, and mice. Journal of Virology **31:**104-111.

86. **Huang, S., T. Kamata, Y. Takada, Z. M. Ruggeri, and G. R. Nemerow.** 1996. Adenovirus interaction with distinct integrins mediates separate events in cell entry and gene delivery to hematopoietic cells. J Virol **70:**4502-8.

87. **Itoh, M., A. Nagafuchi, S. Yonemura, T. Kitani-Yasuda, and S. Tsukita.** 1993. The 220-kD protein colocalizing with cadherins in non-epithelial cells is identical to ZO-1, a tight junction-associated protein in epithelial cells: cDNA cloning and immunoelectron microscopy. J Cell Biol **121:**491-502.

88. **Itoh, M., H. Sasaki, M. Furuse, H. Ozaki, T. Kita, and S. Tsukita.** 2001. Junctional adhesion molecule (JAM) binds to PAR-3: a possible mechanism for the recruitment of PAR-3 to tight junctions. Journal of Cell Biology **154:**491-497.

89. **Jones, E. Y., S. J. Davis, A. F. Williams, K. Harlos, and D. I. Stuart.** 1992. Crystal structure at 2.8 A resolution of a soluble form of the cell adhesion molecule CD2. Nature **360:**232-9.

90. **Jones, T. A., J. Y. Zhou, S. W. Cowan, and M. Kjeldgaard.** 1991. Improved methods for building protein models in electron density maps and the location of errors in these models. Act Crystallogr. **A47:**110-119.

91. **Kasper, C., H. Rasmussen, J. S. Kastrup, S. Ikemizu, E. Y. Jones, V. Berezin, E. Bock, and I. K. Larsen.** 2000. Structural basis of cell-cell adhesion by NCAM. Nat Struct Biol **7:**389-93.

92. **Kaye, K. M., D. R. Spriggs, R. Bassel-Duby, B. N. Fields, and K. L. Tyler.** 1986. Genetic basis for altered pathogenesis of an immune-selected antigenic variant of reovirus type 3 Dearing. Journal of Virology **59:**90-97.

93. **Kerneis, S., A. Bogdanova, J. P. Kraehenbuhl, and E. Pringault.** 1997. Conversion by Peyer's patch lymphocytes of human enterocytes into M cells that transport bacteria. Science **277:**949-52.

94. **Kolatkar, P. R., J. Bella, N. H. Olson, C. M. Bator, T. S. Baker, and M. G. Rossmann.** 1999. Structural studies of two rhinovirus serotypes complexed with fragments of their cellular receptor. Embo J **18:**6249-59.

95. **Kostrewa, D., M. Brockhaus, A. D'Arcy, G. E. Dale, P. Nelboeck, G. Schmid, F. Mueller, G. Bazzoni, E. Dejana, T. Bartfai, F. K. Winkler, and M. Hennig.** 2001. X-ray structure of junctional adhesion molecule: structural basis for homophilic adhesion via a novel dimerization motif. EMBO Journal **20:**4391-4398.

96. **Krasnykh, V., N. Belousova, N. Korokhov, G. Mikheeva, and D. T. Curiel.** 2001. Genetic targeting of an adenovirus vector via replacement of the fiber protein with the phage T4 fibritin. J Virol **75:**4176-83.

97. **Kwong, P. D., R. Wyatt, J. Robinson, R. W. Sweet, J. Sodroski, and W. A. Hendrickson.** 1998. Structure of an HIV gp120 envelope glycoprotein in complex with the CD4 receptor and a neutralizing antibody. Nature **393:**648-659.

98. **Lechner, F., U. Sahrbacher, T. Suter, K. Frei, M. Brockhaus, U. Koedel, and A. Fontana.** 2000. Antibodies to the Junctional Adhesion Molecule Cause Disruption of Endothelial Cells and Do Not Prevent Leukocyte Influx into the Meninges after Viral or Bacterial Infection. The Journal of Infectious Diseases **182:**978-982.

99. **Lee, P. W., E. C. Hayes, and W. K. Joklik.** 1981. Protein σ1 is the reovirus cell attachment protein. Virology **108:**156-163.

100. **Leone, G., R. Duncan, and P. W. K. Lee.** 1991. Trimerization of the reovirus cell attachment protein (sigma 1) induces conformational changes in sigma 1 necessary for its cell-binding function. Virology **184:**758-761.

101. **Li, C. X., and M. J. Poznansky.** 1990. Characterization of the ZO-1 protein in endothelial and other cell lines. J Cell Sci **97 (Pt 2):**231-7.

102. **Liu, Y., A. Nusrat, F. J. Schnell, T. A. Reaves, S. Walsh, M. Ponchet, and C. A. Parkos.** 2000. Human junction adhesion molecule regulates tight junction resealing in epithelia. Journal of Cell Science **113:**2363-2374.

103. **Manchester, M., D. S. Eto, A. Valsamakis, P. B. Liton, R. Fernandez-Munoz, P. A. Rota, W. J. Bellini, D. N. Forthal, and M. B. A. Oldstone.** 2000. Clinical isolates of measles virus use CD46 as a cellular receptor. Journal of Virology **74:**3967-3974.

104. **Manel, N., F. J. Kim, S. Kinet, N. Taylor, M. Sitbon, and J. L. Battini.** 2003. The ubiquitous glucose transporter GLUT-1 is a receptor for HTLV. Cell **115:**449-59.

105. **Martinez-Estrada, O. M., A. Villa, F. Breviario, F. Orsenigo, E. Dejana, and G. Bazzoni.** 2001. Association of junctional adhesion molecule with calcium/calmodulin-dependent serine protein kinase (CASK/LIN-2) in human epithelial caco-2 cells. J Biol Chem **276:**9291-6.

106. **Martin-Padura, I., S. Lostaglio, M. Schneemann, L. Williams, M. Romano, P. Fruscella, C. Panzeri, A. Stoppacciaro, L. Ruco, A. Villa, D. Simmons, and E. Dejana.** 1998. Junctional adhesion molecule, a novel member of the immunoglobulin superfamily that distributes at intercellular junctions and modulates monocyte transmigration. Journal of Cell Biology **142:**117-127.

107. **Masri, S. A., L. Nagata, D. C. Mah, and P. W. Lee.** 1986. Functional expression in Escherichia coli of cloned reovirus S1 gene encoding the viral cell attachment protein σ1. Virology **149:**83-90.

108. **Melikyan, G. B., R. M. Markosyan, H. Hemmati, M. K. Delmedico, D. M. Lambert, and F. S. Cohen.** 2000. Evidence that the transition of HIV-1 gp41 into a six-helix bundle, not the bundle configuration, induces membrane fusion. J Cell Biol **151:**413-23.

109. **Mercier, G. T., J. A. Campbell, J. D. Chappell, T. Stehle, T. S. Dermody, and M. A. Barry.** 2004. A chimeric adenovirus vector encoding reovirus attachment protein σ1 targets cells expressing junctional adhesion molecule 1. Proceedings of the National Academy of Sciences of the United States of America **101:**6188-6193.

110. **Meyer, T. N., C. Schwesinger, and B. M. Denker.** 2002. Zonula occludens-1 is a scaffolding protein for signaling molecules. Galpha(12) directly binds to the Src homology 3 domain and regulates paracellular permeability in epithelial cells. J Biol Chem **277:**24855-8.

111. **Misse, D., M. Cerutti, N. Noraz, P. Jourdan, J. Favero, G. Devauchelle, H. Yssel, N. Taylor, and F. Veas.** 1999. A CD4-independent interaction of human immunodeficiency virus-1 gp120 with CXCR4 induces their cointernalization, cell signaling, and T-cell chemotaxis. Blood **93:**2454-62.

112. **Mitic, L. L., and J. M. Anderson.** 1998. Molecular architecture of tight junctions. Annu Rev Physiol **60:**121-42.

113. **Mitraki, A., S. Miller, and M. J. van Raaij.** 2002. Review: conformation and folding of novel beta-structural elements in viral fiber proteins: the triple beta-spiral and triple beta-helix. J Struct Biol **137:**236-47.

114. **Morrison, L. A., R. L. Sidman, and B. N. Fields.** 1991. Direct spread of reovirus from the intestinal lumen to the central nervous system through vagal autonomic nerve fibers. Proceedings of the National Academy of Sciences USA **88:**3852-3856.

115. **Nagata, L., S. A. Masri, R. T. Pon, and P. W. K. Lee.** 1987. Analysis of functional domains on reovirus cell attachment protein sigma 1 using cloned S1 gene deletion mutants. Virology **160:**162-168.

116. **Nibert, M. L., J. D. Chappell, and T. S. Dermody.** 1995. Infectious subvirion particles of reovirus type 3 Dearing exhibit a loss in infectivity and contain a cleaved σ1 protein. Journal of Virology **69:**5057-5067.

117. **Nibert, M. L., T. S. Dermody, and B. N. Fields.** 1990. Structure of the reovirus cell-attachment protein: a model for the domain organization of σ1. Journal of Virology **64:**2976-2989.

118. **Nicholls, A., K. A. Sharp, and B. Honig.** 1991. Protein folding and association: insights from the interfacial and thermodynamic properties of hydrocarbons. Proteins **11:**281-296.

119. **Ono, N., H. Tatsuo, K. Tanaka, H. Minagawa, and Y. Yanagi.** 2001. V domain of human SLAM (CDw150) is essential for its function as a measles virus receptor. J Virol **75:**1594-600.

120. **Ostrov, D. A., W. Shi, J. C. Schwartz, S. C. Almo, and S. G. Nathenson.** 2000. Structure of murine CTLA-4 and its role in modulating T cell responsiveness. Science **290:**816-9.

121. **Otwinowski, Z., and W. Minor.** 1997. Processing of X-ray diffraction data collected in oscillation mode. Methods in Enzymology **276:**307-326.

122. **Ozaki, H., K. Ishii, H. Arai, H. Horiuchi, T. Kawamoto, H. Suzuki, and T. Kita.** 2000. Junctional adhesion molecule (JAM) is phosphorylated by protein kinase C upon platelet activation. Biochem Biophys Res Commun **276:**873-8.

123. **Ozaki, H., K. Ishii, H. Horiuchi, H. Arai, T. Kawamoto, K. Okawa, A. Iwamatsu, and T. Kita.** 1999. Cutting edge: combined treatment of TNF-alpha and IFN-gamma causes redistribution of junctional adhesion molecule in human endothelial cells. Journal of Immunology **163:**553-557.

124. **Pacitti, A., and J. R. Gentsch.** 1987. Inhibition of reovirus type 3 binding to host cells by sialylated glycoproteins is mediated through the viral attachment protein. Journal of Virology **61:**1407-1415.

125. **Parrott, M. B., K. E. Adams, G. T. Mercier, H. Mok, S. K. Campos, and M. A. Barry.** 2003. Metabolically biotinylated adenovirus for cell targeting, ligand screening, and vector purification. Mol Ther **8:**688-700.

126. **Paul, R. W., A. H. Choi, and P. W. K. Lee.** 1989. The α-anomeric form of sialic acid is the minimal receptor determinant recognized by reovirus. Virology **172:**382-385.

127. **Pelletier, J., R. Nicholson, R. Bassel-Duby, B. N. Fields, and N. Sonenberg.** 1987. Expression of reovirus type 3 Dearing σ1 and σs polypeptides in Escherichia coli. Journal of General Virology **68:**135-145.

128. **Poteete, A. R.** 2001. What makes the bacteriophage lambda Red system useful for genetic engineering: molecular mechanism and biological function. FEMS Microbiol Lett **201:**9-14.

129. **Prota, A. E., J. A. Campbell, P. Schelling, J. C. Forrest, T. R. Peters, M. J. Watson, M. Aurrand-Lions, B. Imhof, T. S. Dermody, and T. Stehle.** 2003.

Crystal structure of human junctional adhesion molecule 1: implications for reovirus binding. Proc. Natl. Acad. Sci. U.S.A. **100:**5366-5371.

130. **Rankin, U. T., Jr., S. B. Eppes, J. B. Antczak, and W. K. Joklik.** 1989. Studies on the mechanism of the antiviral activity of ribavirin against reovirus. Virology **168:**147-158.

131. **Rebai, N., G. Almazan, L. Wei, M. I. Greene, and H. U. Saragovi.** 1996. A p65/p95 neural surface receptor is expressed at the S-G2 phase of the cell cycle and defines distinct populations. European Journal of Neuroscience **8:**273-81.

132. **Rescigno, M., G. Rotta, B. Valzasina, and P. Ricciardi-Castagnoli.** 2001. Dendritic cells shuttle microbes across gut epithelial monolayers. Immunobiology **204:**572-81.

133. **Riesen, F. K., B. Rothen-Rutishauser, and H. Wunderli-Allenspach.** 2002. A ZO1-GFP fusion protein to study the dynamics of tight junctions in living cells. Histochemistry and Cell Biology **117:**307-15.

134. **Rosen, L.** 1960. Serologic grouping of reovirus by hemagglutination-inhibition. American Journal of Hygiene **71:**242-249.

135. **Rubin, D. H., D. B. Weiner, C. Dworkin, M. I. Greene, G. G. Maul, and W. V. Williams.** 1992. Receptor utilization by reovirus type 3: distinct binding sites on thymoma and fibroblast cell lines result in differential compartmentalization of virions. Microbial Pathogenesis **12:**351-365.

136. **Rubin, D. H., J. D. Wetzel, W. V. Williams, J. A. Cohen, C. Dworkin, and T. S. Dermody.** 1992. Binding of type 3 reovirus by a domain of the σ1 protein important for hemagglutination leads to infection of murine erythroleukemia cells. Journal of Clinical Investigation **90:**2536-2542.

137. **Sabin, A. B.** 1959. Reoviruses: a new group of respiratory and enteric viruses formerly classified as ECHO type 10 is described. Science **130:**1387-1389.

138. **Sabin, A. B.** 1957. Viruses in search of a disease. Annals of the New York Academy of Science **67:**250-252.

139. **Schulz, G. E., Schirmer, R.H.** 1976. Principles of Protein Structure. Springer-Verlag, New York.

140. **Segerman, A., J. P. Atkinson, M. Marttila, V. Dennerquist, G. Wadell, and N. Arnberg.** 2003. Adenovirus type 11 uses CD46 as a cellular receptor. J Virol **77:**9183-91.

141. **Shayakhmetov, D. M., T. Papayannopoulou, G. Stamatoyannopoulos, and A. Lieber.** 2000. Efficient gene transfer into human CD34(+) cells by a retargeted adenovirus vector. J Virol **74:**2567-83.

142. **Shiver, J. W., and E. A. Emini.** 2004. Recent advances in the development of HIV-1 vaccines using replication-incompetent adenovirus vectors. Annu Rev Med **55:**355-72.

143. **Simonovic, I., J. Rosenberg, A. Koutsouris, and G. Hecht.** 2000. Enteropathogenic Escherichia coli dephosphorylates and dissociates occludin from intestinal epithelial tight junctions. Cell Microbiol **2:**305-15.

144. **Simons, K., and S. D. Fuller.** 1985. Cell surface polarity in epithelia. Annu Rev Cell Biol **1:**243-88.

145. **Smith, D. K., and H. Xue.** 1997. Sequence profiles of immunoglobulin and immunoglobulin-like domains. J Mol Biol **274:**530-45.

146. **Smith, R. E., H. J. Zweerink, and W. K. Joklik.** 1969. Polypeptide components of virions, top component and cores of reovirus type 3. Virology **39:**791-810.

147. **Spiropoulou, C. F., S. Kunz, P. E. Rollin, K. P. Campbell, and M. B. Oldstone.** 2002. New World arenavirus clade C, but not clade A and B viruses, utilizes alpha-dystroglycan as its major receptor. J Virol **76:**5140-6.

148. **Spriggs, D. R., R. T. Bronson, and B. N. Fields.** 1983. Hemagglutinin variants of reovirus type 3 have altered central nervous system tropism. Science **220:**505-507.

149. **Spriggs, D. R., and B. N. Fields.** 1982. Attenuated reovirus type 3 strains generated by selection of haemagglutinin antigenic variants. Nature **297:**68-70.

150. **Staunton, D. E., V. J. Merluzzi, R. Rothlein, R. Barton, S. D. Marlin, and T. A. Springer.** 1989. A cell adhesion molecule, ICAM-1, is the major surface receptor for rhinoviruses. Cell **56:**849-853.

151. **Stehle, T., and T. S. Dermody.** 2003. Structural evidence for common functions and ancestry of the reovirus and adenovirus attachment proteins. Reviews in Medical Virology **13:**123-132.

152. **Strong, J. E., G. Leone, R. Duncan, R. K. Sharma, and P. W. Lee.** 1991. Biochemical and biophysical characterization of the reovirus cell attachment protein sigma 1: evidence that it is a homotrimer. Virology **184:**23-32.

153. **Sturzenbecker, L. J., M. L. Nibert, D. B. Furlong, and B. N. Fields.** 1987. Intracellular digestion of reovirus particles requires a low pH and is an essential step in the viral infectious cycle. Journal of Virology **61:**2351-2361.

154. **Swofford, D. L.** 1991. Phylogenetic analysis using parsimony, Champagne, Illinois.

155. **Tang, D., J. E. Strong, and P. W. K. Lee.** 1993. Recognition of the epidermal growth factor receptor by reovirus. Virology **197:**412-414.

156. **Tardieu, M., M. L. Powers, and H. L. Weiner.** 1983. Age-dependent susceptibility to reovirus type 3 encephalitis: role of viral and host factors. Annals of Neurology **13:**602-607.

157. **Tardieu, M., and H. L. Weiner.** 1982. Viral receptors on isolated murine and human ependymal cells. Science **215:**419-421.

158. **Tatsuo, H., N. Ono, K. Tanaka, and Y. Yanagi.** 2000. SLAM (CDw150) is a cellular receptor for measles virus. Nature **406:**893-897.

159. **Thompson, J. D., T. J. Gibson, F. Plewniak, F. Jeanmougin, and D. G. Higgins.** 1997. The CLUSTAL_X windows interface: flexible strategies for multiple sequence alignment aided by quality analysis tools. Nucleic Acids Res **25:**4876-82.

160. **Tillman, B. W., T. D. de Gruijl, S. A. Luykx-de Bakker, R. J. Scheper, H. M. Pinedo, T. J. Curiel, W. R. Gerritsen, and D. T. Curiel.** 1999. Maturation of dendritic cells accompanies high-efficiency gene transfer by a CD40-targeted adenoviral vector. J Immunol **162:**6378-83.

161. **Tomko, R. P., R. Xu, and L. Philipson.** 1997. HCAR and MCAR: the human and mouse cellular receptors for subgroup C adenoviruses and group B coxsackieviruses. Proc Natl Acad Sci USA **94:**3352-6.

162. **Tsuruta, Y., L. Pereboeva, J. N. Glasgow, C. L. Luongo, S. Komarova, Y. Kawakami, and D. T. Curiel.** 2005. Reovirus sigma1 fiber incorporated into adenovirus serotype 5 enhances infectivity via a CAR-independent pathway. Biochem Biophys Res Commun.

163. **Tyler, K. L.** 2001. Mammalian reoviruses, p. 1729-1745. *In* D. M. Knipe and P. M. Howley (ed.), Fields Virology, Fourth ed. Lippincott Williams & Wilkins, Philadelphia.

164. **Tyler, K. L., E. S. Barton, M. L. Ibach, C. Robinson, T. Valyi-Nagy, J. A. Campbell, P. Clarke, S. M. O'Donnell, J. D. Wetzel, and T. S. Dermody.**

2004. Isolation and molecular characterization of a novel type 3 reovirus from a child with meningitis. The Journal of Infectious Diseases **189:**1664-1675.

165. **Tyler, K. L., and B. N. Fields.** 1996. Pathogenesis of viral infections, p. 173-218. *In* B. N. Fields, D. M. Knipe, and P. M. Howley (ed.), Fields Virology, Third ed. Lippincott-Raven Press, Philadelphia.

166. **Tyler, K. L., and B. N. Fields.** 1996. Reoviruses, p. 1597-1623. *In* B. N. Fields, D. M. Knipe, and P. M. Howley (ed.), Fields Virology, Third ed. Lippincott-Raven, Philadelphia.

167. **Tyler, K. L., D. A. McPhee, and B. N. Fields.** 1986. Distinct pathways of viral spread in the host determined by reovirus S1 gene segment. Science **233:**770-774.

168. **Tyler, K. L., and N. Nathanson.** 2001. Pathogenesis of viral infections, p. 199-243. *In* D. M. Knipe and P. M. Howley (ed.), Fields Virology, Fourth ed. Lippincott-Raven Press, Philadelphia.

169. **Umeda, K., T. Matsui, M. Nakayama, K. Furuse, H. Sasaki, M. Furuse, and S. Tsukita.** 2004. Establishment and characterization of cultured epithelial cells lacking expression of ZO-1. J Biol Chem **279:**44785-94.

170. **van der Lubben, I. M., F. A. van Opdorp, M. R. Hengeveld, J. J. Onderwater, H. K. Koerten, J. C. Verhoef, G. Borchard, and H. E. Junginger.** 2002. Transport of chitosan microparticles for mucosal vaccine delivery in a human intestinal M-cell model. J Drug Target **10:**449-56.

171. **van Raaij, M. J., E. Chouin, H. van der Zandt, J. M. Bergelson, and S. Cusack.** 2000. Dimeric structure of the coxsackievirus and adenovirus receptor D1 domain at 1.7 A resolution. Structure **8:**1147-55.

172. **van Raaij, M. J., A. Mitraki, G. Lavigne, and S. Cusack.** 1999. A triple β-spiral in the adenovirus fibre shaft reveals a new structural motif for a fibrous protein. Nature **401:**935-938.

173. **Virgin, H. W., IV, R. Bassel-Duby, B. N. Fields, and K. L. Tyler.** 1988. Antibody protects against lethal infection with the neurally spreading reovirus type 3 (Dearing). Journal of Virology **62:**4594-4604.

174. **Virgin, H. W., M. A. Mann, and K. L. Tyler.** 1994. Protective antibodies inhibit reovirus internalization and uncoating by intracellular proteases. Journal of Virology **68:**6719-6729.

175. **Virgin, H. W., K. L. Tyler, and T. S. Dermody.** 1997. Reovirus, p. 669-699. *In* N. Nathanson (ed.), Viral Pathogenesis. Lippincott-Raven, New York.

176. **Vlasak, R., W. Luytjes, W. Spaan, and P. Palese.** 1988. Human and bovine coronaviruses recognize sialic acid-containing receptors similar to those of influenza C viruses. Proc Natl Acad Sci USA **85:**4526-4529.

177. **Vogels, R., D. Zuijdgeest, R. van Rijnsoever, E. Hartkoorn, I. Damen, M. P. de Bethune, S. Kostense, G. Penders, N. Helmus, W. Koudstaal, M. Cecchini, A. Wetterwald, M. Sprangers, A. Lemckert, O. Ophorst, B. Koel, M. van Meerendonk, P. Quax, L. Panitti, J. Grimbergen, A. Bout, J. Goudsmit, and M. Havenga.** 2003. Replication-deficient human adenovirus type 35 vectors for gene transfer and vaccination: efficient human cell infection and bypass of preexisting adenovirus immunity. J Virol **77:**8263-71.

178. **Von Seggern, D. J., S. Huang, S. K. Fleck, S. C. Stevenson, and G. R. Nemerow.** 2000. Adenovirus vector pseudotyping in fiber-expressing cell lines: improved transduction of Epstein-Barr virus-transformed B cells. J Virol **74:**354-62.

179. **Walters, R. W., P. Freimuth, T. O. Moninger, I. Ganske, J. Zabner, and M. J. Welsh.** 2002. Adenovirus fiber disrupts CAR-mediated intercellular adhesion allowing virus escape. Cell **110:**789-99.

180. **Wang, J. H., R. Meijers, Y. Xiong, J. H. Liu, T. Sakihama, R. Zhang, A. Joachimiak, and E. L. Reinherz.** 2001. Crystal structure of the human CD4 N-terminal two-domain fragment complexed to a class II MHC molecule. Proc Natl Acad Sci U S A **98:**10799-804.

181. **Wang, X., D. Y. Huang, S. M. Huong, and E. S. Huang.** 2005. Integrin alphavbeta3 is a coreceptor for human cytomegalovirus. Nat Med **11:**515-21.

182. **Watson, J. D., and F. H. Crick.** 1953. Molecular structure of nucleic acids; a structure for deoxyribose nucleic acid. Nature **171:**737-8.

183. **Weiner, H. L., D. Drayna, D. R. Averill, Jr, and B. N. Fields.** 1977. Molecular basis of reovirus virulence: role of the S1 gene. Proceedings of the National Academy of Sciences USA **74:**5744-5748.

184. **Weiner, H. L., M. L. Powers, and B. N. Fields.** 1980. Absolute linkage of virulence and central nervous system tropism of reoviruses to viral hemagglutinin. Journal of Infectious Diseases **141:**609-616.

185. **Weiner, H. L., R. F. Ramig, T. A. Mustoe, and B. N. Fields.** 1978. Identification of the gene coding for the hemagglutinin of reovirus. Virology **86:**581-584.

186. **Wetzel, J. D., J. D. Chappell, A. B. Fogo, and T. S. Dermody.** 1997. Efficiency of viral entry determines the capacity of murine erythroleukemia cells to support persistent infections by mammalian reoviruses. Journal of Virology **71:**299-306.

187. **Wickman, T. J., P. Mathias, D. A. Cheresh, and G. R. Nemerow.** 1993. Integrins alpha v beta 3 and alpha v beta 5 promote adenovirus internalization but not virus attachment. Cell **73:**309-319.

188. **Williams, L. A., I. Martin-Padura, E. Dejana, N. Hogg, and D. L. Simmons.** 1999. Identification and characterisation of human Junctional Adhesion Molecule (JAM). Molecular Immunology **36:**1175-1188.

189. **Wolf, J. L., G. Cudor, N. R. Blacklow, R. Dambrauskas, and J. S. Trier.** 1981. Susceptibility of mice to rotavirus infection: effects of age and administration of corticosteroids. Infection and Immunity **33:**565-574.

190. **Wolf, J. L., R. S. Kauffman, R. Finberg, R. Dambrauskas, B. N. Fields, and J. S. Trier.** 1983. Determinants of reovirus interaction with the intestinal M cells and absorptive cells of murine intestine. Gastroenterology **85:**291-300.

191. **Wolf, J. L., D. H. Rubin, R. Finberg, R. S. Kaufman, A. H. Sharpe, J. S. Trier, and B. N. Fields.** 1981. Intestinal M cells: a pathway of entry of reovirus into the host. Science **212:**471-472.

192. **Wu, E., S. A. Trauger, L. Pache, T. M. Mullen, D. J. von Seggern, G. Siuzdak, and G. R. Nemerow.** 2004. Membrane cofactor protein is a receptor for adenoviruses associated with epidemic keratoconjunctivitis. Journal of Virology **78:**3897-3905.

193. **Wu, H., P. D. Kwong, and W. A. Hendrickson.** 1997. Dimeric association and segmental variability in the structure of human CD4. Nature **387:**527-530.

194. **Wu, L., N. P. Gerard, R. Wyatt, H. Choe, C. Parolin, N. Ruffing, A. Borsetti, A. A. Cardoso, E. Desjardin, W. Newman, C. Gerard, and J. Sodroski.** 1996. CD4-induced interaction of primary HIV-1 gp120 glycoproteins with the chemokine receptor CCR-5. Nature **384:**179-83.

195. **Xiao, C., C. M. Bator, V. D. Bowman, E. Rieder, Y. He, B. Hebert, J. Bella, T. S. Baker, E. Wimmer, R. J. Kuhn, and M. G. Rossmann.** 2001. Interaction of coxsackievirus A21 with its cellular receptor, ICAM-1. J Virol **75:**2444-51.

196. **Yeung, M. C., M. J. Gill, S. S. Alibha, M. S. Shahrabadi, and P. W. K. Lee.** 1987. Purification and characterization of the reovirus cell attachment protein σ1. Virology **156:**377-385.

197. **Zahraoui, A., D. Louvard, and T. Galli.** 2000. Tight junction, a platform for trafficking and signaling protein complexes. Journal of Cell Biology **151:**F31-F36.

198. **Zhou, L., Y. Luo, Y. Wu, J. Tsao, and M. Luo.** 2000. Sialylation of the host receptor may modulate entry of demyelinating persistent Theiler's virus. J Virol **74:**1477-85.